Invest Manitoba
Open for Business

Open File OF2022-3

Progress report on the study of granitoids in Manitoba: petrogenesis and metallogeny

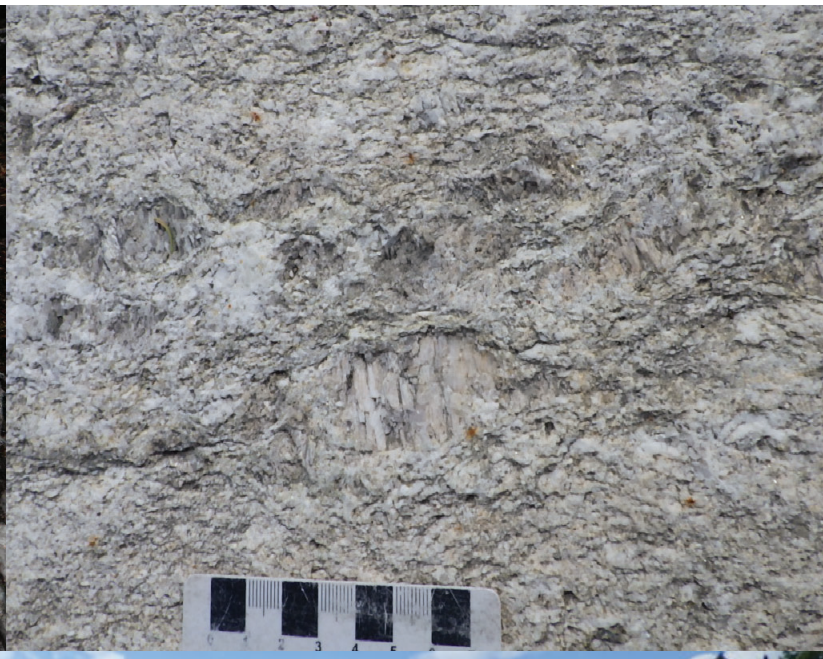

Manitoba

Open File OF2022-3

Progress report on the study of granitoids in Manitoba: petrogenesis and metallogeny

by X.M. Yang
Manitoba Geological Survey
Winnipeg, 2023

Yang, X.M. 2023: Progress report on the study of granitoids in Manitoba: petrogenesis and metallogeny; Manitoba Economic Development, Investment and Trade, Manitoba Geological Survey, Open File OF2022-3, 119 p.

NTS grid: All of Manitoba

Published by:

Manitoba Economic Development, Investment and Trade
Manitoba Geological Survey
360–1395 Ellice Avenue
Winnipeg, Manitoba
R3G 3P2 Canada

Telephone: 1-800-223-5215 (General Enquiry)
204-945-6569 (Publication Sales)
Fax: 204-945-8427
Email: minesinfo@gov.mb.ca
Website: manitoba.ca/minerals

ISBN: 978-0-7711-1640-7

This publication is available to download free of charge at manitoba.ca/minerals.

Front cover photos:

Top left: Outcrop of part of the Corkeram Lake pluton at contact containing mafic volcanic xenoliths from the Lynn Lake greenstone belt.

Top right: Spodumene crystals forming unidirectional solidification texture in the Cat Lake pegmatite.

Bottom: An exploration trench exposing the Cat Lake lithium pegmatite dike associated with S-type granite from the Bird River greenstone belt.

Abstract

The Manitoba Geological Survey initiated a project in 2014 to investigate the petrogenesis and metallogeny of granitoid rocks in Manitoba. The objectives of the project are to identify various petrogenetic types of granitoid rocks and to investigate their geodynamic settings and mineralization potential. This report presents a framework of granitoid rocks from 48 plutons and/or intrusions emplaced into diverse domains (belts) and subprovinces in parts of the Trans-Hudson orogen and western Superior province, respectively, which were examined by reconnaissance mapping, geochemical sampling and laboratory analysis. A variety of petrogenetic types of granitoids (e.g., I-, S- and A-type, tonalite-trondhjemite-granodiorite [TTG], sanukitoid, and adakite-like) were identified and characterized mainly by applying field observations, textures (fabrics), magnetic susceptibilitiy (MS), mineral assemblages, petrography, the presence of mineralization and/or alteration, and geochemical and Nd isotope analytical data in order to evaluate their geodynamic settings, petrogenesis, mineralization potential and metallogeny. A GIS-based database is included in this report, which contains information about the UTM coordinates, field relationship, tectonic unit, petrography, lithogeochemistry and available U-Pb zircon geochronology of 323 granitoid samples.

In particular, critical minerals (e.g., Li, Ta, Cs, Nb, rare-earth elements, U and Cu) related to granitoid intrusions from various tectonic units are evaluated and discussed. The major findings of this study are that muscovite- and/or garnet-bearing granitic rocks (i.e., strongly peraluminous or S-type), commonly characterized by low MS values ($<0.1 \times 10^{-3}$ SI unit), ferroan and calcalkaline affinities, intruded exclusively into and/or occur close to collisional zones (or terrane/domain boundary zones), while to a lesser degree S-type granites also occur in metasediment-dominant basins. Therefore, S-type granites can be used as macro-recognizable geological criteria for subdividing tectonic units. These peraluminous granitoid rocks likely formed in thickened crustal setting(s) due to terrane amalgamation (e.g., continental collision) and are associated genetically with rare metals (e.g., Li, Ta, Cs, Nb, Be)–enriched pegmatite intrusions, and/or may also have potential to host Sn-W mineralization. In contrast, granitoid plutons, consisting dominantly of tonalite, trondhjemite and granodiorite (TTG suites) and characterized by higher MS values ($>0.1 \times 10^{-3}$ SI unit) with magnesian to ferroan, metaluminous to moderately peraluminous and calcic (or tholeiitic) to calcalkaline affinities and mineral assemblages typical of I-type (e.g., amphibole±biotite or biotite±amphibole), are abundant across the Precambrian shield in Manitoba. This suggests that extensive granitoid magmatism contributed greatly to continental crustal growth and expansion in the Archean and Paleoproterozoic, and may be related to plate subduction. Some of the granitoid phases in TTGs contain porphyry Cu-Au (e.g., Cat Lake–Euclid Lake), shear zone-hosted Au (e.g., Little Bear Lake) and skarn Au-Ag mineralization (e.g., Cat Lake).

Geochemical and Nd isotope compositions of the granitoid rocks from diverse domains (belts) in Manitoba provide key information about their parental magmas that were derived from distinct protoliths with different histories of geological evolution. Bedrock mapping aided by geochemical, U-Pb zircon geochronological and Nd isotope study can provide insights into the tectonic evolution of, for example, the Lynn Lake greenstone belt, that was manifested by arc I-type (i.e., the ca. 1879 Ma Farley Lake pluton I), intra-arc extension related A-type (ca. 1872 Ma Farley Lake pluton II), and slab roll-back related adakite-like (ca. 1854 Ma Farley Lake stock) granitoid rocks that are exposed in the Farley Lake area. More importantly, some mineralization may have been generated at a specific stage of the tectonic evolution; for instance, gold mineralization at the Gordon (formerly Farley Lake) mine in the Lynn Lake greenstone belt is genetically associated with the ca. 1854 Ma Farley Lake stock that shows adakite-like geochemical signatures. High-K calcalkaline plutons may have been potential source for U mineralization.

Résumé

En 2014, la Direction des services géologiques du Manitoba a amorcé un projet visant à étudier la pétrogénèse et la métallogénie de roches granitoïdes au Manitoba. Ce projet vise à identifier les différents types pétrogénétiques des roches granitoïdes et à examiner leur environnement géodynamique et leur potentiel de minéralisation. Ce rapport présente un cadre de roches granitoïdes de 48 plutons et/ou intrusions intégrés à divers domaines (ceintures) et sous-provinces dans certaines parties de l'orogène trans-hudsonien et de la partie ouest de la province du Supérieur, respectivement, qui ont été examinées au moyen de la cartographie de reconnaissance, de l'échantillonnage géochimique et d'analyses en laboratoire. Divers types pétrogénétiques de roches granitoïdes (p. ex., types I, S et A, TTG, sanukitoïdes et proches des adakites) ont été identifiés et caractérisés principalement par des observations sur le terrain, la texture (la fabrique), la susceptibilité magnétique (SM), les associations minéralogiques, la pétrographie, la présence de minéralisation et/ou d'altération ainsi que les données d'études isotopiques Nd et géochimiques afin d'évaluer leur environnement géodynamique, leur pétrogénèse, leur potentiel de minéralisation et leur métallogénie. Ce rapport inclut une base de données fondée sur le SIG contenant de l'information sur les coordonnées UTM, la relation sur le terrain, l'unité tectonique, la pétrographie, la lithogéochimie et la géochronologie U-Pb sur zircons disponible de 323 échantillons granitoïdes.

En particulier, les minéraux critiques (p. ex., Li, Ta, Cs, Nb, métaux des terres rares, U et Cu) associés aux intrusions granitoïdes de plusieurs unités tectoniques sont évalués et décrits. Les principales conclusions de cette étude sont que les roches granitiques à muscovite et/ou à grenats (c.-à-d., fortement hyperalumineuses ou de type S), qui se caractérisent généralement par de faibles valeurs de SM ($<0,1 \times 10^{-3}$ unité SI) et par des affinités de nature ferrifère et calco-alcaline, ont pénétré exclusivement dans des zones de collision (ou de zones bordières entre des terranes ou des domaines) ou sont présentes à proximité de telles zones, alors que l'on constate également, dans une moindre mesure, la présence de granits de type S dans des bassins où dominent les métasédiments. On peut donc utiliser les granits de type S comme critères géologiques reconnaissables à grande échelle pour la sous-division des unités tectoniques. Ces roches granitoïdes hyperalumineuses se sont probablement formées dans un ou plusieurs environnements épaissis au sein de la croûte du fait de l'agglomération de la terrane (p. ex., la collision des continents) et sont génétiquement associées aux intrusions de pegmatites enrichies de métaux rares (p. ex., Li, Ta, Cs, Nb, Be), et/ou pourraient aussi contenir des minéralisations en Sn-W. Par contre, les plutons granitoïdes, formés principalement de tonalite, de trondhjémite et de granodiorite (successions de TTG) et caractérisés par des valeurs de SM plus élevées ($>0,1 \times 10^{-3}$ unité SI) avec des affinités allant de magnésienne à ferrifère, de métalumineuse à modérément hyperalumineuses et de calcique (ou tholéiitique) à calco-alcaline et par des assemblages minéraux typiques du type I (p. ex., amphibole±biotite or biotite±amphibole), abondent sur tout le Bouclier précambrien au Manitoba. Cela laisse penser que le vaste magmatisme des granitoïdes a grandement contribué à la croissance et à l'élargissement de la croûte continentale pendant l'Archéen et le Paléoprotérozoïque, et qu'il pourrait être lié à la subduction des plaques. Certaines des phases granitoïdes dans les TTG contiennent du porphyre Cu-Au (p. ex., lacs Cat et Euclid), de l'or situé dans des zones de cisaillement (p. ex., lac Little Bear) et de la minéralisation de skarn Au-Ag (p. ex., lac Cat).

Les compositions géochimiques et isotopiques Nd des roches granitoïdes de divers domaines (ceintures) au Manitoba donnent des renseignements essentiels sur leurs magmas parentaux qui ont été dérivés de protolites distincts associés à différentes étapes de l'évolution géologique. La cartographie du substrat rocheux étayée par l'étude géochimique, géochronologique U-Pb sur zircons et isotopique Nd peut donner des informations sur l'évolution tectonique de, par exemple, la ceinture de roches vertes du lac Lynn, qui s'est manifestée par des roches granitoïdes de type arc I (c.-à-d. pluton I du lac Farley, 1879 Ma environ), de type A formées dans un environnement en extension au sein d'un arc magmatique (pluton II du lac Farley, 1872 Ma) et proches de l'adakite générées par un retournement de la plaque (stock du lac Farley, 1854 Ma environ) qui sont exposées dans la région du lac Farley. Plus important, certaines minéralisations peuvent avoir été générées à un stade précis de l'évolution tectonique; par exemple, la minéralisation aurifère à la mine Gordon (anciennement du lac Farley) située dans la ceinture de roches vertes du lac Lynn est génétiquement associée au stock du lac Farley de 1854 Ma environ, qui montre des signatures géochimiques proches de l'adakite. Les plutons calco-alcalins à forte teneur en potassium peuvent avoir été une source de minéralisation uranifère.

TABLE OF CONTENTS

TABLES

FIGURES

DIGITAL DATA

Introduction

Granitoid rock (*sensu lato*, *s.l.*) is any acid intrusive or plutonic rock with more than 5% modal quartz (Pearce et al., 1984), anorthite (An) content of plagioclase <50 (Hanson, 1978) and silica contents >63 wt. % on anhydrous basis (Le Bas et al., 1986; Middlemost, 1994; Le Maitre et al., 2002). A diversity of granitoids occurs throughout the history of Earth continents, recording key information about when and how the continental crust started to grow, rework, recycle and connect with the mantle geodynamics.

The earliest granitoid is from a ca. 3.456 Ga Paleoarchean tonalite-trondhjemite-granodiorite (TTG) suite (Laurent et al., 2020). Sodic TTGs may have been generated by partial melting, reworking and transformation of early basaltic crust (mafic amphibolite) differentiated from the mantle (e.g., Moyen and Martin, 2012; Polat, 2012), but the nature of their petrogenetic and geodynamic processes have been debated for many years (e.g., Polat and Kerrich, 2001; Martin et al., 2005; Moyen and Martin, 2012; Wyman, 2013; Halla, 2018; Laurent et al., 2020; Moyen et al., 2021; Nadeau et al., 2021; Windley et al., 2021). The conversion of mafic crust into TTGs generated the oldest continental nuclei, known as Archean microcontinents represented by TTG–greenstone terranes (e.g., Condie, 1994; Laurent et al., 2020; Windley et al., 2021; Polat et al., 2022). Comprehensive reviews by Halla et al. (2017) and Halla (2018) on Archean TTGs provide insight into a change in global tectonic regime approximately at the Archean–Proterozoic boundary, manifested by the facts that convergent continental margins with abundant batholiths of potassic granitoids appeared for the first time at 3.0–2.5 Ga involving both mantle-derived and recycled crustal materials. Diverse granitoids (e.g., TTGs, sanukitoid, Closepet-type granitoid, high-K granitoids) caused by increasing crust–mantle interactions reflect a significant change in mantle geodynamics and plate tectonics during the Neoarchean (Halla et al., 2017; Halla, 2018), suggesting that the onset of modern-type plate tectonics operated at 3.0–2.5 Ga although this has been debated over decades. More recently, however, Windley et al. (2021) argue the onset of accretionary circle plate tectonics by the Eoarchean Eon (4.0 Ga) considering available geological dataset worldwide, and both the Wilson circle plate tectonics and accretionary circle plate tectonics have operated since 2.5 Ga at the Neoarchean and Paleoproterozoic boundary.

Studies of high-pressure and high-temperature experimental petrology on granite systems (Bowen, 1928; Tuttle and Bowen, 1958; Rollinson, 1993; Rollinson and Pease, 2021, and references therein) show that granite (*sensu stricto, s.s.*) melts tend to evolve ultimately to the minimum composition at cotectic curve(s) or to eutectic point(s) during fractional crystallization, whereas the first batch of partial melt derived from continental crustal source would also have the minimum or eutectic composition depending on the P-T-X-H_2O conditions (e.g., Yang, 2017; Bonin et al., 2020; Jacob et al., 2021; Moyen et al., 2021; Yang et al., 2021). However, the paths of compositional differentiation for the processes of fractional crystallization and partial melting differ and/or display an opposite trend in an overall temporal sequence when plotting the geochemical composition of granitoid samples on Harker diagrams. Thus, it is essential to establish temporal and spatial relationships of a suite of granitoid samples collected from a pluton via either detailed mapping to determine relative ages or using U-Pb zircon geochronology to determine absolute ages in order to investigate its petrogenesis. The granitoid pluton may have been formed by magmatism between two end member processes, fractionation (of mantle-derived basaltic to intermediate magma) versus partial melting (melt derived from crustal source). This fundmental question has been also debated for decades (see Bonin et el., 2020; Moyen et al., 2021), and it is key to understanding which process has played a dominant role in granitoid petrogenesis that may have also been involved by other mechanisms (e.g., assimilation, magma mixing and mingling) as well as of tectonic settings and related mineralization.

Water solubility in granitic melts is a critical parameter in the study of granite petrogenesis and metallogeny, which has been an important subject of experimental petrology for many decades since the pioneering work was published (Bowen, 1928; Tuttle and Bowen, 1958). Water solubility in granitic melts is a function of pressure, temperature, melt composition, and water activity (Holtz et al., 2001) in terms of experimental work on melting of synthetic and natural granitic rocks at high-P and high-T conditions. Water plays an important role in the generation of granitic melts in the continental crust, where it is more abundant (e.g., Winter, 2014 and references therein). Hydrous melts rise to reach H_2O saturation, releasing a fluid phase, and more fluids would be emanated as they crystallize anhydrous phases (e.g., clinopyroxene, plagioclase). These magmatic fluids and/or hydrous melts may have created separate systems, such as pegmatites or hydrothermal ore deposits. Furthermore, rising hydrous melts will intersect the H_2O-saturated solidus and crystallize at some relatively shallow depth prior to reaching the surface. Hence, hydrous granitic melts tend to form plutons, whereas dry intermediate to acidic melts that would not intersect the positively sloping anhydrous solidus are likely to reach the surface as volcanics to volcaniclastics. Makhluf et al. (2017) suggested that liquidus water contents play a key part in controlling volume of granite melts formed in the lower crust via dehydration reaction in the absence of external (or excess) fluids. In constrast, partial melting of the lithospheric mantle aided by flux of external fluids (e.g., subduction-related fluids/melts) is commonly present underneath the subarc mantle (e.g., Pearce, 1983; Pearce et al., 2005; Winter, 2014).

Based on mineral assemblages, field and petrographic characteristics, geochemical and isotopic (radiogenic Sr-Nd and stable O-S) compositions, Barbarin (1999) divided granitoids into seven lithologic types; ridge 'tholeiitic' granitoids (RTG; plagiogranites), arc 'tholeiitic' granitoids (ATG), amphibole-rich calcalkaline granitoids (ACG), K-rich and K-feldspar-phyric calcalkaline granitoids (KCG), muscovite-bearing peraluminous granitoids (MPG), cordierite-bearing, biotite-rich peraluminous granitoids (CPG), and

peralkaline and alkaline granitoids (PAG). Each of these types forms in a similar geotectonic environment, originating from comparable sources. Therefore, Barbarin (1999) pointed out that a typical association of granitoids formed at a specific stage of the Wilson cycle, linking petrogenesis of granitoids to geodynamic environments (or plate tectonic settings) and growth of continental crust.

Mantle-derived RTG and PAG are the products of extensive fractionation of tholeiitic melts at ocean ridges or alkali basalt melts in continental doming/rifting settings, respectively. Typical of island arcs are mantle-derived ATG together with ACG of presumably mixed crust–mantle origin; the ACG are also mostly characteristic of continental subduction settings, including the huge Cordilleran batholiths. Peraluminous CPG and MPG are generated by crustal anatexis in continental collision or early post-collisional settings. Apart from that, the former collision belts (type area being the Scottish Caledonides) often feature voluminous post-collision uplift-related KCG plutons. CPG and partly MPG overlap with S-type granites (Chappell and White, 1974, 1992). PAG match A-type granites (Eby, 1990), and the other groups are all I-type granites despite their contrasting features, origins and occurrences (Bonin et al., 2020).

Some granitoid rocks display transitional features of I- to S-type in terms of geochemistry; for example, the I/S-type Freistadt biotite granites-granodiorites in the Central European Variscides (René, 2020). This is not surprising because of the unavoidable involvement of both igneous and sedimentary rocks in the source region(s) when parting melting takes place in a terrane collisional zone (e.g., Yang et al., 2019; Frost and Da Prat, 2021), but the type of dominant source rocks may have governed the geochemistry of resultant melts (granitoids). However, this report follows the original definition of Chappell and White (1974, 1992, 2001) and does not investigate this problem because more detailed isotope data (e.g., O, Hf isotopes) are required to do so.

Granite (*s.l.*) classification based on depth (pressure) of source mineralogy and Sr and Yb contents (Zhang et al., 2006) can be important (Yang et al., 2019) and allows grouping of granitoids into four classes: 1) granite derived from partial melting of source rocks at high pressure with garnet left in residual phase has high Sr and low Yb contents; 2) granite formed at medium pressures with granulite facies (composed of plagioclage+garnet+pyroxene±amphibole) as the residual facies has low Sr and Yb or high Sr and Yb contents (depending on the protolith composition); 3) granite formed at low pressures with plagioclase and no garnet in residual phase has low Sr and high Yb contents; and 4) M-type granites related to ophiolites formed by partial melting of gabbro possibly at very low pressures and high temperatures at shallow oceanic crustal levels is manifested by very low Sr and high Yb contents.

Archean TTGs are acknowledged to display poor trends in most geochemical diagrams, albeit having typically plagioclase-rich, sodic, magnesian and metaluminous to weakly peraluminous characteristics (Bonin et al., 2020). Bonin et al. (2020) thought that this is a unique combination of chemical properties, and no other granitic type (Barbarin, 1999) really matches all the features of TTGs. Similar to the classification of Zhang et al. (2006), Moyen and Martin (2012) grouped TTGs into three types in terms of Sr/Y and La/Yb ratios: low-, medium- and high-pressure TTGs.

The geochemical composition of a granitoid rock reflects the result of complex interplay between its magma source (precursor that may have experienced prior geological events; e.g., tectonic reworking, residual mineralogy indicative of physiochemical conditions of magma generation), processes (e.g., partial melting, magma fractionation, assimilation, mixing of magmas), and tectonic setting (characterized by a rock association that is a function of pressure, temperature, water partial pressure, redox condition, and volatile composition). Arculus (1987) suggested that the geochemistry of crust-derived granites mimics the magma source of the continental crust, rather than the geodynamic setting of emplacement. A granitic magma derived from partial melting of an arc-related metasedimentary or meta-igneous rock is likely to inherit the arc signature of an older subduction, displaying depletion of high-field-strength elements (HFSEs) relative to large-ion lithophile elements (i.e., negative Nb–Ta anomalies) in N-MORB (normal mid-ocean–ridge basalt)–normalized spider diagrams (Pearce, 2008; Konopásek et al., 2018). Such geochemical signature is typical of the continental crust (Taylor and McLennan, 2009; Rudnick and Gao, 2010) and would also be inherited by the anatectic melts that are characterized by negative Nb–Ta anomalies (Bonin et al., 2020).

More importantly, mineral deposits may be associated with some granitoid intrusions and/or suites. For example, porphyry Cu (Mo) mineralization is genetically related to volcanic arc to continental arc calcalkaline granitoid intrusions (e.g., Blevin and Chappell, 1995; Blevin, 2004), whereas rare metals (e.g., Li, Cs, Ta, Nb, Be) are hosted in granite pegmatites associated with continental collisional peraluminous S-type granites (*s.s.*; e.g., Černy et al., 1981; Breaks and Moore, 1992; Černý and Ercit, 2005; Yang, 2014a, b; Yang et al., 2019; Yang and Houlé, 2020).

Granitoid rocks are the most abundant type exposed in the Precambrian shield in Manitoba and record important geological information that can be used to infer petrogenesis, sources and tectonic settings of magmas, and can help shed light on the tectonic evolution and mineral potential from regional to local scales. For example, I-type granites, which originated from igneous sources (Chappell and White, 1974, 1992, 2001) and usually display oxidized features with high values of magnetic susceptibility (MS), consistent with the magnetite-series granites of Ishihara (1977, 1981, 2004), have potential for Cu-Mo (Au) mineralization (Blevin and Chappell, 1995; Blevin, 2004). In contrast, S-type granites, which are sourced from sedimentary rocks (Chappell and White, 1974, 1992, 2001) and commonly exhibit reduced features with low MS values, consistent with the ilmenite-series granites of Ishihara (1977, 1981, 2004), are commonly related to Sn-W and rare-metal mineralization (Blevin, 2004). Such generalizations of granitoid types are useful in mineral exploration, despite that exceptions are evident. For example, reduced I-type

and ilmenite-series granites are potentially related to intrusion-related Au mineralization (Lang and Baker, 2001; Blevin, 2004; Yang et al., 2008 and references therein).

Table 1 summarizes some of the key field and petrological characteristics of I- versus S-type granites (*s.l.*), and magnetite- versus ilmenite-series granites, which can be used for identification of granite petrogenetic types and to help assess exploration potential. Porphyry Cu mineralization, for example, needs Cu built up in oxidized (i.e., high fO_2) magmas that commonly result in oxidized magnetite-series and I-type granites, whereas critical metals (e.g., Li, Cs, Ta, Sn and W mineralization) are mainly related to relatively reduced ilmenite-series and S-type granites because enrichment of these metals in magmas requires reduced conditions (i.e., low fO_2; Blevin and Chappell, 1995; Blevin, 2004; Frost and Da Prat, 2021; Yang et al., 2021). Granitoid rocks in large areas of the Precambrian shield in Manitoba, however, have not been adequately characterized in this manner.

In 2014, the Manitoba Geological Survey (MGS) initiated a project to investigate petrogenesis and metallogeny of granitoid rocks in Manitoba. This project is designed as a long-term effort employing a multidisciplinary approach that includes bedrock mapping, petrography, U-Pb geochronology, Nd-isotope analysis and lithogeochemistry. All of the above techniques, together with GIS data compilation and analysis, are used to improve the understanding of granitoid petrogenesis and metallogeny, as well as the relationships to crustal growth and geodynamic settings over time. Since the 2014 field season, the MGS has been carrying out reconnaissance mapping and geochemical sampling of granitoid rocks in southeastern, northwestern, and central to northeastern Manitoba. This report presents the results of the field and laboratory work on the samples collected intermittently during six field seasons and the related laboratory analyses (2015 to 2017, 2019 and 2021). Geochemical composition of these granitoid samples together with some data acquired by former MGS geologists has been used to determine the samples' geochemical affinities, including alkalinity, alumina-saturation state, magnesian and ferroan features (Miyashiro, 1970; Irvine and Baragar, 1971; Maniar and Piccoli, 1989; Rollinson, 1993; Frost et al., 2001; Yang, 2007; Clemens and Stevens, 2021; Rollinson and Pease, 2021) in order to study their petrogenesis and metallogeny.

Methods

In the field, granitoid rocks were mapped and sampled to document the field relationships, textures (fabrics), mineral assemblages, MS and the presence of mineralization and (or) alteration. A Terraplus KT-10 MS meter (maximum sensitivity 0.001×10^{-3} SI units) was used with a pin to measure MS values of natural outcrops or exposures in road cuts; each outcrop was measured at least five times and the average of the measurements was recorded to represent the MS value of the outcrop. Outcrops were sampled using a rock saw or sledgehammer for petrographic and geochemical studies in the laboratories. Sample location was recorded by a GPS device. The MS values were used to assess relatively oxidized and reduced features of granitoid rocks and, together with their mineral assemblages and geochemical characteristics, to classify the granite petrogenetic types (see below).

Major and trace-element contents of all collected samples were analyzed using the 4Lithoresearch package at Activation Laboratories Ltd. (Actlabs) in Ancaster, Ontario. Detailed analytical procedures and methods are described in Data Repository Item DRI2022012, Anderson (2013) and Polat et al. (2016), and can be found on the Actlabs website (www.actlabs.com). An in-house granite standard was used and analyzed multiple times at Actlabs to monitor data quality. Reproducibility of major element analyses was generally better than 5%, and that of trace-element analyses was generally better than 10% of the amount present. A subset of 23 samples was submitted to the University of Alberta Radiogenic Isotope Facility (Edmonton, Alberta) for Sm-Nd isotope analysis. Detailed analytical procedures and methods are contained in DRI2022012. All of these analytical data are presented in this report and provided as a set of Microsoft Excel® tables in DRI2022012 together with a GIS-based shape file of the geochemical and Sm-Nd isotope data.

Geological settings

Manitoba is underlain by three tectonic provinces; the Hearne province, the Trans-Hudson orogen, and the Superior province (Hoffman, 1988; Bailes and Syme, 1989; Corrigan et al., 2009; Stott et al., 2010; Corrigan, 2012; Percival et al., 2006a, b, 2012; Percival, 2007; Parks et al., 2014; Rinne, 2017; Manitoba Geological Survey, 2018), all of which are subdivided into various domains (and/or belts, zones), and basins (Figure 1). Since the granitoid sampling in this study has been carried out in parts of the Trans-Hudson orogen and Superior province so far, this report focuses only on these two tectonic provinces. Figure 1 shows the tectonic division of Manitoba bedrocks and locations of geochemical samples collected in this study. Table 2 lists main features of granitoid rocks from 48 plutons and/or intrusions in different tectonic entities in Manitoba.

Western Superior province in southeastern Manitoba

Southeastern Manitoba is situated in the western Superior province, and is well-known for the occurrences of various mineral resources, such as gold, rare metals, nickel, copper, platinum-group elements (PGE), and chromium. This part of the province is tectonically subdivided, from the north in Bissett to south in Falcon Lake, into the Uchi domain, English River basin, Bird River greenstone belt (i.e., the major part of Bird River domain; Manitoba Geological Survey, 2018), Winnipeg River, and Wabigoon domains (Peck et al., 2000; Bailes et al., 2003; Lemkow et al., 2006; Percival et al., 2006a, b, 2012; Anderson, 2008, 2013; Gilbert et al., 2008, 2013; Duguet et al., 2009; Stott et al., 2010). Granitoid rocks are dominant rock types in the regions, followed by greenstone belts and mafic to ultramafic layered intrusions in abundance (Figure 2).

Table 1: Field, petrographic and lithogeochemical criteria for oxidized and reduced granitoids and petrogenetic types/series.

Criterion	Oxidized	Reduced
Pluton size	Stock, dike, batholith	Stock, dike, batholith
Lithologies	Wide range from mafic, intermediate to felsic	Dominantly felsic
Fabrics	Equigranular, seriate, porphyrytic	Equigranular, heterogeneous
Influences of wallrocks	Significant	Pronounced
Inclusions	Mafic	Restite (commonly granulite)
Magnetic susceptibility	$>0.1 \times 10^{-3}$ SI	$<0.1 \times 10^{-3}$ SI
K-feldspar	Pink, salmon red	Pale grey, white; rarely pinkish
Plagioclase	Commonly pale grey	Grey, white
Quartz	Pale white	Dark, pale white
Hornblende/amphibole	Common	Absence to presence
Biotite	Brownish, dark brown, greenish	Fox red, brownish red
Muscovite	Absence or rare	Common
Garnet	Absence or rare	Presence
Aluminosilicate (e.g., sillimanite, andalusite), cordierite, tourmaline	Absence	Rare to common
Magnetite	Common	Rare to absence
Ilmenite	Presence	Common
Hematite	Rare to presence	Absence
Sphene (titanite)	Common	Rare
Zircon	Presence	Presence
Sulphide minerals	Rare to absence of pyrite, and/or chalcopyrite	Rare to presence of pyrrhotite, and/or pyrite
Apatite	Commonly as inclusions in biotite and amphibole	Commonly as independent (discrete) crystals
Monazite	Rare	Common
Mode of opaque minerals	0.1 to 2.0 volume%	<0.1 volume%
SiO_2	A broad range of SiO_2 contents from basic to acidic	Relatively restricted in composition to high SiO_2 concentrations
Na_2O/K_2O	Commonly >1, Na_2O>3.2 wt. %	Normally <1, Na_2O<3.2 wt. %
Molar ratio of $Al_2O_3/(CaO+Na_2O+K_2O)$	<1.1	>1.1
Alkalinity	Calcalkaline	Calcalkaline
CIPW norms	Diopside or <1% corundum	>1% corundum (except for ilmenite-series I-type granites)
Oxygen fugacity (fO_2)	>ΔFMQ+0.5 (i.e., 0.5 logfO_2 unit above the fayalite-magnetite-quartz buffer)	<ΔFMQ-0.5 (i.e., 0.5 logfO_2 unit below the fayalite-magnetite-quartz buffer)
$\delta^{18}O$	<10‰	>10‰
Initial ratio of $(^{87}Sr/^{86}Sr)_i$	<0.710	>0.710
$\varepsilon_{Nd}(t)$	<0 to >0	<0 to >0
Granitoid petrogenetic types or series (Chappell and White, 1974, 1992, 2001; Ishihara, 1977, 1981, 2004)	I-type and/or magnetite-series; these types of granitoid intrusions formed in magmatic-arc settings, and could be genetically related to porphyry (and/or skarn) Cu, Mo (Au) mineralization. (Note that reduced I-type granites are attributed to ilmenite-series, are emplaced in environments that are away from the convergent margins; see the explanation in the left column).	S-type and/or ilmenite-series granites formed in collisional zones could host Sn (W) mineralization, and are genetically associated with rare metals (e.g., Li, Cs, Ta) deposits hosted in granitic pegamatites. Reduced I-type granites (ilmenite-series) may have been derived from an igneous source region, and are emplaced into a reduced setting (e.g., sedimentary rocks containing graphite or reduced carbon of organic materials) that resulted in the original oxidized magma being transformed to reduced magma/rock through a process of reduction reaction). Intrusion-related Au deposits are genetically associated with reduced, ilmenite-series I-type granitoid intrusions.
Precursor (protolith)	Meta-igneous rocks that had not undergone any sedimentary and/or chemical weathering cycle, which may have ultimately been derived from the mantle.	Metasedimentary rocks, and supracrustal rocks; experienced sedimentary cycle and/or significant chemical weathering.

Note: This table is compiled from Chappell and White, 1974, 1992, 2001; Ishihara, 1977, 1981, 2004; Whalen et al., 1987; Clarke, 1992; Yang, 2014a; Yang et al., 2008, 2019, 2021; Clemens, 2018; Clemens and Stevens, 2021.

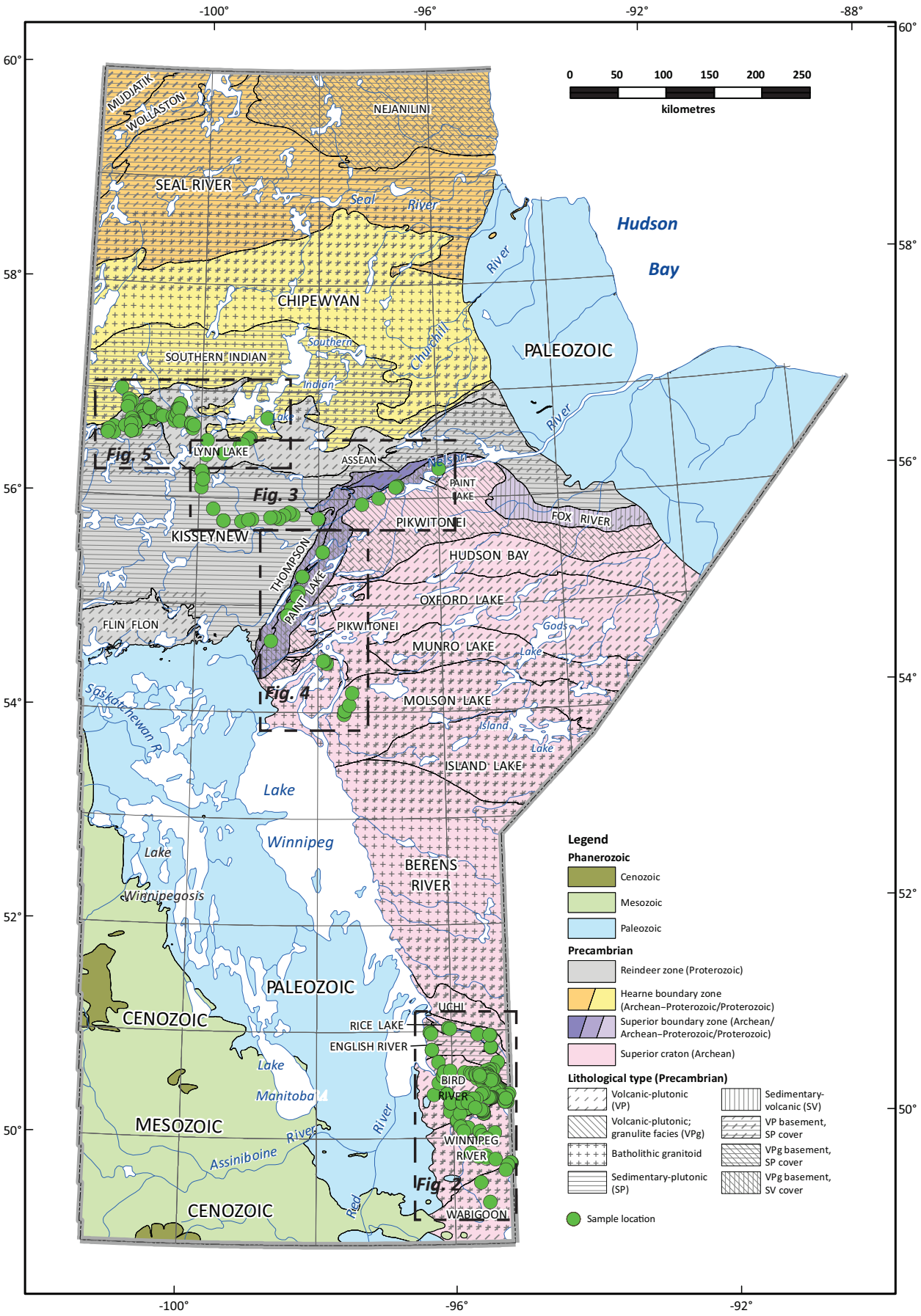

Figure 1: *Tectonic division of Manitoba (after Manitoba Geological Survey, 2018) and localities of granitoid sampling shown as green solid circles from various tectonic units. Dashed boxes reveal approximate locations of Figures 2, 3, 4 and 5. Detailed information about the sample location under NAD 83 UTM coordinate system is indicated in DRI2022012.*

Table 2: Main features of granitoid rocks in different tectonic entities in Manitoba.

Tectonic entity	Intrusion	Code[1]	MS[2] (x 10^{-3} SI)	Index minerals	Petrogenetic types
Uchi domain (UD)	Ross River plutonic suite	1	0.113–24.8	Amphibole, biotite	Magnetite-series, I-type
	Wallace Lake pluton	2	0.088–0.201	Biotite	Magnetite-series, I-type; part may be ilmenite-series, S-type
English River basin (ERB)	Tooth-Turtle intrusive suite	3	1.240–2.660	Biotite	Magnetite-series, I-type
	Black River plutonic suite	4	0.050–9.85	Biotite, amphibole Biotite, garnet, muscovite	Magnetite-series, I-type; part may be ilmenite-series, S-type
	Inconnu pluton I	5	0.168–10.00	Amphibole, biotite	Magnetite-series, I-type
	Inconnu pluton II	5′	0.010–0.150	Muscovite, garnet	Ilmenite-series, S-type
	Great Falls pluton	6	0.533–24.8	Amphibole, biotite	Magnetite-series, I-type
Bird River domain (BRD)	Maskwa Lake batholith I & II	7	0.28–11.70 0.044	Amphibole, biotite Biotite	Magnetite-series, I-type; part may be evolved I-type, ilmenite-series
	Marijane Lake pluton	8	0.251–1.90	Biotite	Magnetite-series, I-type
		8	0.035–0.88	Biotite, muscovite	Ilmenite-series, S-type
	Tin-Osis lakes intrusion	8′	0.037–0.047	Garnet, muscovite	Ilmenite-series, S-type
	Birse Lake pluton	9	0.155–1.51	Amphibole, biotite	Magnetite-series, I-type
		9	0.036–0.085	Biotite, muscovite, garnet	Ilmenite-series, S-type
	Bird River sanukitoid	9′		Amphibole	Magnetite-series, I-type
Winnipeg River domain (WRD)	Lac du Bonnet batholith	10	0.089–19.4	Biotite, amphibole	Magnetite-series, I-type; part may be evolved I-type, ilmenite-series
	Pointe du Bois batholith	11	1.49–45.7	Amphibole, biotite	Magnetite-series, I-type
	Rennie River plutonic suite	12	1.13–34.5	Amphibole, biotite	Magnetite-series, I-type
		12	0.045	Garnet, muscovite	Ilmenite-series, S-type
	Big Whiteshell Lake pluton	13	31.1–62.4	Amphibole, biotite	Magnetite-series, I-type
Wabigoon domain (WD)	Whitemouth Lake pluton	14	3.28–13.5 3.28	Biotite Garnet, muscovite	Magnetite-series, I-type; S-type, magnetite-series
	Falcon Lake igneous complex	15	11.7	Amphibole, biotite	Magnetite-series, I-type
Superior boundary zone (SBZ)	Fox Lake pluton	16	0.088	Biotite	Ilmenite-series, S-type?
	Assean Lake intrusion	17	0.165–3.4	Biotite±hornblende	Magnetite-series, I-type
	Orr Lake intrusion	18	0.716–11.9	Hornblende, biotite	Magnetite-series, I-type
	Jock Lake intrusion	19	0.048	Garnet, muscovite	Ilmenite-series, S-type
	Ospwagan Lake intrusion	20	0.110–0.145	Muscovite, garnet, pyrrhotite	Ilmenite-series, S-type
	Paint Lake pluton	21	0.074–0.077	Biotite, garnet, ±muscovite	Ilmenite-series, S-type
	Grass River pluton	22	1.24–2.01	Biotite, hornblende, ±magnetite	Magnetite-series, I-type
	Setting Lake pluton	23	1.73–6.12	Biotite, hornblende, ±magnetite	Magnetite-series, I-type
	Kiski Lake intrusion	24	10.0–29.6	Biotite, ±magnetite	Magnetite-series, I-type
Munro Lake domain (MOLD)	Jenpeg Dam intrusion	25	0.253–2.03	Hornblende, biotite	Magnetite-series, I-type
Molson Lake domain (MLD)	Nelson River pluton	26	0.164–3.47	Hornblende, biotite	Magnetite-series, I-type
	Paimusk Creek intrusion	26′	0.087–0.092	Biotite, ±muscovite	Ilmenite-series, S-type
Lynn Lake domain (LLD)	Burge Lake pluton	27	0.272–18.0	Biotite, amphibole	Magnetite-series, I-type
	Cockeram Lake pluton	28	0.318–32.9	Biotite, amphibole	Magnetite-series, I-type
	Eldon Lake pluton	29	0.357–12.9	Biotite, amphibole	Magnetite-series, I-type
	Motriuk Lake pluton	30	0.294–7.60	Biotite, amphibole	Magnetite-series, I-type
	Dunphy Lakes batholith	31	0.136–2.90	Amphibole, biotite	Magnetite-series, I-type
	Hughes Lake pluton	32	2.49–17.2	Amphibole, biotite	Magnetite-series, I-type

Notes:
[1] Intrusion code.
[2] MS (magnetic susceptibilty) in SI unit.

Table 2 (continued): Main features of granitoid rocks in different tectonic entities in Manitoba.

Tectonic entity	Intrusion	Code[1]	MS[2] (x 10^{-3} SI)	Index minerals	Petrogenetic types
Lynn Lake domain (LLD)	Farley Lake stock	33	11.2	Amphibole	Adakite-like
	Farley Lake pluton II	34	0.098–3.98	Biotite, amphibole	A-type
	Farley Lake pluton I	35	0.218–54.6	Amphibole, biotite	Magnetite-series, I-type
	Pool Lake pluton	36		Amphibole, biotite	Magnetite-series, I-type
	Counsell Lake pluton	37		Biotite, amphibole	Magnetite-series, I-type
	Late intrusive suite	38		Amphibole, biotite	Magnetite-series, I-type
	Eden Lake pluton	39	0.605–19.9	Amphibole, biotite	Magnetite-series, I-type;
	Ruttan Lake pluton	40	2.44–10.6	Hornblende, biotite	Magnetite-series, I-type
	Turnbull Lake pluton	41	7.09–18.2	Hornblende, biotite	Magnetite-series, I-type
Southern Indian domain (SID)	Vandekerckhove Lake pluton	42	1.51–3.27	Biotite, ±amphibole	Magnetite-series, I-type
	Zed Lake pluton	43	0.30–14.1	Amphibole, biotite	Magnetite-series, I-type;
		43	0.021–0.033	Biotite, ±muscovite, and ±garnet	Part of the Zed Lake pluton; ilmenite-series, S-type
	Little Brightsand Lake pluton	43'	0.018–0.089	Muscovite, garnet, ±biotite	Ilmenite-series, S-type
	Issett Lake pluton	44	0.046–0.085	Muscovite, garnet, ±biotite	Ilmenite-series, S-type
		44	0.215–10.1	Amphibole, biotite	Magnetite-series, I-type
Chipewyan domain (CD)	South Bay intrusion	45	55.0–72.9	Amphibole, biotite	Magnetite-series, I-type
Kisseynew domain (KD)	Notigi Lake intrusive suite	46	0.038–0.43	Garnet, biotite, ±muscovite	Ilmenite-series, S-type
	Wapisu Lake intrusion	47	0.046–0.079	Garnet, biotite, ±muscovite	Ilmenite-series, S-type
	Costello Lake pluton	48	9.70–26.7	Hornblende, biotite	Magnetite-series, I-type

Notes:
[1] Intrusion code.
[2] MS (magnetic susceptibilty) in SI unit.

Uchi domain

The Uchi domain comprises dominantly Neoarchean and Mesoarchean greenstone belts and spatially associated layered intrusions, including the Rice Lake greenstone belt (RLGB) in the westernmost section of the western Superior Province (Stott and Corfu, 1991; Anderson, 2008, 2013; Stott et al., 2010). In southeastern Manitoba, the Uchi domain is flanked to the north by the Berens River domain that is dominated by Mesoarchean granitoids, and to the south by metasedimentary rocks, gneisses, migmatite and granitoid plutonic rocks of the English River basin (Figure 1; Card and Ciesielski, 1986; Breaks, 1991; Stott et al., 2010) overprinted by late strike-slip faults (Stott and Corfu, 1991; Anderson, 2008, 2013). Previous studies suggested that the RLGB records a nearly 300-million-year history (Sanborn-Barrie et al., 2001; Anderson, 2008) of geological evolution involving initial plume magmatism, back-arc, arc and arc-rift magmatism and synorogenic sedimentation within a north-verging subduction-accretion complex developed along the southern margin of the North Caribou superterrane (Figure 2; Percival et al., 2006a, b, 2012; Stott et al., 2010; Anderson, 2013).

English River basin

The English River basin (Stott et al., 2010) or domain is characterized by east-west trending high-grade metasedimentary rocks, paragneisses, and migmatites (Breaks, 1991), which were likely deposited in a synorogenic flysch basin (Hrabi and Cruden, 2006; Percival et al., 2006a, b, 2012). Corfu et al. (1995) considered the depositional age of the English River metasedimentary rocks older than the 2.698 Ga granitoid pluton that cut and was emplaced into the metasedimentary rocks.

The southern margin of the English River basin in southeastern Manitoba is marked by the Bird River greenstone belt that extends to Separation Lake in Ontario in the east (Breaks, 1991; Gilbert et al., 2008).

Bird River greenstone belt

The Neoarchean Bird River greenstone belt includes mafic metavolcanic rocks and the Ni-Cu-PGE-Cr-bearing Bird River sill dated at 2743.0 ±0.5 Ma (Scoates and Scoates, 2013; Sotiriou et al., 2019) and Mayville mafic–ultramafic intrusion dated at 2742.8 ±0.5 Ma (Houlé et al., 2013; Sotiriou et al., 2020; Yang and Houlé, 2020). As a major component of the Bird River domain in southeastern Manitoba, this greenstone belt is part of an east-trending supracrustal belt that extends for 150 km from Lac du Bonnet in the west to Separation Lake (Ontario) in the east (Gilbert et al., 2008). This greenstone belt (Figure 2) is endowed with a unique Li-Ta-Cs-Be-bearing pegmatite resource (e.g., TANCO mine), and Ni-Cu-PGE-Cr minerals associated with mafic–ultramafic intrusions that may have been formed during an extensive Neoarchean Bird River magmatic event (Houlé et al., 2013; Yang

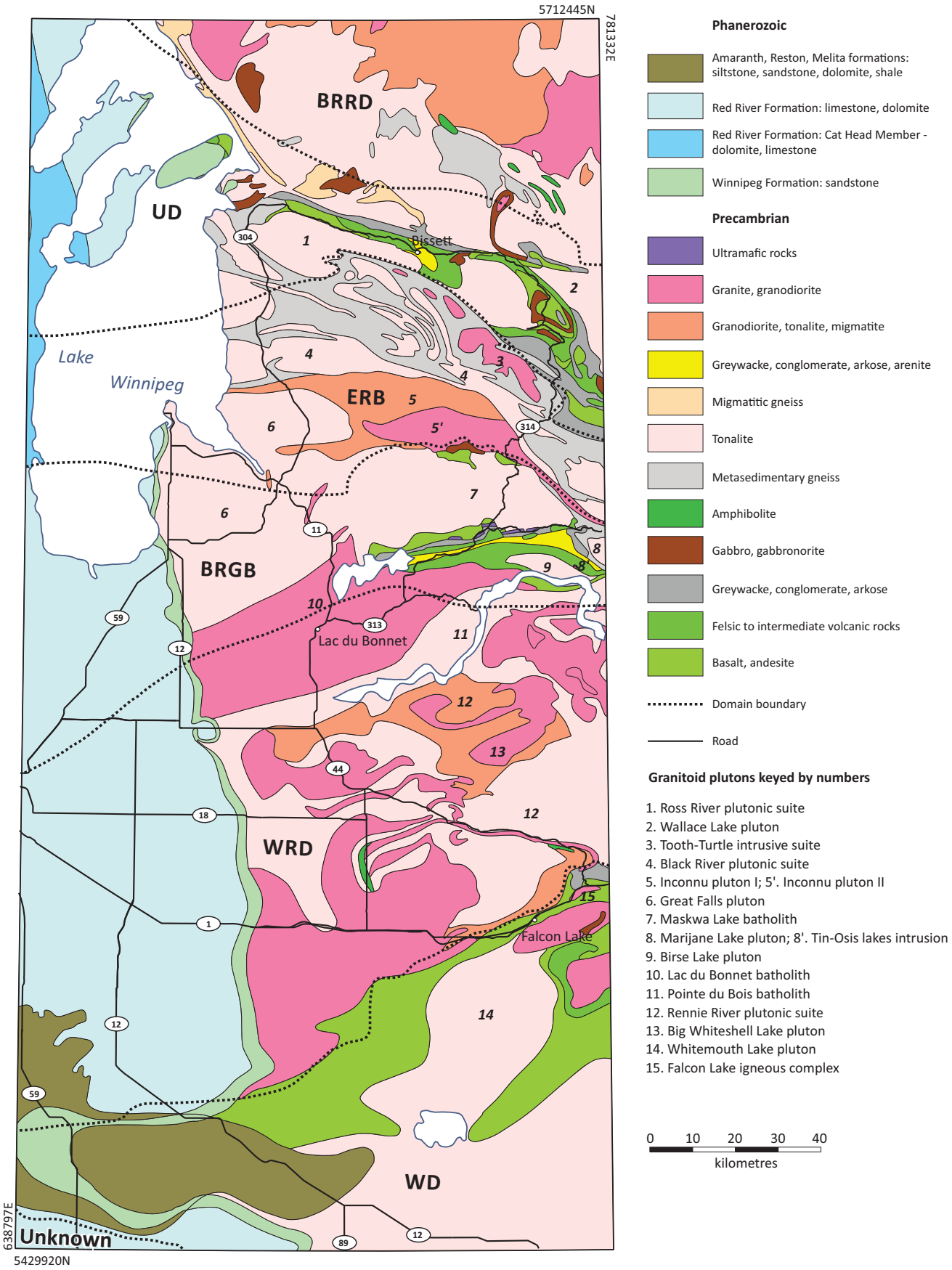

Figure 2: *Simplified geology of southeastern Manitoba, showing the dominance of granitoid rocks in the region. Abbreviations: BRRD, Berens River domain; BRGB, Bird River greenstone belt; ERB, English River basin; UD, Uchi domain; WD, Wabigoon domain; WRD, Winnipeg River domain. Numbered granitoid plutons or batholiths are referred to in the text and Table 2. Nomenclature of tectonic entities or units (see Manitoba Geological Survey, 2018) modified from Percival et al. (2006a, 2012), Gilbert et al. (2008), Stott et al. (2010) and Anderson (2013).*

and Houlé, 2020). This belt is bounded by the Eaglenest Lake shear zone to the south with the Winnipeg River domain (Gilbert et al., 2008).

Winnipeg River domain

The Winnipeg River domain (Figure 2; Stott et al., 2010) is characterized by Neoarchean granitoid rocks with Mesoarchean to Paleoarchean inheritance (Beakhouse, 1991) and by the presence of recycled 3.4–3.0 Ga crustal materials (Corfu, 1988; Percival et al., 2004, 2006b, 2012; Tomlinson et al., 2004; Whalen et al., 2004). Some of the oldest granitoid rocks in this domain have εNd values of –1 to +1, indicating that they may have been derived from much older crustal sources (Tomlinson et al., 2004). In addition, Percival et al. (2006b) also included the 2.9–3.07 Ga volcanic belts as a part of this domain.

Neoarchean tonalite-granodiorite plutons were emplaced between 2.716 and 2.705 Ga, followed by the intrusion of granites at 2.70–2.69 Ga (Corfu, 1988, 1996; Beakhouse, 1991). However, the lack of 2.75–2.71 Ga magmatism in the Winnipeg River domain north of the Wabigoon domain suggests that it had a separate tectonic history before interacting with the adjacent domain after ca. 2.71 Ga (Beakhouse, 1991; Percival et al., 2006b, 2012).

Wabigoon domain

Outcrops of the Wabigoon domain are sporadic and limited in southeastern Manitoba, but are well exposed in western Ontario where the domain is dominated by mafic volcanic rocks (with minor clastic metasedimentary rocks) and tonalite–granodiorite-granite plutons (Blackburn et al., 1991). The volcanic rocks are tholeiitic to calcalkaline, suggesting deposition in ocean crust and arc environments, respectively (Ayer and Davis, 1997; Ayer and Dostal, 2000; Wyman et al., 2000; Wu et al., 2016). These volcanic rocks have Neoarchean (ca. 2.745 to 2.72 Ga) ages (Corfu and Davis, 1992) and contain younger thin clastic metasedimentary sequences with older detrital zircons (>3.0 Ga; Fralick et al., 2006; Percival et al., 2006b).

Superior boundary zone and western Superior province in north-central Manitoba

North-central Manitoba is underlain dominantly by granitoid rocks in various tectonic units, including the Lynn Lake (-Leaf Rapids), Southern Indian and Kisseynew domains, and the Superior boundary zone (SBZ). The SBZ includes the Thompson, Split Lake and Assean Lake domains (Figure 3), flanking the Kisseynew domain to the west and western Superior province in the east.

Central Manitoba is underlain dominantly by granitoid rocks in various tectonic units, including the SBZ, Munro Lake and Molson Lake domains (MLD) of the western Superior province as shown along Highways 6 and 373 between Thompson and Norway House (Figure 4). The Thompson nickel belt (TNB) forms a segment of the SBZ (e.g., Bleeker, 1990), which represents the boundary between the Archean Superior craton and the Paleoproterozoic Trans-Hudson orogen. The TNB consists of Archean basement gneisses, Paleoproterozoic metasedimentary and metavolcanic rocks (Ospwagan Group) and granitic intrusions (Bleeker, 1990; Burnham et al., 2009; Corrigan et al., 2009; Couëslan and Pattison, 2012; Couëslan et al., 2013; Lightfoot et al., 2017; White et al., 2002; Zwanzig et al., 2001, 2003). To the east, the NNE trend of the TNB diffusely changes to a predominantly E–W structural trend of the western Superior province. Areas southeast of the TNB along Highway 373 are underlain by a variety of granitoid rocks that either occur as basement or intrude into supracrustal rocks of the MLD of the Archean Superior province, which are ascribed mainly to Archean TTG suites (Figure 4).

To the west, the TNB is in fault contact with the Kisseynew domain (KD) of the Trans-Hudson orogen (Zwanzig and Bailes, 2010). The transition zone between the TNB and the KD comprises granitoids and sedimentary rocks (Grass River group), part of which grades into turbidites in the KD (Burntwood Group; see Zwanzig and Bailes, 2010; Machado et al., 2011a, b).

Trans-Hudson orogen in northwestern Manitoba

The Trans-Hudson orogen (THO) includes the Lynn Lake (-Leafs Rapids) and Southern Indian domains in northwestern Manitoba, into which a variety of granitoid intrusions are emplaced. The Leaf Rapids domain is comparable to the Lynn Lake domain to the west, based on lithostratigraphic and temporal linkages (Baldwin et al., 1987; Rayner and Corrigan, 2004; Corrigan et al., 2007, 2009; Zwanzig and Bailes, 2010) and thus is attributed simply to the Lynn Lake domain (Figure 1; Manitoba Geological Survey, 2018). The Lynn Lake greenstone belt (LLGB) is well known for its endowment in orogenic Au, magmatic Ni-Cu and volcanogenic Cu-Zn deposits (Beaumont-Smith and Böhm, 2002, 2003, 2004; Yang and Beaumont-Smith, 2015a, b, 2016, 2017; Lawley et al., 2020a, b), and it is an important tectonic element of the Lynn Lake domain in the Reindeer zone of the THO (Stauffer, 1984; Hoffman, 1988; Lewry and Collerson, 1990; Zwanzig and Bailes, 2010; Lawley et al., 2020a, b; Reid, 2021). The LLGB is bounded to the north by the Southern Indian domain (a mixed metasedimentary and metaplutonic domain) and the Chipewyan domain (a continental-arc granitoid batholith); to the south, it is bounded by the metasedimentary KD (Figure 5; Gilbert et al., 1980; Syme, 1985; Zwanzig and Schledewitz, 1992; Zwanzig et al., 1999; Beaumont-Smith and Böhm, 2004; Corrigan et al., 2007, 2009; Zwanzig and Bailes, 2010; Yang, 2021; Martins, 2022).

Field and petrographic descriptions of granitoid rocks

Western Superior province in southeastern Manitoba

Specific granitoid plutons and/or intrusions examined in the western Superior province in southeastern Manitoba and referred in the text are labelled by number(s) in Figure 2. The

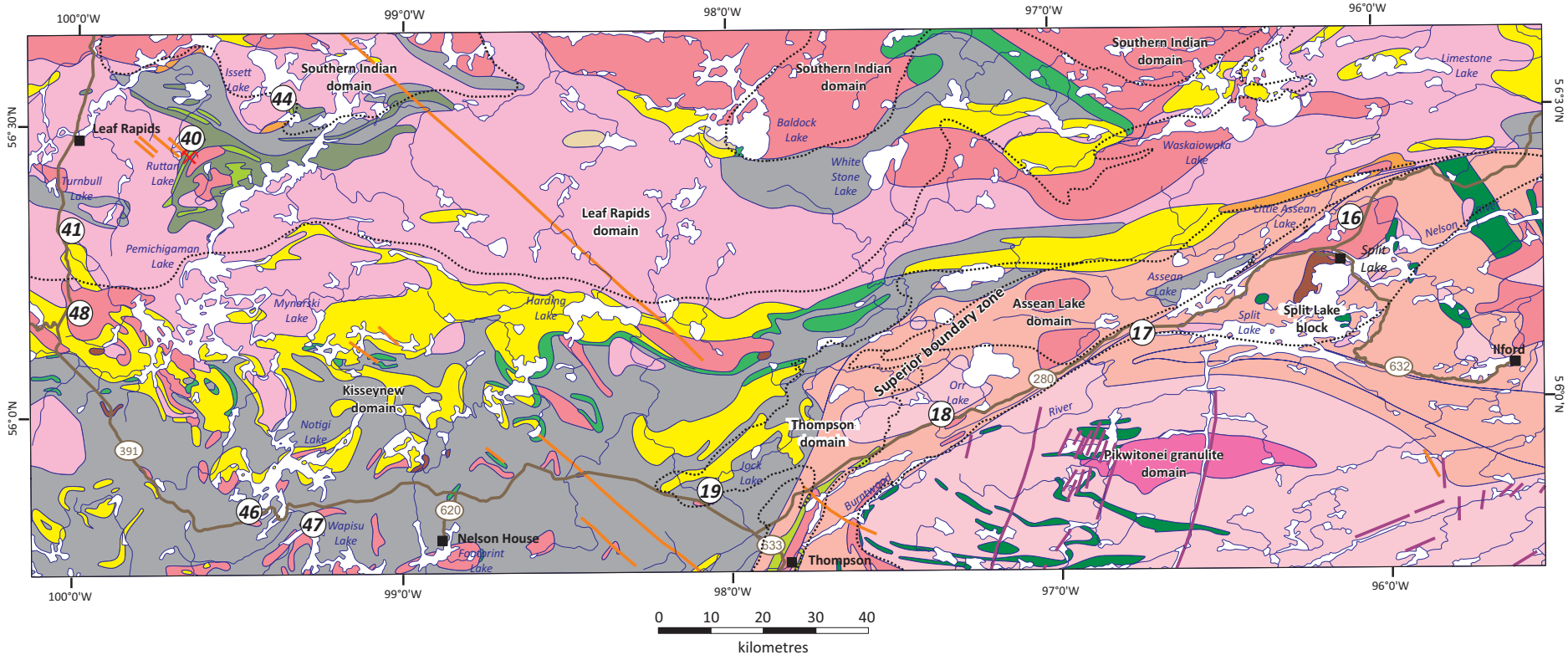

Paleoproterozoic intrusive and supracruatal rocks

- Granite, granodiorite, tonalite
- Tonalite–granodiorite
- Hypersthene tonalite, enderbite
- Migmatite complex
- Arkose, arenite
- Metaconglomerate
- Amphibolite and mafic gneiss
- Psammitic and semipelitic gneiss
- Rhyolite, dacite
- Mafic and intermediate metavolcanic flows
- Granite, granodiorite
- Fox River belt and Ospwagan group metacarbonate and metavolcanic rocks, iron formation

Archean rocks

- Migmatitic gneiss
- Granite, granodiorite
- Tonalite
- Felsic granulite
- Mafic–ultramafic granulite
- Anorthosite

Dike swarm

- Mackenzie dike (ca. 1.27 Ga)
- Molson dike (ca. 1.88 Ga)
- Ruttan Cu-Zn mine (past producer)
- Domain boundary
- Highway

Granitoid plutons keyed by numbers

16. Fox Lake pluton
17. Assean Lake intrusion
18. Orr Lake intrusion
19. Jock Lake intrusion

40. Ruttan Lake pluton
41. Turnbull Lake pluton
44. Issett Lake pluton

46. Notigi Lake intrusive suite
47. Wapisu Lake pluton
48. Costello Lake pluton

Figure 3: *Simplified geology of north-central Manitoba, showing the dominance of granitoid rocks in diverse tectonic units that include the Southern Indian, Leaf Rapids (i.e., Lynn Lake) and Kisseynew domains, and the Superior boundary zone that includes the Thompson, Split Lake and Assean Lake domains. Numbered granitoid plutons or intrusions examined in this study are referred to in the text. Nomenclature of tectonic units or domains is modified from Manitoba Energy and Mines (1986), Zwanzig et al. (2001) and Zwanzig and Bailes (2010).*

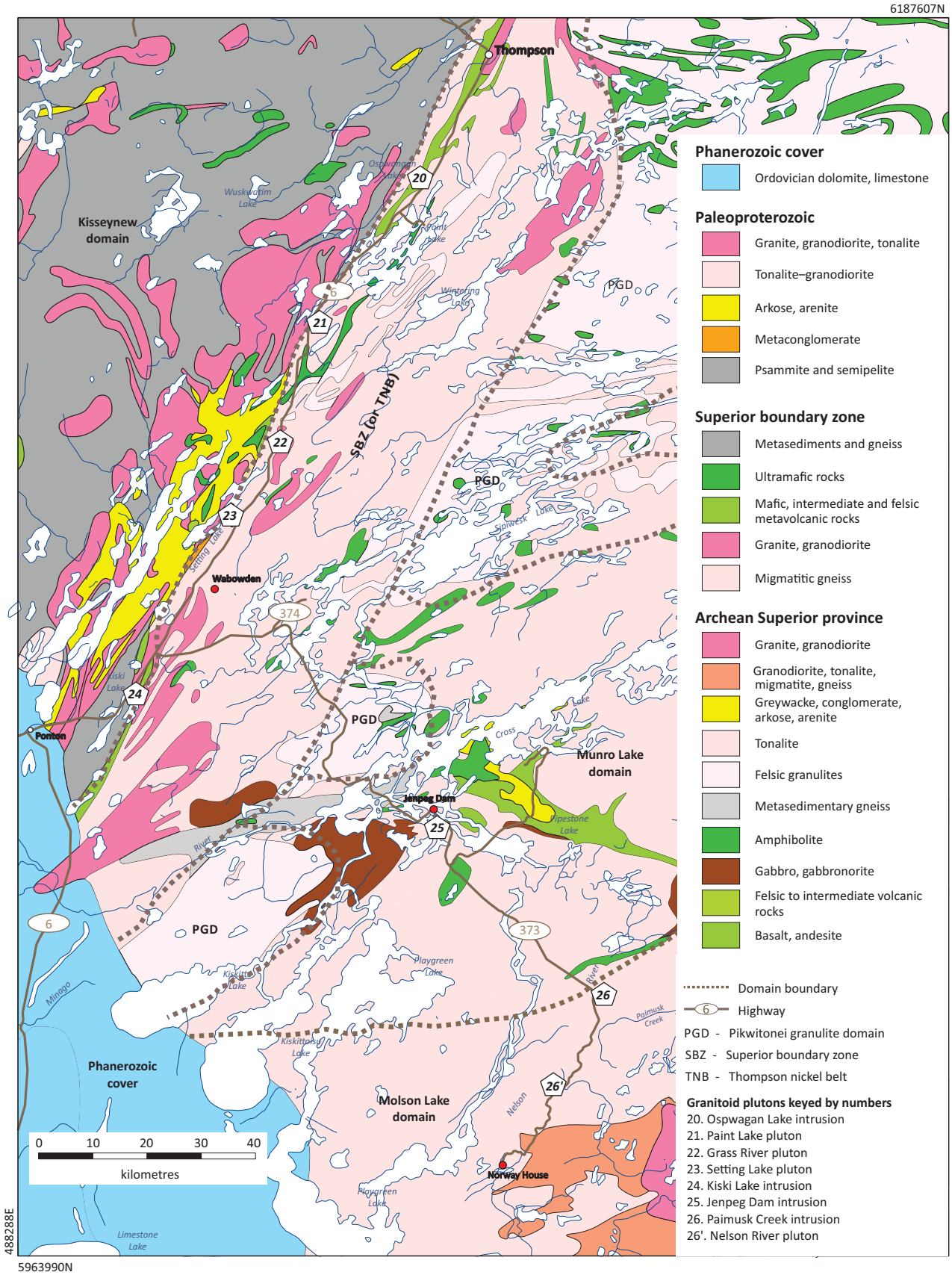

Figure 4: *Simplified geology of central Manitoba, showing the dominance of granitoid rocks in various tectonic units that include the Thompson nickel belt of the Superior boundary zone, and Molson Lake and Munro Lake domains of the Superior province. Numbered granitoid intrusions examined in this study are referred to in the text and Table 2. Nomenclature of tectonic units or domains is modified from Manitoba Energy and Mines (1986); Syme (1998); Zwanzig et al. (2001); Burnham et al. (2009); Heaman et al. (2009), Zwanzig and Bailes (2010) and Manitoba Geological Survey (2018).*

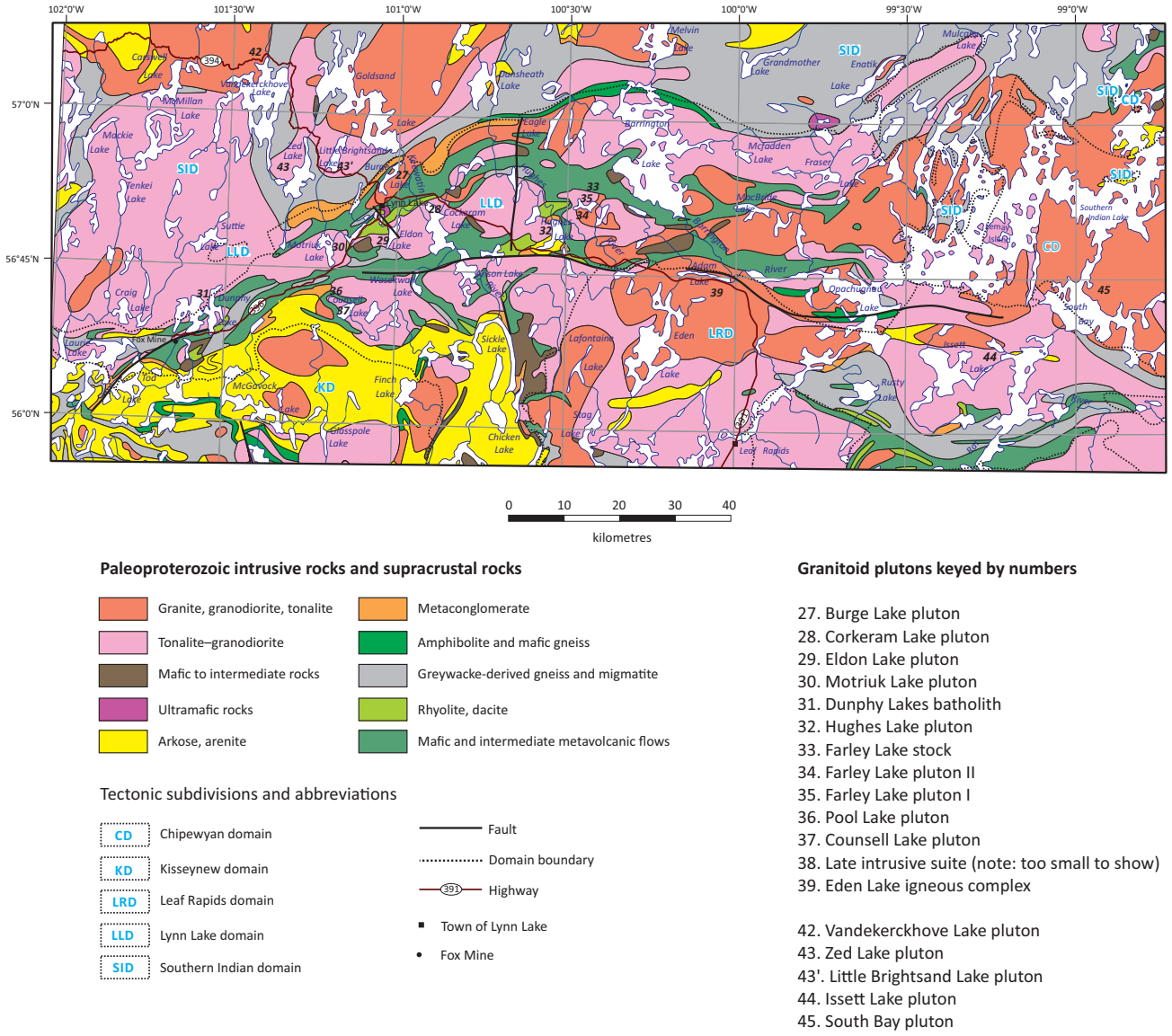

***Figure 5**: Simplified geology of the Lynn Lake greenstone belt and adjacent domains, showing the dominance of granitoid rocks in the region. Numbered granitoid plutons or batholiths are referred to in the text. Nomenclature of tectonic entities or domains modified from Manitoba Energy and Mines (1986) and Zwanzig and Bailes (2010).*

main features of these granitoid plutons are summarized in Table 2. Brief descriptions of granitoid rocks, from north to south, starting in the Uchi domain and ending in the Wabigoon domain, are presented in the following sections.

Granitoid rocks in the Uchi domain

Granitoid rocks examined and sampled in the Uchi domain, which intruded into and/or are in tectonic contact with supracrustal rocks of the RLGB in the Uchi domain, are tonalite and granodiorite plutons of the Ross River plutonic suite and Wallace Lake pluton (numbers 1 and 2, respectively in Figure 2 and Table 2).

Ross River plutonic suite (locality 1)

The Ross River plutonic suite includes two major plutons: the western pluton is a homogeneous, possibly sheet-like intrusion of ca. 2.72 Ga tonalite to granodiorite intruding metavolcanic to metavolcaniclastic rocks of the Bidou assemblage and unconformably overlain to the north by the San Antonio assemblage metasedimentary rocks; and the eastern pluton, known as the Ross River pluton, which intruded volcanic and volcaniclastic rocks of the Bidou and Gem assemblages and is a roughly elliptical body that dominates the central portion of the RLGB (Anderson, 2011). Turek et al. (1989) reported a U-Pb zircon age of 2728 ±8 Ma for a quartz diorite sample from the Ross River pluton. Anderson (2008) reported a U-Pb zircon age of ca. 2724 Ma from granodiorite in the core of the Ross River pluton. These ages are identical within uncertainties, and are interpreted to represent its crystallization age.

The southeastern portion of the Ross River pluton is composed dominantly of granodiorite to tonalite with minor quartz diorite and granite, cut by late quartz-feldspar porphyry and aplite dikes. At the past-producing Ogama-Rockland gold mine

near Long Lake, granodiorite is weakly foliated, medium-grained and equigranular to locally porphyritic, and consists of 30–35% quartz, ~30% plagioclase, up to 10% K-feldspar, and 10–20% amphibole and biotite that are strongly altered to chlorite. Sericitic alteration of feldspars is common. In places, granodiorite is gradational to tonalite and contains inclusions of quartz diorite. Interestingly, quartz diorite displays higher MS values ($0.829–0.930 \times 10^{-3}$ SI) than granodiorite (0.1130×10^{-3} SI), which is consistent with the former being older than the latter and the MS values decreasing with differentiation. However, granodiorite with porphyritic texture (Figure 6a) has very high MS values of up to 24.8×10^{-3} SI (Table 2) where it intrudes gabbro at the northwestern margin of the pluton and includes abundant gabbroic xenoliths, suggesting the wallrocks may have influenced the magnetite content of the granodiorite. It is noted that the Ross River pluton contains shear-hosted Au deposits (e.g., Ogama-Rockland; Zhou et al., 2012, 2016). This suggests a plausible linkage of Au mineralization to the Ross River pluton. Elsewhere, Au-bearing quartz veins in shear zones can be traced back through pegmatite-aplite dikes to the granodiorite, suggesting that they are intrusion-related Au systems (e.g., Thorne et al., 2002; Yang and Lentz, 2005; 2010; Vaughn and Ridley, 2014).

The western pluton of the Ross River plutonic suite consists of medium-grained, equigranular, weakly deformed tonalite to granodiorite. Locally, however, the granitoid rocks are porphyritic and strongly deformed and sheared. In places, numerous quartz veins cut the pluton. These granitoid rocks generally exhibit consistent MS values of $0.152–0.153 \times 10^{-3}$ SI, similar to granodiorite of the Ross River pluton to the east. Collectively, the granitoid rocks of the Neoarchean Ross River plutonic suite are comparable to the magnetite-series granites of Ishihara (1977, 1981, 2004) in terms of their MS values, and to the I-type granitoid rocks of Chappell and White (1974, 1992) on the basis of their mineral assemblages (e.g., amphibole±biotite). These field observations are consistent with the lithogeochemical characteristics of the granitoid rocks reported in Anderson (2008), indicating that they are mainly calcalkaline and metaluminous to moderately peraluminous.

Wallace Lake pluton (locality 2)

The Wallace Lake pluton, part of the Wanipigow River granitic complex in which granitic rocks were dated at 2731 ±10 Ma and 2880 ±9 Ma (Turek et al., 1989), is yet to be dated but is probably ascribed to the 2731 Ma phase based on their similar texture and mineral assemblages. The Wallace Lake pluton is relatively more evolved in terms of mineral assemblage (e.g., the absence of amphibole) than the Ross River plutonic suite and comprises dominantly biotite granite (Figure 6b) that is salmon-red on outcrop surfaces, medium- to coarse-grained, weakly to strongly deformed, and cut by dark quartz veins in places. It is structurally juxtaposed with the RLGB. Wallace Lake granite has low MS values of $0.088–0.201 \times 10^{-3}$ SI (Table 2). Such low MS may reflect the fact that part of the pluton displays relatively reduced conditions, suggesting either S-type or evolved and reduced I-type affinity. Lithogeochemical and isotopic data (this study) confirms this speculation made by Yang (2014a).

Granitoid rocks in the English River basin

Although the English River basin is underlain predominantly by Neoarchean high-grade metasedimentary rocks, derived gneisses and migmatites (Breaks, 1991), various granitoid suites are intruded into this basin, including the Tooth-Turtle intrusive suite, Black River plutonic suite, Inconnu pluton and Great Falls pluton (labelled 3, 4, 5 and 5' as well as 6, respectively, in Figure 2 and Table 2).

Tooth-Turtle intrusive suite (locality 3)

The Tooth-Turtle intrusive suite (Bailes et al., 2003) is composed dominantly of biotite granite at Tooth Lake, where the

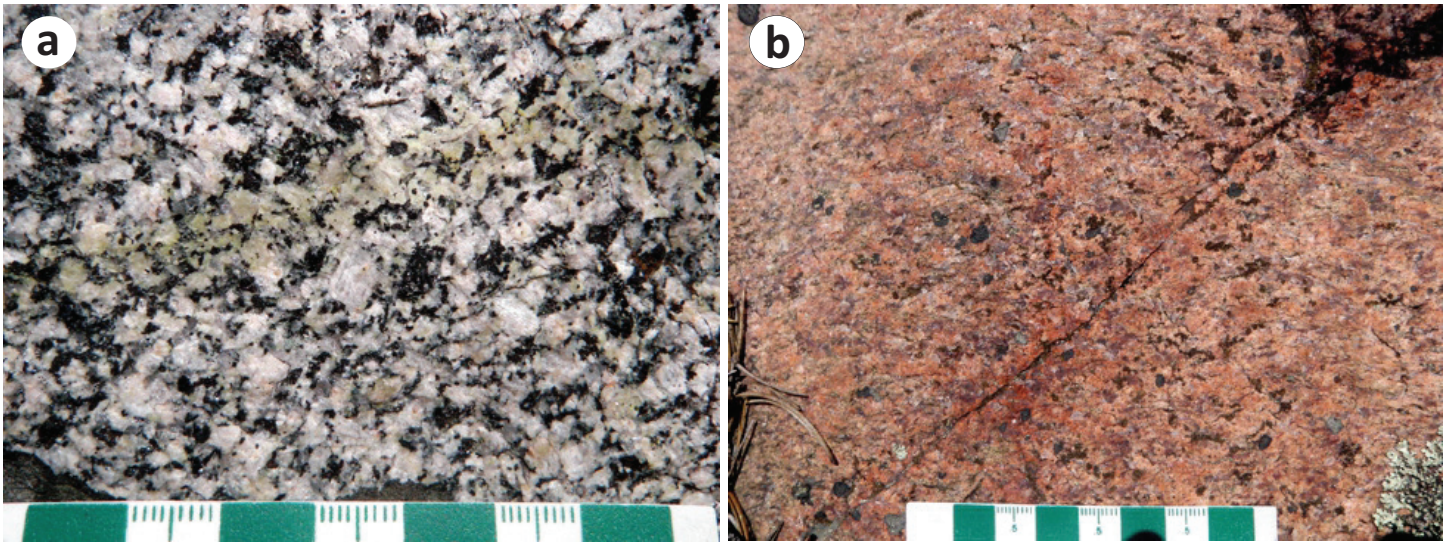

Figure 6: *Field photographs of granitoid rocks from the Rice Lake greenstone belt, Uchi domain, southeastern Manitoba:* ***a)*** *granodiorite with euhedral feldspar phenocrysts, Ross River pluton (UTM Zone 15, 319674E, 5654294N, NAD83);* ***b)*** *salmon-red, medium- to coarse-grained biotite granite, Wallace Lake pluton (UTM 332692E, 5652521N).*

granite is pale grey to whitish, fine- to medium-grained, equigranular and weakly foliated (Figure 7a), and consists of 5–10% biotite, 30–35% quartz and 55–60% feldspar (dominated by K-feldspar, although it is hard to discern it from plagioclase on outcrops). In some places, the granite displays compositional banding, comprising alternating biotite-rich and felsic-rich layers ranging from a few to tens of centimetres in width. Chloritic and sericitic alteration is common. Notably, gossanous patches are ascribed to weathering of sulphide minerals (e.g., pyrite) and/or iron-bearing minerals (e.g., biotite). The granite shows relatively high MS values of 1.24–2.66 × 10^{-3} SI, comparable to the magnetite-series granites of Ishihara (1977, 1981, 2004). Such oxidized features are commonly seen in I-type granites. Pegmatite dikes or ponds, comprising feldspar, quartz and, in places, muscovite and tourmaline, are ubiquitous.

Black River plutonic suite (locality 4)

Granitoid rocks of the Black River plutonic suite vary from diorite, quartz diorite, tonalite and granodiorite to granite, and from massive to foliated or gneissic, suggesting a complex history of tectonomagmatic evolution. A granite sample from this plutonic suite was dated at 2663 ±7 Ma by Turek et al. (1989) using U-Pb zircon geochronology. At outcrop scale, gneissic granodiorite to tonalite is cut by grey quartz diorite, which is, in turn, cut by pinkish to pinkish-grey, equigranular granodiorite and locally by leucogranite. Pinkish gneissic granodiorite is medium- to coarse-grained and consists of 25–30% quartz, 30–35% K-feldspar, 10–15% plagioclase, 20–25% amphibole and 5–10% biotite (Figure 7b). However, ferromagnesian mineral content varies, with some outcrops containing more abundant biotite (up to 20%) than amphibole. This gneissic granodiorite normally shows very high MS values of up to 9.85 × 10^{-3} SI, suggesting a strongly oxidized magnetite-series granite that is comparable to I-type in terms of mineral assemblage.

Some garnet-muscovite-biotite granodiorite, medium- to coarse-grained, deformed as shown by undulatory quartz grains, is composed of 30–35% quartz, 40–45% plagioclase that displays sericitic alteration and non-zonation in composition, and 15–20% microcline with Carlsbad twinning and perthitic lamellae, some showing weak clay alteration; 5% dark brown Fe-rich biotite, minor to 2% muscovite and minor garnet along some fractures showing biotite/chloritic alteration or replacement (Figure 7c, d). This granodiorite displays a very low MS value of 0.050 × 10^{-3} SI (Table 2), consistent with ilmenite-series S-type formed under relatively reduced conditions (e.g., Yang et al., 2008, 2021).

Grey, massive, equigranular, fine- to medium-grained tonalite is also present in the Black River plutonic suite and comprises 20–25% quartz, 45–50% plagioclase, 15–20% amphibole, 10–20% biotite and minor K-feldspar. On many outcrops, massive tonalite is cut by pinkish, massive, equigranular, medium- to coarse-grained granite. Both tonalite and granite exhibit high MS values of 6.973–7.140 × 10^{-3} SI, typical of magnetite-series or I-type granites.

Inconnu pluton (locality 5)

The Inconnu pluton (Černý et al., 1981) was partly mapped in the Cat Creek and Cat Lake–Euclid Lake areas by the MGS (Yang et al., 2012, 2013; Yang, 2014a; Yang and Houlé, 2020). The pluton can be subdivided into two portions: Inconnu pluton I (labelled 5 in Figure 2), consisting of TTGs; and Inconnu pluton II (labelled 5’ in Figure 2), comprising gneissic granite and muscovite±garnet granite. The Inconnu pluton I occurs in the area directly north of Inconnu pluton II, as well as in the area north of the north-northwest–trending Cat Lake–Euclid Lake fault zone (Yang and Houlé, 2020). It consists mainly of coarse-grained, locally porphyritic, pinkish-grey granodiorite, granite and minor monzogranite. Some of these granitoid rocks show heterogeneous texture manifested by very coarse-grained to pegmatitic granite with heterogeneous texture that is locally transitional to homogeneous, massive or porphyritic varieties. The massive to weakly foliated granitoid rocks are characterized by a mineral assemblage of quartz-feldspar(s)-amphibole-biotite±muscovite. Late (quartz-feldspar±muscovite) pegmatite dikes are common within these granitoid rocks.

The Inconnu pluton II is confined to a narrow zone that extends from the area north of Euclid Lake northwestward to the area north of the Trans License road, and northwest of Cat Creek (Yang, 2014a; Yang et al., 2019; Yang and Houlé, 2020). Granitoid rocks are gneissic, light grey to grey and medium-grained; the mineral assemblage includes dark brown (Fe-rich) biotite±greenish amphibole±muscovite±garnet. Dark brown biotite stringers (1–3 mm wide) parallel to the foliation locally wrap around feldspar porphyroclasts. Massive to weakly foliated, medium-grained, muscovite-biotite granodiorite (Figure 7e) contains 45–50% microcline, subhedral to anhedral, with plagioclase inclusions, complex cross-hatched twinning (Figure 7f), and myrmekite (Figure 7g) consisting of worm-like quartz in plagioclase in contact with microcline. This suggests that water was saturated when plagioclase and quartz crystallized simultaneously (e.g., Yang and Lentz, 2005; Yang, 2017 and references therein). The muscovite-biotite granodiorite exhibits a very low MS value of 0.048 × 10^{-3} SI (Table 2), which is typical of the ilmenite-series granites of Ishihara (1981, 2004) or the S-type granites of Chappell and White (1974, 1992). Some outcrops of garnet-bearing granite with MS values of up to 0.15 × 10^{-3} SI that intrude magnetite-bearing gabbroic rocks reflect the influence of oxidized wall-rock on the MS of the granites.

Great Falls pluton (locality 6)

The Great Falls pluton (Bailes et al., 2003), well exposed along Provincial Highway 304 (Figure 2), is composed dominantly of gneissic tonalite to granodiorite to granite, which is cut by granodiorite to leucogranite and younger phases of pegmatite and/or aplite dikes. Medium-grained gneissic tonalite normally contains 20–25% quartz (1–3 mm; locally 5–10 mm), 40–50% plagioclase, 30–35% amphibole and up to 5% biotite. Massive, equigranular, medium- to coarse-grained, locally

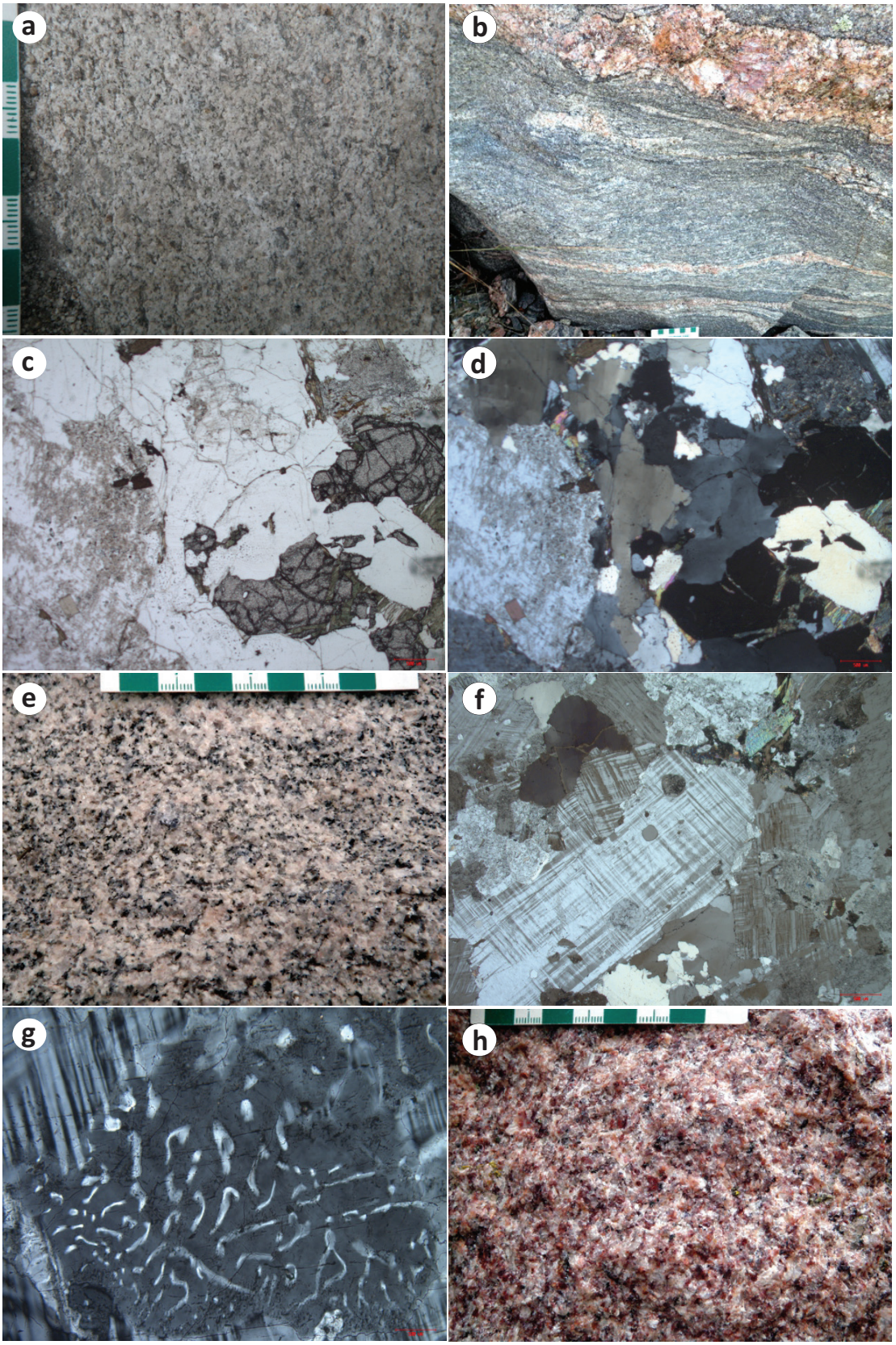

Figure 7: *Field photographs and photomicrographs of granitoid rocks from the English River basin, southeastern Manitoba:* ***a)*** *fine- to medium-grained, weakly foliated biotite granite, Tooth-Turtle intrusive suite (UTM Zone 15N, 337889E, 5623805N, NAD83);* ***b)*** *pinkish-grey, medium- to coarse-grained granodiorite cut by pegmatite dike, Black River plutonic suite (UTM Zone 14N, 699681E, 5627307N, NAD83);* ***c)*** *photomicrograph of medium- to coarse-grained granodiorite containing garnet, biotite and minor muscovite (UTM 329440 E, 5616894N), sample 111-14-232A01 from the Black River plutonic suite, plane-polarized light;* ***d)*** *the same view as (c) under cross-polarized light (XPL);* ***e)*** *weakly deformed, medium-grained muscovite-biotite granodiorite (UTM 313105E, 5613708N), Inconnu pluton II;* ***f)*** *photomicrograph of complex cross-hatched twinning of microcline (K-feldspar) with plagioclase inclusions, sample 111-14-15A01 (same location as [e]), XPL;* ***g)*** *photomicrograph of myrmekite, sample 111-14-15A01 (same location as [e]), XPL;* ***h)*** *pink to red, coarse-grained leucogranite (UTM Zone 14, 704262E, 5613042N, NAD83), Great Falls pluton.*

porphyritic granodiorite consists of 25–30% quartz, 30–35% plagioclase, 10–15% K-feldspar, 20–25% amphibole and up to 5% biotite. Leucogranite is coarse-grained and pink; it consists of 30–35% quartz, 60–65% K-feldspar, minor plagioclase (<5%) and 2–5% biotite (Figure 7h). The tonalite displays high MS values of 8.86–24.8 × 10^{-3} SI, whereas leucogranite has a lower MS value of 0.533 × 10^{-3} SI (Table 2). The MS values indicate that the Great Falls pluton is attributed largely to magnetite-series and I-type granite.

Granitoid rocks in the Bird River greenstone belt

Granitoid rocks in the Bird River greenstone belt (BRGB) that have been recently re-mapped and described by the MGS (Gilbert et al., 2008; Yang et al., 2012, 2013, 2019; Yang, 2014a; Yang and Houlé, 2020) include the Maskwa Lake batholith (Bailes et al., 2003), Marijane Lake pluton, Tin-Osis lakes intrusion, Birse Lake pluton, and sanukitoids (labelled 7, 8, 8', 9, and 9', respectively, in Figure 2 and Table 2). It was noted that sanukitoid rocks occur as small dikes and stocks (Gilbert et al., 2008) that are too small to show in Figure 2, but the UTM locations of the representative samples are shown in DRI2022001. The granitoid rocks are part of the TTGs and represent either the basement of the Neoarchean BRGB (i.e., Maskwa Lake batholith I) or younger plutons (i.e., Maskwa Lake batholith II, Marijane Lake pluton, Birse Lake pluton, Tin-Osis lakes intrusion, sanukitoids) that have intruded and disrupted the supracrustal rocks of the belt. The latter consist of mafic volcanic and synvolcanic intrusive rocks, epiclastic and minor volcaniclastic rocks, and mafic–ultramafic intrusions.

The Mesoarchean granitoid basement represented by the Maskwa Lake batholith I consists mainly of coarse-grained, equigranular, locally gneissic granodiorite, which was intruded, fragmented and brecciated by mid-ocean–ridge basalt (MORB) at the contact zone south of the Cat Creek area (Figure 8a). These rocks display moderate to high MS values of 0.585–2.580 × 10^{-3} SI, similar to those of normal oxidized magnetite-series (Ishihara, 1981) and I-type granites elsewhere (Yang, 2014a; Yang et al., 2008, 2021). Granitoid rocks from the Maskwa Lake batholith I dispay differentiated rare-earth element (REE) patterns with very small negative (or no) Eu anomalies, and small negative Ti anomalies and pronounced negative Nb anomalies in spider diagrams, consistent with those formed in magmatic-arc setting (Yang and Gilbert, 2014; Yang and Houlé, 2020; this study).

Maskwa Lake batholith (locality 7)

The Maskwa Lake batholith I, dated at 2782 ±11 Ma to 2844 ±12 Ma (Wang, 1993) and 2852.8 ±1.1 Ma (Gilbert et al., 2008), is a granodioritic basement intrusion that is geochemically indistinguishable from a younger TTG phase, i.e., the Maskwa Lake batholith II dated at 2725 ±6 Ma (Wang, 1993) cutting the older granodiorite. The younger phase (Figure 8b), which ranges from diorite to tonalite, trondhjemite, granodiorite and granite, intruded mid-ocean–ridge basalt (MORB) that was cut by the Mayville mafic–ultramafic intrusion (2742.8 ±0.8 Ma; Houlé et al., 2013) and the Bird River sill (2743.0 ±0.5 Ma; Scoates and Scoates, 2013). These granitoid rocks have variable MS values of 0.28 to 11.70 × 10^{-3} SI, consistent with magnetite-series and I-type granites. It is noted that some biotite granite outcrops have MS values as low as 0.044 × 10^{-3} SI (Table 2), consistent with evolved I-type granites that exhibit an ilmenite-series signature.

Porphyritic quartz diorite and two-feldspar porphyry are cut by a fine-grained, east-trending gabbro dike, up to 15 m wide, in the southern part of the Maskwa Lake batholith II (labelled 7 in Figure 2). The porphyry is interpreted as a late-stage stock resulting from arc magmatism. It is weekly foliated, contains both plagioclase and K-feldspar phenocrysts, and shows strong sericitic and chloritic alteration; no mafic minerals are discernible in outcrop (Figure 8c). In thin section, orthoclase and plagioclase phenocrysts are up to 10% in fine-grained groundmass consisting of plagioclase, biotite, amphibole, quartz, magnetite and disseminated pyrite (Figure 8d). The orthoclase phenocrysts display erosional edges, are subhedral to euhedral, up to 4.5 mm in length, contain amphibole and biotite inclusions, and are commonly altered to sericite, epidote, and locally to carbonate. This rock shows recrystallization in both groundmass and margins of orthoclase phenocrysts, with very fine-grained plagioclase clusters surrounding the phenocrysts that also display sericite, epidote, or carbonate alteration (Figure 8d).

The TTGs in the BRGB may have been formed in a magmatic-arc setting and therefore have notable potential for porphyry Cu-(Au) mineralization (e.g., Cat Lake–Euclid Lake) associated, for example, with granitoid phases that exhibit potassic alteration. Skarn-type Cu-Au-Ag mineralization is also evident in this area (e.g., Cat Lake; Yang et al., 2013). Lode Au mineralization has been observed in shear zone(s) cutting the central part of the Maskwa Lake batholith (e.g., Little Bear Lake; Kretschmar and McBride, 2015).

Strongly peraluminous granitoid rocks (with muscovite ±garnet and biotite as the dominant ferromagnesian minerals) postdate the TTGs and, together with associated rare-metal–bearing pegmatite intrusions, may have been emplaced during continental collision subsequent to plate subduction (Yang et al., 2013, 2019; Yang and Gilbert, 2014; Yang, 2014a, b). The north-northwest–trending Cat Lake–Euclid Lake shear zone is confined to gneissic, peraluminous granitoid rocks, as well as strongly foliated and mylonitic granitoid rocks. The youngest granitoid intrusive phase is represented by porphyritic sanukitoid-type rocks that occur as dikes, sills or small stocks (Table 2) cutting both supracrustal and granitoid rocks in the belt. These high-Mg rocks display enrichment in both large-ion lithophile and siderophile elements, and show highly fractionated REE patterns with marked heavy REE depletion; the intrusions may have been derived from partial melting of subcontinental lithospheric mantle metasomatized previously by subduction-related components, associated with the collapse of a thickened orogen (Yang and Gilbert, 2014; Yang et al., 2019).

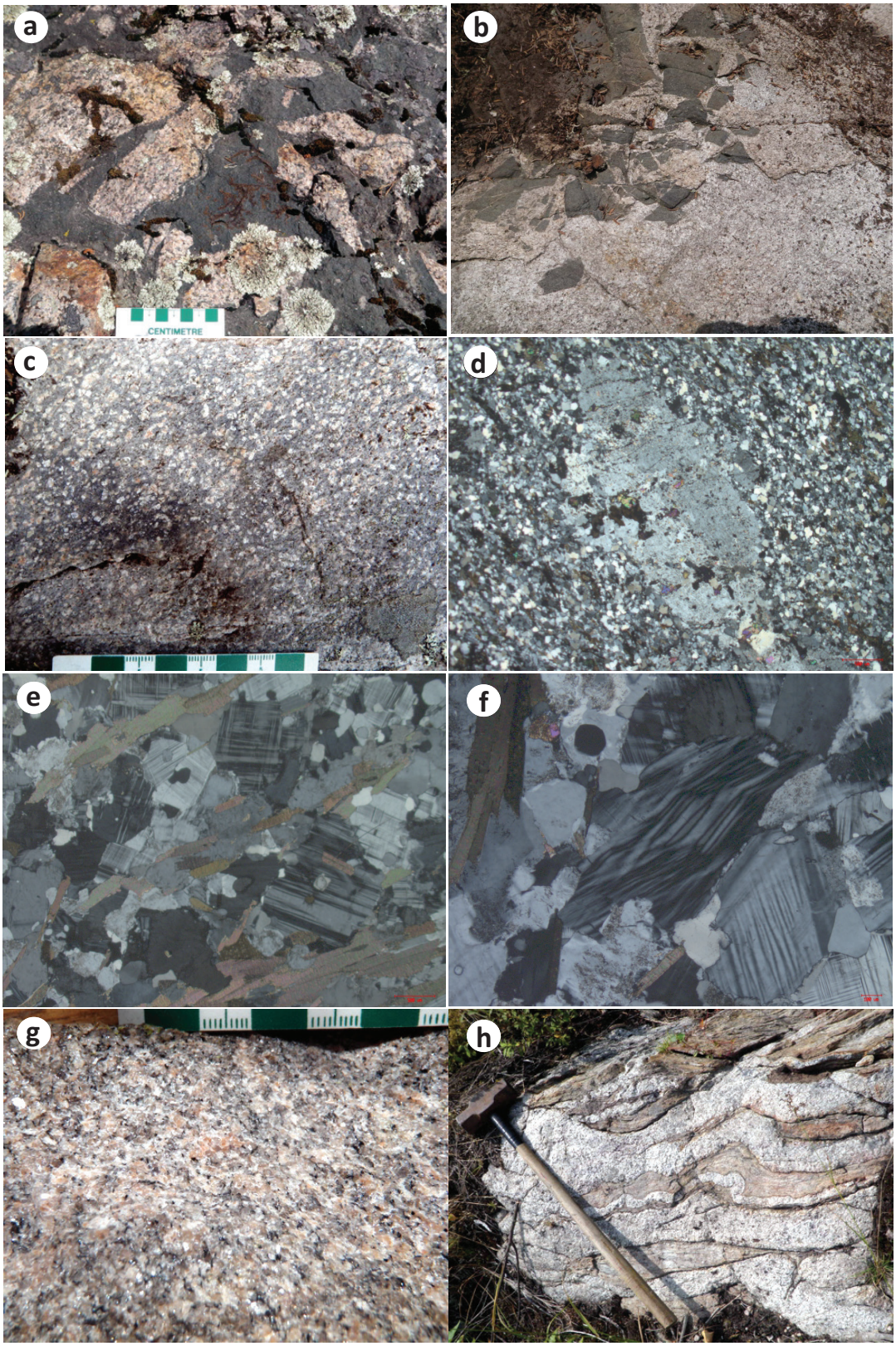

Figure 8: *Field photographs and photomicrographs of granitoid rocks from the Bird River greenstone belt, southeastern Manitoba:* ***a)*** *coarse-grained granodiorite fragmented and brecciated by MORB-type basalt, Maskwa Lake batholith I (UTM Zone 15N, 315328E, 5608468N, NAD83);* ***b)*** *medium-grained granodiorite in the Maskwa Lake batholith II intruding very fine-grained MORB-type basalt and containing basalt fragments (UTM 317746E, 5160077N), width of view is about 1.5 m;* ***c)*** *two-feldspar porphyry, Maskwa Lake batholith II (UTM 324786E, 5597364N);* ***d)*** *photomicrograph of the two-feldspar porphyry shown in (c);* ***e)*** *photomicrograph of gneissic granodiorite, showing biotite laths aligned along foliation (dextral shear sense), Marijane pluton, sample 111-14-200A01 (UTM 346068E, 5589895N), under cross-polarized light (XPL);* ***f)*** *photomicrograph of kinked Albite twinning in plagioclase, sample 111-14-200A01, XPL;* ***g)*** *undeformed, medium-grained, muscovite-biotite granodiorite, Marijane pluton (UTM 343875E, 5587802N);* ***h)*** *medium-grained, muscovite-biotite granite dikes and veins cutting cordierite porphyroblast–bearing greywacke (UTM 343421E, 5585389N), Tin-Osis lakes intrusion. Abbreviation: MORB, mid-ocean–ridge basalt.*

Marijane Lake pluton (locality 8)

The Marijane Lake pluton (labelled 8 in Figure 2) is unique in the BRGB for containing both biotite granodiorite (2645.6 ±1.3 Ma; Gilbert et al., 2008) and muscovite-biotite granodiorite to granite, although their cutting relationship was not observed in outcrops. The biotite granodiorite is medium- to coarse-grained and equigranular to gneissic, and comprises 25–30% quartz, 20–30% K-feldspar, 20–35% plagioclase, 10–20% biotite and minor or no amphibole (<5%). Gneissic texture is manifested by 5–10% biotite laths aligned along foliation, (dextral shear sense), wrapping around subhedral to anhedral plagioclase (20–25%; some displaying sericite alteration) with Albite twinning, anhedral microcline (25–30%) displaying typical cross-hatched twining, and anhedral quartz (25–30%) showing undulose extinction (Figure 8e). Some Albite twinning shows kinked bands (Figure 8f). It displays MS values of 0.251–1.90 × 10^{-3} SI, consistent with magnetite-series and I-type granites. In contrast, the two-mica granodiorite contains up to 5% muscovite and is massive, equigranular and medium- to coarse-grained in most outcrops (Figure 8g), and displays consistently very low MS values of 0.035–0.088 × 10^{-3} SI (Table 2), typical of ilmenite-series and S-type granites.

Tin-Osis lakes intrusion (locality 8')

Granite to pegmatitic granite in the Tin Lake and Osis Lake area (Drayson, 2016), termed the Tin-Osis lakes intrusion (labelled 8' in Figure 2; Table 2; see Yang et al., 2019), contains up to 10% muscovite and minor pink garnet, and is massive, equigranular and medium- to coarse-grained in most outcrops, and displays consistently very low MS values (0.037–0.047 × 10^{-3} SI; Table 2), typical of reduced ilmenite-series and S-type granites.

It is noted that medium-grained muscovite-biotite (±garnet) granite intruding the Booster Lake Formation (2712 ±17 Ma; Gilbert et al., 2008) metasedimentary rocks contains cordierite porphyroblasts (Gilbert et al., 2008; Yang, 2014a); both are deformed and folded (Figure 8h). The presence of metasedimentary xenoliths in the muscovite-bearing granite, together with its low MS values and the cordierite-bearing metasedimentary country rocks, suggests that the redox conditions of the granite intrusion may have been influenced by the wallrock composition to some extent, although they are considered to be largely inherited from the source rocks (cf. Ishihara, 1981, 2004).

The Tin-Osis lakes granite contains 30–35% subhedral to euhedral K-feldspar, 25–30% anhedral quartz, 25–30% subhedral plagioclase, 5–10% euhedral to subhedral muscovite, and in some cases, up to 5% euhedral to subhedral, brown to green biotite. The granite has an inequigranular texture in which the major rock-forming minerals range from 0.5 to 5 mm in length. The quartz crystals often display undulatory extinction, suggesting that these rocks have been variably deformed. The K-feldspar grains often display Tartan twinning, indicative of microcline. The plagioclase grains display Albite twinning, which in some cases taper indicative of weak deformation. Accessory minerals include biotite, garnet, cordierite, apatite, ilmenite, monazite, zircon, and gahnite ($ZnAl_2O_4$; Yang et al., 2019). Garnet commonly contains inclusions of quartz and muscovite, and biotite usually contains monazite and/or zircon inclusions that display radiation halos.

Some parts of the Tin-Osis lakes intrusion can be termed leucogranite as they contain less than 5% ferromagnesian minerals (Drayson, 2016; Yang et al., 2019). These leucogranites are characterized by the presence of muscovite, garnet, sillimanite and tourmaline. The leucogranites are medium-grained, equigranular, and consists of 30% subhedral K-feldspar (1–5 mm), 30% anhedral quartz (1–2 mm), 25% euhdral to subhedral plagioclase (1–5 mm), 10% euhedral muscovite (1–2 mm), and up to 3% euhedral garnet (2–5 mm). Accessory minerals include ilmenite, biotite, gahnite, ±sillimanite, and ±tourmaline. Gahnite is absent, unless biotite is present; they almost exclusively occur together (Yang et al., 2019). Where sillimanite is present, it commonly occurs with muscovite as a halo surrounding euhedral garnet crystals. Locally, sillimanite alters to muscovite. Where tourmaline is present, it occurs as large discrete crystals, or as inclusions in garnet. Notably, larger K-feldspar crystals contain inclusions of euhedral, sericitized feldspars and muscovite. At the contact with metasedimentary rock (greywacke), there is exclusively biotite in the metasedimentary rock and abundant muscovite in the granite.

Birse Lake pluton (locality 9)

The Birse Lake pluton (labelled 9 in Figure 2) was dated at 2723.2 ±0.7 Ma (Gilbert et al., 2008). This pluton varies in lithologies from quartz diorite to tonalite, granodiorite, muscovite-bearing granite and garnet-bearing granite. Texturally, both equigranular and porphyritic varieties are evident in the tonalite and granodiorite, and massive and foliated varieties are present. The strongly peraluminous muscovite- and garnet-bearing granites are mostly present in the eastern end of the pluton, where it was emplaced into metasedimentary rocks. However, such strongly peraluminous phases appear absent in the western end, where rare-metal pegmatite deposits occur (e.g., Tanco; Gilbert et al., 2008, 2013). Deformed, coarse-grained, porphyritic granodiorite displays moderate MS values of 0.155–1.51 × 10^{-3} SI (Table 2) and consists of 30–35% quartz, 30–35% K-feldspar, 20–25% plagioclase and 20–25% amphibole. Locally, inclusions of fine-grained, dark mafic rock are evident in the granodiorite. Together with the MS values, it suggests that the western portion of the pluton is of magnetite-series and I-type, which may be favourable for Cu-Au mineralization (e.g., Blevin, 2004; Ishihara, 2004). The garnet/muscovite granite has very low MS values of 0.036–0.085 × 10^{-3} SI (Table 2), consistent with ilmenite-series and S-type granites that are favourable for rare-metal and/or Sn-W mineralization (Chappell and White, 1974, 1992; Ishihara, 1977, 1981, 2004; Yang et al., 2019). Coexistence of different petrogenetic types of granitoid rocks in the Birse Lake pluton is worthy of further study, and may provide new clues regarding the source and origin of the Tanco pegmatites (e.g., Martins and Kremer, 2012).

Bird River sanukitoid rocks (label 9')

The Bird River sanukitoid-type rocks labelled as 9' in Table 2 are porphyritic and occur mostly as dikes, sills or small stocks that are too small to show in Figure 2. They cut both the supracrustal and granitoid rocks in the BRGB. Gilbert et al. (2008) noticed that the sanukitoid rocks are characterized by the presence of subhedral to euhedral plagioclase, K-feldspar and hornblende phenocrysts that account for 40 to 50% and are embedded in a finer groundmass of feldspar, amphibole, biotite, chlorite, quartz, Fe-Ti oxide minearals, and ±quartz.

Granitoid rocks in the Winnipeg River domain

Lac du Bonnet batholith (locality 10)

Although part of the Lac du Bonnet batholith (labelled 10 in Figure 2) extends into the BRGB, most of it is considered part of the Winnipeg River domain. This batholith, dated at 2660 ±3 Ma (Wang, 1993), may represent a stitching intrusion that welded the adjacent tectonic blocks of the BRGB and Winnipeg River domain (Yang, 2014a; Yang et al., 2019).

The Lac du Bonnet batholith (Černý et al., 1981) is a composite pluton, dominated by pinkish, medium- to coarse-grained granodiorite, granite and leucogranite with minor quartz diorite and monzonite, that is cut by late simple pegmatite dikes (comprising quartz–K-feldspar±biotite±muscovite) without notable internal metasomatism. Biotite granite is pinkish, massive, medium- to coarse-grained and equigranular, and typically contains 25–30% quartz, 45–50% K-feldspar, 10–15% plagioclase and 10–15% biotite (Figure 9a). Some of the K-feldspar crystals locally occur as phenocrysts up to 1.5 cm in length. Compared to the biotite granite, leucogranite (Figure 9b) has higher quartz (30–35%) and K-feldspar (up to 60%), but low biotite (5–10%) and minor plagioclase (<5%). Notably, biotite granite has higher MS values (up to 19.4 × 10^{-3} SI) than leucogranite (up to 5.0 × 10^{-3} SI), but both fall in the field of magnetite-series and normal I-type granites. Goad and Černý (1981) suggested that the biotite granite and leucogranite were unrelated in origin because of distinctively different rare-earth element patterns. Some evolved biotite granite displays MS values as low as 0.044 × 10^{-3} SI (Table 2), consistent with reduced I-type granites that exhibit the ilmenite-series signature.

Pointe du Bois batholith (locality 11)

The Pointe du Bois batholith (labelled 11 in Figure 2) in the Winnipeg River domain consists mainly of gneissic tonalite, granodiorite and granite, although massive equigranular granitoid rocks dated at 2729 ±8.7 Ma (Wang, 1993) are also present. In outcrops, the gneissic tonalite to granodiorite is commonly cut by pinkish-grey, equigranular biotite granite (Figure 9c). In places, it is also cut by mafic dikes up to 1 m thick, but often contains subrounded to angular gabbroic xenoliths. Pinkish pegmatite-aplite dikes commonly crosscut the gneissic tonalite to granite. Both the gneissic and massive granitoid rocks display relatively high MS values of 1.49–18.0 × 10^{-3} SI, although some highly evolved leucogranite has MS values as low as 0.089 × 10^{-3} SI. It is noted that an exposure of grey gneissic tonalite has exceptionally high MS values of up to 45.7 × 10^{-3} SI (Table 2). This gneissic tonalite is medium-grained and magnetic, consisting of biotite-rich layers alternating with felsic layers ranging from several to tens of centimetres in width (Figure 9d). The biotite-rich layers contain 1–5% magnetite, and minor amphibole. A dark grey, fine-grained gabbro dike cuts the gneissic tonalite and is cut by pink pegmatitic granite dikes. Generally, these granitoid rocks with varied amounts of amphibole (10–25%) and biotite (5–15%) are comparable to the magnetite-series granites of Ishihara (1977, 1981, 2004) and I-type granites of Chappell and White (1974, 1992) in terms of their MS values and mineral assemblages.

Rennie River plutonic suite (locality 12)

The Rennie River plutonic suite (labelled 12 in Figure 2) is composed of many lithologies from tonalite to granodiorite to granite, with textures ranging from porphyritic to seriate, equigranular and gneissic. At the south margin, it contains garnet-muscovite–bearing granite cut by biotite (±muscovite±tourmaline)-quartz-feldspar pegmatite dikes. Pinkish, massive, porphyritic granodiorite comprises 30–35% K-feldspar phenocrysts that are euhedral to subhedral and 2–3 cm in length, together with a few quartz phenocrysts up to 2 cm in size, in a medium- to coarse-grained groundmass of quartz, K-feldspar, plagioclase and biotite (Figure 9e). In some outcrops, the porphyritic granodiorite varies to seriate textures and is cut by fine- to medium-grained, pinkish massive granite. It was noted that most of the granitoid rocks in this plutonic suite display consistently high MS values of 1.13–34.5 × 10^{-3} SI (Table 2), typical of magnetite-series and I-type granites.

The Rennie River plutonic suite contains garnet-muscovite–bearing granodiorite to granite at its southern margin; the distribution of these strongly peraluminous granites coincides with the southern boundary of the Winnipeg River domain. The granodiorite is pale greyish-white to pinkish-grey on fresh surface, massive and equigranular, and consists of 30–35% quartz, 40–45% K-feldspar, 20–25% plagioclase, 5% biotite, minor muscovite and up to 1% garnet (Figure 9f). It has a very low MS value of 0.045 × 10^{-3} SI (Table 2), consistent with ilmenite-series (Ishihara, 1977, 1981, 2004) and S-type granites (Chappell and White, 1974, 1992) and reflecting relatively reduced conditions of emplacement (cf. Blevin, 2004). W. Mandziuk (pers. comm., 2014) considered that the garnet-bearing granitoid rocks were formed from granite magmas contaminated by metasedimentary rocks. Elongated and folded greywacke xenoliths are present in the granite, which is cut by pinkish pegmatite dikes that also contain notable garnet and muscovite.

Halden et al. (2007) dated zircon crystals with sector zonation from the Caddy Lake granite, and obtained an age of emplacement of 2687 ±7 Ma. This granite could be part of the Rennie River plutonic suite (Yang, 2014a; Yang et al., 2019).

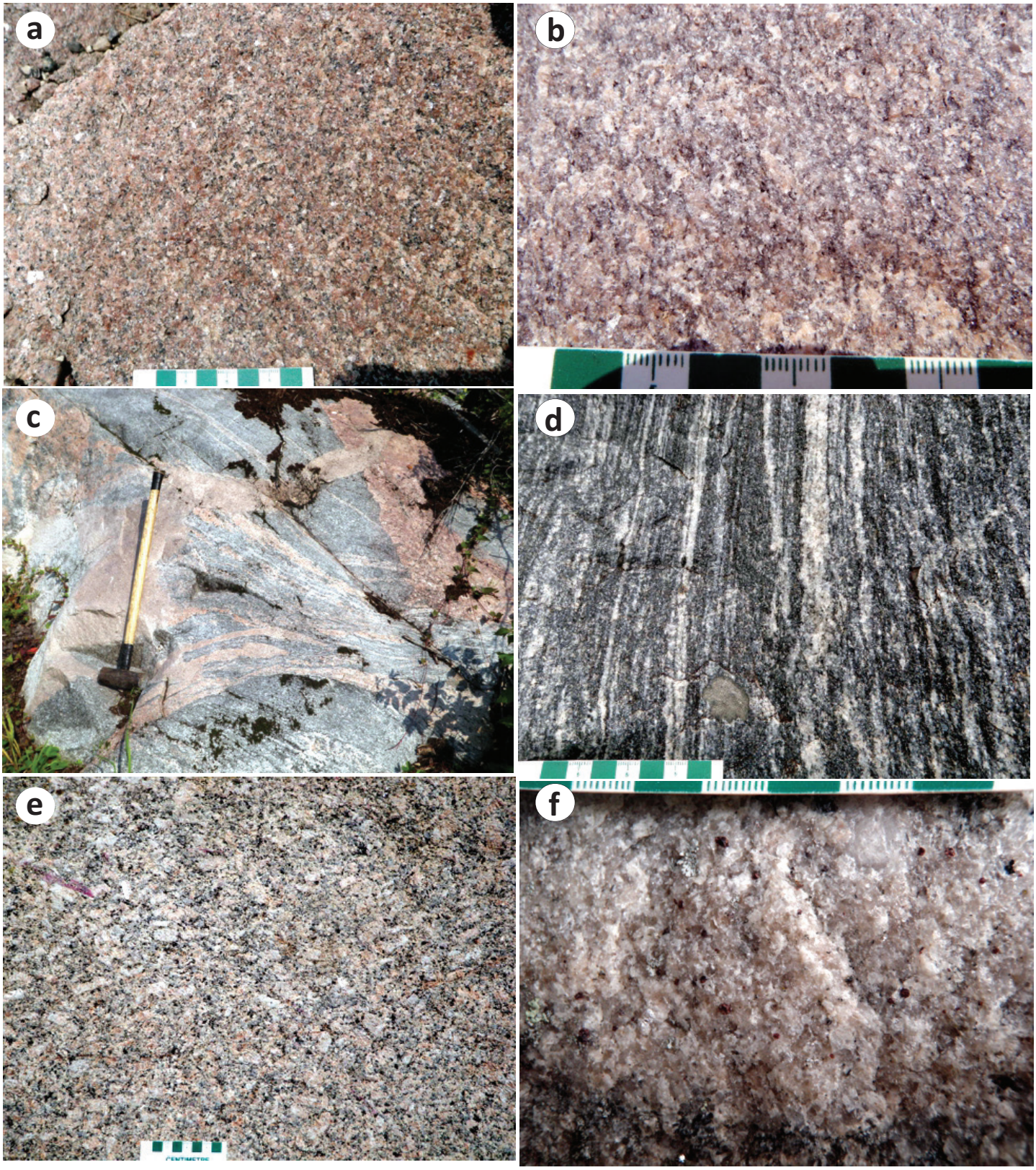

***Figure 9**: Field photographs of granitoid rocks from the Winnipeg River domain, southeastern Manitoba: **a)** pink, medium-grained biotite granite, Lac du Bonnet batholith (UTM Zone 15N, 301921E, 5578488N, NAD83); **b)** medium-grained leucogranite, Lac du Bonnet batholith (UTM 304788E, 5579115N); **c)** grey, medium-grained, gneissic tonalite cut by pink biotite granite, Pointe du Bois batholith (UTM 319078E, 5572003N); **d)** grey, medium-grained, gneissic tonalite (with very high MS values of up to 45.7 × 10^{-3} SI), showing gneissic fabrics consisting of alternating biotite-rich and felsic layers, Pointe du Bois batholith (UTM 294166E, 5559908N); **e)** pink porphyritic granodiorite with megacrystic K-feldspar as phenocrysts, Rennie River plutonic suite (UTM 313534E, 5553590N); **f)** medium-grained, massive, garnet-bearing granite, Rennie River plutonic suite (UTM 339676E, 5516634N).*

Big Whiteshell Lake pluton (locality 13)

The Big Whiteshell Lake pluton (labelled 13 in Figure 2) is dominated by granodiorite and granite, although tonalite and quartz diorite also occur locally. In terms of texture, massive, equigranular and foliated to gneissic varieties are present. Granitoid rocks in this pluton are characterized by high MS values of up to 62.4 × 10^{-3} SI (Table 2), typical of magnetite-series granites and reflecting oxidized conditions of emplacement (Ishihara, 1981, 2004; Blevin, 2004). They are ascribed to I-type granites of Chappell and White (1974, 1992), based on the presence of amphibole and biotite and the absence of aluminous silicates (i.e., muscovite, garnet, cordierite).

Granitoid rocks in the Wabigoon domain

Whitemouth Lake pluton (locality 14)

The Whitemouth Lake pluton (labelled 14 in Figure 2) is sporadically exposed in the Wabigoon domain of southeastern Manitoba. A Rb-Sr isochron age of 2664 ±50 Ma was interpreted to represent its minimum age of intrusion (Manitoba Geological Survey, 2006). This large batholith consists of massive granodiorite to granite and, in places, gneissic tonalite and granodiorite. At outcrop scale, multiple phases of granitoid rocks coexist and are cut by pink pegmatite (Figure 10a). Pinkish, fine- to medium-grained leucogranite, consisting of 35–40% quartz, 55–60% K-feldspar, 1–5% biotite and minor plagioclase, occurs in places. Notably, the leucogranite or alkali-feldspar granite shows high MS values of up to 13.5 × 10^{-3} SI. In addition, on the northern margin of the pluton, gneissic muscovite-garnet-biotite granite intrudes a grey foliated tonalite phase that shows moderate MS values of 3.28 × 10^{-3} SI (Table 2), consistent with the magnetite-series granites of Ishihara (1981, 2004). However, such strongly peraluminous granite is typical of S-type in terms of the presence of muscovite and garnet (up to 1%), suggesting that the redox condition of this S-type granite may have been buffered by oxidized wallrocks. Alternatively, however, the presence of primary pyrrhotite in the granite may explain its relatively high MS value, suggesting that the redox condition of this S-type granite magma could be reduced to have formed sulphide-saturated magma (e.g., Yang, 2012; Yang et al., 2019).

Falcon Lake intrusive complex (locality 15)

The Falcon Lake intrusive complex (FLIC; labelled 15 in Figure 2) is a composite, layered and compositionally zoned intrusion that intrudes the Wabigoon domain. Mandziuk et al. (1989) demonstrated that the FLIC is an Archean composite intrusion comprising gabbroic rocks, diorite, granodiorite and quartz monzonite with complex internal contacts. Halden et al. (2007) retrieved zircon grains with typical sector zoned cores and mantled by oscillatory zoned overgrowths from three major phases of FLIC, suggestive of their crystallization from magmas. Halden et al. (2007) used laser-ablation inductively coupled plasma–mass spectrometry to date the zircons and obtained U-Pb ages of emplacement (or crystallization) for the FLIC between 2733 ±15 Ma and 2723 ±9 Ma, suggesting a product of Neoarchean magmatism. New data acquired by this study for three fractions of zircon recovered from a monzogranite (sample 111-14-283A01) are concordant to variably discordant and define a well-constrained chord, suggesting only recent Pb-loss and yielding a weighted average $^{207}Pb/^{206}Pb$ age of 2695.74 ±0.95 Ma (or 2696 ±1 Ma; mean square of weighted deviates = 0.99, P = 0.37). These geochronology data suggest a complexity of the FLIC which several episodes of granitoid magmatism between ca. 2733 Ma and 2696 Ma.

The quartz monzonite in the FLIC occurs in the core of the complex and is massive and medium-grained, locally with a few euhedral K-feldspar phenocrysts up to 2.2 cm in length

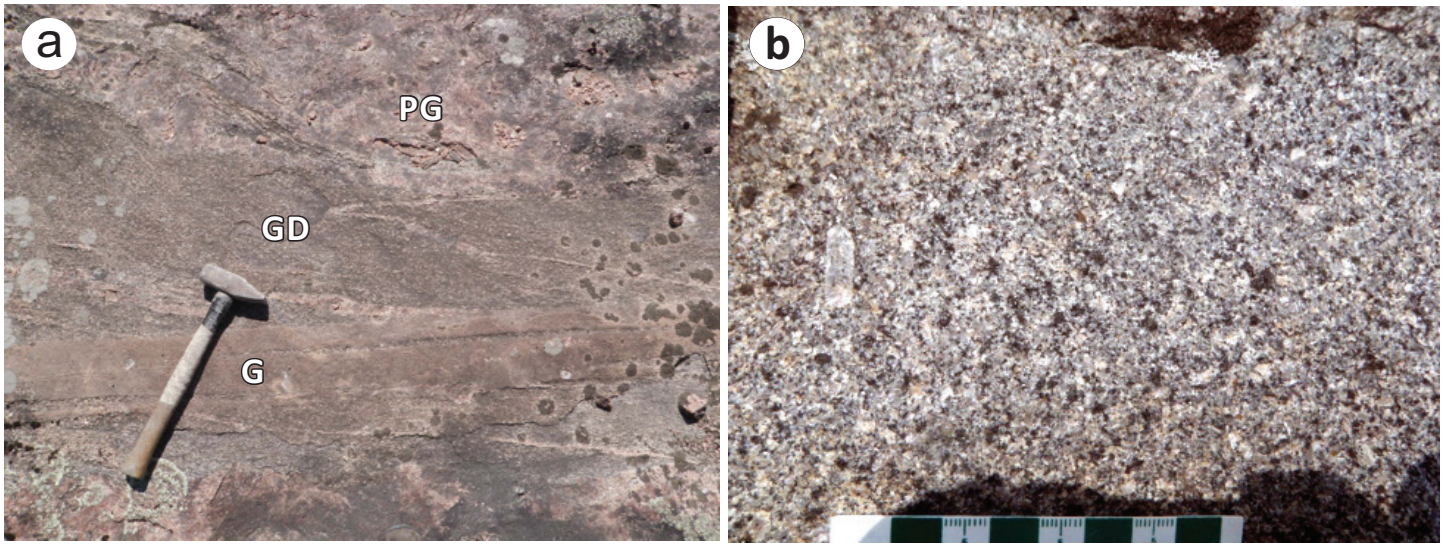

Figure 10: *Field photographs of granitoid rocks from the Wabigoon domain, southeastern Manitoba:* ***a)*** *granodiorite (GD) cut by fine-grained granite (G) and pegmatitic granite (PG), Whitemouth Lake pluton (UTM Zone 15N, 318467E, 5479806N, NAD83);* ***b)*** *medium-grained quartz monzonite with a few euhedral K-feldspar phenocrysts, Falcon Lake intrusive complex (UTM 337410E, 5511611N).*

(Figure 10b); this rock contains 30–35% hornblende, 30–40% plagioclase, 20–25% K-feldspar and 5–10% quartz. The quartz monzonite has a moderately high MS value of 11.7 × 10^{-3} SI. Notably, sulphide-bearing breccia pipes, occurring in the quartz monzonite or along the contact between quartz monzonite and granodiorite, are interpreted to have formed from a late volatile-rich phase of this igneous complex (Mandziuk et al., 1989).

Discussion

Archean granitoid rocks of the western Superior province in southeastern Manitoba exhibit variable mineral assemblages, fabrics and MS values, and thus can be ascribed to different petrogenetic types, e.g., magnetite-series versus ilmenite-series (Ishihara, 1977, 1981, 2004) and I-type versus S-type (Chappell and White, 1974, 1992, 2001) as described above. No A-type granitoids have yet been identified (Yang and Houlé, 2020). Generally, the field and petrological features of granitoid rocks are a function of the interplay between magma sources, tectonic settings, magmatic processes and erosion levels (e.g., Blevin and Chappell, 1995; Pearce, 1996; Blevin, 2004; Yang, 2007, 2017; Yang et al., 2008, 2011), which are reflected also in their temperatures, pressures, chemical and isotopic compositions, and redox conditions of formation (i.e., fO_2). Field relationships established by reconnaissance mapping can provide important constraints for the evaluation of petrogenesis and metallogeny of granitoid rocks in southeastern Manitoba.

Although MS measurements provide a first-order means of screening different petrogenetic types of granitoid rock in the field, detailed investigations of petrography, petrology and lithogeochemistry provide more information about magmatic processes, emplacement conditions and metallogeny. Blevin (2004) suggested that metallogenic potential of granitoid rocks could be assessed by investigation of their geochemical characteristics, degree of compositional evolution, degree of fractionation and oxidation state. These parameters are largely controlled by the precursors of the granitoid rocks (Chappell and White, 1974, 2004; Ishihara, 1977, 1981, 2004), petrogenetic processes and geodynamic settings responsible for their formation (Pearce et al., 1984; Whalen et al., 1987, 2004). The most important factor is their oxidation state, which greatly affects the geochemical behaviour of metals in their derivative magmas. The criteria summarized in Table 1 can be used for identification of relatively reduced and oxidized granitoid rocks in the field.

A major finding of this study in the western Superior province (southeastern Manitoba) is that S-type granites occur in or nearby terrane boundary zones, indicating that S-type granite can be used as a geological marker for collisional zones between tectonic blocks (Yang, 2014a; Yang et al., 2019). More importantly, rare-metals (Li, Cs, Ta, Nb, Be) mineralization hosted in granitic pegmatites (i.e., Tanco) are genetically associated with S-type granite intrusions.

Superior boundary zone and the Munro Lake and Molson Lake domains

Granitoid rocks from the Superior boundary zone (SBZ), including parts of the Thompson nickel belt, Split Lake block and Assean Lake domain (Figures 1, 3), are briefly described below, focusing on the Fox Lake pluton, Assean Lake, Orr Lake and Jock Lake intrusions (localities 16–19, respectively, in Table 2 and Figure 3), as well as the Ospwagan Lake intrusion, Paint Lake pluton, Grass River pluton, Setting Lake pluton, and Kiski Lake intrusion (localities 20–24, respectively, in Table 2 and Figure 4) in the Thompson nickel belt as part of the SBZ. To the southeast of the SBZ, granitoid bodies emplaced into the Munro Lake and Molson Lake domains include the Jenpeg Dam intrusion, Nelson River pluton, and Paimusk Creek intrusion (localities 25, 26 and 26', respectively, in Table 2 and Figure 4). Details about the nature and geological history of the SBZ, as well as its interaction with the Trans-Hudson orogen, were discussed in many papers (e.g., Böhm et al., 1999, 2003; Corkery, 1985; Corkery et al., 2000; Zwanzig et al., 2001, 2003; White et al., 2002; Corrigan et al., 2009; Kuiper et al., 2011).

Granitoid rocks in the Superior boundary zone

Fox Lake pluton (locality 16)

Granite of the Fox Lake pluton is texturally homogeneous, massive and medium- to coarse-grained, although the presence of variably foliated to mylonitic phases has been reported (Corkery, 1985). The granite is pinkish grey to light grey on fresh and weathered surfaces (Figure 11a) and comprises 4–7% biotite (3–4 mm), 30–35% anhedral quartz (4–6 mm), 40–50% K-feldspar laths (5–7 mm) and 10–15% plagioclase (2–7 mm). Feldspars display diffuse edges, likely related to sericitic alteration. The lack of foliation or gneissosity in this pluton suggests it may be younger than the Orr Lake and Assean Lake intrusions described below. This granite has low MS values (<0.088 × 10^{-3} SI), suggesting that it is an ilmenite-series granite. Biotite is the only ferromagnesian mineral in this granite, and hornblende is absent. Whole-rock geochemistry of one granite sample taken from the Fox Lake pluton (DRI2022012) reveals that it is an evolved I-type granite with ilmenite-series characteristics (e.g., Yang et al., 2008).

Assean Lake intrusion (locality 17)

Previous studies indicated that several different types of granitoid rocks occur at Assean Lake, displaying Mesoarchean ages of ca. 3.2 to 3.1 Ga (for details, see Böhm et al., 1999, 2000, 2003, 2018). These granitoid rocks from part of the Assean Lake intrusion include strongly foliated to gneissic, medium- to coarse-grained, equigranular granodiorite to granite, and granitic orthogneiss. The granodiorite has compositional banding (Figure 11b) and consists of 5–10% biotite (±hornblende), 25–30% quartz (1–3 mm), 30–40% plagioclase (2–3 mm) and 10–15% K-feldspar (3–4 mm). Two groups of fabrics are evident: one

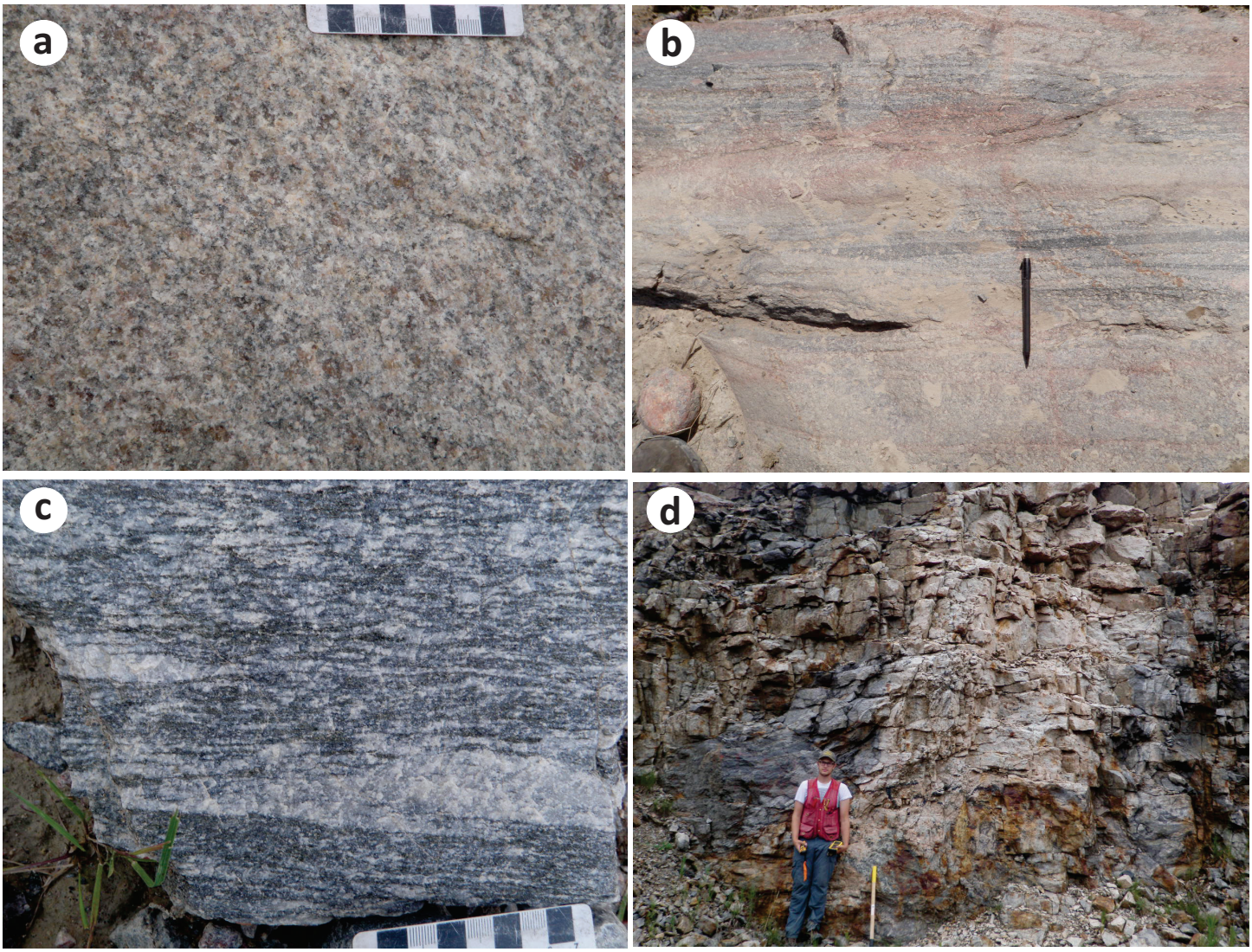

Figure 11*: Field photographs of granitoid rocks from the Superior boundary zone:* ***a)*** *medium- to coarse-grained, massive biotite granite, Fox Lake pluton (UTM 682470E, 6244232N; NAD83, Zone 14);* ***b)*** *medium-grained gneissic granodiorite, Assean Lake intrusion (UTM 637210E, 6224513N);* ***c)*** *medium-grained granite gneiss, Orr Lake intrusion (UTM 619820E, 6213084N);* ***d)*** *garnet-muscovite–bearing pegmatite and pegmatitic granite dike intrusive into paragneiss, Jock Lake intrusion (557399E, 6191948N).*

trending ~090° overprinted by another trending ~070°. These fabrics are common in this part of the SBZ, reflecting the older Archean east-trending structures overprinted by younger east-northeast–trending Paleoproterozoic structures (e.g., Corkery et al., 2000). The gneissic granodiorite and granite have MS values of 0.165–3.4 × 10^{-3} SI, consistent with I-type and magnetite-series granite (Table 2).

Orr Lake intrusion (locality 18)

Medium- to coarse-grained granitic gneiss (Figure 11c) is a major phase of the Orr Lake intrusion. The gneissosity (~240°/85°) seems to parallel the main Trans-Hudsonian fabric in this part of the SBZ (e.g., Zwanzig et al., 2001), which is curved around the promontory structure northeast of Thompson (Kuiper et al., 2011). This granitic gneiss shows strongly compositional layering, with apparent alternation of mafic- and felsic-enriched layers. It is noted that the layers rich in ferromagnesian minerals (biotite, ±hornblende±magnetite) display very high MS values of >30 × 10^{-3} SI, whereas layers rich in felsic minerals (quartz and feldspar) have low MS values of 0.5–1.5 × 10^{-3} SI. Overall, outcrops of the granitic rocks display MS values in the range 0.716–11.9 × 10^{-3} SI, consistent with I-type and magnetite-series granites elsewhere in the Superior province (e.g., Yang et al., 2008; Yang, 2014a).

Jock Lake intrusion (locality 19)

The Jock Lake intrusion cuts sulphide (pyrite and pyrrhotite) and hornblende-bearing garnet-biotite-quartz-plagioclase paragneiss (Figure 11d). The main components of this intrusion are very coarse-grained to pegmatitic granite and pegmatite that occur mostly as dikes cutting the paragneiss. The granitic rocks are massive and consist of quartz, K-feldspar and minor garnet, muscovite and local tourmaline. Graphic texture is common in the pegmatites, pointing to co-crystallization of quartz and K-feldspar. These granitic rocks are very low in MS (0.048–0.055 × 10^{-3} SI), indicating that they belong to S-type and ilmenite-series granites.

Ospwagan Lake intrusion (locality 20)

Five granitoid intrusions, i.e., the Ospwagan Lake intrusion (locality 20), Paint Lake pluton (locality 21; Machado et al., 2011a), Grass River pluton (locality 22), Setting Lake pluton (locality 23) and Kiski Lake intrusion (locality 24), in the Thompson nickel belt (TNB), were examined and sampled (Figure 4; Table 2).

The Ospwagan Lake intrusion is a composite pluton emplaced into the boundary between the KD to the west and the TNB to the east (Figures 1, 4). This intrusion consists of granodiorite, granite, garnet-muscovite pegmatitic granite and granitic pegmatite. The pluton was dated by Machado et al. (2011a) using monazite U-Pb geochronology with a minimum age of 1806 ±5 for a weakly deformed granitoid sample and an age of 1772 ±2 Ma for a sample from a garnet-biotite granite sheet within the Ospwagan Group metasedimentary rocks. These ages likely reflect felsic magmatism related to the collisional event of the THO with the Superior craton. The ages are much younger than the 1.88 Ga rifting event along the margin of the Superior craton and the resultant ultramafic bodies hosting the Thompson nickel deposits that are emplaced into the metasedimentary rocks of the Ospwagan group (Macek and Bleeker, 1989; Thompson Nickel Belt Geology Working Group, 2001; Rayner et al., 2006; Burnham et al., 2009; Heaman et al., 2009; Couëslan and Pattison, 2012; Couëslan et al., 2013; Lightfoot et al., 2017).

The garnet-muscovite pegmatitic granite is light grey on fresh surface and weathers pale white (Figure 12a). It is coarse-grained to pegmatitic, massive and equigranular, but varies to fine- to medium-grained at the contact with the wallrock. This granite cuts the Ospwagan group sulphide-bearing (pyrrhotite, ±pyrite) biotite gneiss containing porphyroblastic garnet. The granite consists dominantly of anhedral quartz, K-feldspar and minor muscovite flakes and garnet (0.5–2 mm; Figure 12a). Locally, trace disseminated pyrrhotite (0.1–0.3 mm) is evident, which shows weak to moderate magnetism albeit the lack of magnetite. This leads to the garnet-muscovite granite displaying slightly higher MS values of 0.110-0.145 × 10^{-3} SI (Table 2) compared to those of typical S-type and ilmenite-series granites (Yang et al., 2008, 2019; Yang, 2014a). However, this granite belongs to S-type coined by Chappell and White (1974, 1992, 2001) and ilmenite-series granites defined by Ishihara (1977, 1981, 2004) in terms of the rock-forming mineral assemblage and the presence of magnetic pyrrhotite that requires a relatively reduced granitic melt (e.g., Whalen and Chappell, 1988; Yang, 2012).

Paint Lake pluton (locality 21)

The Paint Lake pluton is a composite granitoid body dominated by granite and granodiorite that are cut by garnet-muscovite pegmatite dikes.

The granite is medium- to coarse-grained, locally very coarse-grained, equigranular and massive, but is locally porphyritic and contains subhedral K-feldspar phenocrysts up to 2 cm. It consists of 10–15% biotite (partly altered to chlorite and iron oxide), 25–28% anhedral quartz (3–5 mm), 50–55% K-feldspar (3–5 mm) and 10–15% plagioclase laths (2–4 mm) that display diffuse grain boundaries (Figure 12b), and minor garnet. The granodiorite cut by the granite is medium- to coarse-grained, massive, equigranular, but locally porphyritic in texture. It consists of 20–25% quartz (3–5 mm), 45–55% K-feldspar (5–7 mm), 15–20% biotite (1–3 mm) that is present as aggregates. Garnet-muscovite pegmatite (Figure 12c) dikes up to 3 m in width cuts both the granite and granodiorite. Magnetic susceptibility values of the garnet-bearing granite and granodiorite in the Paint Lake pluton are low ranging from 0.074 to 0.077 × 10^{-3} SI, typical for ilmenite-series and S-type granites.

Although the age of the granitoid rocks described above is unknown, it is noted that granitic pegmatites from northeast of Paint Lake were dated at 1848 ±8 Ma to 1785 ±1 Ma by Machado et al. (2011a, b) using zircon and monazite U-Pb geochronology, suggesting that the collision between the basement of the THO (amalgamated Sask-Hearne craton) and the Superior province took place as early as at ca. 1850 Ma (Machado et al., 2011b).

Grass River pluton (locality 22)

The Grass River pluton consists of a medium- to coarse-grained, and gneissic granitoid body varying in composition and textures from gneissic granite to granodiorite, felsic migmatite and orthogneiss that are intruded by medium- to coarse-grained, massive, equigranular granite. The gneissic granodiorite displays compositional banding (Figure 12d) with mafic-mineral enriched segregation layers that are foliated and folded with a dominant foliation striking 022°, the dominant structural trend observed in this part of the TNB. These mafic-rich bands (0.3 to 5 cm in width) are comprised of biotite±hornblende±magnetite alternating with felsic layers that consist of quartz, plagioclase, K-feldspar, and biotite±hornblende. The gneissic granodiorite has MS values of 1.24 × 10^{-3} to 2.01 × 10^{-3} SI, typical for I-type or magnetite-series granite (Table 2).

Massive granite occurs in dikes and stocks cutting the gneissic unit. This granite (Figure 12e) is less deformed, massive and composed of 25–30% quartz (2–3 mm), 40–50% K-feldspar (2–4 mm), 10–15% biotite (1–3 mm; altered to chlorite and magnetite), minor plagioclase, and minor discrete magnetite. It has similar MS values as the gneissic granitoid phases, and therefore is also attributed to the I-type and magnetite-series granites defined by Chappell and White (1974) and Ishihara (1977), respectively.

A grey gneiss sample similar to the gneissic granodiorite was dated by Machado et al. (2011a), who suggested that this rock could be Archean (~2658 Ma) but was affected by relatively high-temperature metamorphism leading to zircon growth at ca. 1802 Ma.

Setting Lake pluton (locality 23)

The Setting Lake pluton is a complex composite intrusive body comprising granodiorite gneiss and migmatitic rocks ranging from monzonite to quartz syenite to granite. A monzonite sample taken at the southern end of Setting Lake was dated at 1835 +4/–3 Ma, and a granodiorite gneiss sample from the

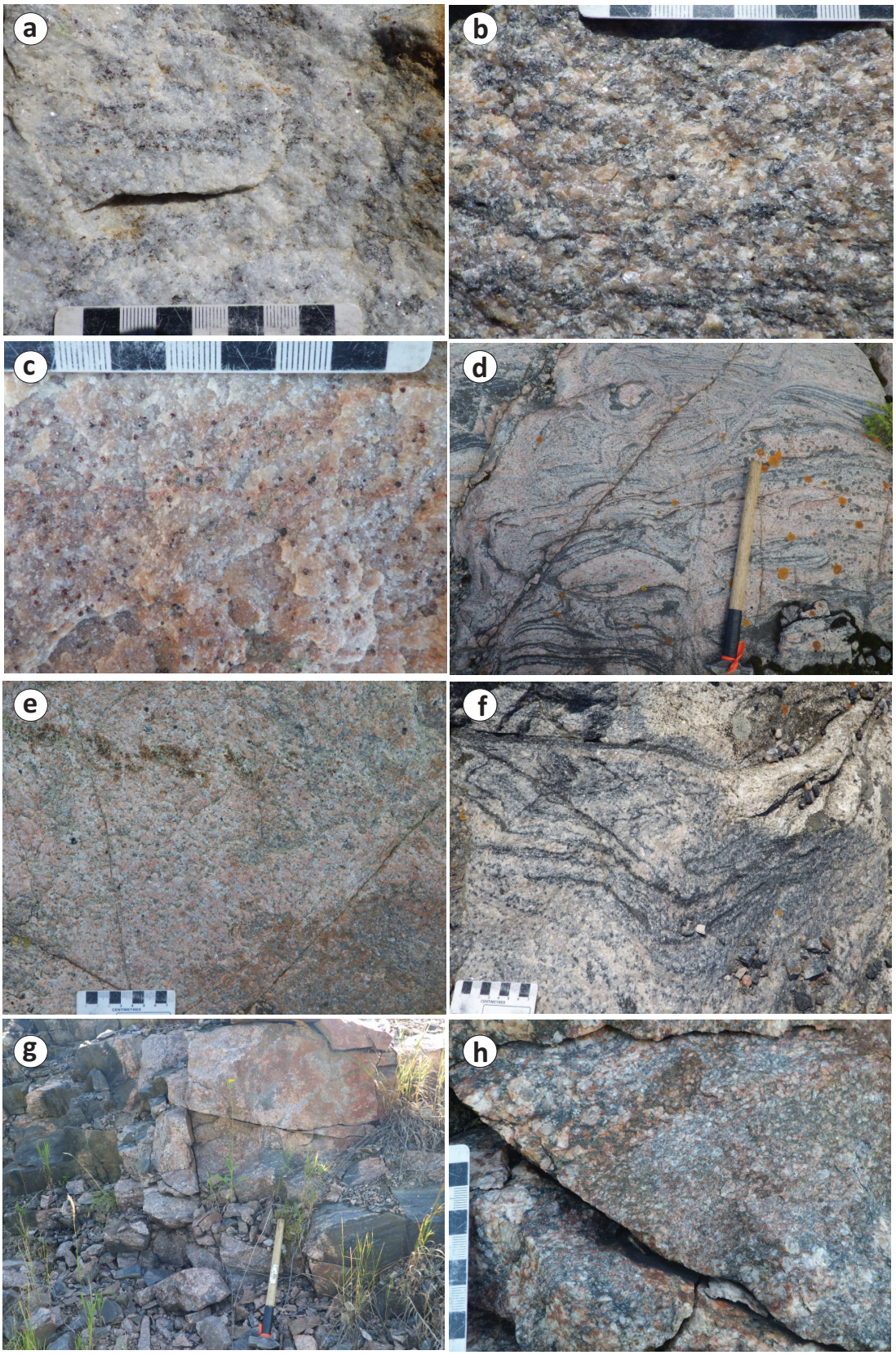

***Figure 12**: Field photographs of granitoid rocks from the Thompson nickel belt of the Superior boundary zone, central Manitoba: **a)** fine-grained to pegmatitic garnet-muscovite granite, Ospwagan Lake intrusion (UTM Zone 14, 561856E, 6157314N, NAD 83), present as a dike, 10 to 15 m wide, cutting pyrrhotite-bearing biotite gneiss of the Ospwagan group; **b)** medium- to coarse-grained garnet-biotite granite, Paint Lake pluton (UTM 540583E, 6131651N); **c)** garnet-biotite (±muscovite) granitic pegmatite, Paint Lake pluton (UTM 540617E, 6131591N); **d)** medium- to coarse-grained gneissic granite, Grass River pluton (UTM 535017E, 6110786N); **e)** coarse-grained, massive, equigranular granite, which intrudes into the gneissic granite, Grass River pluton (UTM coordinates as [d]); **f)** medium-grained gneissic granite, Setting Lake pluton (UTM 524952E, 6091324N); **g**) pegmatite dike cutting mafic gneiss, Kiski Lake intrusion (UTM 507962E, 6064991N); **h**) extremely heterogeneous granitic pegmatite, Kiski Lake intrusion (same UTM coordinates as [g]).*

Favel Island yielded 1878 ±34 Ma (Zwanzig et al., 2003). Metamorphic monazite crystals from a foliated granodiorite at the northern end of Setting Lake yielded a concordant age of 1768 ±2 Ma, which is younger than the age range of 1818 ±2 Ma to 1788 ±2 Ma acquired from monazite in granitic pegmatites (Machado et al., 2011a). These ages obtained from the Setting Lake pluton reflect a prolonged history of magmatism (~1890–1830 Ma) and metamorphism recorded in the TNB as a result of convergence between the amalgamated Sask-Hearne craton basement of the THO and the Superior province (Machado et al., 2011a, b).

The granodiorite gneiss is medium- to coarse-grained, folded, and displays compositional bands. The mafic bands showing a moderate to strongly magnetic feature are composed of biotite, magnetite and variably hornblende, intercalating with felsic domains comprised of quartz, plagioclase, K-feldspar, biotite and minor hornblende (Figure 12f). MS values registered for the rock range from 1.73×10^{-3} to 6.12×10^{-3} SI, typical of I-type and the magnetite-series granites (Table 2).

Partial melt (leucosome) veins and pegmatitic dikes are commonly observed in the granodiorite gneiss. These dikes consist dominantly of quartz, feldspars, and minor biotite±muscovite.

Kiski Lake intrusion (locality 24)

The Kiski Lake granite and granitic pegmatite intrusion intrudes in mafic to intermediate gneiss (Figure 4). A granite sample taken from east of Kiski Creek was dated by U-Pb zircon geochronology at 1866 to 1862 Ma (Zwanzig et al., 2003). An up to 3 m wide granitic pegmatite dike exposed on a road cut displays extreme heterogeneity in texture and mineralogy (Figure 12g). The granitic pegmatite comprises megacrystic K-feldspar (up to 4 cm, subhedral to rounded, weakly deformed) and anhedral quartz (0.2 to 0.6 cm) in fine- to medium-grained groundmass including aggregates of biotite and magnetite (Figure 12h). The textural variations are porphyritic, seriate, and pegmatitic on the outcrop. This granitic pegmatite displays relatively high MS values of 10.0 to 29.6×10^{-3} SI (Table 2), which is ascribed to the derivate fractionated from I-type and magnetite-series granite magmas.

Granitoid rocks in the Munro Lake and Molson Lake domains

Jenpeg Dam intrusion (locality 25)

The Jenpeg Dam intrusion is part of the Archean TTG suite that constitutes the core of the Munro Lake domain in the western Superior province. Tonalite from this intrusion is medium to light grey on both weathered and fresh surfaces. It is medium- to coarse-grained, massive, and equigranular, but locally it is porphyritic. In the porphyritic variety of the tonalite, phenocrysts of euhedral plagioclase laths (up to 3 cm) are embedded in a medium-grained groundmass consisting of quartz, plagioclase, biotite and hornblende, and minor K-feldspar (1–2%; Figure 13a). Notably, some plagioclase phenocrysts contain biotite (~0.5–1.5 mm) inclusions, suggesting that the granitic melts may have been water-enriched. The non-porphyritic variety of the tonalite contains 20–25% quartz (1–3 mm), 40–50% plagioclase (3–4 mm), 5–10% K-feldspar laths (3–4 mm), 10–15% biotite (2–3 mm), and 5–10% hornblende (2–3 mm), similar to the mineral assemblage of the groundmass of the porphyritic tonalite.

In the porphyritic granodiorite, quartz (up to 1 cm) and euhedral to subhedral K-feldspar are homogeneously distributed in a fine- to medium-grained groundmass of quartz, plagioclase, K-feldspar, and biotite (Figure 13b). Generally, this granodiorite is a more evolved phase indicated by the presence of quartz phenocrysts and lack of amphibole. The phenocryst assemblage suggests that quartz co-crystallized with K-feldspar within a magma chamber before the granodiorite ultimately emplaced into the upper crust. Relative to the tonalite described above, more evolved granodiorite may be used for pressure estimation based on coexisting quartz and K-feldspar in the phenocryst assemblage (e.g., Yang, 2017), providing critical information about the erosion level and erosion rate of the intrusion given its absolute age is determined.

The tonalite and granodiorite from the Jenpeg Dam intrusion have MS values of 0.253 to 2.03×10^{-3} SI, falling into the field of normal I-type and magnetite-series granites.

Pinkish, simple pegmatite (quartz-feldspar-biotite±muscovite) dikes cutting the Jenpeg Dam intrusion are commonly observed.

Nelson River pluton (locality 26)

The Nelson River pluton is a meta-igneous complex, comprising various textural varieties: gneissic, massive, and equigranular to porphyritic to megacrystic. Mafic xenoliths are common as illustrated by a medium-grained, approximately 1.2 m gabbroic xenolith (Figure 13c, d) that displays sharp to diffuse contacts with the host granitoid rock. Deformed and foliated mafic inclusions are also evident, with various shapes (e.g., elongated, irregular, subrounded) and sizes (e.g., as small as a few cm up to a few metres across). It is not uncommon to see mafic xenoliths with gradational contacts with the host granitoids.

Medium- to coarse-grained, locally megacrystic, pinkish granite is widely present in the Nelson River pluton. It consists of 25–27% quartz (3–5 mm), 55–60% K-feldspar (5–6 mm; locally up to 2 cm), 5–10% plagioclase and 3–5% biotite. Pegmatitic phases composed of quartz, K-feldspar and biotite occur either as dikes or as isolated pods or patches within the pluton, suggesting that these pegmatitic rocks may have been resulted from fractionation of the same magma as the host granite.

Porphyritic, pinkish, massive granodiorite usually contains 5–10% K-feldspar phenocrysts (1–2 cm) in a medium- to coarse-grained groundmass that consists of 20–25% quartz (1–3 mm), 40–45% plagioclase (2–4 mm), 10–15% K-feldspar (2–6 mm), 10–15% biotite (1–3 mm) and minor hornblende.

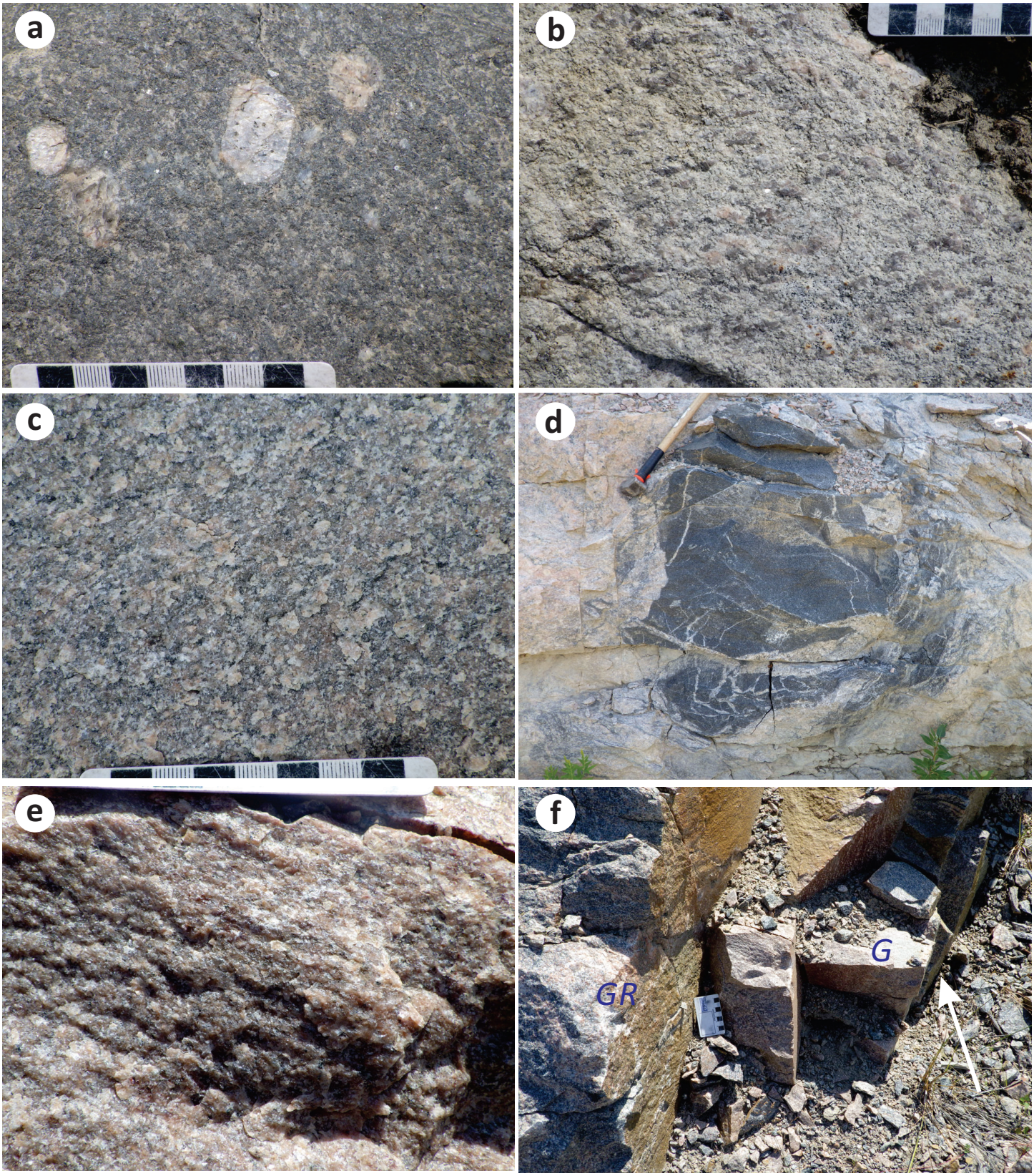

Figure 13: *Field photographs of granitoid rocks from the Munro Lake and Molson Lake domains of the western Superior province, central Manitoba:* ***a)*** *porphyritic tonalite with euhedral plagioclase phenocrysts (up to 3 cm) embedded in medium-grained groundmass (note: biotite inclusions in plagioclase), Jenpeg Dam intrusion, MOLD (UTM Zone 14, NAD 83; 565980E, 6041515N);* ***b)*** *porphyritic granodiorite with quartz and K-feldspar phenocrysts in medium-grained groundmass, Jenpeg Dam intrusion, MOLD (UTM 562272E, 6043709N);* ***c)*** *massive, medium-grained biotite (±muscovite) granite, Paimusk Creek intrusion, MLD (UTM 592193E, 6010865N);* ***d)*** *medium- to coarse-grained pinkish granodiorite with dark grey, fine- to medium-grained gabbroic xenolith, Nelson River pluton, MLD (UTM 584055E, 5988156N);* ***e)*** *fine- to medium-grained equigranular granite, Nelson River pluton, MLD (UTM 584612E, 59920794N);* ***f)*** *granite (G) shown in (e) occurring as a dike cutting medium- to coarse-grained granodiorite (GR; same UTM location as [d]).*

Cutting the coarse-grained granite and granodiorite is a late, pinkish grey, massive, medium-grained, equigranular granite (Figure 13e, f). This granite is present as dikes (or small stocks) consisting of 25–30% quartz (2–3 mm), 50–55% K-feldspar (2–4 mm), 5–10% plagioclase (2–4 mm), and 2–5% biotite (1–2 mm). This leucogranite is an evolved granite exhibiting MS value of 1.86×10^{-3} SI, likely belonging to evolved I-type and magnetite-series granites.

The Nelson River granitoids have MS values of 0.164 to 3.47×10^{-3} SI, comparable to normal I-type and magnetite-series granites elsewhere in Manitoba (Yang, 2014a).

Paimusk Creek intrusion (locality 26')

The Paimusk Creek granitic intrusion emplaced along the boundary of the Munro Lake and Molson Lake domains (Figure 4). This granite is pinkish on fresh surface, and pinkish grey on weathered surface. It is medium-grained, massive, equigranular, without apparent structural fabrics. It consists of 25–30% anhedral quartz (2–3 mm), 50–55% subhedral K-feldspar laths (2–4 mm), 5–10% plagioclase (2–4 mm), 5–10% biotite (1–2 mm), and minor muscovite.

This granite displays relatively reduced features manifested by low MS values of 0.087 to 0.092×10^{-3} SI, typical for S-type and ilmenite-series granites (Table 2).

Trans-Hudson orogen

Granitoid intrusions were examined and sampled from the Paleoproterozoic Trans-Hudson orogen (THO) including parts of the Lynn Lake greenstone belt (LLGB), Southern Indian (SID), and Kisseynew domains (KD). The localities of these intrusions are numbered (Figures 3, 5; Table 2). A brief description of the field and petrographic characteristics for each intrusion in the tectonic units is presented in the following sections.

Granitoid rocks in the Lynn Lake domain

Granitoid rocks from the LLGB, a major component of the Lynn Lake domain (LLD; Figures 1, 5), have been mapped and described by the MGS (Gilbert et al., 1980; Gilbert, 1993; Yang and Beaumont-Smith, 2015a, b, 2016, 2017; Yang, 2016, 2019a, 2021). The granitoid intrusions that are the focus of this report are the Burge Lake, Cockeram Lake, Eldon Lake and Motriuk Lake plutons; the Dunphy Lakes batholith; and the Hughes Lake pluton, Farley Lake stock and Farley Lake plutons I and II; Pool Lake and Counsell Lake plutons, Late intrusive suite; and Eden Lake, Ruttan Lake and Turnbull Lake plutons (localities 27–41, respectively, in Table 2 and Figures 3 and 5). These granitoid rocks are divided into pre-Sickle (or Pool Lake) and post-Sickle intrusive suites based on their field and temporal relationships to the syntectonic molasse–type sedimentary rocks of the Sickle group (Norman, 1933; Milligan, 1960; Gilbert et al., 1980; Baldwin et al., 1987; Zwanzig et al., 1999; Beaumont-Smith and Böhm, 2002, 2003, 2004; Anderson et al., 2005; Yang and Beaumont-Smith, 2015a, b; Yang, 2021; Lawley et al., 2020b).

Burge Lake pluton (locality 27)

The Burge Lake pluton (Figure 5) consists mainly of granodiorite and intrudes the Wasekwan group supracrustal rocks and the Ralph Lake conglomerate (Yang and Beaumont-Smith, 2015a; Yang, 2021). This pluton was dated at 1857 ±2 Ma (Beaumont-Smith et al., 2006), cutting the Ralph Lake conglomerate that was thought to be comparable to the Sickle group (Lawley et al., 2020a, b), and is thus assigned to the post-Sickle intrusive suite (Yang and Beaumont-Smith, 2015a; Manitoba Agriculture and Resource Development, 2021; Yang, 2021). The granodiorite is weakly to moderately foliated, medium- to coarse-grained, equigranular and locally porphyritic (Figure 14a). It is typically composed of 10–15% biotite (3–5 mm), 35–45% subhedral to euhedral plagioclase laths (3–8 mm), 10–15% pinkish K-feldspar, 25–30% anhedral or subrounded quartz (2–5 mm), and accessory minerals, including magnetite, zircon, apatite and titanite. Hornblende is mostly replaced by biotite. Sericitic and chloritic alteration of feldspar and biotite, respectively, is common. The granodiorite at Burge Lake displays MS values ranging from 0.272 to 12.6×10^{-3} SI, and locally up to 18.0×10^{-3} SI (Table 2), suggesting that it is a normal I-type (Chappell and White, 1974, 1992) and magnetite-series (Ishihara, 1981; Yang and Beaumont-Smith, 2015b) granodiorite. The Burge Lake granodiorite is noted to exhibit adakite-like features, and may be related to orogenic gold mineralization (Yang, 2021).

Cockeram Lake composite granitoid pluton (locality 28)

The Cockeram Lake pluton (Figure 5), intruding the Wasekwan group, is attributed to the pre-Sickle intrusive suite, as it was dated at 1876 +8/–6 Ma (Baldwin et al., 1987) and stitches the northern and southern belts of the LLGB. This pluton contains a range of rock types, including quartz diorite, tonalite, granodiorite and granite. Thus, it is a composite granitoid pluton. In places, the granodiorite intrudes quartz diorite (Figure 14b) and tonalite, and then is intruded by more evolved granite. The granodiorite is pinkish grey, medium- to coarse-grained, equigranular to locally porphyritic and foliated. Xenoliths of mafic to intermediate volcanic rocks are commonly present. The granodiorite consists of 20–25% anhedral quartz (0.5–0.8 mm), 25–35% subhedral plagioclase laths (5–12 mm), 20–25% K-feldspar (10–12 mm) and 10–15% hornblende (0.5–1 mm; mostly altered to biotite), along with accessory Fe-oxide minerals (e.g., magnetite). It has MS values of up to 17.5×10^{-3} SI, which are lower than quartz diorite (up to 32.9×10^{-3} SI), comparable to those of I-type granites of Chappell and White (1974) and magnetite-series granite of Ishihara (1981). The granodiorite is cut by a fine- to medium-grained granite that contains up to 35% quartz but less than 10% biotite, and has much lower MS values (near 0.63×10^{-3} SI), also typical of I-type or magnetite-series granite.

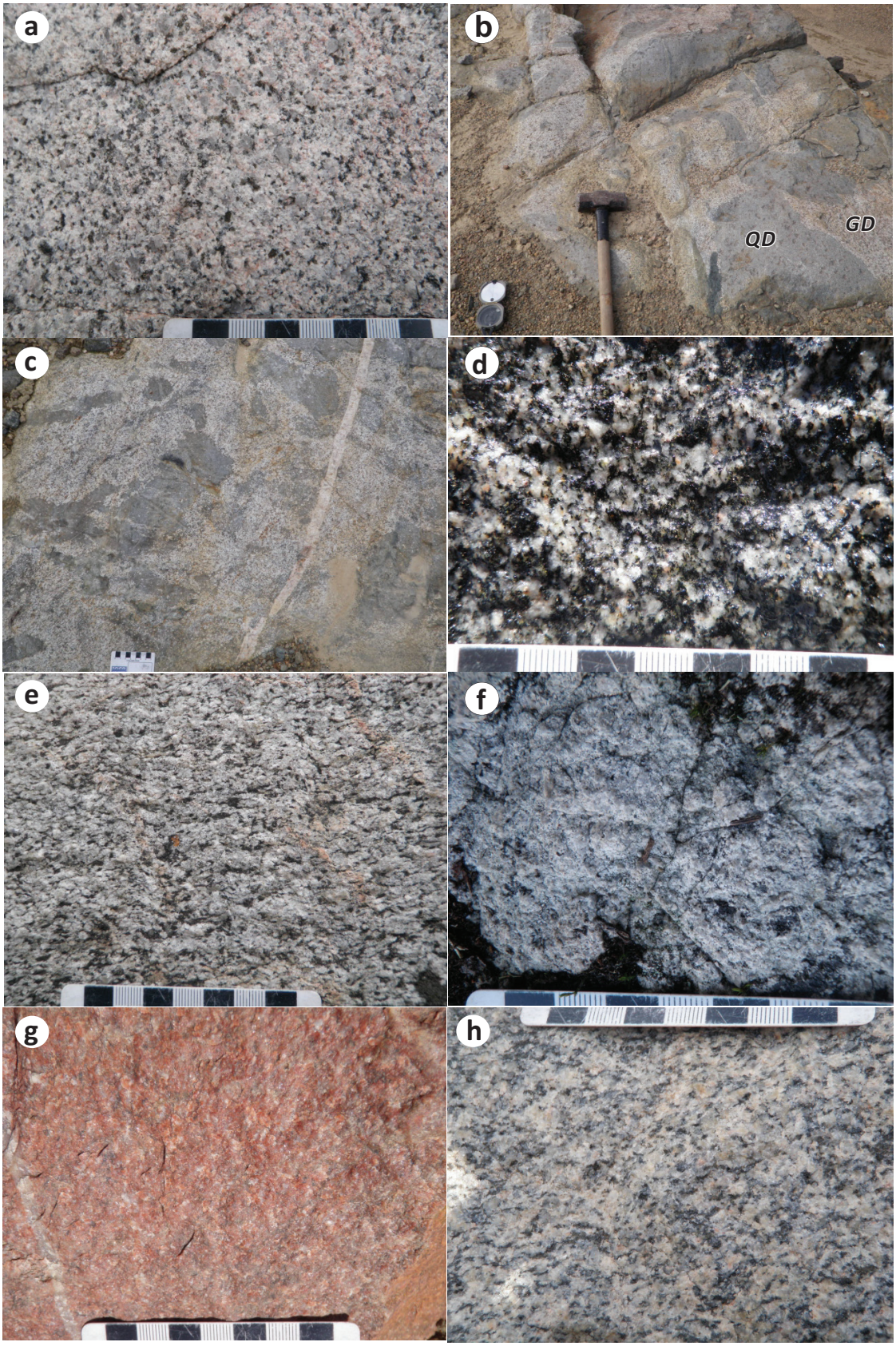

Figure 14: *Field photographs of granitoid rocks from the Lynn Lake domain:* ***a)*** *medium- to coarse-grained granodiorite, Burge Lake pluton (UTM Zone 14, 375947E, 6307963N, NAD 83);* ***b)*** *intrusive breccia indicative of a younger granodiorite (GD) intruding an earlier quartz diorite (QD) phase, Cockeram Lake pluton (UTM 386832E, 6303025N);* ***c)*** *medium-grained tonalite with irregular xenoliths of plagioclase-phyric basalt cut by a late, thin pegmatite dike, Eldon Lake pluton (UTM 3757761E, 6298253N);* ***d)*** *medium-grained tonalite, Motriuk Lake pluton (UTM 365499E, 6295322N);* ***e)*** *foliated medium-grained granodiorite, Dunphy Lake batholith (UTM 345251E, 6288790N);* ***f)*** *porphyritic granite, Hughes Lake pluton (UTM 406205E, 6298477N);* ***g)*** *fine- to medium-grained quartz syenite, Hughes Lake pluton (UTM 408236E, 6294050N);* ***h)*** *medium-grained granodiorite, Farley Lake pluton I (UTM 412105E, 6306254N).*

Eldon Lake pluton (locality 29)

The Eldon Lake pluton (Figure 5) is a component of the pre-Sickle intrusive suite in the LLGB. This pluton contains tonalite, quartz diorite and minor quartz monzonite. The tonalite weathers pale grey to beige and is grey on fresh surfaces. It is medium- to coarse-grained, equigranular and locally porphyritic, and consists of 10–15% amphibole that is replaced mostly by biotite, 20–25% quartz (5–7 mm, locally up to 10 mm), 60–65% plagioclase and minor K-feldspar (<5%). In places, many irregular xenoliths of fine-grained plagioclase-phyric basalt are present in the tonalite (Figure 14c). These xenoliths are texturally similar to plagioclase-phyric basalt of the Wasekwan group in the LLGB (Yang and Beaumont-Smith, 2015a, 2017). The Eldon Lake pluton displays MS values of 0.357–12.9 × 10^{-3} SI, comparable to relatively oxidized I-type (Chappell and White, 1974, 1992) and magnetite-series (Ishihara, 1977, 1981) granites.

Motriuk Lake pluton (locality 30)

The Motriuk Lake pluton (Figure 5) is composed dominantly of medium- to coarse-grained tonalite (Figure 14d) that is locally cut by fine-grained granite dikes. The tonalite consists of 20–25% biotite (pseudomorph after hornblende) and minor amphibole relicts, 20–25% quartz (3–5 mm), 50–55% plagioclase and minor K-feldspar (<10%). It is noted that some biotite is altered to chlorite and magnetite, and some plagioclase crystals in fractures are stained to a reddish colour. The fine-grained granite contains 5–10% biotite, 30–35% quartz, 40–45% K-feldspar and 10–20% plagioclase. The MS measurements indicate that both tonalite and granite in the Motriuk Lake pluton are relatively oxidized, with MS values of 0.94–7.60 × 10^{-3} SI, typical of I-type and magnetite-series granites (Table 2).

Dunphy Lakes batholith (locality 31)

The Dunphy Lakes batholith (Figure 5) consists mainly of granodiorite and tonalite, which are emplaced into the boundary of the LLD and SID. Two tonalite samples taken from the eastern portion of Dunphy Lake yielded ages of 1847 ±2 Ma and 1829 ±2 Ma (Beaumont-Smith and Böhm, 2003), suggesting that this batholith is a post-Sickle intrusion. The granodiorite is medium-grained, foliated and equigranular (locally porphyritic), and consists of 20–25% quartz (3–4 mm), 45–55% plagioclase, 10–15% K-feldspar and 10–15% biotite (Figure 14e). The tonalite, however, contains notable amphibole relicts (up to 5%) in the ferromagnesian minerals (15–20%; dominated by biotite and hornblende). This rock also contains 20–25% quartz, 50–60% plagioclase and minor K-feldspar (<10%). The granodiorite and tonalite at Dunphy Lakes display MS values of 0.136–2.90 × 10^{-3} SI, consistent with I-type or magnetite-series granites (Table 2).

Hughes Lake pluton (locality 32)

The Hughes Lake pluton (Figure 5) comprises mainly granite and quartz diorite, and is locally intruded by quartz syenite to leucogranite dikes. This pluton intrudes dark green aphyric basalt with disseminated pyrrhotite in the northern belt of the LLGB, and is unconformably overlain by polymictic conglomerate and arkosic sandstone of the Sickle group. A quartz diorite sample from the Hughes Lake pluton yielded a U-Pb zircon age of 1876 +8/–7 Ma (Baldwin et al., 1987), identical to that of the Cockeram Lake pluton, which is also a pluton of the pre-Sickle intrusive suite. The granite at Hughes Lake is medium-grained and equigranular to porphyritic (Figure 14f). It is pinkish on fresh surfaces and consists of 2–3% biotite, 30–35% quartz, 55–60% K-feldspar and 5–10% plagioclase. Locally, chlorite veinlets occur along cleavage planes in the granite. It is noted that late-stage reddish quartz syenite to leucogranite dikes locally intrude the pluton and the volcanic country rocks. The quartz syenite (Figure 14g) is fine- to medium-grained and consists of 10–15% quartz (0.1–1 mm, locally up to 4 mm), 80–85% K-feldspar and 1–2% magnetite (0.2–0.3 mm). Locally, narrow veinlets (<1 mm wide) of quartz, pyrite, ±magnetite±biotite occur in the quartz syenite dikes, which have MS values of up to 17.2 × 10^{-3} SI. The Hughes Lake granite displays consistent MS values of 2.49–3.00 × 10^{-3} SI, typical of I-type and magnetite-series granite.

Farley Lake stock (locality 33)

The Farley Lake stock (Figure 5) comprises diorite to quartz diorite exposed on the south wall of the East pit at the Gordon mine (formerly Farley Lake mine; Yang and Beaumont-Smith, 2016). A quartz diorite sample was dated at 1854.4 ±2.4 Ma, attributed to post-Sickle intrusions in the LLGB (Yang and Lawley, 2018). The quartz diorite is light to dark grey on weathered and fresh surfaces, fine- to medium-grained, massive, equigranular and moderately to strongly foliated (Figure 15a). It consists of 2–10% anhedral quartz (1–3 mm), 40–50% plagioclase laths (1–4 mm) with diffuse grain boundaries, 30–40% hornblende (1–3 mm) and minor biotite. Disseminated pyrite occurs locally. In places, reddish granitic aplite veins cut the quartz diorite, which displays a relatively high MS value of 11.2 × 10^{-3} SI. A chlorite-altered quartz diorite sample in drillcore from the Farley Lake deposit was reported to contain 0.6 g/t Au; this quartz diorite appears to occur as a dike cutting the sedimentary rocks of the Wasekwan group, including banded iron formation (Beaumont-Smith et al., 2000).

Farley Lake pluton II (locality 34)

The Farley Lake pluton II is a younger phase of the Farley Lake intrusive suite, consisting of granodiorite and granite to leucogranite. The granodorite is pinkish on fresh surfaces and weathers beige to tan. It is medium- to coarse-grained, foliated and equigranular to locally porphyritic. This granodiorite consists of 5–8% hornblende (partly altered to biotite), 25–27% quartz, 30–40% plagioclase, 25–30% K-feldspar and minor discrete biotite flakes (Figure 15b). In places, the feldspar laths are present as phenocrysts (locally up to 20 mm) with diffuse grain edges due to sericitic alteration. Trace sulphide minerals are locally present.

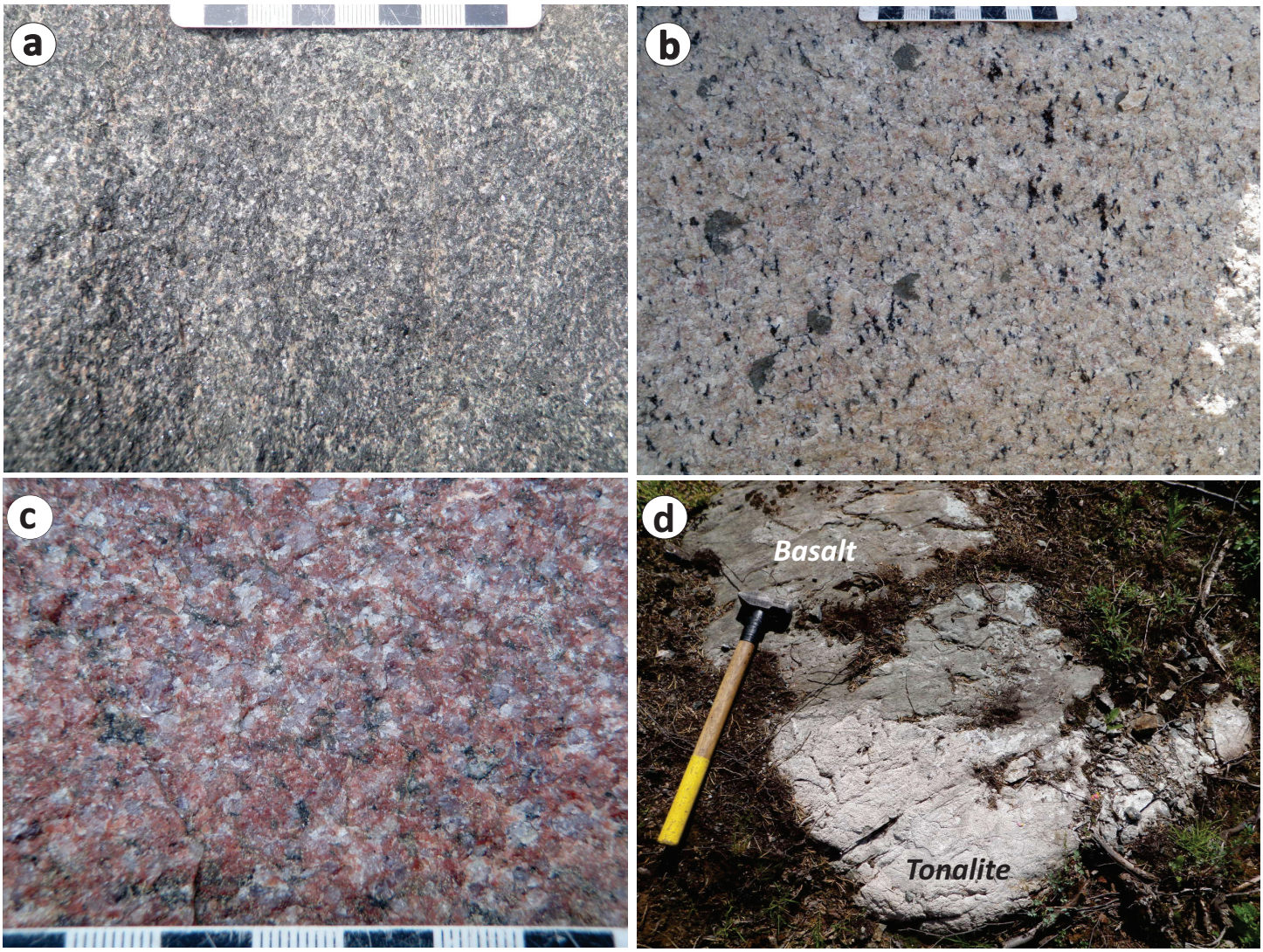

Figure 15: *Outcrop photographs of Farley Lake stock, Farley Lake pluton II and Farley Lake pluton I from the Lynn Lake greenstone belt:* ***a)*** *medium-grained quartz diorite, Farley Lake stock (UTM 412074E, 6307468N, NAD 83);* ***b)*** *medium- to coarse-grained foliated granodiorite, Farley Lake pluton II (UTM 411174E, 6301508N);* ***c)*** *medium-grained leucogranite, Farley Lake pluton II (subunit 7a; UTM 411699E, 6304064N); d) fine- to medium-grained tonalite dikes from the Farley Lake pluton I, cutting aphyric to plagioclase-phyric basalt (UTM 412191E, 6306575N).*

This granodiorite, dated at 1872.6 ±2.5 Ma (Yang and Lawley, 2018), exhibits very low MS values of 0.085 × 10^{-3} SI, consistent with reduced I-type and ilmenite-series granites elsewhere (cf. Yang et al., 2008).

The granite and leucogranite occur as dikes to small stocks, cutting the early phase of Farley Lake pluton I (Yang and Beaumont-Smith, 2016). They are light pinkish to pinkish red on fresh surfaces, medium-grained, massive and equigranular. They consist of 30–35% quartz (3–5 mm), 55–65% reddish K-feldspar laths (3–5 mm) with sharp crystal edges, minor plagioclase, ~5% biotite and trace magnetite (Figure 15c). The granite typically lacks hornblende, and can be termed leucogranite where biotite content is below 5%. This evolved granite displays relatively high MS values of up to 3.98 × 10^{-3} SI, consistent with I-type and magnetite-series granites. Geochemically, the granodiorite to leucogranite from the Farley Lake pluton II displays A-type characteristics (Yang and Lawley, 2018).

Farley Lake pluton I (locality 35)

The Farley Lake pluton I (Figure 5) comprises tonalite, granodiorite and granite, and minor related pegmatitic and aplitic dikes. The tonalite intrudes aphyric to plagioclase-phyric basalt (Figure 15d; Yang and Beaumont-Smith, 2016) in the area south of Farley Lake. The tonalite is fine- to medium-grained, grey to light grey, equigranular but moderately foliated and locally porphyritic. It consists of 15–25% quartz, 50–60% plagioclase, 15–20% amphibole and minor biotite. Chloritic alteration is common. The tonalite displays very high MS values (up to 54.6 × 10^{-3} SI) in a zone within 100 m of its contact with the Wasekwan volcanic rocks; these values are much higher than the typical values for the tonalite, which range from 0.3 to 10.0 × 10^{-3} SI.

The dominant phase in the Farley Lake pluton I is medium- to coarse-grained, equigranular to locally porphyritic, foliated granodiorite. It was dated at 1879.4 ±4.3 Ma (Yang and Lawley, 2018). The granodiorite weathers greyish pink to light beige and

consists of 20–30% anhedral quartz, 25–35% subhedral plagioclase laths, 20–25% K-feldspar, 5–10% biotite (±hornblende) and accessory iron-oxide minerals (Figure 14h). It has MS values of 0.3–24.1 × 10^{-3} SI, typical of the I-type granite of Chappell and White (1974) and the magnetite-series granite of Ishihara (1981). Granite is subordinate in the pluton and contains slightly higher K-feldspar and quartz than the granodiorite. Also, it is attributed to I-type or magnetite-series granite in terms of its mineral assemblage and MS values in the rage 0.2–2.5 × 10^{-3} SI.

Pool Lake pluton (36)

The Pool Lake pluton is a part of the 1876 Ma Pool Lake plutonic suite (Gilbert et al., 1980; Baldwin et al., 1987) intruding the 1892 to 1889 Ma supracrustal rocks of the Wasekwan group, and thus is attributed to pre-Sickle intrusive suite (Yang and Beaumont-Smith, 2015a, 2016, 2017; Yang, 2019a, 2021; Manitoba Agriculture and Resource Development, 2021). This pluton consists mainly of tonalite to granodiorite with minor quartz diorite and feldspar-phyric porphyry. The granodiorite from the Pool Lake pluton is pinkish on fresh surfaces and weathers beige to tan, and is medium- to coarse-grained, foliated and equigranular to locally porphyritic. It consists of 5–8% hornblende (partly altered to biotite), 3–5% discrete biotite flakes, 20–30% quartz, 30–45% plagioclase and 20–25% K-feldspar, and accessory Fe-oxide minerals (e.g., magnetite). The mineral assemblage of Pool Lake granodiorite is consistent with magnetite-series I-type granites in the LLGB and elsewhere in the world.

Counsell Lake pluton (37)

The 1891 Ma Counsell Lake pluton is a pre-Sickle intrusion (Yang, 2019a), consisting mainly of granodiorite, granite, and tonalite to quartz diorite. The granodiorite is commonly medium- to coarse-grained, massive, equigranular to locally porphyritic and weakly to moderately foliated. It weathers greyish pink to light beige and consists of 20–30% anhedral quartz, 25–35% subhedral plagioclase, 20–25% K-feldspar, 5–10% hornblende±biotite, and accessory Fe-oxide minerals. Some of the porphyritic variety contains 5% quartz phenocrysts up to 1.2 cm across (Figure 16a), suggesting relatively shallow emplacement into the Wasekwan group supracrustal package. Less commonly, granite in this pluton contains slightly higher K-feldspar and quartz contents than the granodiorite, whereas tonalite is relatively enriched in plagioclase and hornblende, and lacks (or has <10%) K-feldspar. Quartz diorite occurs mostly as marginal phases of the Counsell Lake pluton. Quartz diorite is fine- to medium-grained, massive, equigranular and moderately to strongly foliated. It consists of 5–10% anhedral quartz, 50–60% plagioclase with diffuse grain boundaries, 20–30% hornblende, and minor biotite. Where the rock lacks quartz or contains <5% quartz, it is termed diorite.

Late intrusive suite (38)

In the LLGB, the Late intrusive suite (Yang and Beaumont-Smith, 2015a, b, 2016, 2017; Yang, 2019a, 2021) consists of quartz-feldspar porphyry, pegmatite and/or aplite, which occur mostly as dikes or small intrusions that are too small to show in Figure 5. These dikes tend to be isolated, relatively less deformed and apparently not associated with any of the larger intrusions mapped at surface. These intrusives have an unclear relationship to the pre- and post-Sickle intrusive suites and are therefore ascribed to the Late intrusive suite. A quartz-feldspar porphyry dike (up to 10 m wide) south of Boiley Lake contains ~2% magnetite phenocrysts that are cubic to subhedral (1–3 mm), together with quartz and K-feldspar embedded evenly in a felsic groundmass (Figure 16b). The presence of magnetite phenocrysts

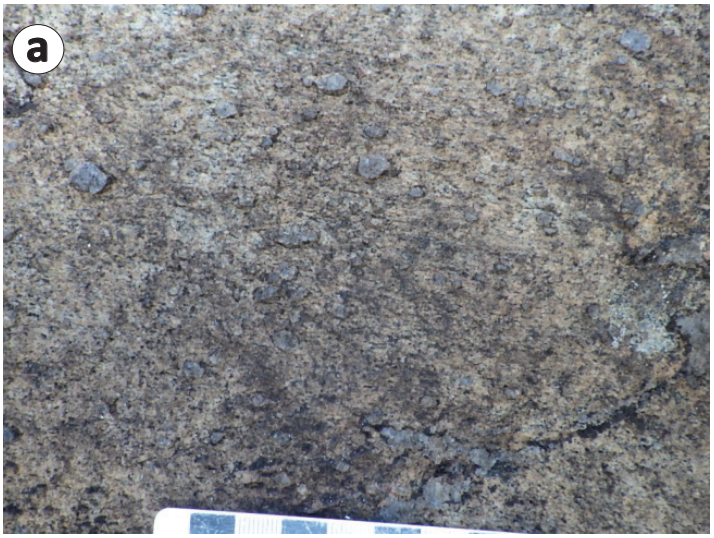

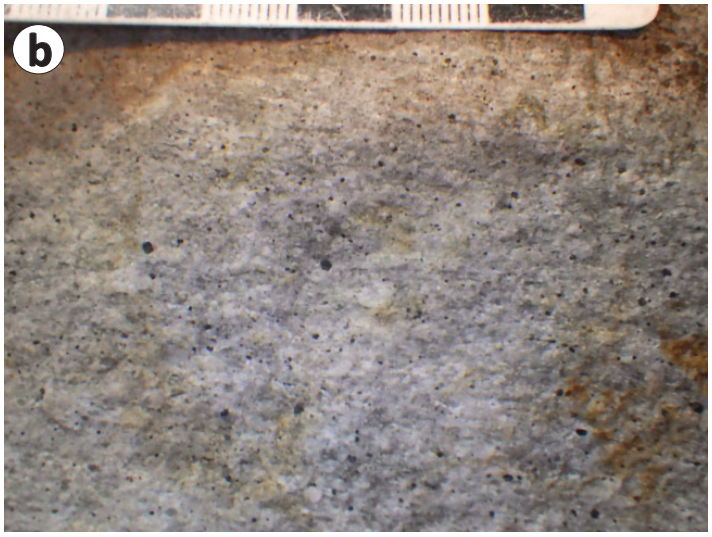

Figure 16: *Outcrop photographs of the Counsell Lake pluton and Late intrusive suite in the Lynn Lake greenstone belt:* ***a)*** *foliated, medium- to coarse-grained porphyritic granodiorite with quartz phenocrysts (2–5 mm; UTM Zone 14, 365201E, 6283371N, NAD 83), the Counsell Lake pluton;* ***b)*** *massive quartz-feldspar porphyry with up to 2% euhedral to subhedral magnetite (up to 3 mm) phenocrysts, Late intrusive suite (UTM 363619E; 6283902N).*

indicates that the dike may have formed in relatively oxidized conditions. Hydrothermal fluids associated with such oxidized intrusion(s) can effectively scavenge and transport gold (e.g., Boyle, 1979), and thus may have played a role in Au mineralization.

Eden Lake pluton (39)

The Eden Lake pluton (Halden and Fryer, 1999) in the Leaf Rapids domain (LRD), thought comparable to the LLD in terms of lithostratigraphic correlation and ages (Rayner and Corrigan, 2004; Corrigan et al., 2007, 2009; Zwanzig and Bailes, 2010; Manitoba Geological Survey, 2018), was examined and sampled (Yang and Beaumonth-Smith, 2015b). This pluton is labelled in the locality of 39 (Figure 5) and Table 2.

Various phases of granitoid rocks in the Eden Lake pluton were dated at 1871–1818 ±1.2 Ma (Turek et al., 2000; Manitoba Geological Survey, 2006). These phases include foliated tonalite, granodiorite, monzogranite, quartz diorite and aegirine-bearing monzonite, as well as pegmatite and aplite (Halden and Fryer, 1999; Mumin, 2002). In this report, the focus is on two granodiorite phases (one porphyritic, the other equigranular); carbonatite and associated rare-earth element mineralization within the Eden Lake complex were studied previously by Mumin (2002) and Chakhmouradian et al. (2008), and are not discussed in this report. Porphyritic granodiorite containing K-feldspar megacrysts displays strong foliation and consists of 40–45% K-feldspar (15–26 mm), 15–25% plagioclase, 20–25% quartz, 15–20% biotite (pseudomorph after hornblende) and 1–2% magnetite (Figure 17a). The K-feldspar–megacrystic granodiorite has high MS values of up to 19.9 × 10^{-3} SI. Foliated, equigranular granodiorite is commonly observed on Highway 391 north of Eden Lake and cuts foliated tonalite, both of which are cut by pegmatite and aplite (Figure 17b). This granodiorite displays MS values of 0.605–6.73 × 10^{-3} SI. Overall, the majority of granitoids in this area are comparable to oxidized I-type and magnetite-series granites on the basis of mineral assemblage and MS values

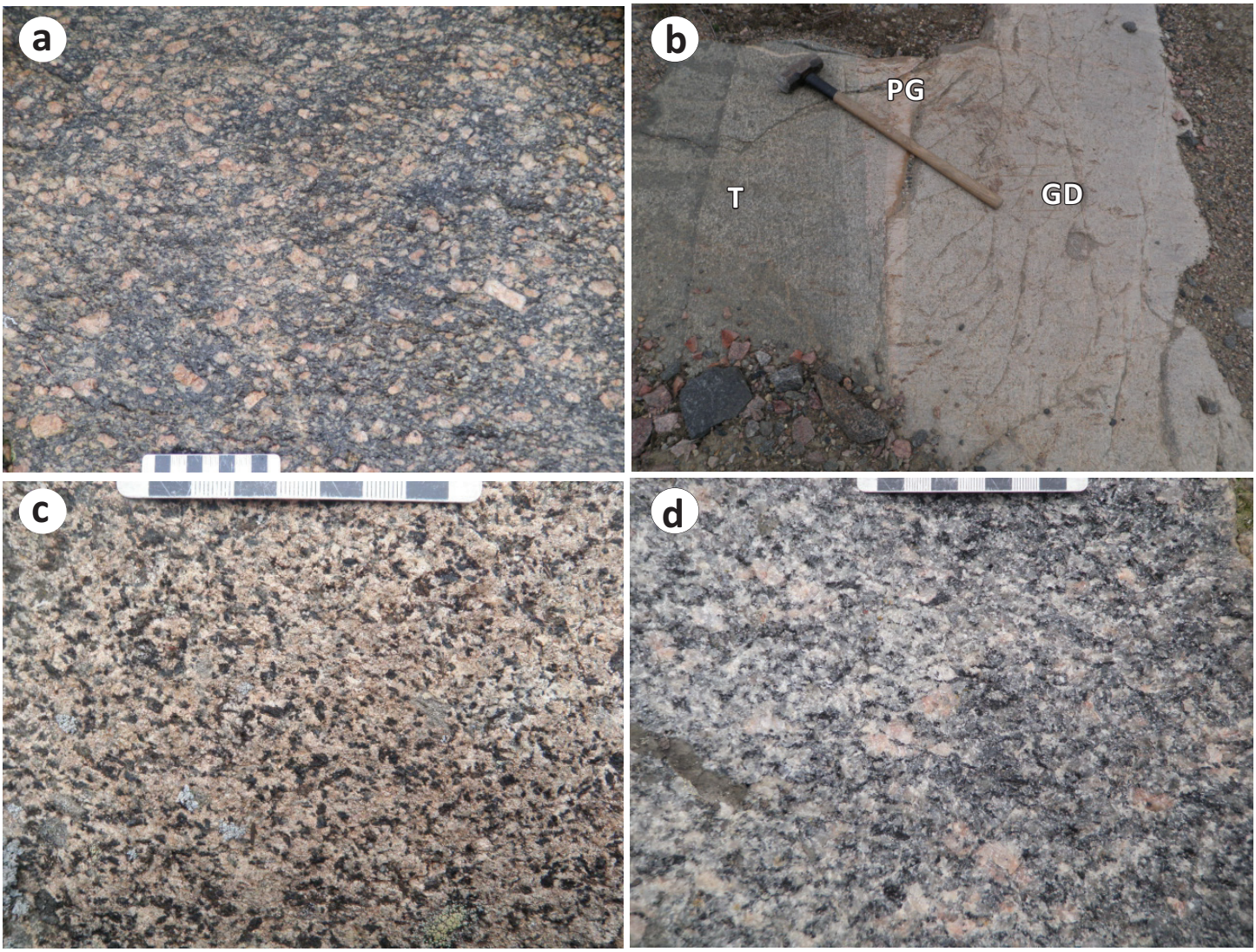

Figure 17: *Field photographs of granitoid rocks from the Leaf Rapids domain:* ***a)*** *K-feldspar megacrysts in porphyritic granodiorite, Eden Lake igneous complex (UTM Zone 14, 423687E, 6291480N, NAD 83);* ***b)*** *foliated, medium-grained tonalite (T) cut by foliated granodiorite (GD) and pegmatite/aplite (PG), Eden Lake igneous complex (UTM 425753E, 6290886N);* ***c)*** *medium- to coarse-grained quartz monzonite, Ruttan Lake pluton (UTM 459422E, 6259658N);* ***d)*** *foliated porphyritic granodiorite, Turnbull Lake pluton (UTM 436557E, 6241927N).*

(Table 2), although the aegirine-bearing monzonite described by Halden and Fryer (1999) may be of A-type (cf. Whalen et al., 1987; Barbarin, 1999).

Ruttan Lake pluton (40)

The Ruttan Lake pluton is a composite granitoid body ranging in composition from quartz monzonite to quartz diorite, granodiorite and granite. This pluton intruded supracrustal rocks of the 1883–1874 Ma Rusty Lake belt of the LRD (Baldwin et al., 1987; Corrigan et al., 2009), which is host to the world-class Ruttan Cu-Zn deposit (Figure 3; Ames et al., 2002; Anderson et al., 2005).

The quartz monzonite is medium grey on fresh surface and weathers reddish grey (Figure 17c). It is medium- to coarse-grained, equigranular, massive and locally moderately foliated. It consists of 15–20% hornblende (3–5 mm), 5–10% biotite (3–5 mm), 25–30% plagioclase laths (3–5 mm) and 15–20% K-feldspar (4–5 mm). The quartz monzonite is cut by fine- to medium-grained granite, aplite and pegmatite dikes.

The granite is dominantly medium-grained, equigranular and massive. It consists of 5–7% biotite flakes (1–2 mm), 25–30% anhedral quartz (2–4 mm), 30–40% K-feldspar (2–5 mm) and 15–20% plagioclase laths (2–4 mm) that display diffuse boundaries. Simple pegmatitic pods to dikes (composed mostly of feldspar, quartz and biotite±muscovite) occur locally in the granite. Also commonly seen are variably shaped xenoliths (e.g., elongate, irregular to subrounded) of greywacke, basalt and amphibolite up to 5 m across. Magnetic susceptibility values of the granite are relatively high, ranging from 2.44 to 10.6 × 10^{-3} SI, consistent with typical magnetite-series and I-type granites elsewhere.

Turnbull Lake pluton (locality 41)

The Turnbull Lake pluton is emplaced into the southern portion of the LRD (Figure 5). It is composed dominantly of foliated porphyritic granodiorite that is cut by subordinate, fine- to medium-grained, pinkish equigranular granite to leucogranite. The porphyritic granodiorite is grey to pinkish grey and contains 5–10% megacrystic subhedral K-feldspar phenocrysts (20–30 mm in length; Figure 17d) in a medium- to coarse-grained groundmass composed of 10–15% biotite (5–10 mm), 1–5% hornblende (8–10 mm), 20–25% quartz (5–10 mm), 20–25% plagioclase laths (5–10 mm), 10–15% K-feldspar (5–10 mm) and minor magnetite (3–5 mm). A roughly east-west foliation trend is defined by aligned feldspars and biotite, generally paralleling the dominant, regional structural trend. The leucogranite is fine- to medium-grained, locally coarse-grained, pinkish to pinkish red, massive and equigranular. It contains 2–5% biotite, 25–30% quartz, 40–50% K-feldspar and 5–10% plagioclase. The feldspar laths exhibit diffuse edges, indicative of sericitic and clay alteration.

Both the foliated granodiorite and massive leucogranite have relatively high MS values of 7.09–18.2 × 10^{-3} SI, typical of magnetite-series and I-type granites. It is worth noting that this granite is similar to evolved I-type granites observed elsewhere, such as in the Lynn Lake greenstone belt (Yang and Beaumont-Smith, 2016, 2017) and in the Appalachians of southwestern New Brunswick (Yang et al., 2008).

Granitoid rocks in the Southern Indian domain

Vandekerckhove Lake pluton (42)

The Vandekerckhove Lake pluton in the Southern Indian domain (SID) is composed dominantly of gneissic granite to granodiorite, locally cut by late pegmatite and aplite dikes. The gneissic granite (Figure 18a**)** is medium-grained and equigranular, and consists of 30–35% quartz, 30–35% K-feldspar, 20–25% plagioclase, 1–5% biotite (locally up to 10% in mafic-rich bands), and minor amphibole. This granite generally exhibits consistent MS values of 1.52–3.27 × 10^{-3} SI, comparable to magnetite-series granite (Ishihara, 1977, 1981, 2004) in terms of MS values and to I-type granitoid rocks (Chappell and White, 1974, 1992) on the basis of mineral assemblages (i.e., biotite±amphibole).

Zed Lake pluton (43)

The Zed Lake pluton is a composite pluton comprising quartz diorite, tonalite, granodiorite and leucogranite, cut by muscovite (±garnet)–bearing pegmatite dikes. Quartz diorite is grey on fresh surfaces and weathers beige to pale grey. It is medium- to coarse-grained, massive, equigranular and locally porphyritic, and consists of 10–15% quartz, 15–20% biotite (pseudomorphic after hornblende) and amphibole, and 60–70% plagioclase (Figure 18b); disseminated pyrite is locally present. The tonalite contains more quartz than the quartz diorite, but the modal percentages of the other mineral phases are similar. Granodiorite is widespread along the shore of Zed Lake and consists of 25–28% quartz, 35–45% plagioclase, 15–25% K-feldspar and 5–10% biotite. Very coarse-grained to pegmatitic leucogranite (Figure 18c), which occurs locally, consists dominantly of quartz and feldspar, with minor muscovite (±garnet) and rare biotite. Pegmatite dikes and sheets are common in the Zed Lake pluton. Rafts of recrystallized fine-grained greywacke (consisting of quartz, feldspar and biotite) up to 2 m in length commonly occur within the pegmatite, similar to the Little Brightsand Lake pluton that comprises pegmatitic granite (Figure 18d) and pegmatite-bearing muscovite and/or garnet. Interestingly, the major granitoid phases of the Zed Lake pluton display a range of MS values from 0.30 × 10^{-3} to 14.1 × 10^{-3} SI (Table 2), consistent with typical magnetite-series or normal I-type granite elsewhere. The leucogranite, however, has much lower MS values of 0.021–0.033 × 10^{-3} SI, which are compatible with those of ilmenite-series and S-type granites.

A sample of two-mica tonalite from the Zed Lake pluton was dated at 1785 ±1.5 Ma (Beaumont-Smith and Böhm, 2002), much younger than the post-Sickle (or Pool Lake) intrusive suite that stitches the northern and southern belts of the LLGB (Milligan,

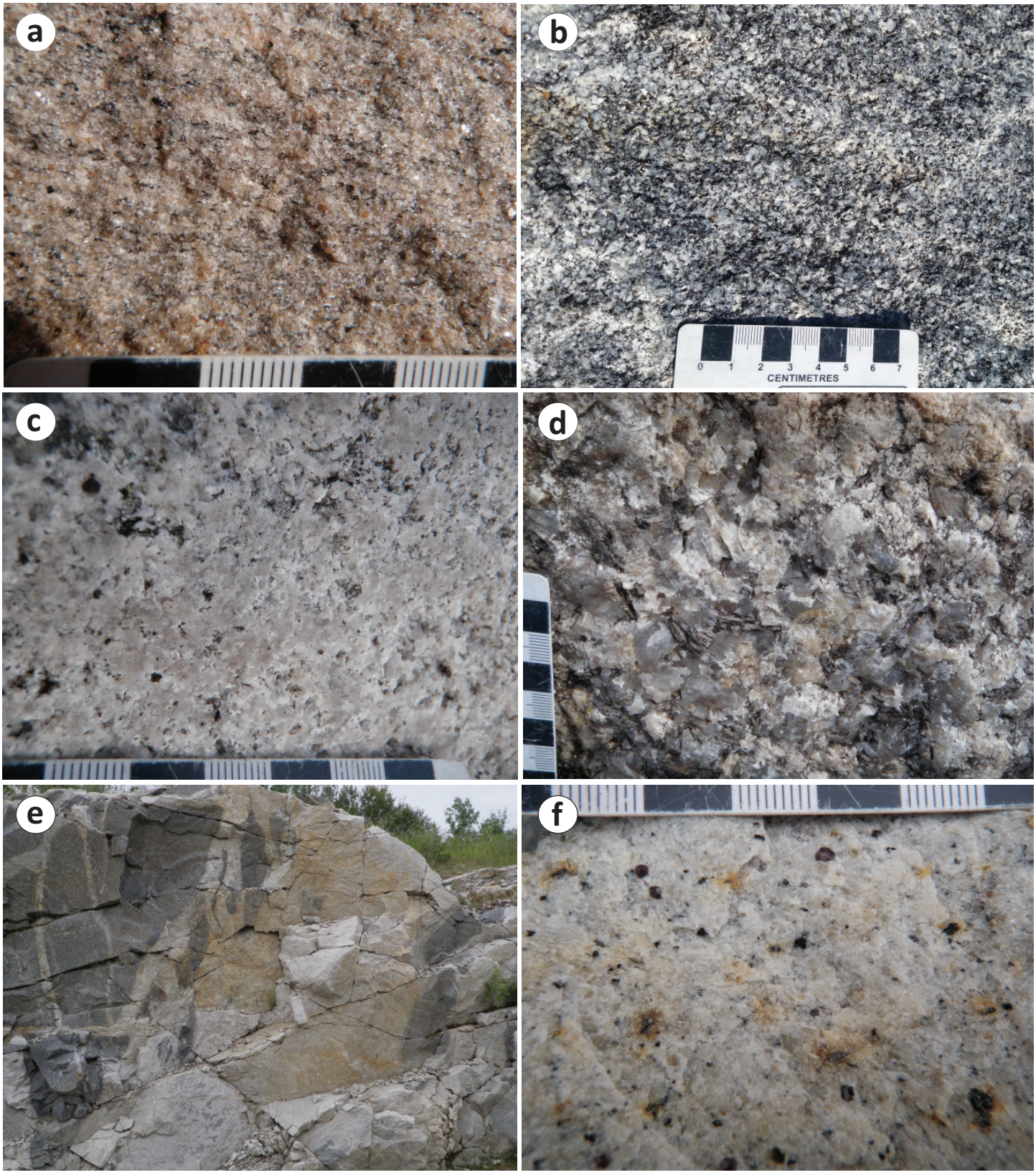

Figure 18: *Field photographs of granitoid rocks from the Southern Indian domain:* ***a)*** *medium-grained granite with weak gneissic fabric, Vandekerckhove Lake pluton (UTM Zone 14, 353570E, 6329018N, NAD 83);* ***b)*** *medium-grained quartz diorite, Zed Lake pluton (UTM 363749E, 6314690N);* ***c)*** *coarse-grained leucogranite, Zed Lake pluton (UTM 361293E, 6315643N);* ***d)*** *pegmatitic muscovite granite, Little Brightsand Lake pluton (UTM 367736E, 6312308N);* ***e)*** *medium-grained garnet-muscovite granite intruded into foliated tonalite, Issett Lake pluton (UTM 4867914E, 6276099N); height of roadcut face is ~8 m;* ***f)*** *medium-grained garnet-muscovite granite, Issett Lake pluton, same location as [e]).*

1960; Gilbert et al., 1980; Baldwin et al., 1987; Zwanzig et al., 1999). This two-mica tonalite could be related to the S-type or ilmenite-series phases of the Zed Lake pluton, as indicated by the presence of muscovite. A garnet-bearing tonalite–monzogranite from the Southern Indian domain was dated at 1846 ±3 Ma by Rayner and Corrigan (2004), suggesting an age range of ca. 1846–1785 Ma for the emplacement of strongly peraluminous S-type granites in the SID.

Little Brightsand Lake pluton (43')

The Little Brightsand Lake pluton comprises two-mica granite, quartz-feldspar porphyry and pegmatite/aplite, mainly exposed and occurring as small intrusions and dikes in Zed Lake greywacke in the northwestern corner of the map area (Figure 5). The two-mica granite is medium- to coarse-grained, undeformed, massive, equigranular and locally porphyritic, and consists of 25–35% anhedral quartz (2–4 mm), 55–60% subhedral to euhedral feldspar (2–4 mm), 4–5% biotite and about ~1% muscovite (Yang, 2021). Thus, this two-mica granite can be termed leucogranite, and it becomes finer in grain size toward the contact with greywacke hostrocks. The contact between the greywacke and two-mica granite is sharp and wavy to irregular, and concentrates biotite aggregates on the greywacke side, typical of contact metamorphism caused by the two-mica granite intrusion.

The granitic rocks from the Little Brightsand Lake pluton have extremely low MS values of 0.018 × 10^{-3} to 0.089 × 10^{-3} SI, consistent with typical S-type granites (Yang and Beaumont-Smith, 2015b; Yang et al., 2019; Yang, 2021).

Issett Lake pluton (44)

The Issett Lake pluton (Figures 3 and 5) contains garnet-muscovite granite that intrudes strongly foliated tonalite (Figure 18e, f). The garnet-muscovite granite is creamy-white on fresh surface and weathers to pale white. It is medium-grained, massive and equigranular. This granite typically contains euhedral, red to dark red garnet crystals (2–3 mm, locally up to 5 mm) and minor muscovite flakes (~1%); it also contains 3–5% biotite (2–3 mm), 30–35% quartz, 50–55% whitish-cream K-feldspar laths (3–4 mm) and 10–15% subhedral to euhedral plagioclase (3–4 mm). Locally, it contains trace disseminated pyrite. This granite has very low MS values of 0.046–0.085 × 10^{-3} SI, typical of S-type and ilmenite-series granites.

Tonalite from the Issett Lake pluton is strongly foliated and medium- to coarse-grained, and consists of 15–17% biotite (pseudomorph after hornblende; minor relict amphibole), 20–25% quartz (3–5 mm), 50–55% subhedral to anhedral plagioclase (3–6 mm in length) with diffuse grain boundaries and 5–10% K-feldspar. Compared to the garnet-muscovite granite described above, the tonalite shows higher MS values, ranging from 0.215 to 10.1 × 10^{-3} SI, consistent with normal magnetite-series and I-type granites (Table 2).

South Bay intrusion (45)

The South Bay intrusion (locality 45 in Figure 5) is dominated by strongly foliated porphyritic quartz monzonite with distinctive K-feldspar megacrysts (Figure 19a). This quartz monzonite phase is cut by late-stage, foliated, medium-grained and equigranular granite and pegmatite dikes (Figure 19b). The porphyritic quartz monzonite typically contains 20–25% euhedral to subhedral K-feldspar megacrysts (20–40 mm in length) and up to 5% subhedral quartz phenocrysts (~20 mm) embedded in a medium- to coarse-grained groundmass comprising quartz, biotite, hornblende, K-feldspar, ±plagioclase, and magnetite. The groundmass consists of 20–25% biotite, 5–10% prismatic hornblende (3–5 mm), 15–25% quartz and 10–15% feldspar. This megacrys-

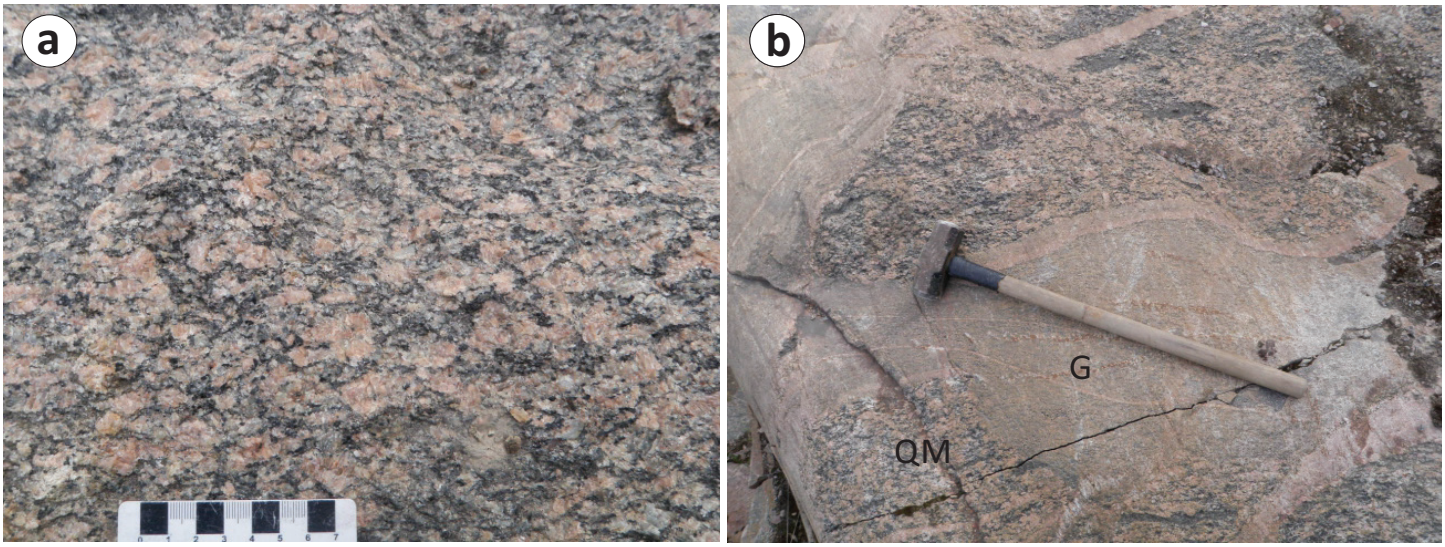

Figure 19: *Field photographs of granitoid rocks from the Southern Indian Lake domain:* ***a)*** *megacrystic K-feldspar in foliated porphyritic quartz monzonite, South Bay intrusion (UTM Zone 14, 504604E, 6296357N, NAD 83);* ***b)*** *medium-grained granite (G) intruded into foliated megacrystic quartz monzonite (QM), South Bay intrusion, same location as (a).*

tic K-feldspar quartz monzonite displays very high MS values of 55.0–72.9 × 10^{-3} SI, indicating that it is a highly oxidized I-type or magnetite-series granite.

The K-feldspar megacrystic quartz monzonite observed in this study is petrographically similar to that of the Chipewyan/Wathaman batholith, as well as other granitoid phases mapped elsewhere in the Southern Indian Lake area (e.g., Kremer, 2008; Martins, 2015; Martins et al., 2022) and at Northern Indian Lake (Kremer and Martins, 2014). A sample of undeformed, K-feldspar megacrystic monzogranite that is mesoscopically indistinguishable from the Chipewyan/Wathaman batholith and containing rafts of folded metasedimentary rocks described by Lenton and Corkery (1981) at Pukatawakan Bay of Southern Indian Lake was dated at 1829 ±1 Ma by Rayner and Corrigan (2004). This age is much younger than those for the Chipewyan/Wathaman batholith (1.87–1.85 Ga; MacHattie, 2001; Corrigan et al., 2009), which prompted Rayner and Corrigan (2004) to suggest that the ca. 1.83 Ga intrusions may represent either a later pulse of the Chipewyan/Wathaman batholith or part of the ca. 1.83 Ga Nueltin suite described by Peterson et al. (2002).

Granitoid rocks in the Kisseynew domain

Granitoid rocks examined and sampled in the KD include granodiorite to garnet-bearing granite and garnet-muscovite-bearing granite of the Notigi Lake intrusive suite (locality 46), garnet-bearing granodiorite of the Wapisu Lake intrusion (locality 47), and granodiorite to granite at Costello Lake (locality 48; see Figure 3; Table 2).

Notigi Lake intrusive suite (locality 46)

Numerous dikes, plugs and small stocks of garnet-bearing granite, grouped into the Notigi Lake intrusive suite (NLIS), intrude paragneiss and migmatite of the Burntwood group (Murphy and Zwanzig, 2007). These granite bodies typically contain up to 5% pinkish to dark red garnet associated with 3–5% dark brown biotite and local minor muscovite. They occur as dikes ranging from a few centimetres to 10 m in width (Figure 20a) and are texturally heterogeneous although massive and equigranular phases are also present, ranging from fine-grained to pegmatitic (Figure 20b). Some of the small intrusions display the coexistence of pegmatitic and medium- to coarse-grained phases (Figure 20c) that form a network of dike-like intrusions within the paragneiss and migmatitic rocks. This strongly suggests that these granitic melts may not have been transported very far from the source region (e.g., Brown, 2010) and clearly indicates that they are derived from partial melting of metasedimentary rocks.

The NLIS granite bodies consist commonly of 30–35% quartz, 50–55% feldspars with diffuse crystal edges, 1–5% biotite, trace to 5% garnet, and local muscovite and trace sulphides, such as pyrite and pyrrhotite. Potassium feldspar is generally the dominant feldspar in the NLIS granitic phases, although granodiorite phases are also present. Granodiorite is medium-grained, massive and equigranular, and contains 40–45% plagioclase (2–3 mm), 10–15% K-feldspar (2–4 mm), 25–30% quartz (2–3 mm) and 5–10% biotite flakes (2–3 mm). Local trace sulphide disseminations are evident, with notable presence of weakly magnetic pyrrhotite. Granodiorite is intruded, fragmented and brecciated by garnet-bearing coarse-grained to pegmatitic granite that seems to form networks on exposed surfaces (Figure 20d).

The NLIS granite and granodiorite phases display very low MS values, normally in the range 0.038–0.065 × 10^{-3} SI, which classifies them as peraluminous S-type (Chappell and White, 1974, 1992, 2001) and ilmenite-series granites (Ishihara, 1977, 1981, 2004). A few higher readings (up to 0.43 × 10^{-3} SI) are interpreted to be due to the presence of weakly magnetic pyrrhotite.

The NLIS described in this report does not include the ca. 1885 Ma, alkaline, K-feldspar–phyric, monzonitic to syenogranitic suite (northeastern Kisseynew domain) at Footprint Lake described in Whalen et al. (2008). The Footprint Lake plutonic suite is interpreted to be formed by low-degree partial melting of subduction-modified subcontinental lithospheric mantle (Whalen et al., 2008).

Wapisu Lake intrusion (locality 47)

The Wapisu Lake intrusion is a small stock comprising garnet-bearing granodiorite intruded into garnet-biotite-feldspar-quartz paragneiss to migmatitic rocks. The granodiorite is fine- to locally medium-grained, light grey, massive and equigranular. It is composed of 5% biotite (0.5–1 mm), 25%–30% quartz (0.5–1.5 mm), 45–55% feldspar laths (1–3 mm) that display diffuse edges, and minor pinkish-red euhedral garnet (1–3 mm). The granodiorite is cut by pegmatite dikes containing K-feldspar, quartz, garnet, biotite and local muscovite. It is worth noting that the Wapisu Lake granodiorite displays very low MS values of 0.046–0.079 × 10^{-3} SI, suggesting that it represents peraluminous S-type granite as defined by Chappell and White (1974) and ilmenite-series granite as defined by Ishihara (1977), which is further evidenced by the presence of magmatic reddish garnet.

Costello Lake pluton (locality 48)

The Costello Lake pluton comprises fairly homogeneous, massive and equigranular granite and granodiorite but displays relatively high MS values (9.70–26.7 × 10^{-3} SI) compared to other intrusive rocks in the KD described above. The granite is fine-grained and pinkish grey on both fresh and weathered surfaces (Figure 20e), and consists of 2–5% biotite (0.5–1 mm), 30–35% quartz (0.5–1.5 mm), 40–50% feldspar (1–3 mm) and 10–15% plagioclase (1–3 mm). Locally, it is cut by simple pegmatite dikes (composed of feldspar+quartz+biotite). The granodiorite (Figure 20f) is medium- to coarse-grained and grey to light pinkish grey, and consists of 10–15% biotite, 5–7% horn-

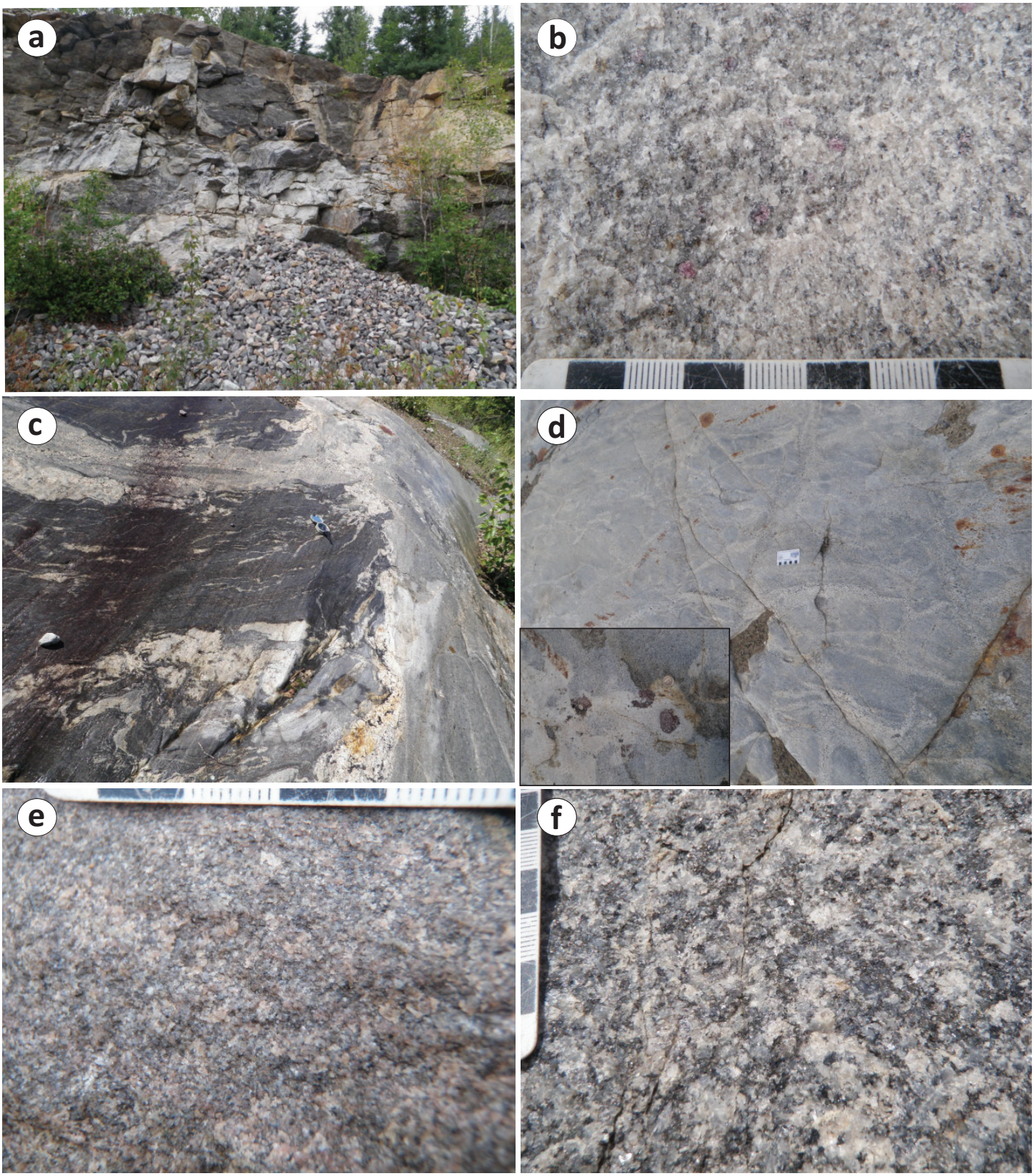

***Figure 20**: Field photographs of granitoid rocks from the Kisseynew domain: **a)** medium- to coarse-grained garnet-bearing granite dikes of the Notigi Lake intrusive suite intruding biotite-garnet-quartz-feldspar paragneiss (height of the quarry wall is about 8 m; UTM Zone 14, 477353E, 6189313N, NAD 83); **b)** medium-grained, massive, garnet-bearing granite (close-up the dike shown in [a]); **c)** medium- to coarse-grained to pegmatitic garnet-bearing granites (at least two phases) in gneissic to migmatitic protolith, Notigi Lake intrusive suite (UTM 474562E, 6189738N); **d)** medium-grained granodiorite intruded and fragmented by garnet-bearing pegmatitic granite, Notigi Lake intrusive suite (UTM 521718E, 6195505N); inset is an enlargement of the pale phase in veins or veinlets in the lower left corner, which contains garnet crystals larger than 1.5 cm; **e)** fine-grained granite, Costello Lake pluton (UTM Zone 14, 435867E, 5224857N); **f)** medium- to coarse-grained granodiorite, Costello Lake pluton (UTM 437743E, 6233556N).*

blende (2–4 mm), 20–25% quartz (3–5 mm), 35–40% plagioclase (4–6 mm) and 10–15% K-feldspar (3–5 mm). The mineral assemblages and MS values of both the granite and granodiorite in this pluton are clearly indicative of I-type and magnetite-series.

Geochemical characteristics of granitoid rocks

Whole-rock geochemical analyses of 323 granitoid samples, including 10 from H.P. Gilbert (unpublished data, 2008), 14 from Beaumont-Smith (2008), 30 from Yang et al. (2019) and 269 from Yang (unpublished data, 2014, 2015, 2016, 2017), are compiled in this report as Data Repository Item DRI2022012. The samples were collected from 48 intrusions and/or plutons (Figures 2 to 5; Table 2) emplaced in various tectonic units of the Archean Superior province and Paleoproterozoic Trans-Hudson orogen (Figure 1). In addition, a subset of 26 samples, including 22 from the western Superior province and four from the Lynn Lake greenstone belt, was selected for Sm-Nd isotope analysis together with the lithogeochemical data to investigate their sources, magmatic processes, and tectonic settings of emplacement, and the results are reported also in DRI2022012. More importantly, potential of some mineralization can be evaluated via geochemical characterization of the granitoid samples, which may have formed at specific stages and/or favorable geological conditions during crustal growth, reworking and evolution throughout the history of Earth.

Figure 1 demonstrates that sampling is geographically concentrated in southeastern and central Manitoba (western Superior province) as well as in northwestern Manitoba (Reindeer zone of Trans-Hudson orogen), and readily accessible at road side, quarries and/or natural exposures mostly close to highways. Some samples were collected from lake shore exposures, for instance, in the Bird River and Lynn Lake greenstone belts. In the following sections, this report presents the geochemical characteristics of the granitoids, and discusses petrogenetic types and metallogenic potential as well as provides some insights on tectonic evolution.

Before presenting the geochemical data, it is necessary to introduce two geochemical parameters: the Gottini index (τ) [= $(Al_2O_3 - Na_2O)/TiO_2$; unit in wt. %], and the Rittmann serial index (σ) [= $(Na_2O + K_2O)^2/(SiO_2 - 43)$; unit in wt. %]. Grasso (1968) proposed to use τ values to discriminate mantle- from crust-derived volcanic rocks. Rittmann (1973) adopted the Gottini index (τ) together with his own serial index (σ) to differentiate volcanic rocks formed in orogenic from anorogenic settings. In fact, the Rittmann serial index (σ) can also be used to define alkalinity of igneous rocks (Yang, 2007), and the Gottini index (τ) can be used to investigate the degree of magmatic differentiation. Both the σ and τ values together with other geochemical parameters and/or elemental ratios of the 323 samples reported in this study are listed also in DRI2022012.

Geochemistry of granitoid rocks from the western Superior province in southeastern Manitoba

Uchi domain (UD)

Classification

This section uses major- and trace-elements diagrams, for example, the total alkalis versus SiO_2 (TAS) and Zr/TiO_2 versus Nb/Y ratios, to classify granitoid samples collected from the UD. Seven samples from the Ross River plutonic suite and two from the Wallace Lake pluton in the UD fall into the fields of granodiorite to granite in the TAS diagram (Figure 21a) of Middlemost (1994). Total (Na_2O+K_2O) contents of these samples increase with increasing silica contents. The granitoid rocks have values of the Rittmann serial index (σ) ranging from 1.1 to 2.0, belonging to calcic- (or tholeiitic) to calcalkaline series (Yang, 2007) and comparable to subalkaline rocks of Irvine and Baragar (1971). Intriguingly, philosophic aspects of Rittmann's earlier work on magmatological tectonics has been highly praised for years (Musumeci et al., 2022 and references therein), requiring more attention when characterizing magmatic rocks including granitoid rocks.

It is noted that all samples display Na_2O/K_2O ratios >1 (ranging from 1.18 to 4.17) except for one sample from the Wallace Lake pluton, which has a Na_2O/K_2O ratio of 0.85 and contains 4.26% K_2O and 74.89% SiO_2 (DRI2022012). This sample belongs to high-K calcalkaline series based on the K_2O versus SiO_2 diagram (not shown) of Peccerillo and Taylor (1976).

In terms of the Shand index (Maniar and Piccoli, 1989), the UD granitoid samples are mainly alumina-saturated and attributed to subaluminous to moderately peraluminous, except for one sample that is metaluminous (Figure 21b). This geochemical feature suggests that the UD granitoids are I-type because their aluminum saturation index (ACNK) <1.1 (Chappell and White, 1974, 1992, 2001), supported also by their relatively high MS values (Table 2). Thus, they are most likely formed by partial melting of igneous source rocks.

On the SiO_2 versus Fe* and MALI plots (not shown), all samples are magnesian and attributed to calcic to calcalkalic granitoids in terms of the geochemical classification of Frost et al. (2001). Note that $Fe^* = FeO^T/(FeO^T+MgO)$, and $MALI = Na_2O+K_2O-CaO$; unit in wt. %. Based on the relationship of Zr contents versus ($10^4Ga/Al$) ratio proposed by Whalen et al. (1987), most of the UD granitoid samples are located in the field of I- and S-type (not shown), except for one sample from the Wallace Lake pluton that is plotted in the field of A-type, suggesting that this sample with high ($10^4Ga/Al$) ratio may have resulted from magmatic fractionation.

Using the Cross, Iddings, Pirsson, Washington (CIPW) normative albite (Ab)-anorthite (An)-orthoclase (Or) ternary diagram of Barker (1979) to portray the UD granitoid samples (Figure 22a) indicates that the Ross River plutonic suite samples are tonalite to trondhjemite, typical of sodium-rich TTG, whereas samples in

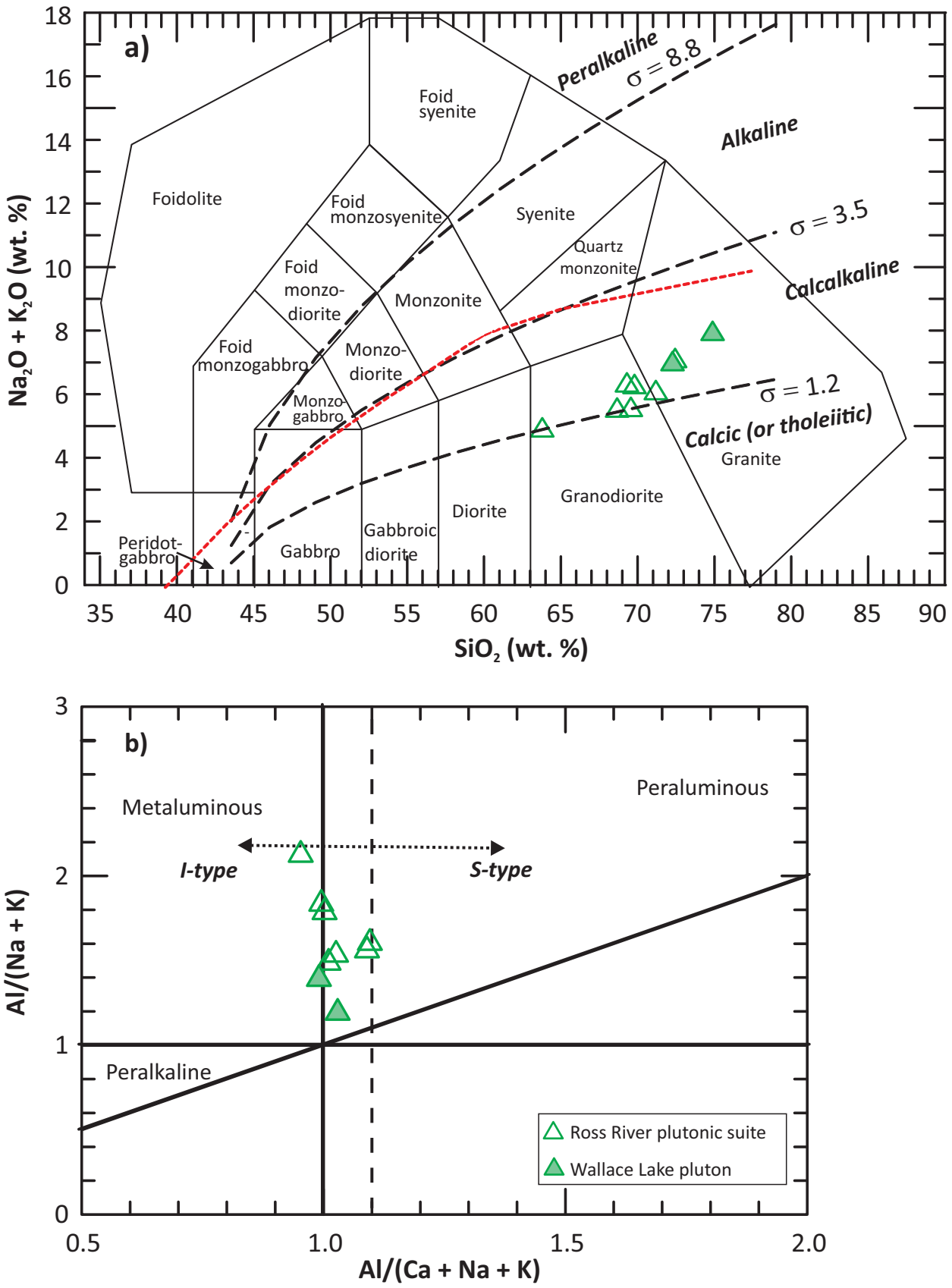

Figure 21: *Chemical classification of granitoids from the Uchi domain based on alkalinity and alumina-saturation index:* ***a)*** *total alkalis (Na_2O+K_2O) versus SiO_2 (TAS; wt. %) diagram (fields from Middlemost, 1994); the boundary (red dashed line) between alkaline and subalkaline series from Irvine and Baragar (1971); the Rittmann serial index σ = $(Na_2O+K_2O)^2/(SiO_2–43)$, unit in wt. % (Rittmann, 1973); using σ values to further subdivide granitoids into calcic (tholeiitic), calcalkaline, alkaline and peralkaline series (Yang, 2007);* ***b)*** *Shand index plot (fields from Maniar and Piccoli, 1989); ACNK = $Al_2O_3/(CaO+Na_2O+K_2O)$, ANK = $Al_2O_3/(Na_2O+K_2O)$, unit in mole; vertical dashed line indicates ACNK = 1.1, a key parameter discriminating S- and I-type granites (Chappell and White, 1974).*

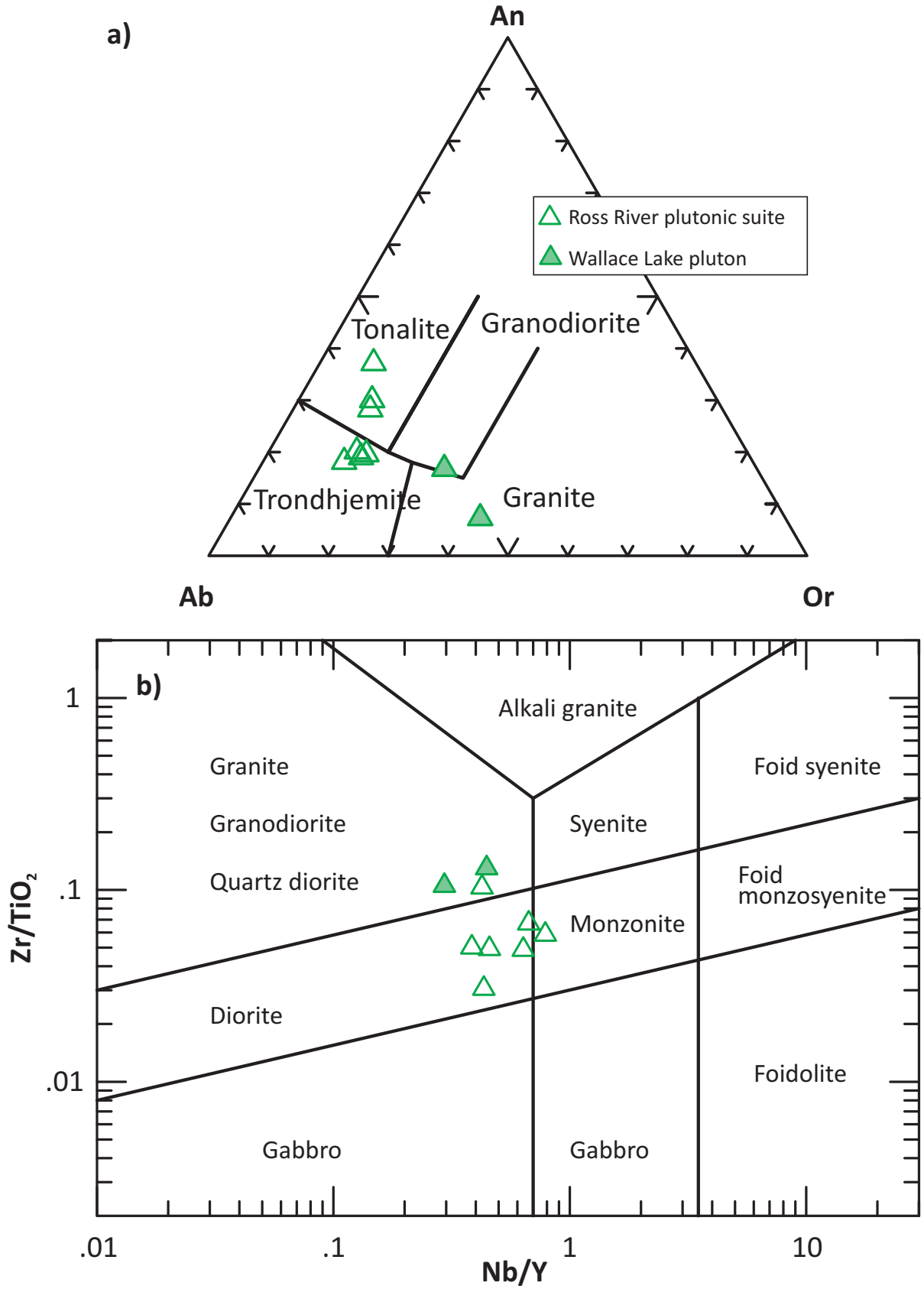

Figure 22: *Chemical classification of granitoids from the Uchi domain in terms of CIPW normative compositions and HFSE:* ***a****) Ab-An-Or ternary diagram (fields from Barker, 1979);* ***b****) plot of Zr/TiO_2 versus Nb/Y (after Pearce, 1996). Abbreviations: Ab, albite; An, anorthite; CIPW, Cross, Iddings, Pirsson, Washington; HFSE, high-field-strength element; Or, orthoclase.*

the Wallace Lake pluton are relatively potassium-rich granite to granodiorite, atypical of Archean TTG. On the Zr/TiO_2 versus Nb/Y diagram (Figure 22b) that uses immobile HFSEs and is thought to be equivalent to the TAS diagram (Pearce, 1996), the UD granitoids are mostly located in the fields of diorite to granite, and only one sample from the Ross River plutonic suite plots as monzonite due to its higher Nb/Y ratio of 0.79 (DRI2022012). Accordingly, this sample is ascribed to be alkaline based on its Nb/Y ratio of >0.7 (Pearce, 1996), but it is calcalkaline based on its σ value of 1.4 (Yang, 2007) as indicated by the TAS diagram (Figure 21a), consistent with the feature of CIPW norms. The high Nb/Y ratio of calcalkaline rocks is interpreted as contamination of continental crust that exhibits both high Nb content (19 ppm) and Nb/Y ratio (0.79; Wedepohl, 1995), and particularly by contamination of the upper continental crust (Rudnick and Gao, 2010).

Trace-element characteristics

Granitoid rocks in the Ross River plutonic suite display relatively high Sr, Ba, but low Rb, Cs contents of large-ion lithophile elements (LILEs). These rocks show low Rb/Sr ratios ranging from 0.05 to 0.13 and relatively high K/Rb ratios of 274–661 (DRI2022012), suggesting that the granitoid magmas derived from a moderately evolved to unevolved source region (e.g., Blevin, 2004; Yang et al., 2019) have undergone limited low degree fractionation. In contrast, the Wallace Lake pluton high-K calcalkaline granites have relatively high Rb, Cs, but low Sr, Ba concentrations, and have high Rb/Sr ratios of 0.65–1.89 and consistently moderate K/Rb ratios of 283–312 (DRI2022012), indicating the granite magmas derived from a moderately evolved source have been experienced relatively high degree of fractionation.

Figure 23a shows chondrite-normalized REE patterns of the UD granitoid rocks, demonstrating fractionation of light relative to heavy REEs, and enrichment and/or depletion of REE abundances compared with the chrondrite values. Granitoid samples from the Ross River plutonic suite show a moderately to strongly light rare-earth element–enriched and heavy rare-earth element–depleted profiles, with small negative to moderately strong positive Eu anomalies, as indicated by Eu/Eu* values of 0.83–1.73 (DRI2022012). Granite samples from the Wallace Lake pluton display very similar light rare-earth element–enriched and HREE-depleted patterns with notably negative Eu anomalies, indicated by Eu/Eu* values of 0.44–0.61 (Figure 23a). This suggests that plagioclase may have played a role in their magmatic evolution. Their total REE abundances are higher with lower La/Yb ratios than those in the Ross River plutonic suite, suggestive of their difference in origin.

Figure 23b shows N-MORB–normalized extended trace-element profiles of the UD granitoid rocks, revealing that they are enriched in incompatible elements and have pronounced negative Nb, Ti and P anomalies. This is a typical arc signature, suggesting that these granitoids may have formed in a magmatic-arc setting (e.g., Prouteau et al., 1999, 2001; Pearce et al., 2005; Pearce, 2008; Yang et al., 2008; Anderson, 2013; Windley et al., 2021).

Granitoid samples from the Ross River plutonic suite have much higher Sr/Y and La/Yb ratios compared with the Wallace Lake pluton (Figure 24a), suggesting that they may have different origins. The former is attributed to medium- to low-pressure TTG that is manifested by the presence of garnet in the source region (Zhang et al., 2006; Moyen and Martin, 2012); the positive correlation between Sr/Y and La/Yb ratios is likely to reflect magmatic fractionation. The latter is not TTG, lacking of garnet but containing feldspar in the source region. The UD granitoids all plot in the field of volcanic-arc granitoids (Figure 24b) proposed by Pearce et al. (1984) in terms of Rb (ppm) and Y+Nb (ppm) contents.

Whalen and Hildebrand (2019) noticed that A-type granitoids have higher concentration of Nb+Y than those emplaced into magmatic arc and/or formed by slab failure magmatism, and arc granitoids display lower Nb/Y and La/Yb ratios than those of slab failure. Based on these geochemical parameters, none of the UD granitoid rocks are A-type, but they are likely to have formed in magmatic arc or by slab failure magmatism (Figure 25a, b).

In summary, the UD granitoid rocks are mostly attributed to Archean TTG suite with typical features of I-type granites, which formed in a magmatic-arc regime. Inter-intrusion variation may be ascribed to differences in their petrogenetic processes, e.g., degree of fractionation, supracrustal contamination, and magma sources.

English River basin (ERB)

Classification

Granitoid samples collected from the ERB are classified on the basis of their major- and trace-element compositions, using the TAS, Shand index and Zr/TiO_2 versus Nb/Y diagrams. Two samples collected from the Tooth-Turtle intrusive suite, seven from the Black River plutonic suite, 32 from the Inconnu pluton and 10 from the Great Falls pluton in the ERB are plotted in the TAS diagram of Middlemost (1994), falling into the fields of granodiorite to granite (Figure 26a). Kushner (2016) described lithogeochemical characteristics of part of the Inconnu pluton in the Cat Creek area (Mayville) based on four samples collected in 2015 as a part of this study (DRI2022012). Total (Na_2O+K_2O) contents are unevenly distributed and do not exhibit any discernable relationship with silica contents in the TAS diagram, reflecting that these granitoid intrusions are unlikely petrogenetically related. These granitoid rocks mostly have σ values between 1.2 and 3.5, typical of the calcalkaline series (Yang, 2007). Two samples from the Inconnu pluton have σ values less than 1.2, belonging to the calcic- (or tholeiitic) series. Together, the ERB granitoids are comparable to subalkaline rocks of Irvine and Baragar (1971).

The ERB granitoid samples can be grouped into two subgroups: one with Na_2O/K_2O ratios >1 (ranging from 1.01 to 5.10) and the other with Na_2O/K_2O ratios <1 (ranging from 0.31 to 0.99). The former is part of TTGs with I-type characteristics (Table

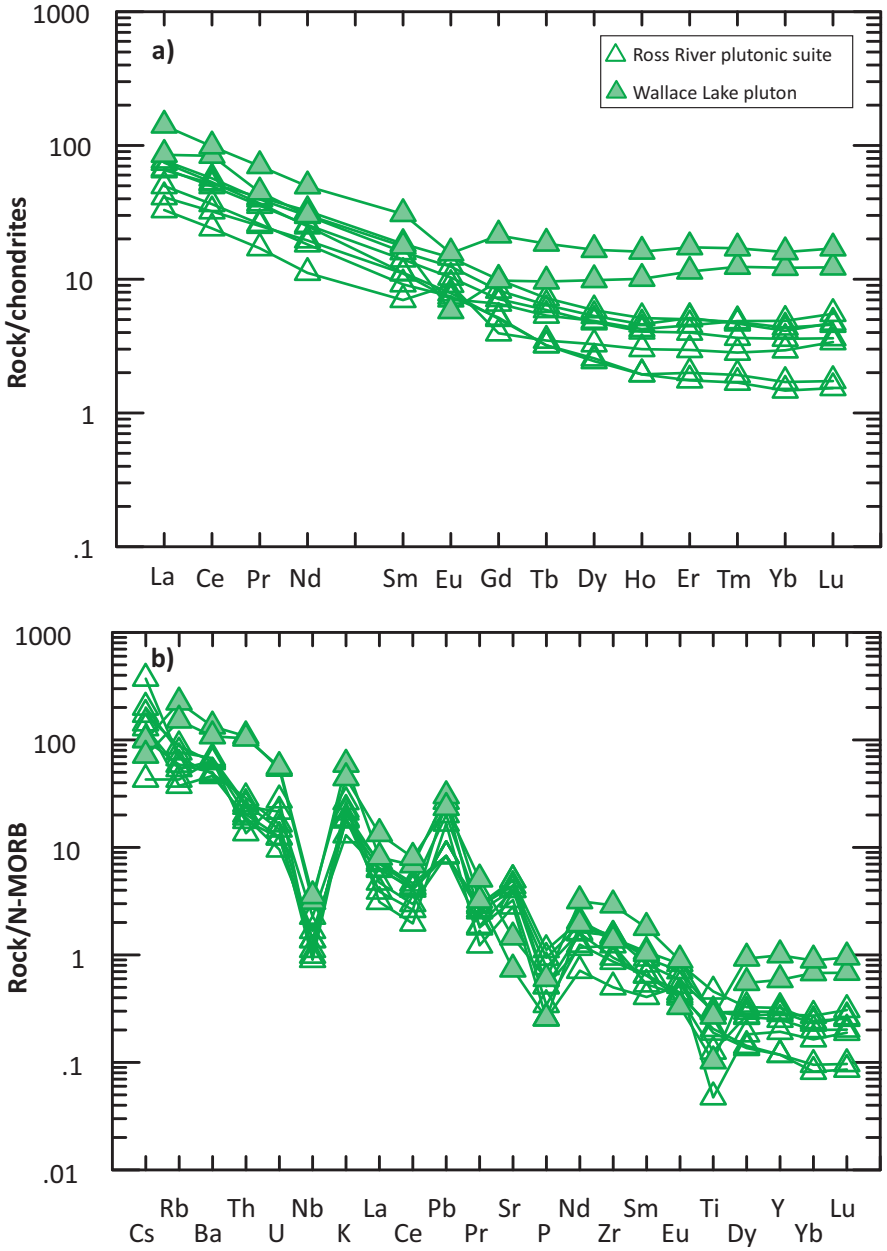

Figure 23: *Trace-element patterns of granitoid rocks from the Uchi domain:* ***a)*** *chondrite-normalized rare-earth element patterns;* ***b)*** *N-MORB–normalized extended trace-element profiles. Normalizing values from Sun and McDonough (1989). Abbreviation: N-MORB, normal mid-ocean–ridge basalt.*

1), whereas the latter belongs to high-K evolved granitoids, some of which are S-type granites. Two samples with remarkable Ta, Nb and Be enrichment (one pegmatitic granite and one spodumene pegmatite) from the Inconnu pluton II (Yang and Houlé, 2020) have abnormally high Na_2O/K_2O ratios of 9.56 to 19.29 (DRI2022012), which are genetically related to strong fractionation of S-type granites emplaced into a collisional zone between the ERB to the north and BRGB to the south (Yang, 2014a; Yang et al., 2019). The high Na_2O/K_2O ratios of these two samples may have been likely caused by sodic metasomatism of internal magmatic fluids derived from S-type intrusions that commonly have low Na_2O/K_2O ratios of <1 (Table 1).

In terms of the Shand index (Maniar and Piccoli, 1989), the granitoid samples from the ERB are mostly alumina-saturated and attributed to subaluminous to strongly peraluminous, except for few samples that are metaluminous (Figure 26b). The geochemical features suggest that some of the ERB granitoid rocks are I-type based on their ACNK of <1.1, whereas some of them are ascribed to S-type with ACNK values >1.1 (Chappell and White, 1974, 1992, 2001). This is consistent with the discrimination result based on MS values and mineral assemblages (Table 2).

On the SiO_2 versus Fe* and MALI plots (not shown) of Frost et al. (2001), granitoid samples in the Tooth-Turtle intrusive suite, and most samples in the Black River plutonic suite and the Great Falls pluton are magnesian, whereas the samples in the Inconnu pluton are either magnesian at lower SiO_2 (<70 wt. %) or ferroan at higher silica that are mostly of S-type (Yang et al., 2019). The ERB granitoid samples are attributed to calcic, calcalkalic to alkali-calcic, consistent with the result of using the TAS diagram

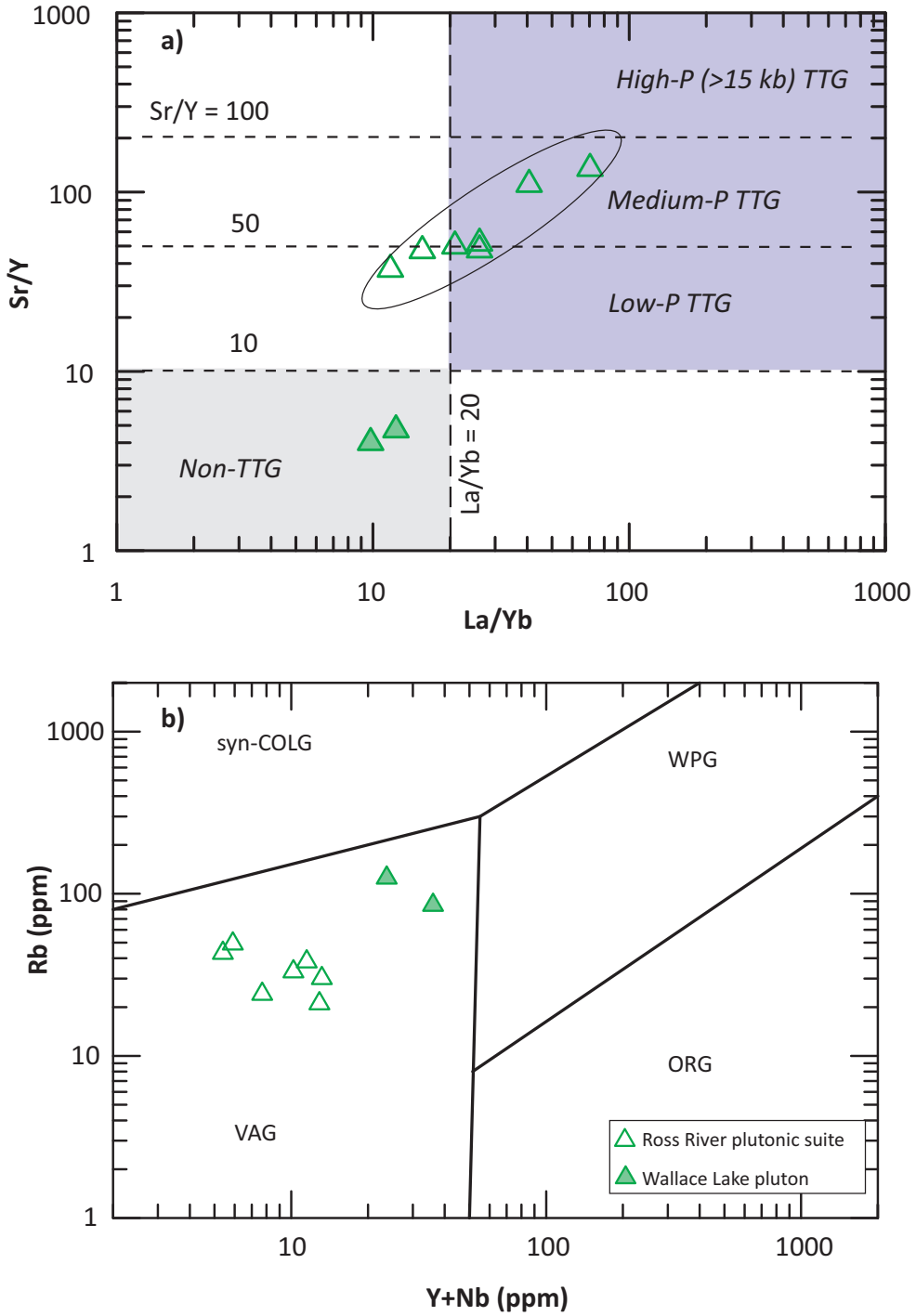

Figure 24: *Discrimination plots for granitoid rocks from the Uchi domain:* ***a)*** *La/Yb versus Sr/Y diagram; boundaries used to define TTG types from Moyen and Martin (2012);* ***b)*** *tectonomagmatic discrimination diagram of (Y+Nb) versus Rb (after Pearce et al., 1984). Abbreviations: ORG, ocean-ridge granitoid; syn-COLG, syncollisional granitoid; TTG, tonalite-trondhjemite-granodiorite; VAG, volcanic-arc granitoid; WPG, within-plate granitoid.*

linked with the Rittmann serial index (Figure 26a). Based on the relationship of Zr contents versus (10^4Ga/Al) ratios (Whalen et al., 1987), most samples plot in the field of I- and S-type (not shown), although some of the samples from the Inconnu pluton fall into the field of A-type. These samples having high (10^4Ga/Al) ratios but low Zr contents (<40 ppm; see DRI2022012) must not be A-type, but may have resulted from magmatic fractionation.

Use of the CIPW Ab-An-Or ternary diagram of Barker (1979) to portray the ERB granitoid rocks (Figure 27a) indicates that samples from the Tooth-Turtle intrusive suite and Great Falls pluton are tonalite to trondhjemite typical of sodium-rich TTG, whereas samples in the Black River plutonic suite and Inconnu pluton display an array of relatively sodium-rich granodiorite transitioning to potassium-rich granite to granodiorite, covering TTG and S-type granites. On the Zr/TiO_2 versus Nb/Y diagram (Figure 27b), the ERB granitoid samples are located in the fields of diorite to granite, some in the monzonite and syenite fields, and few extend into the field of foid syenite. This variation is

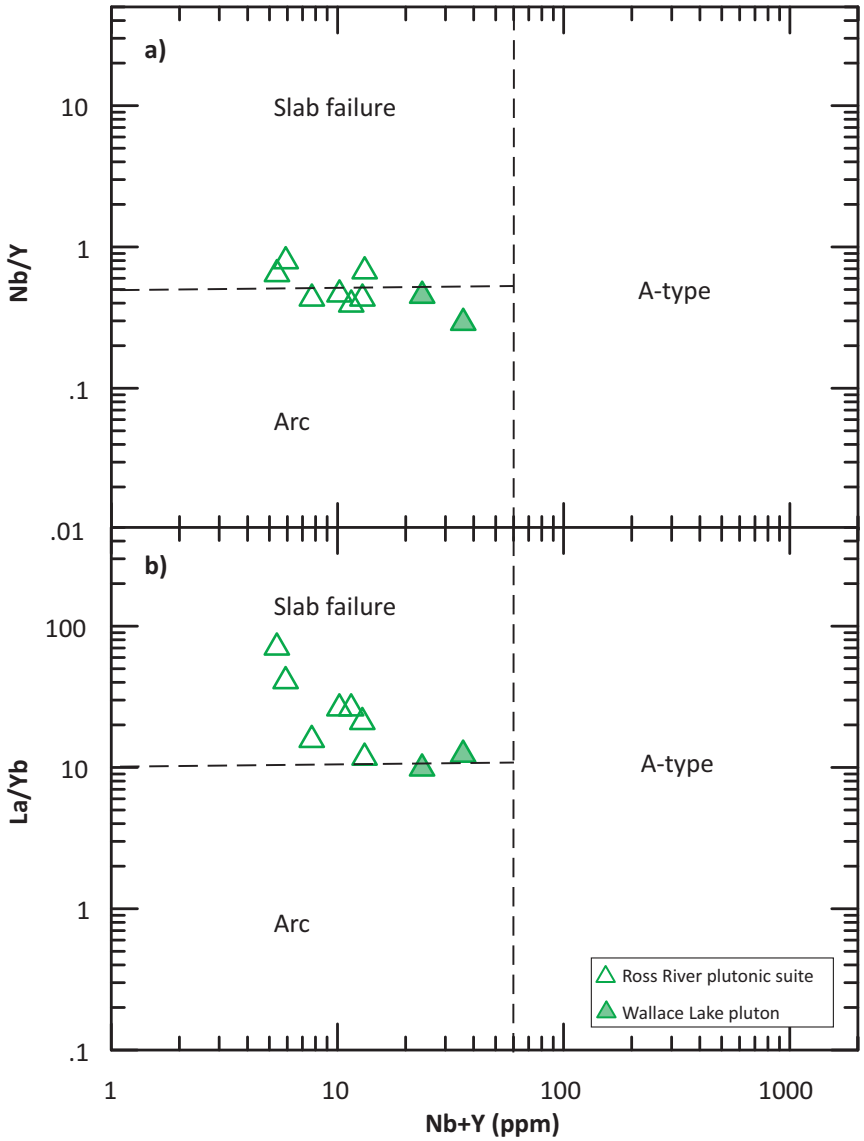

Figure 25: *Discrimination plots of Nb/Y versus Nb+Y (ppm) and La/Yb versus Nb+Y (ppm) for granitoid rocks from the Uchi domain. Boundaries for slab-failure, arc and A-type granitoids from Whalen and Hildebrand (2019).*

due to their relatively higher Nb/Y ratios of >0.7 (DRI2022012). Although these samples may be alkaline based on their Nb/Y ratios (Pearce, 1996), they are mostly calcalkaline based on their σ values ranging from 1.2 to 3.5 (Yang, 2007) as indicated by the TAS diagram (Figure 26a). The high Nb/Y ratios of the ERB calc-alkaline granitoid rocks are likely attributed to contamination of continental crust that exhibits both high Nb content (19 ppm) and Nb/Y ratio (0.79; Wedepohl, 1995), and particularly by contamination of the upper continental crust (Rudnick and Gao, 2010).

Trace-element characteristics

Granitoid rocks in the ERB mostly display variable and relatively high Sr, Ba but low Rb, Cs contents of LILEs, although some of the granite and associated pegmatitic and/or aplitic samples from the Inconnu pluton have high Rb and Cs concentrations. Collectively, the ERB granitoid rocks show a large range of Rb/Sr ratios ranging from 0.07 to 45.27; also, notably, intra- and inter-intrusion variation in Rb/Sr ratios are evident. Such characteristics are interpreted to stem from magmatic fractionation and different magmatic sources (i.e., I- and S-type; Yang et al., 2019). This is also indicated by highly variable K/Rb ratios ranging from 28 to 515 (DRI2022012), suggesting that the granitoid magmas may have been derived from an evolved to unevolved source region (e.g., Blevin, 2004; Yang et al., 2019).

The chondrite-normalized REE patterns of the ERB granitoid rocks shown in Figure 28 indicate enrichment of light rare-earth elements (LREE) relative to heavy rare-earth elements (HREE) and varied enrichment in REE abundances compared with the chrondrite values, except for few pegmatitic to aplitic rocks associated with S-type intrusion of the Inconnu pluton (Figure 28b). These granitoid samples show moderately to strongly LREE-enriched and HREE-depleted profiles, without or with small to moderate negative or moderately strong positive Eu anomalies, as indicated by Eu/Eu* values of 0.29 to 4.21 (see DRI2022012). This suggests that the feldspars played a role in the formation of the ERB intrusions either as a fractionating phase of granitoid

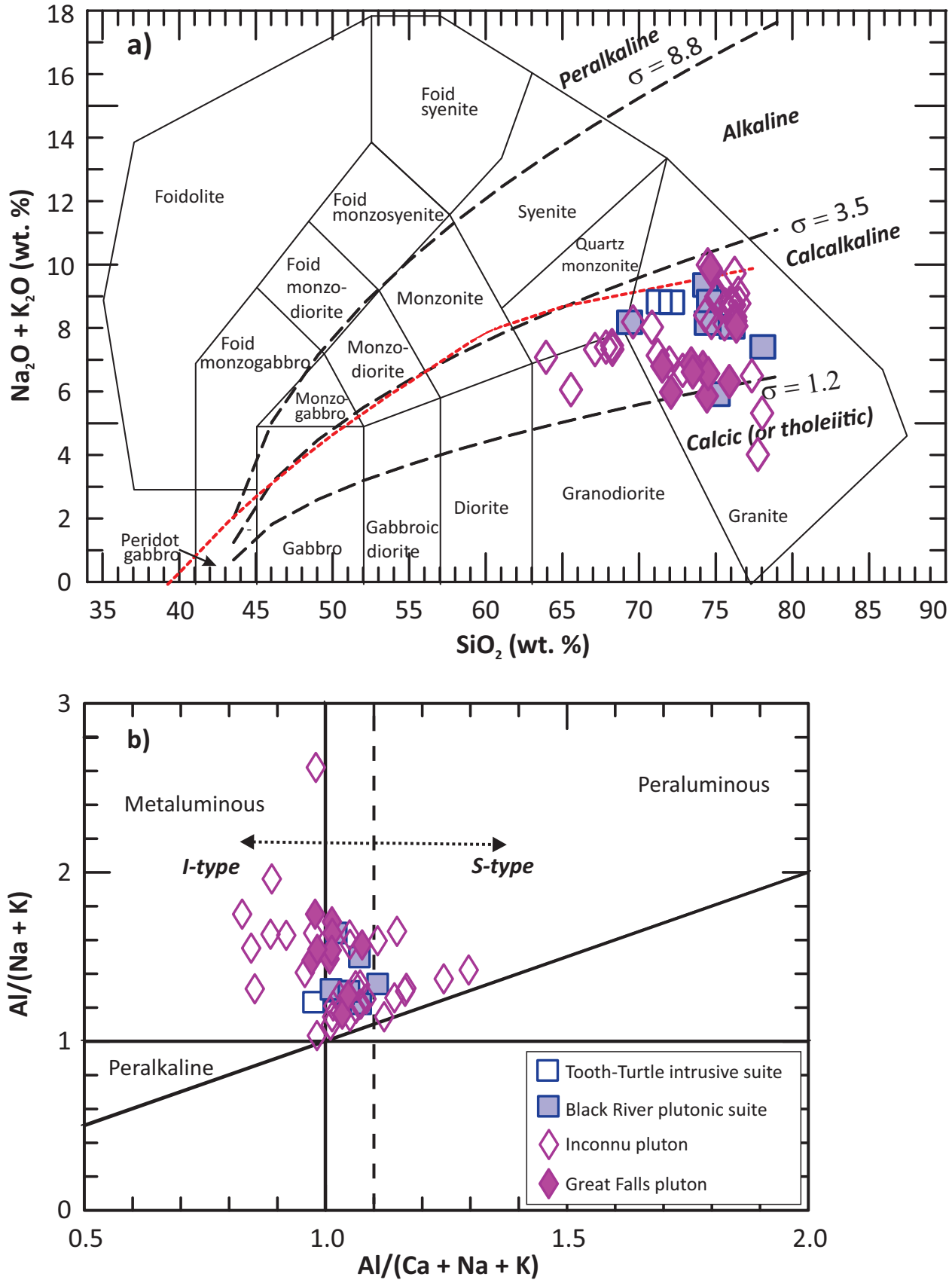

Figure 26: *Chemical classification of granitoids from the English River basin based on alkalinity and alumina-saturation index:* ***a)*** *total alkalis (Na_2O+K_2O) versus SiO_2 (TAS; wt. %) diagram (the fields from Middlemost, 1994); the boundary (red dashed line) between alkaline and subalkaline series from Irvine and Baragar (1971); the Rittmann serial index σ = $(Na_2O+K_2O)^2/(SiO_2–43)$, unit in wt. % (Rittmann, 1973); using σ values to further subdivide granitoids into calcic (tholeiitic), calcalkaline, alkaline and peralkaline series (Yang, 2007);* ***b)*** *Shand index plot (fields from Maniar and Piccoli, 1989); ACNK = $Al_2O_3/(CaO+Na_2O+K_2O)$, ANK = $Al_2O_3/(Na_2O+K_2O)$, unit in mole; vertical dashed line indicates ACNK = 1.1, a key parameter discriminating S- and I-type granites (Chappell and White, 1974).*

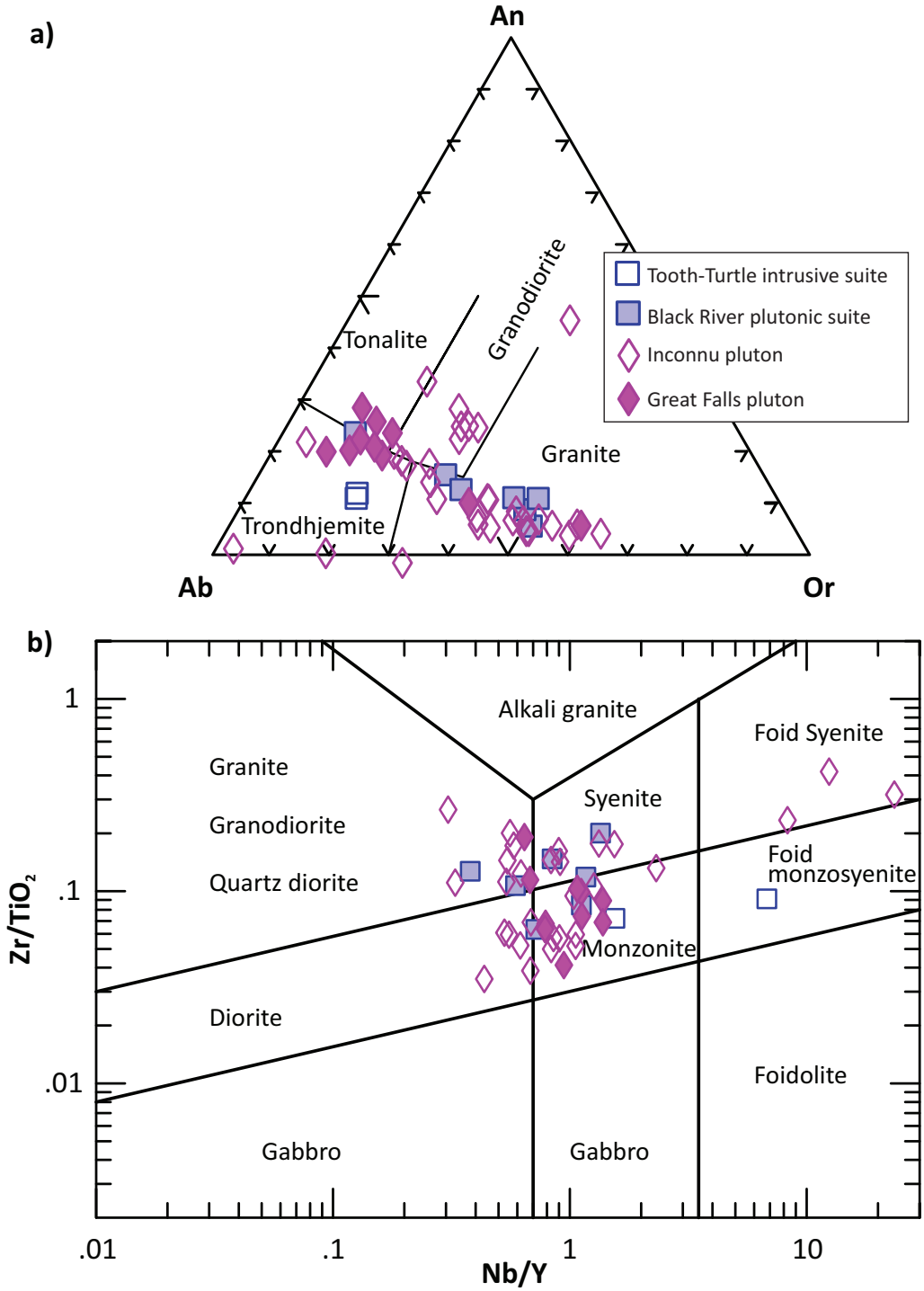

Figure 27: *Chemical classification of granitoids from the English River basin in terms of CIPW normative compositions and HFSE:* ***a****) Ab-An-Or ternary diagram (fields from Barker, 1979);* ***b****) plot of* Zr/TiO_2 *versus Nb/Y (after Pearce, 1996). Abbreviations: Ab, albite; An, anorthite; CIPW, Cross, Iddings, Pirsson, Washington; HFSE, high-field-strength element; Or, orthoclase.*

magmas or as a residual phase in the source region. For example, the values of Eu/Eu* in the Tooth-Turtle intrusive suite are 0.80 to 0.92, suggesting that feldspar did not significantly separate from the magmas during its petrogenesis. In contrast, some of the Inconnu pluton S-type granites have lower values of Eu/Eu* from 0.29 to 0.50, revealing that a significant amount of feldspars were likely present in their source region as residual phases whilst the magmas were extracted from the soure region (Yang et al., 2019).

Figure 29 shows N-MORB–normalized extended trace-element profiles of the ERB granitoid rocks, revealing that they are enriched in incompatible elements and have pronounced negative Nb, Ti and P anomalies. This is a typical arc signature, suggesting that these granitoids may have formed in a magmatic-arc setting (e.g., Prouteau et al., 1999, 2001; Pearce et al., 2005; Pearce, 2008; Anderson, 2013). However, the S-type granites from the Inconnu pluton also show similar trace-element signatures (Figure 29b), but display more enrichment in LILEs, e.g.,

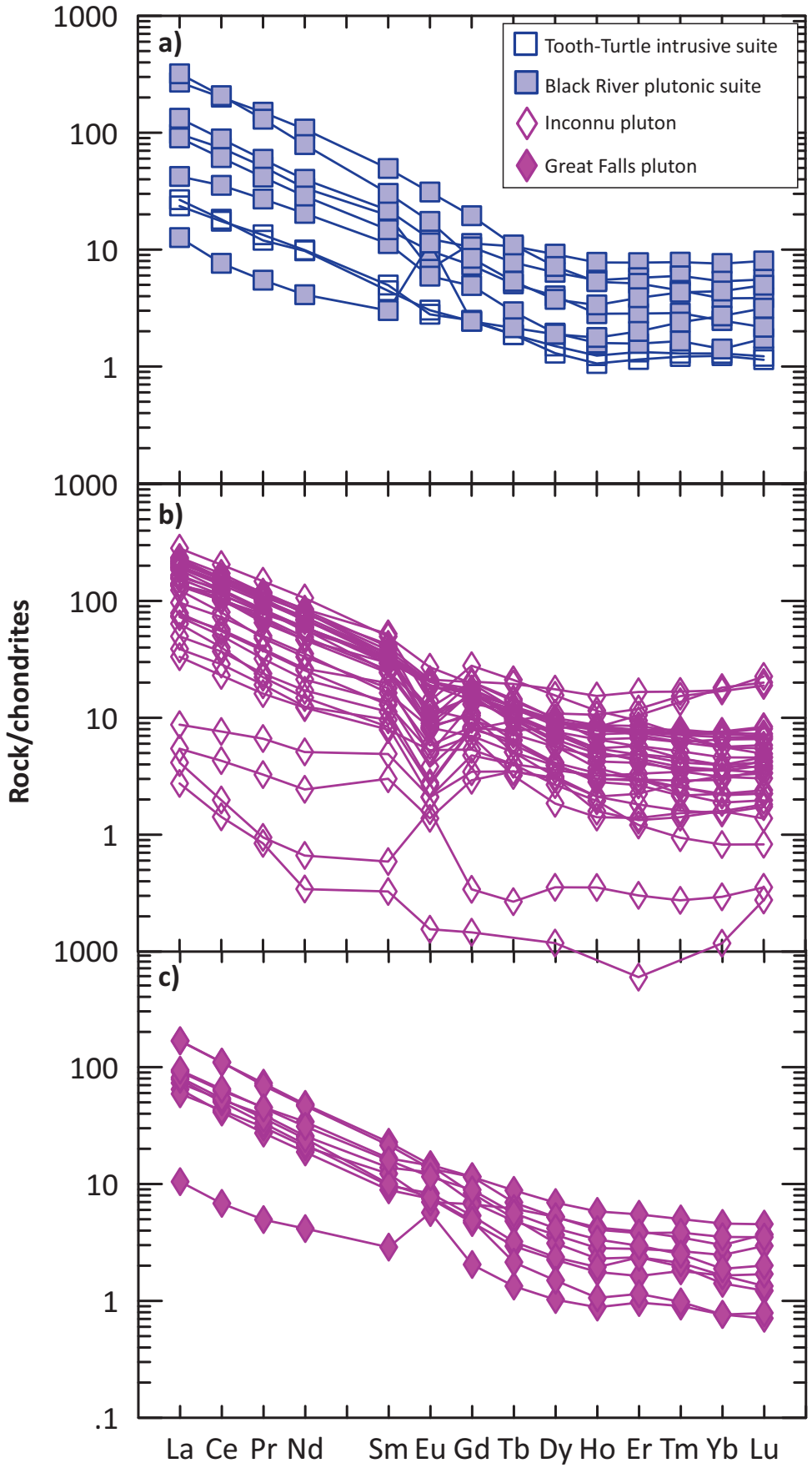

Figure 28: *Chondrite-normalized rare-earth element patterns of granitoid rocks from the English River basin:* ***a)*** *samples from the Tooth-Turtle intrusive suite and Black River plutonic suite;* ***b)*** *samples from the Inconnu pluton;* ***c)*** *samples from the Great Falls pluton. Normalizing values from Sun and McDonough (1989).*

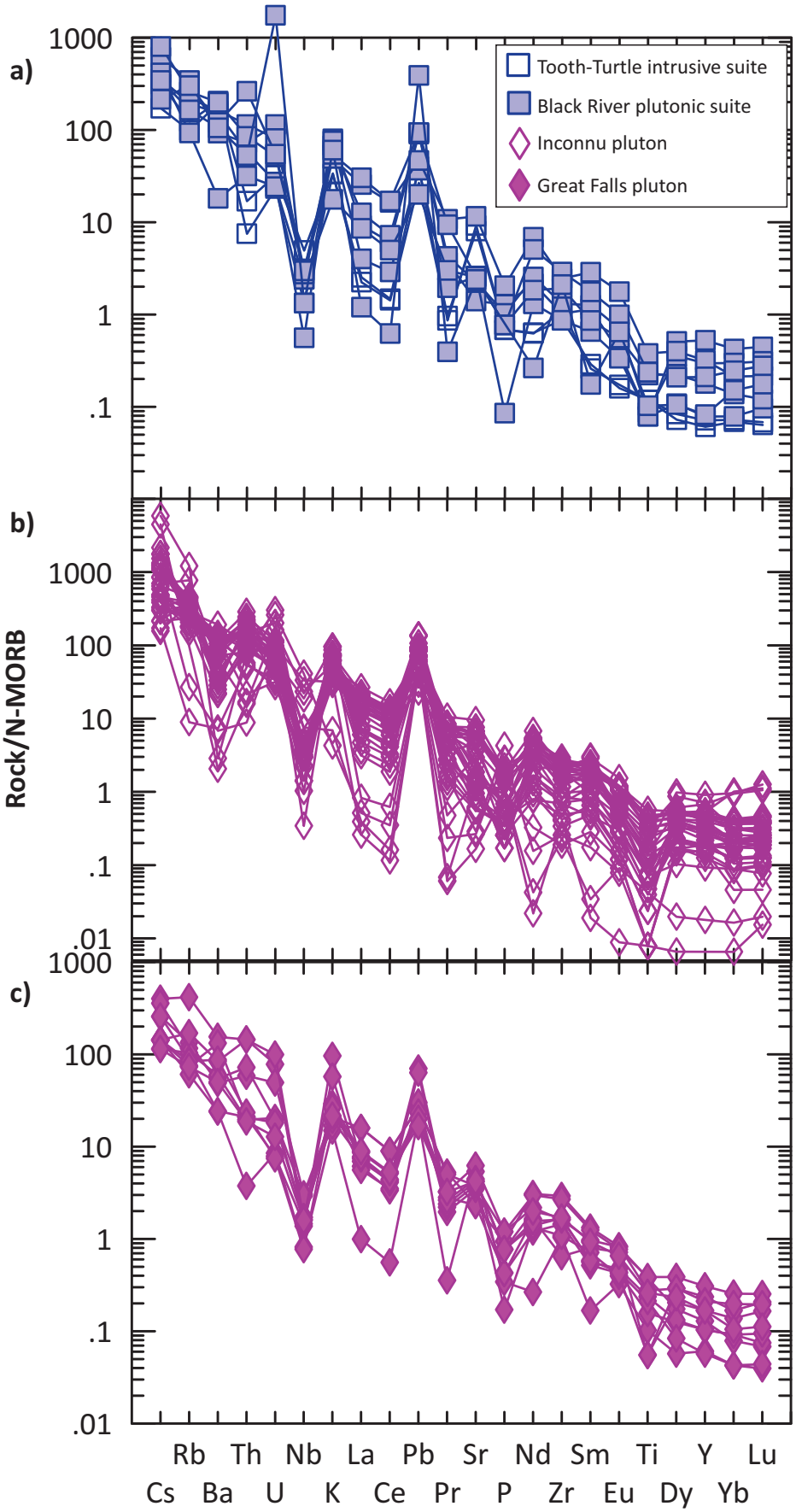

***Figure 29**: N-MORB–normalized extended trace-element profiles of granitoid rocks from the English River basin: **a)** samples from the Tooth-Turtle intrusive suite and Black River plutonic suite; **b)** samples from the Inconnu pluton; **c)** samples from the Great Falls pluton. Normalizing values from Sun and McDonough (1989). Abbreviation: N-MORB, normal mid-ocean–ridge basalt.*

Cs being >1000 times higher than the normalized values of Sun and McDonough (1989). This is interpreted by the sedimentary source rocks of S-type granites that had largely inherited the geochemical characteristics of their provenance, probably derived from arc rocks (Yang et al., 2019; Yang and Houlé, 2020).

Granitoid samples from the ERB display varied Sr/Y and La/Yb ratios ranging from very high to low values (Figure 30a), which are attributed either to TTGs whose responsible magmas were derived from different depths or to S-type granites (non-TTGs) resulting from partial melting of metasedimentary rocks in a thickened crust due to terrane collision (Yang et al., 2019). This suggests the ERB contains granitoid intusions of different origins. The Tooth-Turtle intrusive suite is likely high-pressure TTG, whereas the Black River plutonic suite, the Great Falls pluton and part of the Inconnu pluton (i.e., phase I) are attributed to medium- to low-pressure TTG, that is manifested by the presence of garnet in the source region (e.g., Zhang et al., 2006; Moyen and Martin, 2012). The Inconnu pluton (i.e., phase II) are S-type granites that occur within the terrane boundary zone (Figure 2) that is in fact a collision zone (Yang et al., 2019). Intra-intrusion variation in Sr/Y and La/Yb ratios that show positive correlation is likely caused by magmatic fractionation. The S-type granites of the Inconnu pluton II are distinct from TTG, lacking of garnet but containing feldspar in their source region.

The ERB granitoid rocks mostly plot in the field of volcanic-arc granitoids (Figure 30b) proposed by Pearce et al. (1984) in

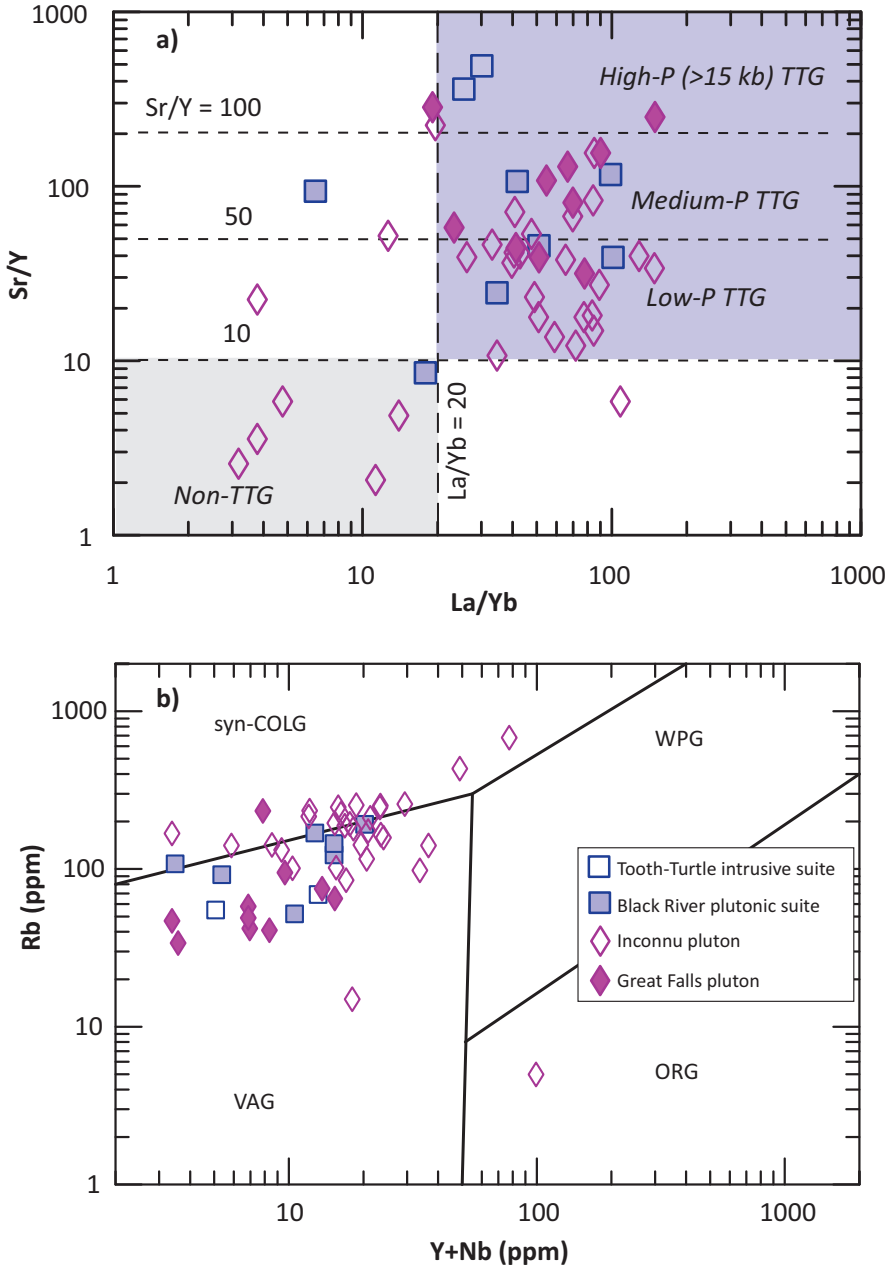

Figure 30: *Discrimination plots for granitoid rocks from the English River basin:* ***a)*** *La/Yb versus Sr/Y diagram; the boundaries used to define TTG types are from Moyen and Martin (2012);* ***b)*** *tectonomagmatic discrimination diagram of (Y+Nb) versus Rb (after Pearce et al., 1984). Abbreviations: ORG, ocean-ridge granitoid; syn-COLG, syncollisional granitoid; TTG, tonalite-trondhjemite-granodiorite; VAG, volcanic-arc granitoid; WPG, within-plate granitoid.*

terms of their Rb and Y+Nb contents, whereas the S-type granites of the Inconnu pluton II belong to syn-collisonal granites.

The ERB granitoid rocks display many similarities to those formed by slab failure magmatism in magmatic-arc environments (Figure 31a, b), which are different from A-type granitoids that have much higher concentrations of Nb+Y as pointed out by Whalen and Hildebrand (2019). Furthermore, arc granitoids display lower Nb/Y and La/Yb ratios than those of slab failure magmatism. Based on these geochemical parameters, none of the ERB granitoid rocks are A-type, which are likely to have formed by magmatic arc to slab failure magmatism.

In summary, the ERB granitoid rocks are mostly attributed to Archean TTGs with typical features of I-type granites, which formed in a magmatic-arc setting, but part of the Inconnu pluton (phase II) belongs to the S-type granites formed in a collisional zone. Intra-variation in geochemical composition is likely due to magmatic fractionation, while inter-intrusion variation may have been ascribed to differences in their petrogenetic processes (e.g., degree of fractionation, supracrustal contamination, and magma sources).

Bird River domain (BRD)

Bedrock mapping conducted recently by the MGS (Gilbert et al., 2008; Yang and Houlé, 2020) indicates that the Neoarchean BRGB, a major part of the Bird River domain (BRD), comprises supracrustal rocks and associated mafic–ultramafic intrusive

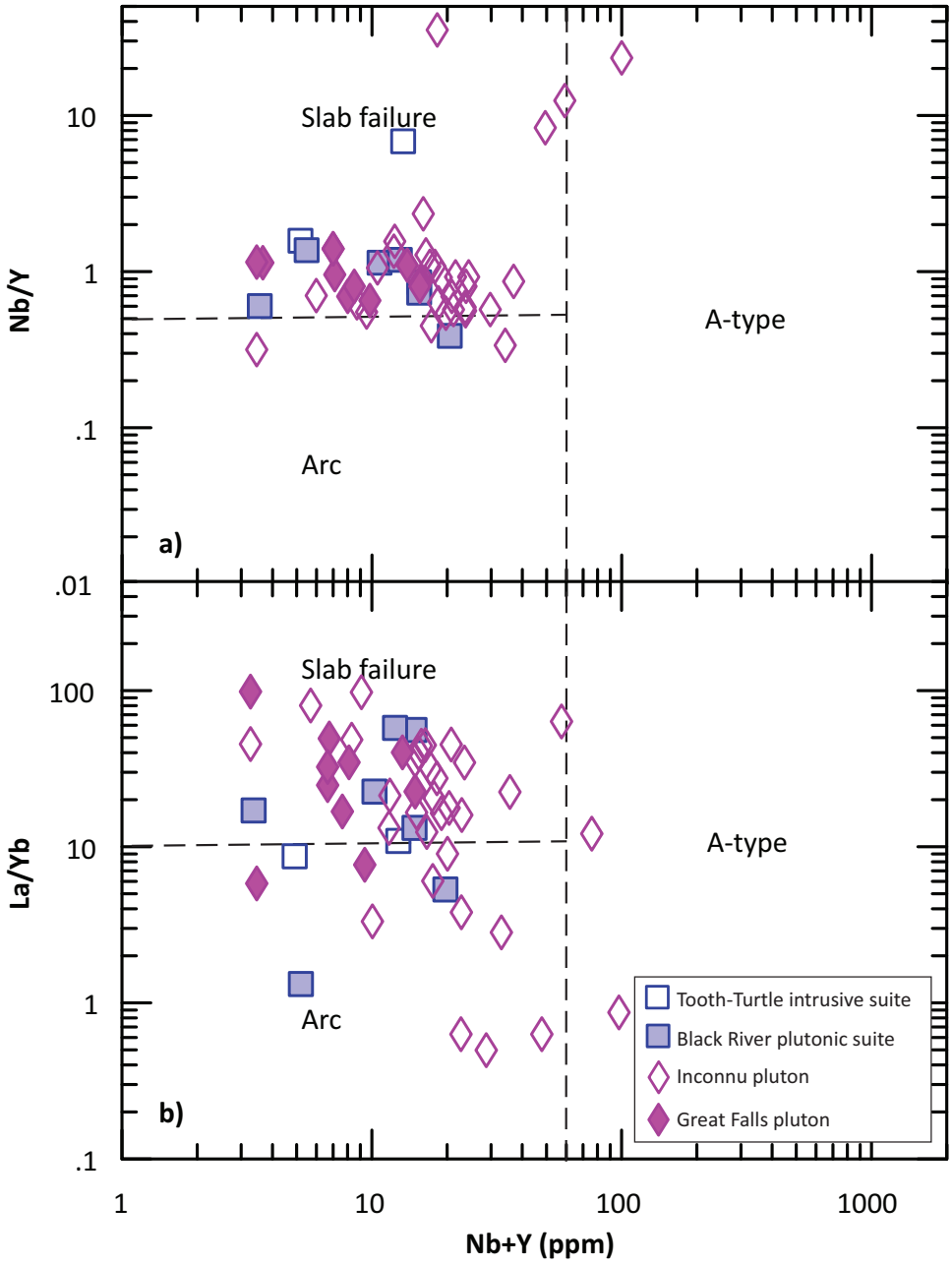

Figure 31: *Discrimination plots of Nb/Y versus Nb+Y (ppm) and La/Yb versus Nb+Y (ppm) for granitoid rocks from the English River basin. Boundaries for slab-failure, arc and A-type granitoids from Whalen and Hildebrand (2019).*

rocks emplaced and/or deposited atop the Mesoarchean granitoid basement and intruded by various Neoarchean granitoid plutons and/or intrusions (ca. 2.70 to 2.65 Ga). Uplifting induced extension resulted in deposition of epiclastic sedimentary rocks (e.g., polymictic conglomerate, greywacke, and siltstone to mudstone) in local synorogenic basin(s), which overlay unconformably the supracrustal sequences; late Neoarchean intrusions cut the entire supracrutal and epiclastic packages.

In the following sections, the major geochemical characteristics are presented of Mesoarchean granitoid rocks from the basement (i.e., the Maskwa Lake batholith I), and of the Neoarchean granitoids (i.e., the Maskwa Lake batholith II, Marijane Lake pluton, Tin-Osis lakes intrusion, Birse Lake pluton, Bird River sanukitoid; see Figure 2 and Table 2) cutting the basement of the BRGB, respectively. As part of this study, Drayson (2016) described the geochemical features of granitic rocks in the Tin-Osis lakes area. Sotiriou et al. (2019, 2020) presented an extensive geochemical dataset on the anorthosite complexes (i.e., the Bird River sill, Mayville intrusion) and associated supracrustal rocks intruded by the Neoarchean phases of TTG from the Maskwa Lake batholith II, and suggested that the BRGB may have formed in a continental backarc geodynamic setting, consistent with the conclusions of MGS mapping (e.g., Gilbert et al., 2008; Yang and Houlé, 2020).

Basement granitoid rocks: classification

Based on major-element composition, the basement granitoid rocks of the BRGB represented by the Mesoarchean phases of the Maskwa Lake batholith I (Table 2) fall dominantly within the fields of granodiorite and granite in the TAS diagram, although two samples plot in the fields of quartz diorite and monzonite, respectively (Figure 32a). All samples are subalkaline based on the definition of Irvine and Baragar (1971), and most are calcic (tholeiitic) in terms of alkalinity (σ <1.2, see DRI2022012; Yang, 2007), except for a few that plot in the calcalkalic and alkali-calcic fields (1.2<σ <3.5; Figure 32b). Based on the Fe* index (Frost et al., 2001), these granitoids are dominantly magnesian, although a few evolved phases fall into the ferroan field (Figure 32c). On the Shand index plot (Figure 32d), they are weakly to moderately peraluminous, although a sheared granite (sample 111-13-190C01; solid red reverse triangle) that was termed muscovite-biotite schist based on texture and mineral assemblage in the field is strongly peraluminous due to the presence of secondary muscovite. In addition, sample 111-13-221A01 is metaluminous. Using an ACNK of 1.1 as the boundary for differentiating I-type (<1.1) from S-type (>1.1) granites (Figure 32d; Chappell and White, 1974), the basement granitoid rocks are I-type, and therefore most likely derived from partial melting of igneous source rocks that typically contain titanite and apatite (e.g., Bruand et al., 2020). More interestingly, these rocks display a range of lithologies from TTG to granite (Figure 32e), typical of Archean TTG suites (Barker, 1979). This is also consistent with the observation on the TAS diagram (Figure 32a) that the granitoid rocks span a wide compositional space.

The basement granitoid rocks of the BRGB display a range of σ values from 0.01 to 3.48 (DRI2022012), suggesting that they are calcic to calcalkaline as defined by Yang (2007). This is consistent with the classification results obtained in Figure 32b and is also confirmed by variation in their Nb/Y ratios that are consistently less than 0.7 on the Zr/TiO_2 versus Nb/Y plot (Figure 32f), typical of subalkaline affinity (Pearce, 1996). In addition, these granitoid rocks exhibit varied Zr/TiO_2 ratios that are mostly higher than 0.05, reflecting relatively evolved characteristics (Figure 32f), although sample 111-12-28B01 falls into the field of unevolved gabbro.

Basement granitoid rocks: trace-element geochemistry

The basement granitoid rocks in the Maskwa Lake batholith I have low Rb (up to 180 ppm), relatively high Sr (up to 196 ppm) and Ba (up to 5080 ppm) contents, with low Rb/Sr ratios that are mostly <1 (DRI2022012), suggesting a limited degree of magmatic fractionation after separation from the magma source. However, the granitoids display variable K/Rb ratios that range from 116 to 563 but are mostly higher than 200, indicating that their sources were unevolved to moderately evolved (cf. Blevin, 2004). This is consistent with their moderate abundances of transitional elements (e.g., Cr, Co, Ni).

Chondrite-normalized REE patterns of the basement granitoid rocks show moderately to strongly LREE–enriched and HREE–depleted profiles, mostly with small negative Eu anomalies as indicated by the Eu/Eu* values of 0.33–0.94. Some granite samples, however, do not have Eu anomalies (Eu/Eu* = 0.97–1.00; Figure 33a). The abundances of total REE vary remarkably, ranging from a few up to 650 times chondritic values. Also, LREE and HREE are moderately to strongly fractionated, manifested by chrondrite-normalized ratios of $(La/Yb)_N$ ranging from 3 to 120. Intra-HREE fractionation, however, is relatively weak, with $(Gd/Yb)_N$ ratios ranging from 0.9 to 2.5 (DRI2022012).

Primitive-mantle–normalized extended trace-element profiles of the basement granitoid rocks show that they are enriched in incompatible elements, with pronounced negative Nb, Ta and Ti anomalies (Figure 33b). This is a typical arc signature, suggesting that these granitoids may have been formed in an arc-type setting (e.g., Rollinson, 1993; Pearce and Peate, 1995; Pearce et al., 2005; Pearce, 2008; Yang et al., 2008; Anderson, 2013).

On the Pearce et al. (1984) discrimination diagram, all granitoid samples fall in the field of volcanic arc granitoids (Figure 34a). On the plot of log τ versus log σ (not shown), all samples fall in the field of orogenic belts and island arcs. Note that τ values range from 28.86 to 90.05 (DRI2022012), consistent with characteristics of granitoids from unevolved to moderately evolved source(s) that are also indicated by the moderate to high K/Rb ratios described above. On the plot of Nb/Ta versus Zr/Sm (Figure 34b), the basement granitoid rocks display relatively low Nb/Ta ratios (<17.4) and high Zr/Sm ratios (>25.2) when compared to primitive mantle, MORB, oceanic-island basalt and island-arc basalt, and are more similar to Archean TTG and/or adakite

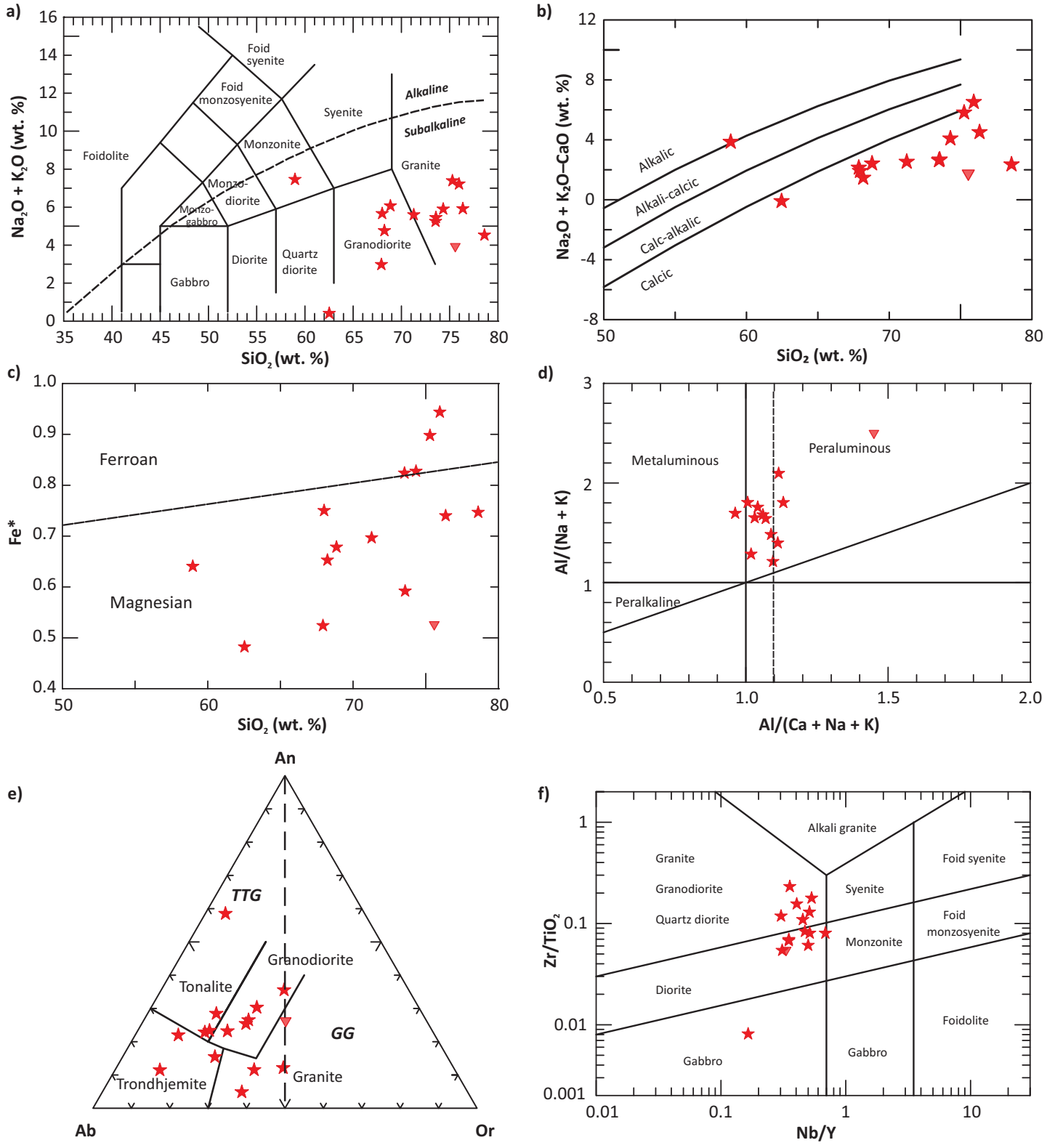

Figure 32: *Chemical classification of the basement granitoid rocks of the Maskwa Lake batholith I from the Bird River greenstone belt:* ***a)*** *total alkalis (Na_2O+K_2O) versus SiO_2 (TAS; wt. %) diagram (fields from Middlemost, 1994); boundary between alkaline and subalkaline series from Irvine and Baragar (1971);* ***b)*** *plot of MOLI (i.e., $Na_2O+K_2O–CaO$) vs. SiO_2; wt. %; after Frost et al. (2001);* ***c)*** *classification of ferroan versus magnesian granitoids ($Fe^* = FeO^t/(FeO^t+MgO)$; wt. %; from Frost et al. (2001);* ***d)*** *Shand index plot (fields from Maniar and Piccoli, 1989); ACNK = $Al_2O_3/(CaO+Na_2O+K_2O)$, ANK = $Al_2O_3/(Na_2O + K_2O)$, moles; vertical dashed line indicates ACNK = 1.1, a key parameter discriminating S- and I-type granites (Chappell and White, 1974);* ***e)*** *Ab-An-Or ternary diagram (fields from Barker, 1979);* ***f)*** *plot of Zr/TiO_2 versus Nb/Y (after Pearce, 1996). Note: solid red reverse triangle indicates muscovite-biotite schist sampled from a shear zone cutting the basement granitoid.*

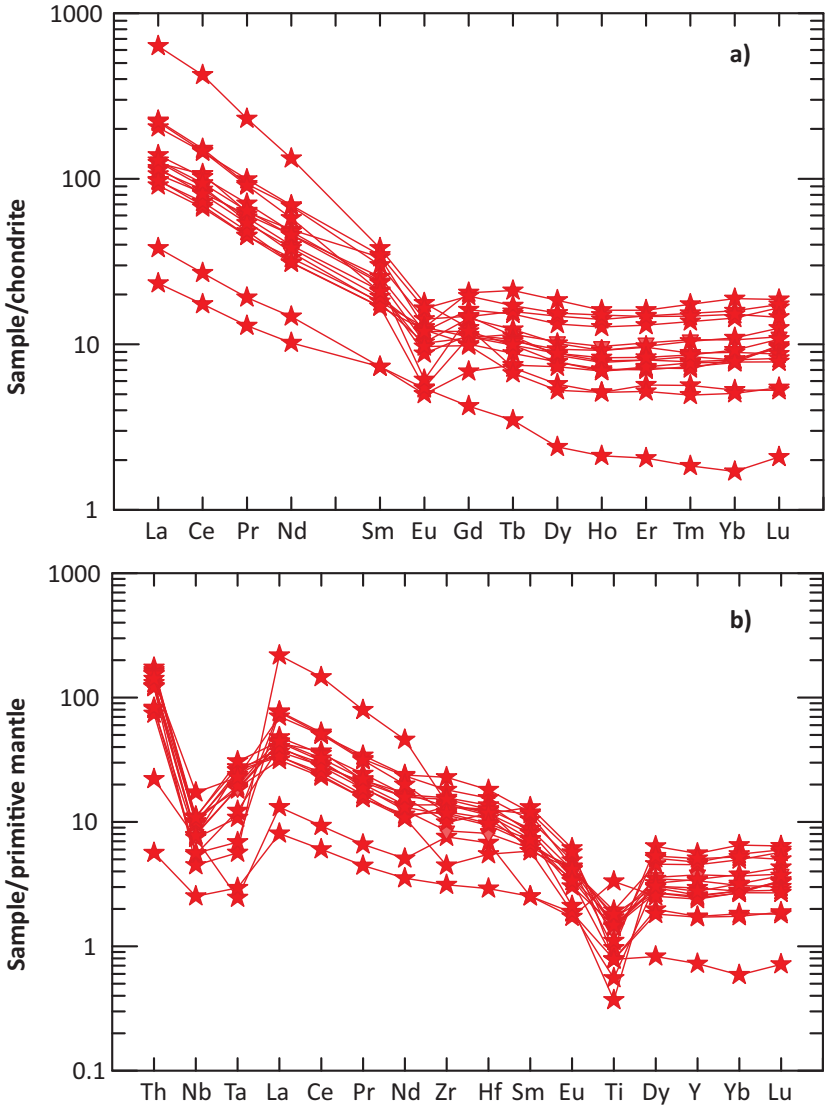

Figure 33: *Trace-element profiles for the basement granitoid rocks of the Maskwa Lake batholith I from the Bird River greenstone belt:* ***a)*** *chondrite-normalized rare-earth–element plot;* ***b)*** *primitive-mantle–normalized extended trace-element plot (normalizing values from Sun and McDonough, 1989).*

(Foley et al., 2002). This suggests that these granitoid rocks may have been derived from partial melting of amphibolite (Foley et al., 2002) in a volcanic-arc environment. However, on the plot of Sr/Y versus La/Yb, the granitoid rocks can be subdivided into two groups: one with Sr/Y<10 and La/Yb<20 located in the non-TTG field, and the other with 50>Sr/Y>10 and La/Yb>20, located in the low-pressure TTG field (Figure 35; Moyen and Martin, 2012). Relatively low La/Yb and Sr/Y ratios in the granitoids can be explained by plagioclase fractionation in a closed system, which consequently leads to negative Eu anomalies (Figure 33a). Alternatively, partial melting of the source region may have taken place at relatively shallow crustal levels, involving plenty of plagioclase (e.g., juvenile mafic crustal material).

It is noteworthy that TTGs can be subdivided into low, medium and high subtypes in terms of HREE contents. These subtypes correspond to high-, medium- and low-pressure partial melting, respectively, of the source region (Moyen, 2011; Moyen and Martin, 2012). The TTG subtype with low HREE concentration (Moyen, 2011), low Nb and Ta, and high Sr displays a geochemical signature of modern adakite, requiring the TTG melt to be in equilibrium with a significant amount of garnet and some rutile in the source region where plagioclase is absent or unstable under high pressure (>15 kb). The absence of plagioclase in the source region (residue), where it is unstable because of P–T conditions, or the absence of physical separation of plagioclase from the ascending magma in a closed system (e.g., shallow magma chamber; Prouteau et al., 1999) is required to preserve the geochemical characteristics of adakite-type melts inherited from putative slab melting (Defant and Drummond, 1990; Drummond and Defant, 1990). In contrast, the 'low-pressure' TTG group (Moyen, 2011) shows high HREE, Nb and Ta but lower Sr, consistent with the presence of plagioclase in the source region (residue) but a smaller amount of garnet and no rutile. The 'medium pressure' group falls in between. Plagioclase, rutile and garnet are strongly pressure dependent, so that three sub-types of TTGs

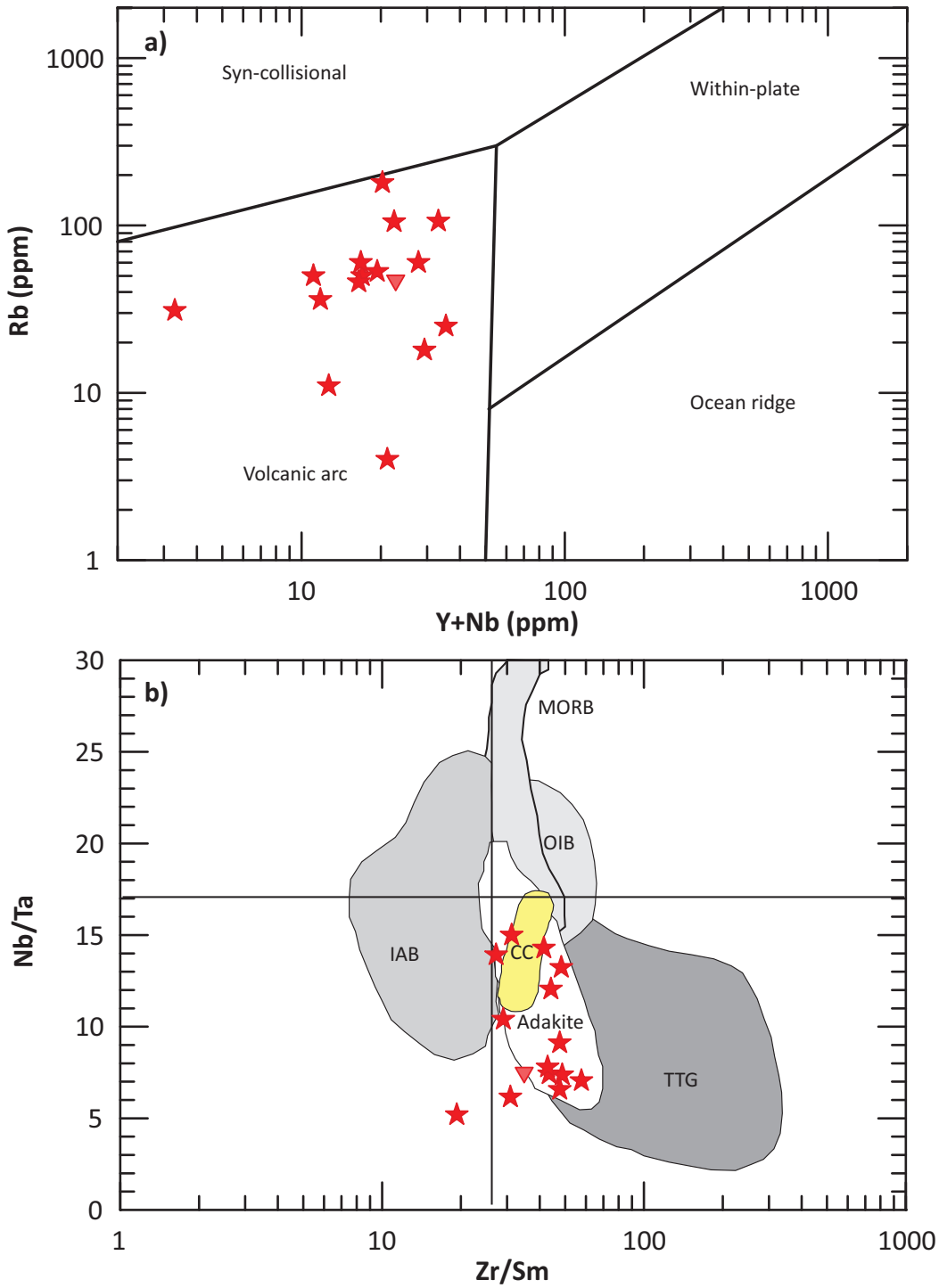

Figure 34: *Tectonomagmatic discrimination diagram for the granitoid rocks of the Maskwa Lake batholith I from the Bird River greenstone belt:* ***a)*** *plot of (Y+Nb) versus Rb (after Pearce et al., 1984);* ***b)*** *plot of Zr/Sm versus Nb/Tb (after Foley et al., 2002); primitive-mantle Na/Ta and Zr/Sm ratios are 17.4 and 25.2, respectively (Sun and McDonough, 1989). Abbreviations: CC, continental crust; IAB, island-arc basalt; MORB, mid-ocean–ridge basalt; OIB, oceanic-island basalt; TTG, tonalite-granodiorite-trondhjemite.*

can be interpreted in terms of depth of partial melting that implicitly takes place in an arc environment linked to plate subduction.

The granitoid rocks of the Maskwa Lake batholith I are comparable to the low-pressure subtype of TTG proposed by Moyen and Martin (2012), which may exhibit the geochemical characteristics of non-TTG owing to differentiation (Figure 35), likely involving plagioclase (Figure 33) in a closed system. In addition, these granitoids generally display calcic, magnesian and weakly to moderately peraluminous affinities. These features, together with constraints from trace-element geochemistry, suggest that the granitoid rocks may have been generated by partial melting of amphibolites derived from mafic protoliths at relatively low pressure in an arc-like setting (e.g., Windley and Garde, 2009;

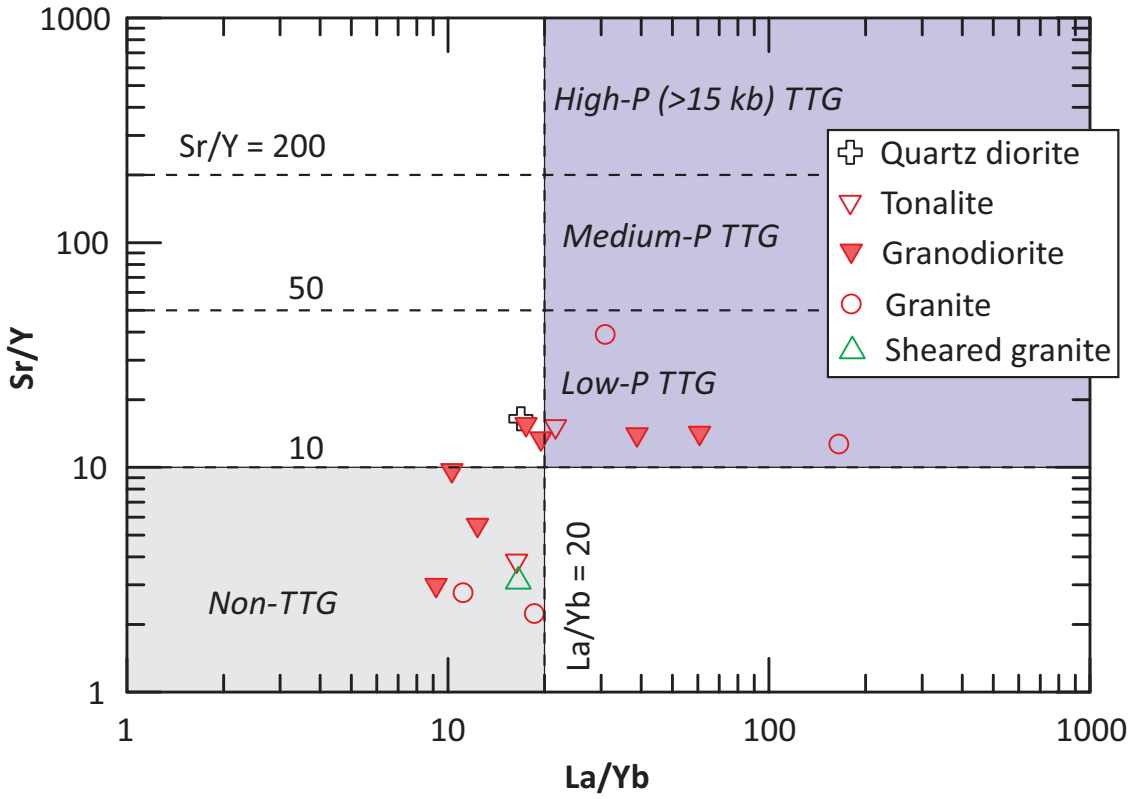

Figure 35: *Plot of La/Yb versus Sr/Y for the granitoid rocks of the Maskwa Lake batholith I from the Bird River greenstone belt. The boundary between Sr/Y and La/Yb ratios used to define TTG and subtypes is from Moyen and Martin (2012).*

Bruand et al., 2020), together constituting part of a newly formed continental basement in the BRGB.

In summary, major- and trace-element composition of the Mesoarchean granitoids from the BRGB basement (i.e., the Maskwa Lake batholith I) are characterized mainly by sodium-rich, calcic (or tholeiitic), peraluminous and magnesian magmatic affinities, although exceptions of few samples are evident that may have resulted from magmatic differentiation. The granitoid rocks are attributed mostly to low-pressure TTGs with I-type signatures and may have been emplaced into a volcanic (island)-arc setting, whose parental magmas were likely produced by partial melting of amphibolite at relatively low pressure.

Neoarchean granitoid rocks: classification

Neoarchean granitoid samples collected from the Maskwa Lake batholith II, Marijane Lake pluton, Tin-Osis lakes intrusion, Birse Lake pluton, and Bird River sanukitoid (Table 2; DRI2022012) are plotted on the TAS (Figure 36a) and Shand index diagrams (Figure 36b), respectively, and compared with the Mesoarchean basement granitoid rocks described above in order to investigate their commonalities and differences. The samples from the Maskwa Lake batholith II fall into the fields of diorite, granodiorite to granite (Figure 36a). Their total (Na_2O+K_2O) contents increase generally with increasing silica contents in the TAS diagram, consistent with magmatic fractionation. These granitoid rocks mostly have values of the Rittmann serial index (σ) between 1.2 and 3.5, typical of calcalkaline series (Yang, 2007), although some samples have σ values less than 1.2, belonging to calcic- (or tholeiitic) series. Together, these granitoids are comparable to subalkaline rocks of Irvine and Baragar (1971). The granitoid rocks in the Maskwa Lake batholith II show many similarities with the basement granitoids in the Mesoarchean Maskwa Lake batholith I, although the latter appears to have relatively lower total (Na_2O+K_2O) contents and more variable silica concentrations.

Seven granitoid samples taken from the Marijane Lake pluton mostly plot in the field of granite, and one falls in the field of monzonite and one in the granodiorite field (Figure 36a). They are calcalkaline in terms of their σ values between 1.2 and 3.5, except for the granodiorite sample being calcic as its σ value is less than 1.2. Five samples collected from the Tin-Osis lakes intrusion (Drayson, 2016; Yang et al., 2019) plot in the granite field of the TAS diagram (Figure 36a), and one sample taken from the country rock (greywacke) is also plotted on this diagram for comparison. Intriguingly, this metasedimentary rock is located in the granodiorite field, similar to granodiorite to some extent in silica and total alkali concentration. The Tin-Osis lakes granites are mostly calcalkaline based on their σ values between 1.2 and 3.5, and one granite and the metasediment samples are calcic (tholeiitic) due to σ values of less than 1.2 (Figure 36a). Again, they are subalkaline based on the classification of Irvine and Baragar (1971). Thirteen samples from the Birse Lake pluton spread in the fields of granodiorite and granite, and show positive correlation between total (Na_2O+K_2O) and silica contents in the TAS diagram (Figure 36a). These samples are subalkaline

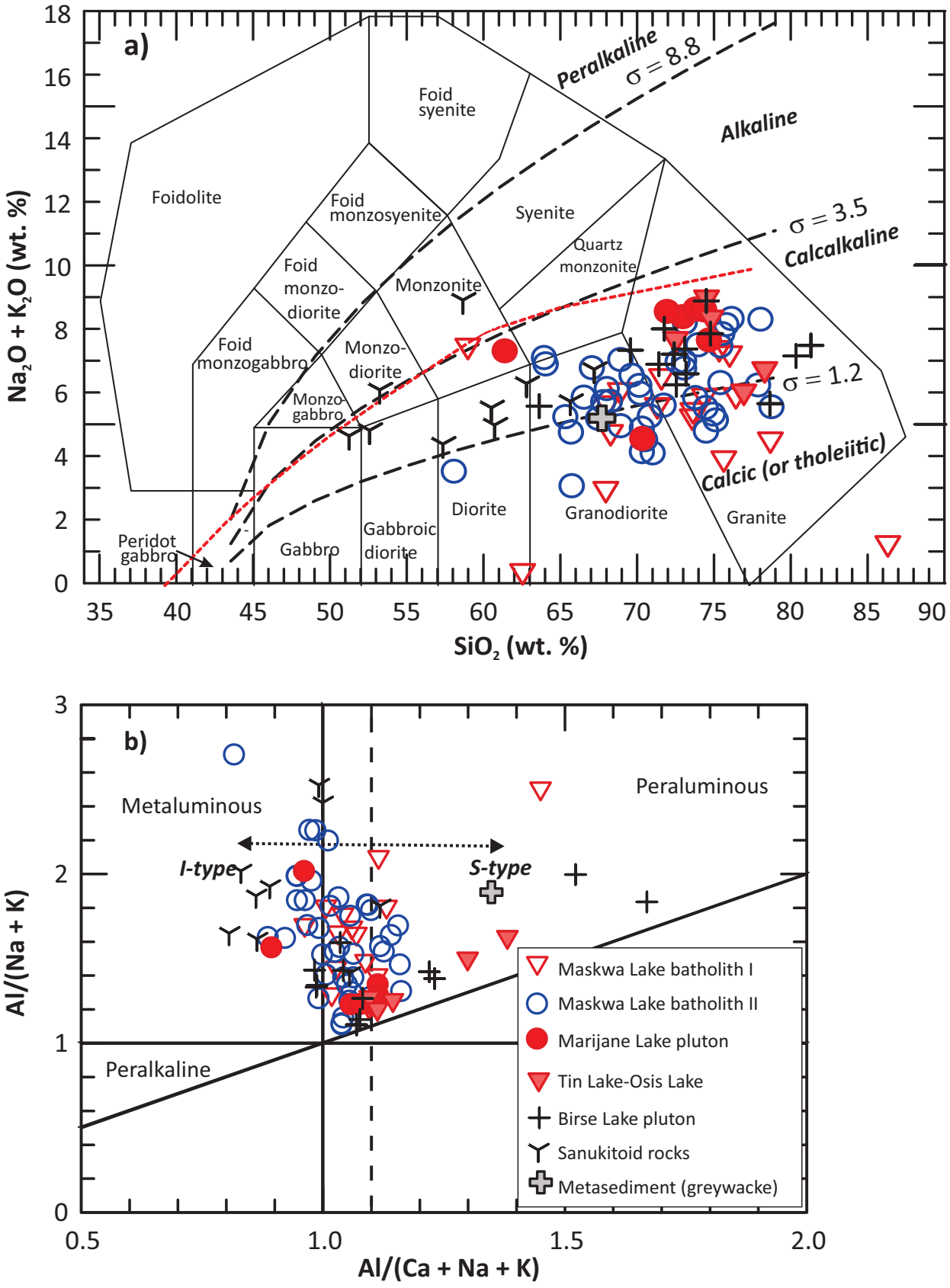

Figure 36: *Chemical classification of the Neoarchean granitoid rocks from the Bird River greenstone belt in terms of alkalinity and alumina-saturation index:* ***a)*** *total alkalis (Na_2O+K_2O) versus SiO_2 (TAS; wt. %) diagram (fields from Middlemost, 1994); the boundary (red dashed line) between alkaline and subalkaline series from Irvine and Baragar (1971); the Rittmann serial index σ = $(Na_2O+K_2O)^2/(SiO_2–43)$, unit in wt. % (Rittmann, 1973); using σ values to further subdivide granitoids into calcic (tholeiitic), calcalkaline, alkaline and peralkaline series (Yang, 2007);* ***b)*** *Shand index plot (fields from Maniar and Piccoli, 1989); ACNK = $Al_2O_3/(CaO+Na_2O+K_2O)$, ANK = $Al_2O_3/(Na_2O+K_2O)$, unit in mole; vertical dashed line indicates ACNK = 1.1, a key parameter discriminating S- and I-type granites (Chappell and White, 1974).*

and calcalkaline in terms of their alkalinities (Irvine and Baragar, 1971; Yang, 2007).

Ten samples taken from the Bird River sanukitoid (H.P. Gilbert, unpublished data, 2008) display a large range in compositions from gabbro, gabbroic diorite, diorite, to monzodiorite and monzonite (Figure 36a). They are dominantly subalkaline, attributing to calcalkaline based on their σ values, although two samples belong to the alkaline series. Compared to the other Neoarchean granitoid rocks in the BRGB, the Bird River sanukitoid rocks mostly have consistently high values of Mg# ranging from 55.8 to 68.3, although two samples display relatively lower Mg# values of 35.8 to 42.6 (DRI2022012). Also, the sanukitoids exhibit high Na_2O/K_2O ratios of 1.25 to 4.96, except for one sample showing a low Na_2O/K_2O ratio of 0.22.

On the Shand index plot of Maniar and Piccoli (1989), the granitoid samples from the Maskwa Lake batholith II, Marijane Lake pluton, Tin-Osis lakes intrusion and Birse Lake pluton are mostly alumina-saturated and attributed to subaluminous to strongly peraluminous. Some of the samples, however, are metaluminous (Figure 36b). The Bird River sanukitoid rocks are exclusively metaluminous, typically with ACNK <1.0. The geochemical features suggest that most of the BRGB granitoid rocks including the basement granitoids in the Maskwa Lake batholith I are I-type because their ACNK <1.1, and the Tin-Osis lakes intrusion and parts of the Marijane Lake and Birse Lake plutons are ascribed to S-type with ACNK values >1.1 (Chappell and White, 1974, 2001). This is consistent with the discrimination result based on MS values and mineral assemblages (Table 2). However, six samples from the Maskwa Lake batholith II are strongly peraluminous, despite the fact of their ACNK values >1.1, but are attributed to evolved I-type because of the absence of at least one diagnostic indicator mineral (e.g., muscovite, garnet; Chappell and White, 1974, 1992, 2001; Yang et al., 2019).

Plotting the BRGB granitoid samples on the CIPW normative Q' versus ANOR classification diagram (Figure 37a) of Streckeisen and Le Maitre (1979) shows that the Maskwa Lake batholith comprises a variety of lithologies ranging from quartz monzodiorite, calc tonalite, tonalite, granodiorite, through monzogranite, syenogranite to alkali-feldspar granite. Both the Mesoarchean basement granitoids in the Maskwa Lake batholith I and Neoarchean granitoids in the Maskwa Lake batholith II are dominantly calcic and extend to calcalkalic in the diagram of MALI versus SiO_2 (Figure 37b). This is largely in agreement with the discriminant results of the TAS diagram (Figure 36a) in combination with the Rittmann serial index σ, and further illustrates that these rocks follow the calcic to calcalkalic trends, commonly seen in Archean TTGs. The S-type granites of the Tin-Osis lakes intrusion and from parts of the Marijane Lake pluton and Birse Lake plutons are mostly plotted in the fields of monzogranite, syenogranite to even alkali-feldspar granite, whereas I-type granites are more scattered (Figure 37a). The Bird River sanukitoids span from monzogabbro, monzonite, quartz monzonite, through tonalite to granodiorite (Figure 37a), and vary from calcic to alkalic series (Figure 37b).

On the CIPW Ab-An-Or ternary diagram of Barker (1979), the granitoid samples from the Maskwa Lake batholith fall mainly into the fields of trondhjemite, tonalite and granodiorite, typical of sodium-rich TTG; some samples extend to the granite field (Figure 38a). The basement granitoids from the Maskwa Lake batholith I appear to have more Or component than the Maskwa Lake batholith II, suggesting that the fractionation degrees of the Meso- and Neo-Archean granitoid rocks are different or involving different degrees of crustal contamination (see the section of Sm-Nd isotopic systematics below and the Nd isotope data in DRI2022012). The Marijane Lake pluton is mainly composed of granite, but two samples are granodiorite and tonalite. It is noted that the five granite samples in the Marijane Lake pluton display a negative correlation between An and Or components (Figure 38a) and those with low An contents are S-type granite. The Tin-Osis lakes intrusion consists dominantly of granite, and only one sample together with the greywacke is plotted in the trondhjemite field. The granitoid samples from the Birse Lake pluton show a consistent compositional array of granite extending to granodiorite, pointing to a magmatic fractionation trend of An and Ab declining with increasing Or components, except for one sample falling into the field of trondhjemite. Again, the Or-rich and An-poor phases in the Birse Lake pluton are exclusively S-type. Ten samples from the Bird River sanukitoid are scattered in the Ab-An-Or ternary diagram, including trondhjemite, tonalite and granodiorite. Any correlation among their Ab, An and Or compositions cannot be discernable for Bird River sanukitoid rocks (Figure 38a).

On the Zr/TiO_2 versus Nb/Y diagram (Figure 38b), the BRGB granitoid samples are mainly clustered in the fields of diorite to granite, which collectively display subalkaline affinities (e.g., Pearce, 1996). Exceptions are that two samples from the Maskwa Lake batholith II plot in the monzonite field, and four sampels fall into the syenite field (including one from the Marijane Lake pluton, two from the Tin-Osis lakes intrusion and one from the Birse Lake pluton), because these four samples display relatively high Nb/Y ratios of >0.8 (DRI2022012). Although these samples may be alkaline based on the Nb/Y ratios (Pearce, 1996), they are mostly calcalkaline on the basis of their σ values between 1.2 and 3.5 (Yang, 2007) as indicated by the TAS diagram (Figure 36a). The high Nb/Y ratios of the BRGB calcalkaline granitoid rocks are likely attributed to contamination of continental crust that exhibits both high Nb content (19 ppm) and Nb/Y ratio (0.79; Wedepohl, 1995), in particularly by contamination of the upper continental crust (Rudnick and Gao, 2010).

Based on the relationship of Zr contents versus (10^4Ga/Al) ratios (Whalen et al., 1987), most of the BRGB granitoid samples plot in the field of I- and S-type (not shown), although some of the samples from the Marijane Lake pluton, Tin-Osis lakes intrusion and Birse Lake pluton fall into the field of A-type. These samples having high (10^4Ga/Al) ratios but low Zr contents (<40 ppm) may have resulted from magmatic fractionation, whereas those having high Zr contents (>100 ppm; see DRI2022012) are

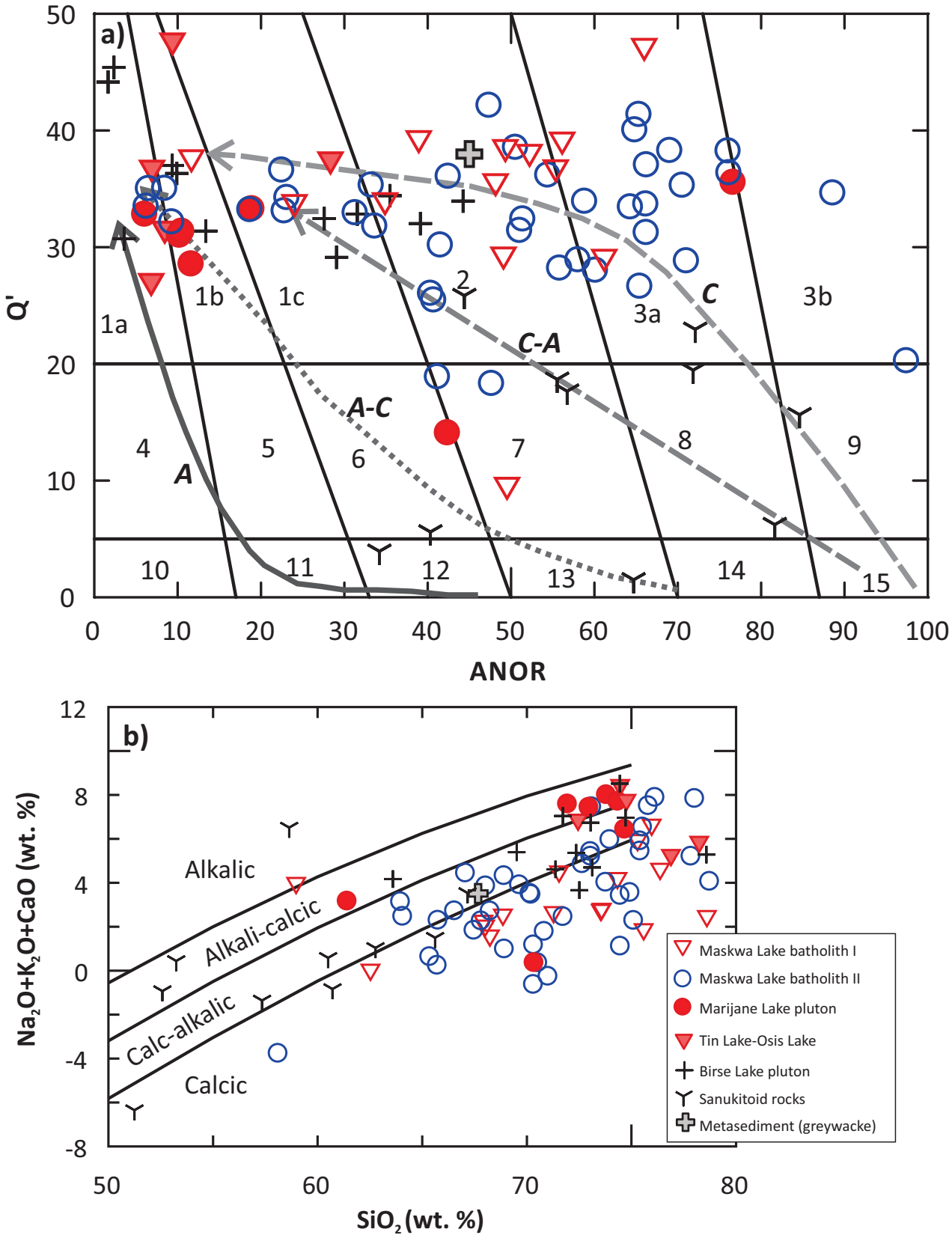

Figure 37: *Classification of the Neoarchean granitoid rocks from the Bird River greenstone belt, based on* ***a)*** *the CIPW normative Q' vs. ANOR diagram of Streckeisen and Le Maitre (1979). Q' = 100*qz/(qz+or+ab+an); ANOR = 100*an/(an+or). Rock units: 1a, alkali-feldspar granite; 1b, syenogranite; 1c, monzogranite; 2, granodiorite; 3a, tonalite; 3b, calc tonalite; 4, alkali-feldspar quartz syenite; 5, quartz syenite; 6, quartz monzonite; 7, quartz monzodiorite; 8, quartz diorite; 9, quartz gabbro; 10, alkali-feldspar syenite; 11, syenite; 12, monzonite; 13, monzogabbro; 14, diorite; 15, gabbro. Coarse dashed and solid lines with arrows indicate interpreted differentiation trends of different magmatic suites (after Whalen and Frost, 2013): C, calcic; C-A, calcalkali; A-C, alkali-calcic; A, alkali; and* ***b)*** *diagram of MALI versus SiO_2 (wt. %); MALI = Na_2O+K_2O–CaO, unit in wt. % (after Frost et al., 2001). Abbreviations: ab, albite; an, anorthite; CIPW, Cross, Iddings, Pirsson, Washington; or, orthoclase; qz, quartz.*

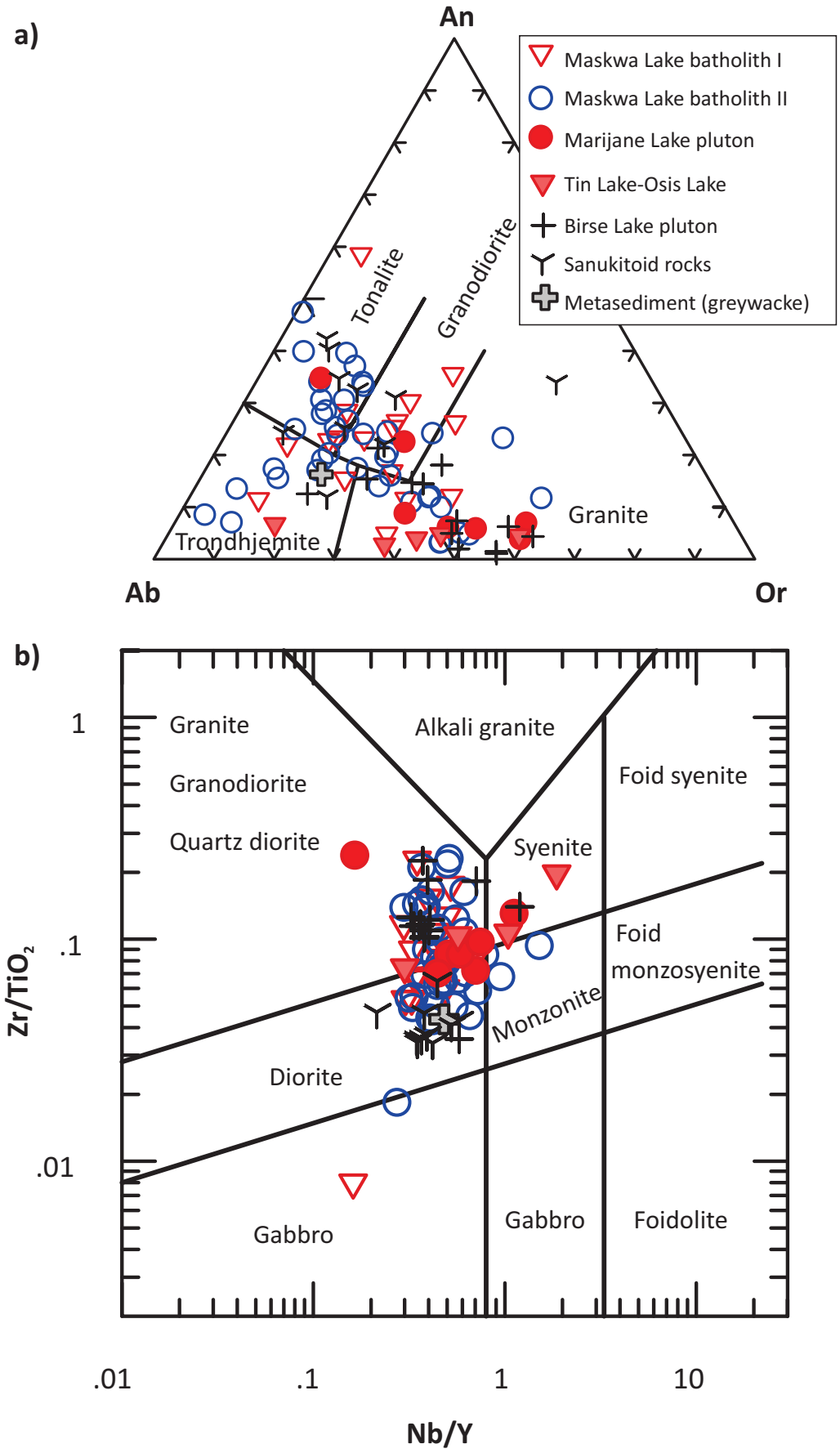

Figure 38: *Chemical classification of the Neoarchean granitoids from the Bird River greenstone belt in terms of CIPW normative compositions and HFSEs:* ***a****) Ab-An-Or ternary diagram (fields from Barker, 1979);* ***b****) plot of Zr/TiO_2 versus Nb/Y (after Pearce, 1996). Abbreviations: Ab, albite; An, anorthite, CIPW, Cross, Iddings, Pirsson, Washington; HFSE, high-field-strength element; Or, orthoclase.*

likely controlled by the nature of their source rocks (e.g., Yang et al., 2008, 2019).

Neoarchean granitoid rocks: trace-element geochemistry

Similar to the Mesoarchean basement granitoid rocks, the Neoarchean granitoid rocks in the Maskwa Lake batholith II display a large range but relatively low Rb contents ranging from 1 to 286 ppm, relatively high Sr (up to 605 ppm) and Ba (up to 1148 ppm) contents, mostly with low Rb/Sr ratios (<1; see DRI2022012). Such features reflect a limited degree of magmatic fractionation after magma separation from the source region, although few evolved samples show relatively high Rb/Sr r(atios ranging from 1.2 to 6.6. However, the Neoarchean granitoid rocks display variable K/Rb ratios that range from 32 to 681, but are mostly higher than 200 indicating that their sources were unevolved to moderately evolved (cf. Blevin, 2004). This is consistent with their low to moderate concentrations of transitional elements (e.g., Cr, Co, Ni).

Trace-element profiles of the BRGB granitoid samples are presented in Figure 39; the left panel (Figure 39a, c, e, g, i, k) shows chondrite-normalized REE patterns, and the right panel (Figure 39b, d, f, h, j, l) shows N-MORB–normalized extended trace-element profiles for the samples from different plutons (or intrusions). Compared to the basement granitoid rocks (Figure 39a), the granitoid rocks from the Maskwa Lake batholith II show consistently enriched REE patterns, with moderately to strongly enriched LREE relative to HREE and mostly with small to strongly negative Eu anomalies indicated by Eu/Eu* values of 0.19–0.91. Some samples, however, do not display or show slightly positive Eu anomalies (Eu/Eu* = 0.94–1.11; Figure 39c). The abundances of LREE vary from 50 to 350 times chondritic values, with HREE contents varying from 3 to 35 times chondritic values (Figure 39c). LREE and HREE are moderately fractionated, manifested by chrondrite-normalized ratios of $(La/Yb)_N$ ranging from 3 to 39. Intra-HREE fractionation, however, is relatively weak, with $(Gd/Yb)_N$ ratios ranging from 0.5 to 2.5 (DRI2022012). N-MORB–normalized extended trace-element profiles of the granitoid rocks from the Maskwa Lake batholith II show that they are enriched in LILEs (e.g., Cs, Rb), with pronounced negative Nb (Ta), Ti and P anomalies (Figure 39d), resembling those of the basement granitoids from the Maskwa Lake batholith I (Figure 39b). Some samples display remarkably positive Pb anomalies. The trace-element profiles of these granitoids are consistent with those of typical arc rocks, suggesting that they may have formed in an arc-like setting (e.g., Rollinson, 1993; Pearce and Peate, 1995; Pearce, 2008; Yang et al., 2008; Windley et al., 2021).

Windley et al. (2021) compiled and investigated a large dataset of geochemical analyses, and reviewed the literature of major Archean cratons worldwide, comparing with Phanerozoic subduction zone geochemistry. They point out that the enrichment of LILEs, LREE, Th, U and Pb, coupled with the depletion of Nb (Ta) and Ti, in Archean igneous rocks can be best explained by subduction zone geodynamic and petrogenetic processes. Windley et al. (2021) show that all the geochemical characteristics are collectively consistent with a subduction zone origin for the Eoarchean to Mesoarchean TTGs and do not show any major change in Th-Nb-Pb-Ti-LREE systematics between Eoarchean and Mesoarchean times, suggesting that the onset of plate tectonics on Earth may have been much earlier than previously thought (e.g., Pease et al., 2008; Percival et al., 2012).

Chondrite-normalized REE patterns, and N-MORB–normalized extended trace-element profiles for granitoids samples from the Marijane Lake pluton are shown in Figure 39e and 39f. The granitoid samples exhibit LREE enriched and HREE depleted patterns, with slight to moderate Eu anomalies (Eu/Eu* ranging from 0.21 to 0.81; Figure 39e). It is noted that sample 111-14-206A01 is a pegmatitic granite with much lower REE contents than the other samples, and displays a distinct REE pattern, e.g., slightly enriched LREE [i.e., $(La/Yb)_N$ of 1.9] and moderately elevated HREE relative to middle REE [i.e., $(Gd/Yb)_N$ of 0.3], with a high Eu positive anomaly (Eu/Eu* = 1.68). From Dy to Lu, the REE pattern of this sample intersects with that of other samples from the Marijane Lake pluton, indicating a different process involved in the genesis of the pegmatite granite (e.g., internal fluids aided fractionation of amphibole; Yang et al., 2008). The granite samples display LILEs enriched profiles, with pronounced negative Nb (Ta), Ti, and P anomalies (Figure 39f) as well as remarkable Pb positive anomalies. The trace-element profiles of these granitoids are consistent with those of typical arc rocks. As mentioned previously, part of the Marijane Lake granites is S-type granite formed by partial melting of metasedimentary rocks that must have inherited geochemical signatures of arc rocks (Yang et al., 2019).

The granite samples from the Tin-Osis lakes intrusion mostly display a 'seagull wing-like' flat REE pattern, without pronounced differentiation of LREE relative to HREE but with moderate to large negative Eu anomalies (Eu/Eu* = 0.02–0.47; Figure 39g). These samples have relatively low $(La/Yb)_N$ ratios of 0.5 to 5.2 and low $(Gd/Yb)_N$ ratios of 0.4 to 1.6 (DRI2022012). One granite sample, however, shows a slightly (or shallow) enriched REE pattern with a small negative Eu anomaly (Eu/Eu* = 0.70), similar to that of greywacke (Eu/Eu* = 0.52) although with a notable difference in the degree of LREE enrichment relative to HREE. While the Tin-Osis lakes intrusion is S-type showing distinct REE patterns from the arc-related I-type granitoids of TTGs that display much steeper REE patterns with much less pronounced negative Eu anomalies in the BRGB, they are generally comparable to the S-type part of the Birse Lake pluton (Figure 39i). These geochemical characteristics strongly suggest that the sources of the S-type granites did not have a garnet residue and formed at shallower depth than the I-type granitoids in the TTG suite derived from deeper magma sources containing an appreciable amount of garnet (e.g., Martin et al. 2005; Zhang et al., 2006; Moyen and Martin, 2012). Some of the S-type granites have low REE abundances and flat REE patterns (Figure 39g) that likely resulted from fractionation of LREE rich minerals (e.g., monazite; Clarke, 1992; Rollinson, 1993), leading to their REE patterns gradually becom-

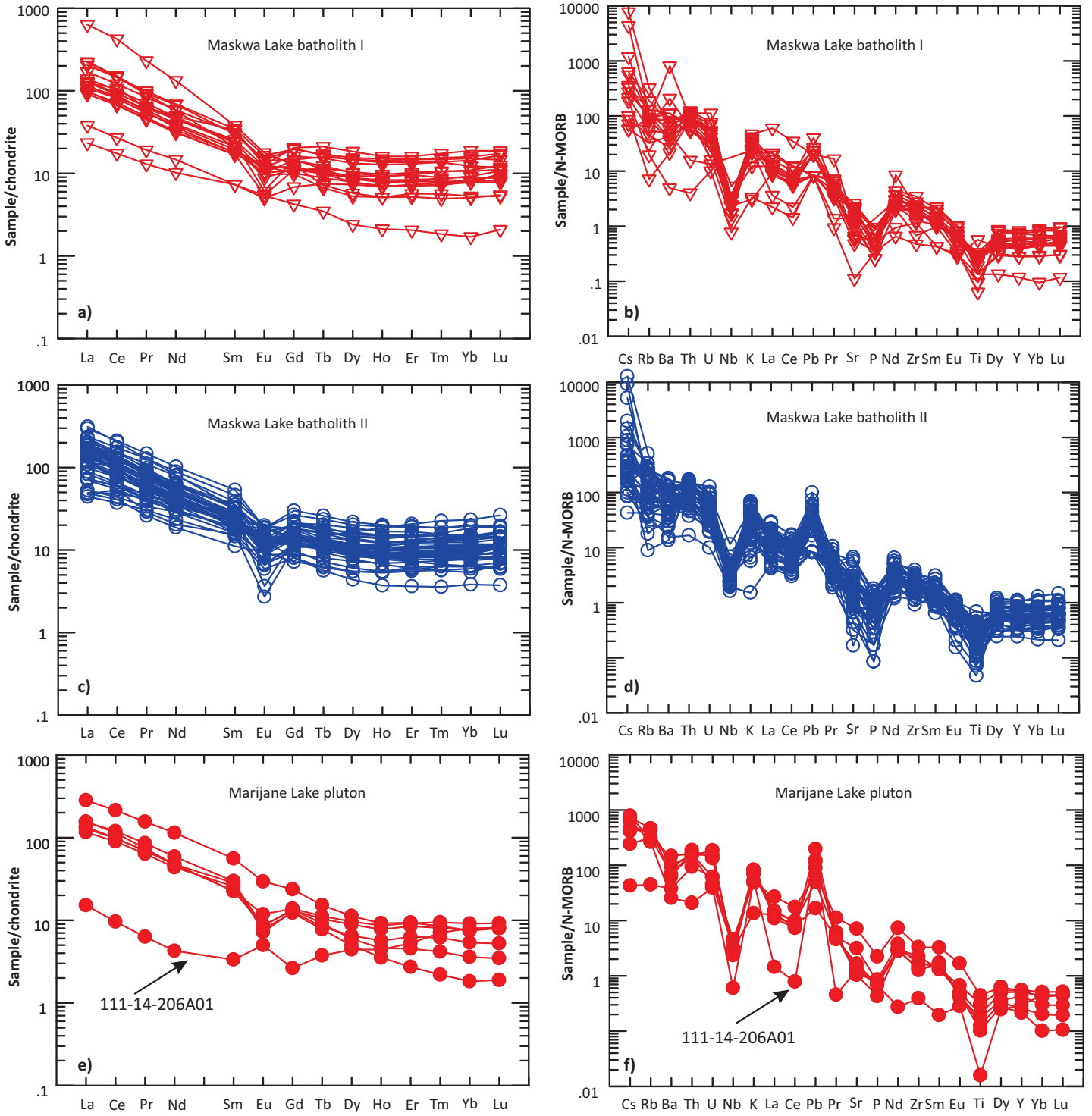

Figure 39: *Trace-element profiles for the Neoarchean granitoid rocks from the Bird River greenstone belt: left panel* ***a)****,* ***c)****,* ***e)****,* ***g)****,* ***i)*** *and* ***k)*** *chondrite-normalized rare-earth–element plot; right panel* ***b)****,* ***d)****,* ***f)****,* ***h)****,* ***j)*** *and* ***l)*** *N-MORB–normalized extended trace-element plot. Normalizing values from Sun and McDonough (1989).*

ing flatter with more pronounced negative Eu anomalies due to fractional crystallization of feldspars (plus monazite) as indicated by the Tin-Osis lakes intrusion and the Birse Lake pluton (e.g., sample 111-14-291A01; Figure 39i). On the N-MORB–normalized multi-element plot (Figure 39h), the S-type granites show relative enrichments in LILEs (e.g., Cs, Rb, K), U, Th, with pronounced negative Nb (Ta), Ti, Sr, and Ba anomalies. Their multi-element patterns are similar to those of the S-type part of the Birse Lake pluton (Figure 39j), although the elemental abundances are variable, likely reflecting source heterogeneities. The greywacke sample shows a similar multi-elemental profile to the S-type granites, although the former has relatively higher elemental abundances (Figure 39h), consistent with the interpretation that its provenance must have inherited geochemical signatures (e.g., pronounced negative Nb, Ta, Ti anomalies) of magmatic-arc rocks (Yang et al., 2019).

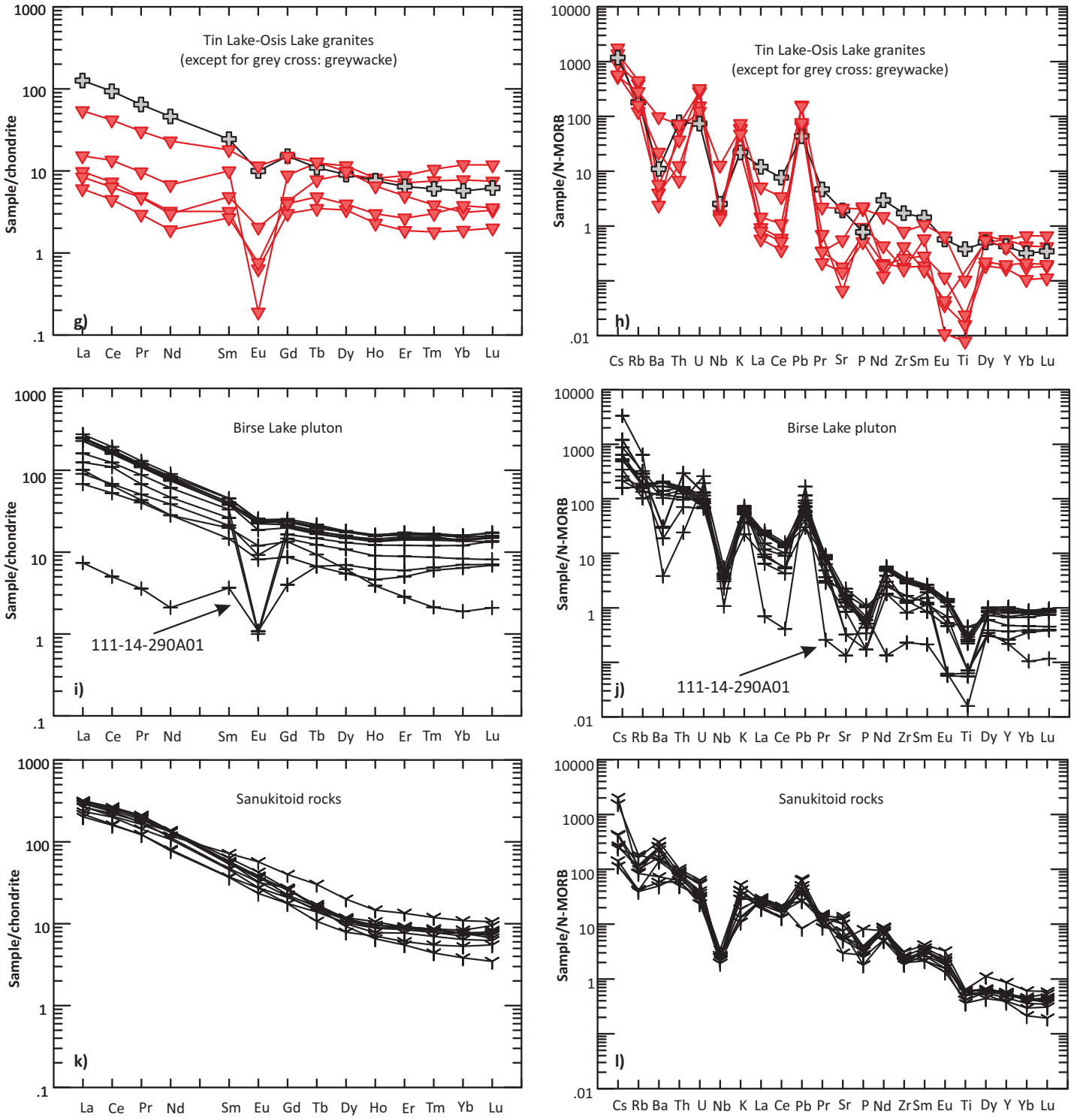

Figure 39 (continued): *Trace-element profiles for the Neoarchean granitoid rocks from the Bird River greenstone belt: left panel* ***a), c), e), g), i)*** *and* ***k)*** *chondrite-normalized rare-earth–element plot; right panel* ***b), d), f), h), J)*** *and* ***l)*** *N-MORB–normalized extended trace-element plot. Normalizing values from Sun and McDonough (1989).*

The samples from the Bird River sanukitoid exhibit consistently smoother and much more enriched LREE patterns without notable Eu anmoalies (Eu/Eu* = 0.81 to 1.09; Figure 39k) compared with those granitoids regardless of I- and S-type from the BRGB. They show consistent enrichment in LILEs (Cs, Rb, K, Ba, Sr), typical positive Pb and pronounced negative Nb (Tb), Ti and P anomalies (Figure 39l), also consistent with those of magmatic-arc rocks. However, these high-Mg rocks display enrichment in both the LILEs and siderophile elements (see DRI2022012 and the above descriptions of their major-element composition), and display highly fractionated REE patterns with marked HREE depletion, indicative of their unique petrogenesis (e.g., Beakhouse and Davis, 2005; Halla et al., 2017; Hildebrand et al., 2018; Yang et el., 2019). Stern et al. (1989) referred sanukitoids

to the plutonic equivalents of mantle-derived LILE-enriched trachyandesites (or high-Mg andesites) that contain 55–60% SiO_2, >0.6 Mg#, >200 ppm Cr, >100 ppm Ni, >500 ppm Sr, <0.1 Rb/Sr, and enriched LREEs without Eu anomalies. Furthermore, Martin et al. (2010) demonstrated that Archean sanukitoids formed only after 3.0 Ga. The peak in sanukitoid formation was at around 2.7 Ga, which coincides with the coeval peak in formation of gold mineralization and crustal formation; both sanukitoids and gold deposits require similar conditions of subducted slabs and interaction with metasomatized mantle. Lin and Beakhouse (2013) suggested that increasing collisions of accretionary orogens at that time would have led to more slab breakoffs and the influx of asthenospheric mantle in sub-arc mantle wedges, which resulted in generation of sanukitoid magmas and associated gold-bearing hydrothermal fluids. This model is consistent with known geological relations in many Neoarchean orogens, including the Bird River belt (Gilbert et al., 2013; Yang and Gilbert, 2014; Yang et al., 2019; Yang and Houlé, 2020).

On the plot of Sr/Y versus La/Yb ratios, the Neoarchean granitoid rocks from the BRGB can be subdivided into two groups: one with Sr/Y<10 and La/Yb<20 plotted in the non-TTG field, and the other with 100>Sr/Y>10 and La/Yb>20, located in the fields of low-pressure and medium-pressure TTG (Figure 40a; Moyen and Martin, 2012). Relatively low La/Yb and Sr/Y ratios in the granitoids can be explained by plagioclase fractionation in a closed system, which consequently led to moderately negative Eu anomalies (Figure 39a, c, e, g, and i). Alternatively, partial melting of the source region may have taken place at relatively shallow crustal level and involving plenty of plagioclase (e.g., juvenile mafic crustal material). Most of the Neoarchean granitoid samples fall in the field of volcanic-arc granitoids, but the S-type granites mostly plot in the field of syncollisional granitoids (Figure 40b) on the tectonomagmatic discrimination diagram of Pearce et al. (1984). On the plot of log τ versus log σ (not shown), all samples fall in the field of orogenic belts and island arcs. Note that τ values range from 12.7 up to 5050; DRI2022012). Interestingly, S-type granites of the Tin-Osis lakes intusion and parts of the Marijane Lake and Birse Lake plutons display higher τ values and ACNK (Figure 36b), consistent with their sources (sedimentary rocks) being rich in alumina-bearing minerals (e.g., clays). In constrast, the Bird River sanukitoids have consistently low τ values of 12.7 to 28.9, suggesting that their mantle sources are rich in Na_2O and TiO_2 (in Fe-Ti oxides).

On the Nb/Y and La/Yb versus Nb+Y discrimination diagrams of Whalen and Hildebrand (2019), the Neoarchean granitoid rocks from the BRGB are straddled around the boundary between slab failure magmatism and magmatic-arc environments (Figure 41a, b), and none of the samples are located in the field of A-type granitoids that have much higher concentrations of Nb+Y. The sanukitoid samples have higher Nb/Y and La/Yb ratios than those of magmatic-arc rocks, and are therefore interpreted to be formed by slab failure magmatism (Hildebrand et al., 2018; Whalen and Hildebrand, 2019). Based on these geochemical parameters, none of the BRGB granitoid rocks are A-type, but are likely to have formed in magmatic arc or by slab failure magmatism.

In summary, the Neoarchean BRGB granitoid rocks are mostly attributed to Archean TTG suite with typical features of I-type granites, which formed in a magmatic-arc setting. The Tin-Osis lakes intusion and parts of the Marijane Lake and Birse Lake plutons are S-type granites that formed in a thickened crust due to terrane collision (Yang, 2014a, b; Yang et al., 2019). Intra-variation in geochemical composition is likely due to magmatic fractionation, while inter-intrusion variation may have been ascribed to differences in their petrogenetic processes (e.g., degree of fractionation, supracrustal contamination, and magma sources). The Bird River sanukitoid rocks cutiing the Neoarchean Maskwa Lake batholith II likely formed by slightly late slab-failure magmatism associated with slab roll-back and/or break off.

Winnipeg River (WRD) and Wabigoon domains (WD)

Classification

The granitoid samples from the WRD and WD are classified in this section using major- and trace-elements diagrams of the TAS, and Zr/TiO_2 versus Nb/Y (Figure 42a, b), respectively. Twelve samples collected from the Lac du Bonnet batholith, 11 from the Pointe du Bois batholith, 14 from the Rennie River plutonic suite and three from the Big Whiteshell Lake pluton in the WRD together with three samples from the WD (DRI2022012) fall dominantly into the field of granite in the TAS diagram (Figure 42a); only two samples from the Pointe du Bois batholith are located in the granodiorite field. Intra-intrusion variation in total (Na_2O+K_2O) contents increasing with increasing silica contents is evident in some plutons (e.g., the Pointe du Bois batholith), but not so in others (e.g., the Rennie River plutonic suite). The granitoid rocks have values of Rittmann serial index (σ) exclusively ranging from 1.2 to 3.5, belonging to the calcalkaline series (Yang, 2007), with only one sample in the Rennie River plutonic suite having a σ value below 1.2 attributed to the calcic- (or tholeiitic) series. Thus, all samples from the WRD and WD are comparable to subalkaline rocks of Irvine and Baragar (1971).

The WRD granitoids appear to be relatively rich in K_2O, with varied Na_2O/K_2O ratios (DRI2022012). The granitoid samples taken from the Lac du Bonnet batholith display low Na_2O/K_2O ratios <1 (ranging from 0.49 to 0.98) and consistently high silica contents ranging from 71.50 to 77.62 wt. %, except for one sample that has a Na_2O/K_2O ratio of 2.26 and contains 66.47 wt. % SiO_2. These rocks are exclusively of the high-K calcalkaline series based on the K_2O versus SiO_2 diagram (not shown) of Peccerillo and Taylor (1976), except for the low silica sample being of the calcalkaline series. The granitoids in the Pointe du Bois batholith exhibit varied Na_2O/K_2O ratios ranging from 0.59 to 2.97, consistent with high-K calcalkaline to calcalkaline series. Similarly, the granitoid samples from the Rennie River plutonic suite have more variable Na_2O/K_2O ratios ranging from 0.54 to 4.43, attributed dominantly to high-K calcalkaline and extending to

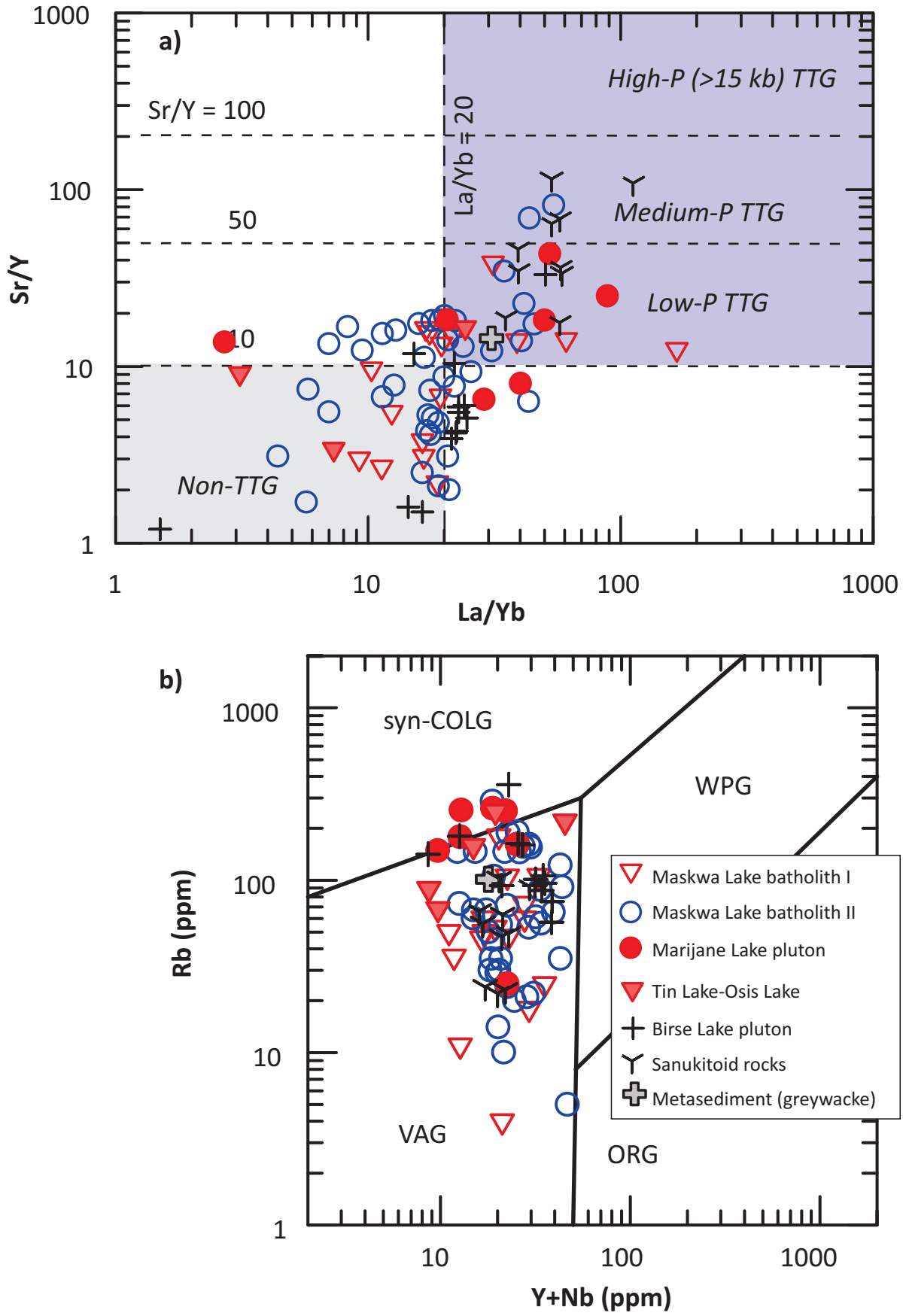

Figure 40: *Tectonomagmatic discrimination diagram for the Neoarchean granitoid rocks from the Bird River greenstone belt:* ***a)*** *plot of La/Yb versus Sr/Y; the boundary between Sr/Y and La/Yb ratios used to define TTG and subtypes is from Moyen and Martin (2012);* ***b)*** *plot of (Y+Nb) versus Rb (after Pearce et al., 1984). Abbreviations: ORG, ocean-ridge granitoid; syn-COLG, syncollisional granitoid; TTG, tonalite-trondhjemite-granodiorite; VAG, volcanic-arc granitoid; WPG, within-plate granitoid.*

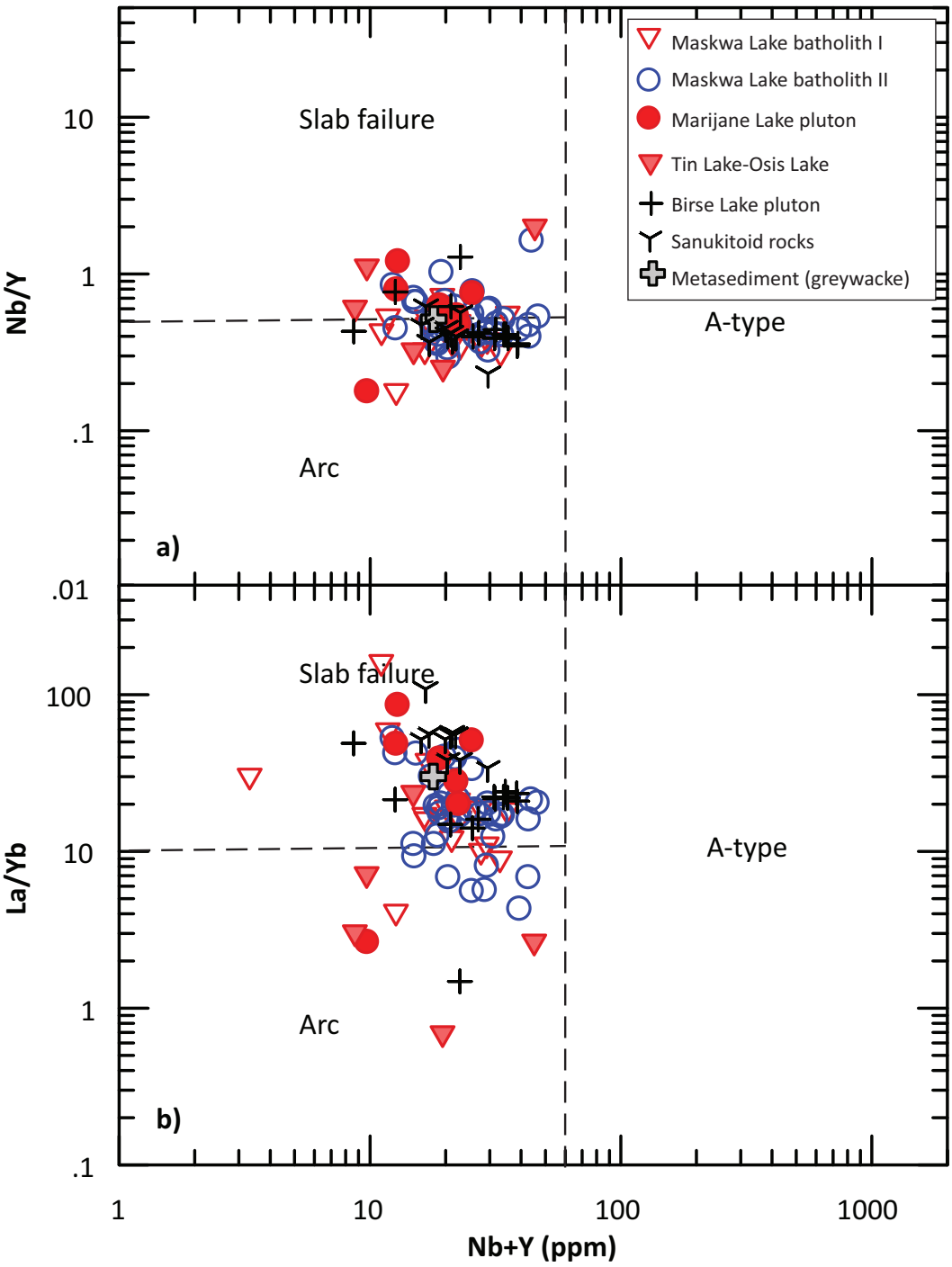

Figure 41: *Discrimination plots of Nb/Y versus Nb+Y (ppm) and La/Yb versus Nb+Y (ppm) for the Neoarchean granitoid rocks from the Bird River greenstone belt. Boundaries for slab-failure, arc and A-type granitoids from Whalen and Hildebrand (2019).*

calcalkaline to arc-tholeiitic series in terms of the K_2O versus SiO_2 relationship defined by Peccerillo and Taylor (1976). The samples from the Big Whiteshell Lake pluton are potassic-rich with Na_2O/K_2O ratios of 0.51 to 0.88, and are high-K calcalkaline. The WD granitoid samples shows a relatively small variation in Na_2O/K_2O ratios of 0.95 to 1.42, plotting in the field of high-K calcalkaline series (not shown) of Peccerillo and Taylor (1976).

On the SiO_2 versus Fe* and MALI plots (not shown), most of the graintoid samples from the WRD and WD are magnesian and attributed to calcic to calcalkalic granitoids based on the geochemical classification of Frost et al. (2001). Few evolved samples extend to the field of ferroan granitoids. Based on the relationship of Zr contents (ppm) versus (10^4Ga/Al) ratios proposed by Whalen et al. (1987), some of the WRD granitoid samples with Zr concentrations higher than 300 ppm (DRI2022012) plot in the field of A-type, indicating that they are possibly A-type. However, the other WRD samples together with the WD samples containing Zr contents less than 250 ppm fall into the field of I- and S-type (not shown) or extend into the A-type field, suggesting

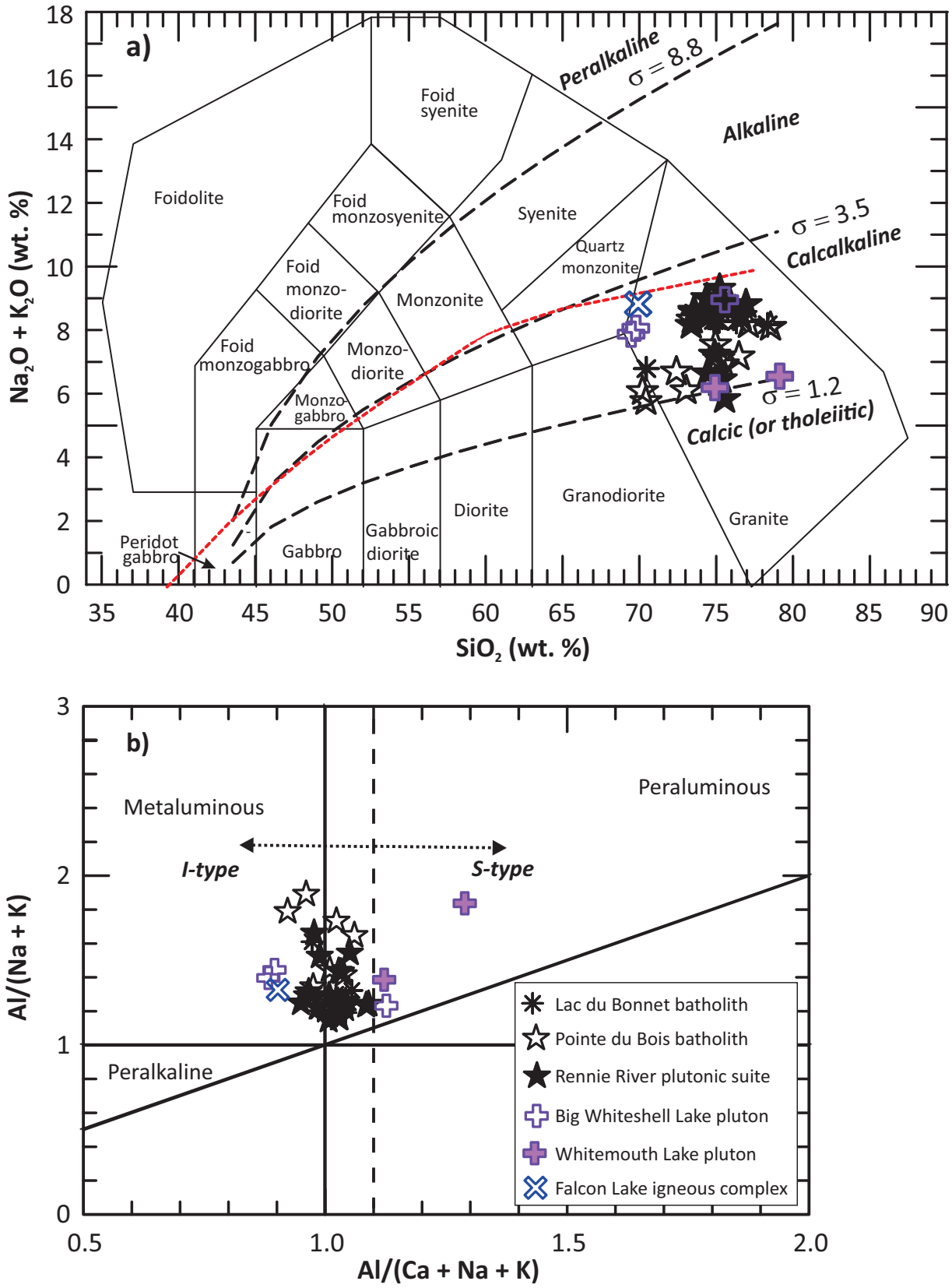

Figure 42: *Chemical classification of granitoids from the Winnipeg River and Wabigoon domains based on alkalinity and alumina-saturation index:* ***a)*** *total alkalis (Na_2O+K_2O) versus SiO_2 (TAS; wt. %) diagram (fields from Middlemost, 1994); boundary (red dashed line) between alkaline and subalkaline series from Irvine and Baragar (1971); Rittmann serial index σ = $(Na_2O+K_2O)^2/(SiO_2–43)$, unit in wt. % (Rittmann, 1973); using σ values to subdivide granitoids further into calcic (tholeiitic), calcalkaline, alkaline and peralkaline series (Yang, 2007);* ***b)*** *Shand index plot (fields from Maniar and Piccoli, 1989); ACNK = $Al_2O_3/(CaO+Na_2O+K_2O)$, ANK = $Al_2O_3/(Na_2O+K_2O)$, unit in mole; vertical dashed line indicates ACNK = 1.1, a key parameter discriminating S- and I-type granites (Chappell and White, 1974).*

that their high (10^4Ga/Al) ratios may have resulted from magmatic fractionation.

In terms of the Shand index (Maniar and Piccoli, 1989), the granitoid samples from the WDR and WD are metaluminous to moderately peraluminous, except for three samples (i.e., one from the Rennie River plutonic suite and two from the Whitemouth Lake pluton) that are strongly peraluminous (Figure 42b). Their geochemical compositions suggest that these granitoid rocks are dominantly I-type due to an ACNK <1.1 (Chappell and White, 1974, 2001), which is supported by their relatively high MS values (Table 2), and consistent with likely derivation from partial melting of igneous source rocks. However, the three granite samples with ACNK >1.1 are likely S-type and emplaced into a terrane boundary zone.

The WRD and WD granitoid samples are portrayed in the CIPW normative albite (Ab)-anorthite (An)-orthoclase (Or) ternary diagram of Barker (1979) to show their compositional variation (Figure 43a). The samples from the Lac du Bonnet batholith are dominantly granite with only one sample plotting in the tonalite field, indicative of evolved features of potassic-rich granites, typically increasing Or with decrasing An components. Similarly, the other samples are straddled along the boundaries dividing the fields of trondhjemite and tonalite, and granodiorite and granite, showing the compositional trend present in the Lac du Bonnet batholith. Such a chemical variation evident both in intra- and inter-intrusion is ascribed to magmatic fractionation commonly seen in Archean TTGs. On the Zr/TiO_2 versus Nb/Y diagram (Figure 43b), the WRD and WD granitoid samples are mostly clustered among the fields of diorite, monzonite, syenite and granite. Based on the classification of Pearce (1996), the samples with high Nb/Y ratios (>0.8) and higher Zr contents (>300 ppm) are probably alkaline, but those with lower Nb/Y ratios (<0.8) and lower Zr contents (<250 ppm) are probably subalkaline (DRI2022012). However, use of Nb/Y ratios to classify granitoid rocks seem to conflict with the discriminant result based on the TAS diagram (Figure 42a) using σ values that suggest the WRD and WD rocks are dominantly calcalkaline series. The high Nb/Y ratio of calcalkaline rocks may be interpreted by contamination of continental crust, in particular for those rocks lacking of sodic-amphibole and/sodic-pyroxene (e.g., Barbarin, 1999; Yang, 2007; Yang et al., 2021).

Trace-element geochemistry

Granitoid rocks in the WRD and WD display moderate to relatively high Sr, Ba, but low Rb, Cs contents of LILEs. Most of these rocks show extremely to moderately low Rb/Sr ratios ranging from 0.01 to 0.99. However, some exposures with relatively high Rb/Sr ratios ranging from 1.04 to 4.90 are evident in the Lac du Bonnet batholith and Rennie River plutonic suite of the WRD, indicative of higher degree of magmatic fractionation (DRI2022012). The WRD and WD granitoids have a range of K/Rb ratios of 112 to 1233, suggesting that the granitoid magmas derived from an evolved to unevolved source region (e.g., Blevin, 2004). Note that sample 111-14-255A01, with K/Rb ratio of 1233, from the Rennie River plutonic suite, also has a very high La/Yb ratio of 197.6 and a Sr/Y ratio of 1370, consistent with typical Archean sanukitoids in the BRGB and elsewhere (e.g., Halla et al., 2017).

Figure 44 shows chondrite-normalized REE patterns in the left panel, and N-MORB–normalized extended trace-element profiles in the right panel, respectively, for the WRD and WD granitoid rocks. The granitoid samples from the Lac du Bonnet batholith demonstrate a strong fractionation of LREE relative to HREEs with moderately to pronounced negative Eu anomalies (Eu/Eu* values of 0.41 to 0.75), except for two samples showing moderate enrichment and/or depletion of REE abundances compared with the chrondrite values, with positive Eu anomalies (Eu/Eu* values of 1.45 to 2.57; Figure 44a). Some of the samples show convex downward patterns, especially in the HREE (Tb to Lu), reflecting hornblende played a key role either in the fractionating assemblage or in residues of the magma source (e.g., Rollinson, 1993; Yang et al., 2008; Rollinson and Pease, 2021). The Pointe du Bois batholith samples show moderately to strongly LREE-enriched and HREE-depleted profiles (Figure 44c), with small negative to strong positive Eu anomalies, as indicated by Eu/Eu* values of 0.37 to 0.95 (DRI2022012). Granite samples from the Rennie River plutonic suite display varied profiles from LREE-enriched and HREE-depleted patterns with notably negative Eu anomalies indicated by Eu/Eu* values of 0.33–0.76, through flat REE patterns with notable Eu anomalies (Eu/Eu* = 0.47–0.53), to LREE enriched with remarkably positive Eu anomalies (Eu/Eu* = 2.36–10.90; Figure 44e; DRI2022012). This indicates that plagioclase may have played a role in their magmatic evolution, and that some rocks contain feldspar culmulate, suggesting that the Rennie River plutonic suite has a complex genesis likely involving diverse magmatic processes. Two different REE patterns are present in the Big Whiteshell Lake pluton; one characterized by moderately enriched LREE with notable negative Eu anomaly, and another with strongly enriched LREE, positive Eu anomaly (Figure 44g) and relatively low REE abundance. Two granitoid samples in the Whitemouth Lake pluton show less LREE enrichment than monzogranite in the Falcon Lake igneous complex (Figure 44i) from the WR, although both show slightly negative to no Eu anomalies (Eu/Eu* = 0.90–0.99).

N-MORB–normalized extended trace-element profiles of the WRD and WD granitoid rocks (Figure 44b, d, f, h, and j) reveal that they are enriched in incompatible elements (e.g., Cs, Rb), display positive Pb, and have pronounced negative Nb, Ti and P anomalies. This is a typical arc signature, suggesting that these granitoids may have formed in a magmatic-arc setting (e.g., Prouteau et al., 1999, 2001; Pearce et al., 2005; Anderson, 2013). It is noted that an evolved tonalite sample (111-14-235B01) from the Pointe du Bois batholith contains 49.3 ppm U (DRI2022012; Figure 44d), which is unusually high for Archean TTGs.

Granitoid samples from the WRD and WD have relatively high but varied Sr/Y and La/Yb ratios (Figure 45a). The granitoids in the Lac du Bonnet batholith display a large range of Sr/Y

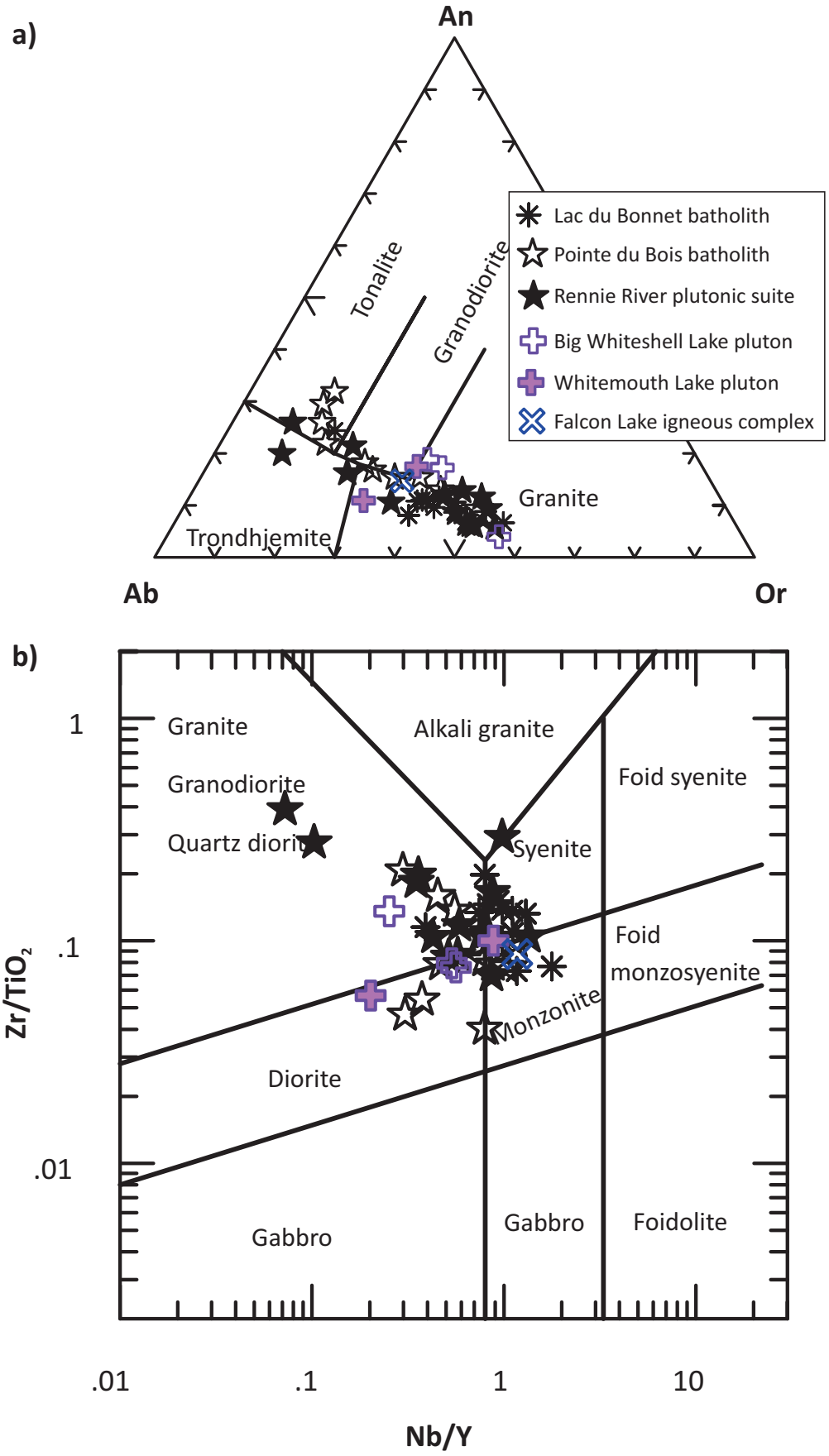

Figure 43: *Chemical classification of granitoids from the Winnipeg River and Wabigoon domains in terms of their CIPW normative compositions and HFSE:* ***a****) Ab-An-Or ternary diagram (fields from Barker, 1979);* ***b****) plot of Zr/TiO_2 versus Nb/Y (after Pearce, 1996). Abbreviations: Ab, albite; An, anorthite; CIPW, Cross, Iddings, Pirsson, Washington; HFSE, high-field-strength element; Or, orthoclase.*

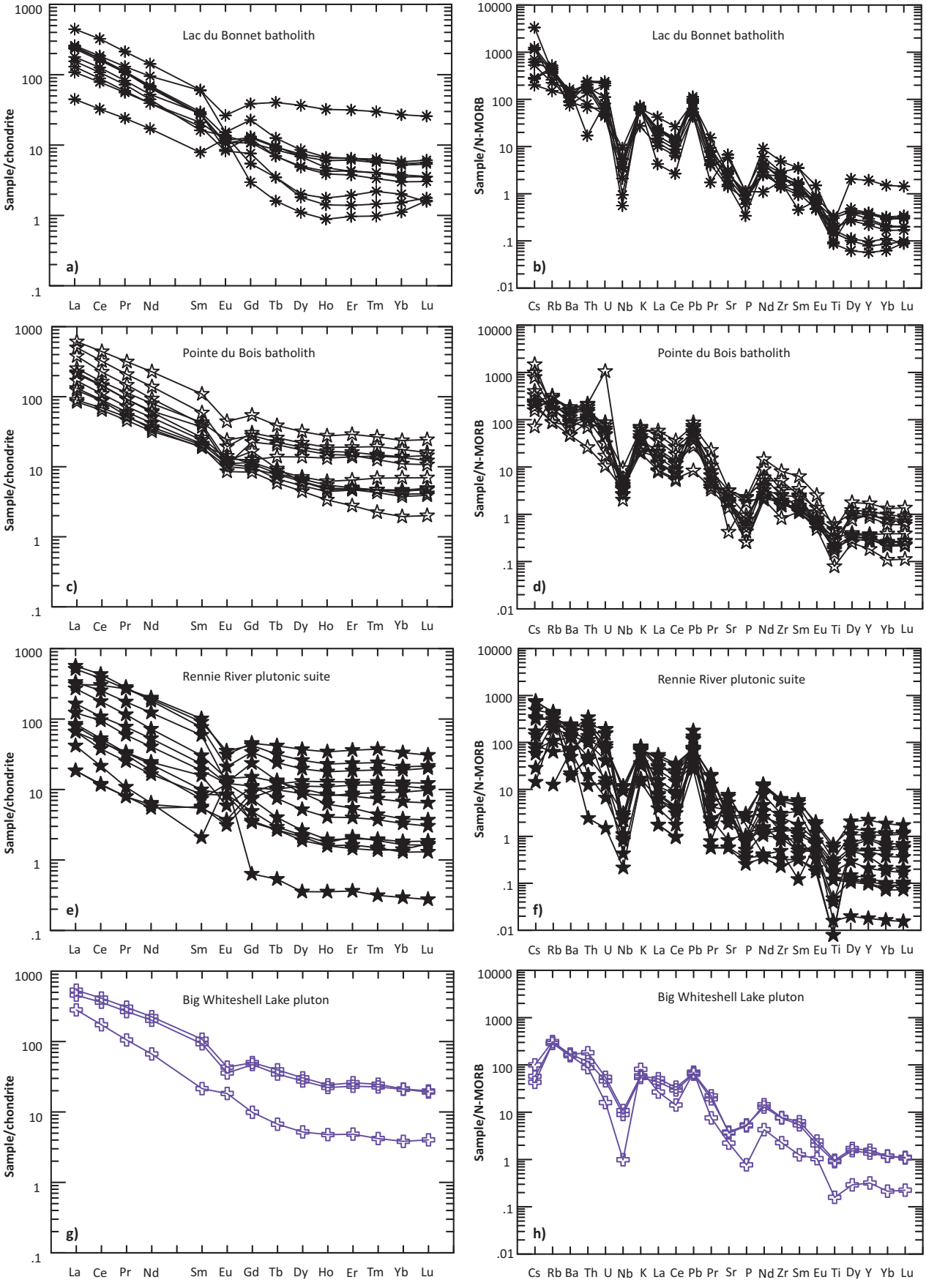

Figure 44: *Trace-element patterns of granitoid rocks from the Winnipeg River and Wabigoon domains: left panel* ***a), c), e), g), i)*** *chondrite-normalized rare-earth element patterns; right panel* ***b), d), f), h), j)*** *N-MORB–normalized extended trace-element profiles. Normalizing values from Sun and McDonough (1989).*

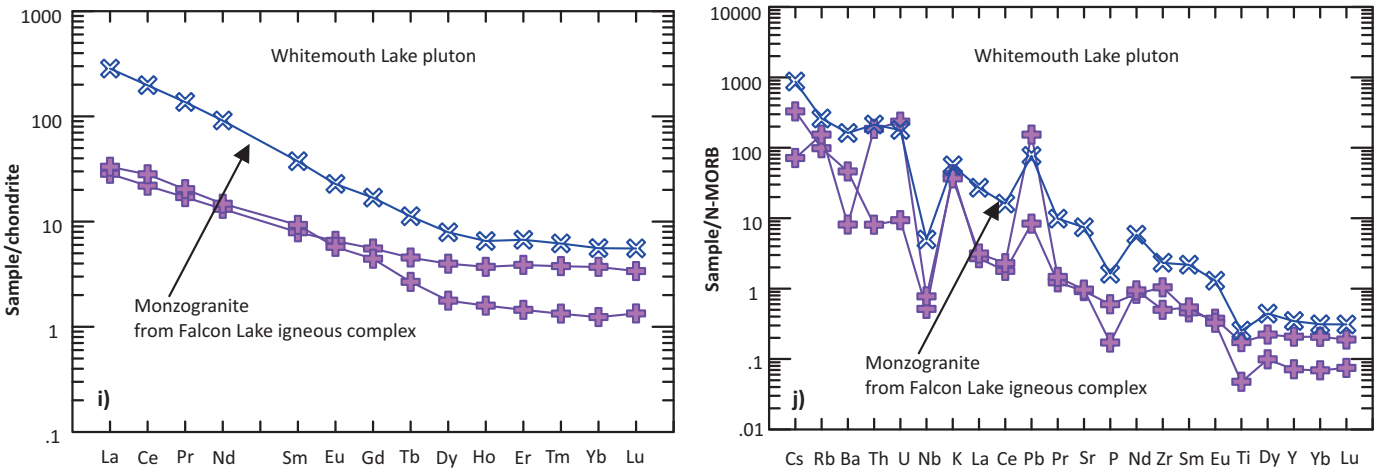

Figure 44 (continued): *Trace-element patterns of granitoid rocks from the Winnipeg River and Wabigoon domains: left panel* ***a), c), e), g), i)*** *chondrite-normalized rare-earth element patterns; right panel* ***b), d), f), h), j)*** *N-MORB–normalized extended trace-element profiles. Normalizing values from Sun and McDonough (1989).*

and La/Yb ratios and mostly resemble medium- to low-pressure TTGs, indicating the presence of garnet in their source region (Moyen and Martin, 2012); two samples plot in the non-TTG field, likely reflecting magmatic fractionation of feldspars that led to decrease in both the Sr/Y and La/Yb ratios in the residual melts. The Pointe du Bois batholith samples are mainly attributed to low-pressure TTG, and three samples have lower Sr/Y (<10) but relatively high La/Yb (>20), atypical of TTG. Granitoids from the Rennie River plutonic suite can be divided into two groups based on Sr/Y and La/Yb ratios: medium- to low-pressure TTG; and non-TTG. The latter lacks of garnet but contains feldspar in its source region. Again, granitoids in the Big Whiteshell Lake pluton show low-pressure TTG to atypical TTG composition. Two Whitemouth Lake pluton samples and one sample of the Falcon Lake igneous complex from the WD also show features of low- to medium-pressure TTGs. Kepezhinskas et al. (2022) point out that granitoids with Sr/Y ratios <40 and Y>15 ppm represent magmatic-arc signatures. In fact, these WRD samples plot in the field of non-TTG (Figure 45a) as described previously and have very low Sr/Y ratios (<10) but high Y contents ranging from 23.8 to 62.6 ppm (DRI2022012), suggesting that they may have formed in a magmatic-arc regime.

Figure 45b shows distribution of the WRD and WD granitoid samples on the Rb versus Y+Nb discrimination diagram of Pearce et al. (1984), indicating that the WD and most WRD samples are located in the field of volcanic-arc granitoids. However, some of the WRD samples extend to the fields of syncollisional and within-plate granitoids. For example, the Lac du Bonnet batholith samples straddle along the boundary between the volcanic-arc and syncollisional granitoids, and one falls into the A-type granite field. This can be explained by crustal contamination and extensive fractionation involving hornblende. Such explanation is also applicable to most samples of the Rennie River plutonic suite and the Big Whiteshell Lake pluton. However, part of the Rennie River plutonic suite is S-type granite (Table 2) as reported before (Yang, 2014a; Yang et al., 2019), consistent with geochemical features of the syncollisional (Pearce et al., 1984) and/or post-collisional granites (Sylvester, 1998).

Plotting the WRD and WD granitoid samples on the Nb/Y versus Nb+Y (ppm) and La/Yb versus Nb+Y (ppm) diagrams of Whalen and Hildebrand (2019) reveals that most of them fall into the field of slab failure magmatism, some in the field of arc, and few into the A-type granite field (Figure 46a, b). Athough A-type granitoids have higher concentration of Nb+Y than those emplaced into magmatic arc and/or formed by slab failure magmatism, the high Y contents (>15 ppm) are actually a diagnostic charcteristic of arc rocks (e.g., Kepezhinskas et al., 2022) and Y behaves similarly to Yb in magmatic system (Rollinson and Pease, 2021). Thus, arc granitoids must have lower Nb/Y and La/Yb ratios than those of slab failure magmatism. Based on these geochemical parameters, the WRD and WD granitoids are likely to have formed in magmatic arc or by slab failure magmatism.

In summary, the granitoid rocks from the Winnipeg River and Wabigoon domains are mostly attributed to Archean TTG suite with typical features of I-type granites, which formed in magmatic-arc regime and related slab failure magmatism. Inter-intrusion variation may have been ascribed to differences in their petrogenetic processes, e.g., degree of fractionation, supra-crustal contamination, and magma sources. Parts of the Rennie River plutonic suite from the WRD and Whitemouth Lake pluton from the WD are S-type granites formed at collisional zones between domain boundaries.

Geochemistry of granitoid rocks from the Superior boundary zone, Munro Lake and Molson Lake domains

Geochemical characteristics of 24 granitoid samples collected from 12 plutons/intrusions (i.e., Fox Lake, Assean Lake, Orr Lake, Ospwagan Lake, Paint Lake, Grass River, Setting Lake, Kiski Lake, Jenpeg Dam, Nelson River, and Paimusk Creek; see Figure 4), including 16 samples from the Superior boundary zone (SBZ), 3 from the Munro Lake (MOLD) and 5 from the Molson

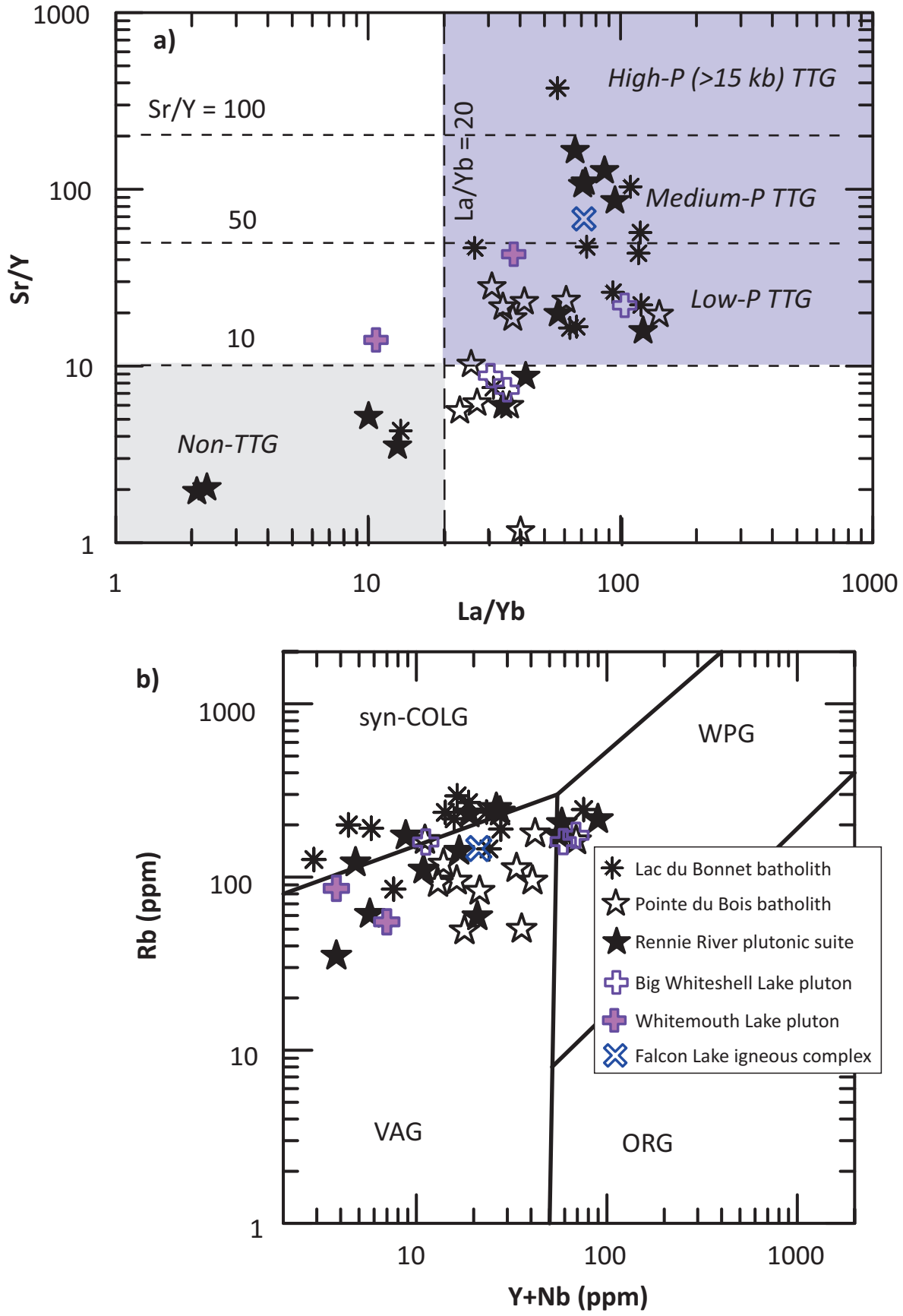

Figure 45: *Discrimination plots for granitoid rocks from the Winnipeg River and Wabigoon domains:* ***a)*** *La/Yb versus Sr/Y diagram; boundaries used to define TTG types from Moyen and Martin (2012);* ***b)*** *tectonomagmatic discrimination diagram of (Y+Nb) versus Rb (after Pearce et al., 1984). Abbreviations: ORG, ocean-ridge granitoid; syn-COLG, syncollisional granitoid; TTG, tonalite-trondhjemite-granodiorite; VAG, volcanic-arc granitoid; WPG, within-plate granitoid.*

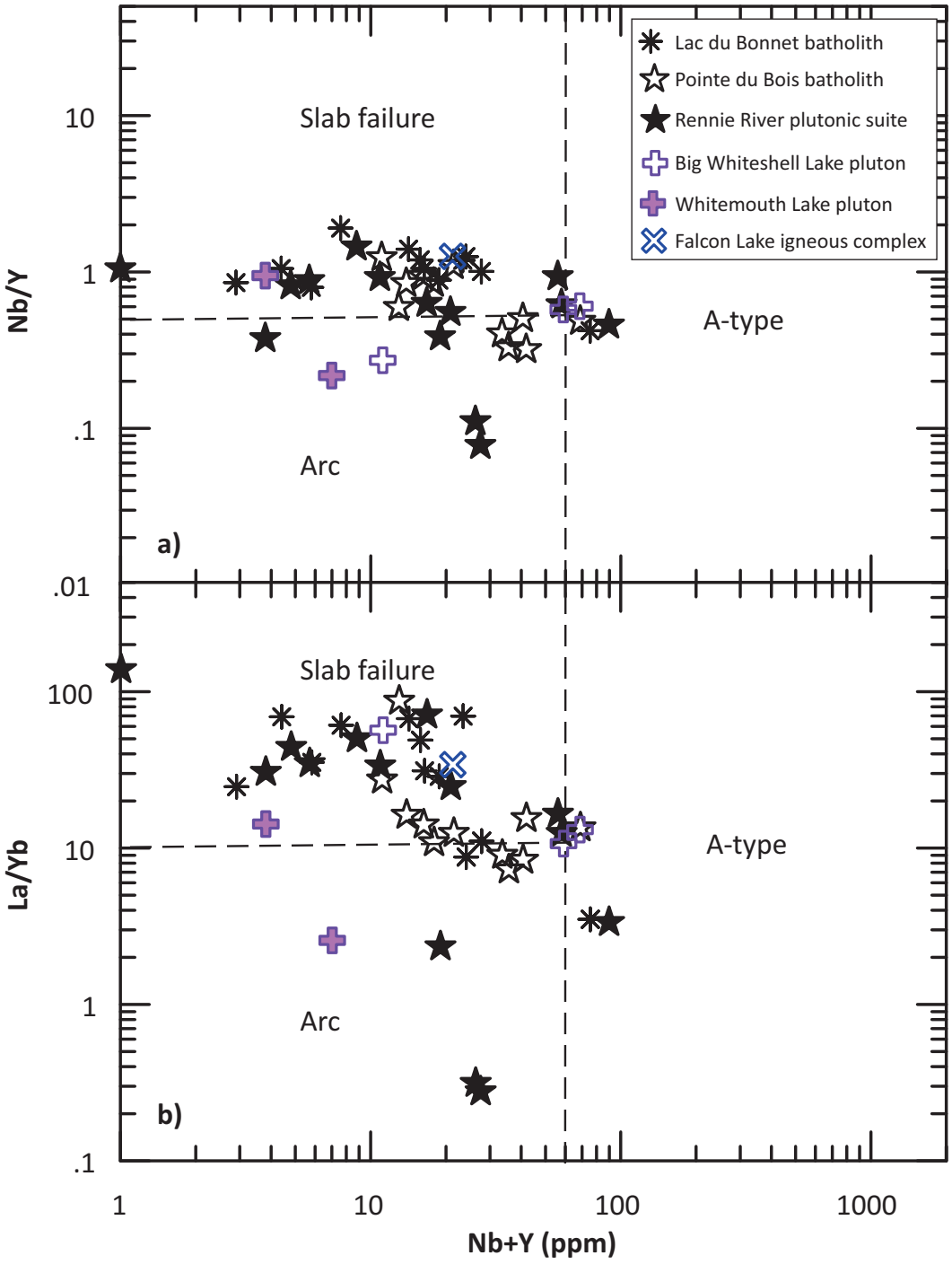

Figure 46: *Discrimination plots of Nb/Y versus Nb+Y (ppm) and La/Yb versus Nb+Y (ppm) for granitoid rocks from the Winnipeg River and Wabigoon domains. Boundaries for slab-failure, arc and A-type granitoids from Whalen and Hildebrand (2019).*

Lake domains (MLD) are described and discussed together in the following section.

Classification

On the TAS diagram (Figure 47a), most of the SBZ granitoid samples, with SiO_2 contents ranging from 69.78 to 74.99 wt. % (see DRI2022012), are located in the field of granite, and one sample from the Setting Lake pluton falls in the granodiorite field. Based on the Rittmann serial index (σ) calculations, the SBZ samples mostly have σ values between 1.2 and 3.5, belonging to the calcalkaline series (Yang, 2007), whereas one sample from the Ospwagan Lake intrusion has a σ value of 4.1 that is attributed to alkaline series, and one sample from the Orr Lake intrusion with σ value of 1.0 that is calcic (or tholeiitic). Except of the Ospwagan Lake intrusion sample, all other SBZ samples belong to the subalkaline series according to Irvine and Baragar (1971). The MOLD and MLD granitoid samples all plot in the granite field and display σ values that range from 1.2 to 3.5, belonging to the calcalkaline series that is comparable to subalkaline series defined by Irvine and Baragar (1971).

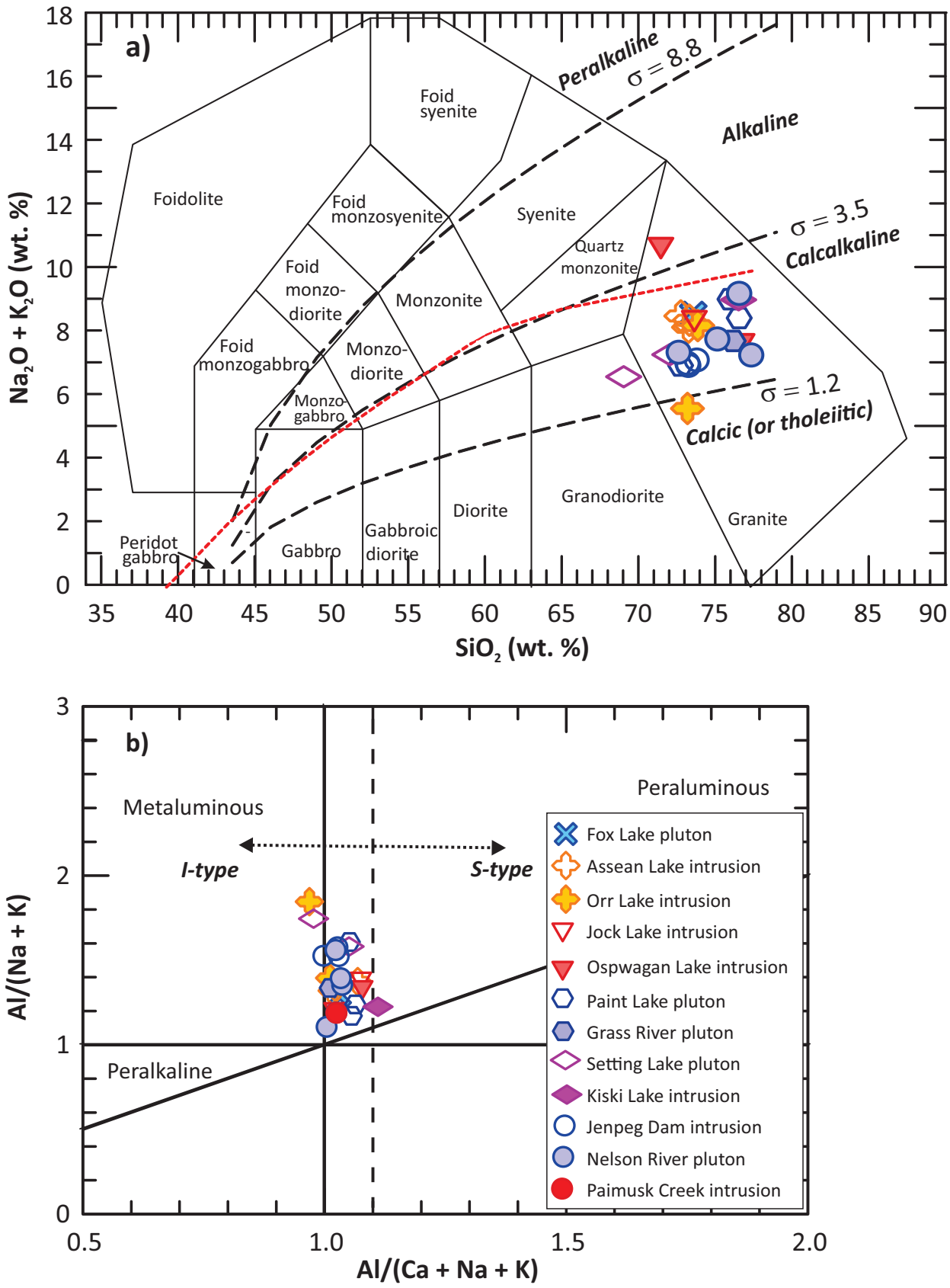

Figure 47: *Chemical classification of granitoids from the Superior boundary zone as well as the Munro Lake and Molson Lake domains based on alkalinity and alumina-saturation index:* ***a)*** *total alkalis (Na_2O+K_2O) versus SiO_2 (TAS; wt. %) diagram (fields from Middlemost, 1994), plotted on the anhydrous basis; boundary (red dashed line) between alkaline and subalkaline series from Irvine and Baragar (1971); Rittmann serial index σ = $(Na_2O+K_2O)^2/(SiO_2–43)$, unit in wt. % (Rittmann, 1973); using σ values to further subdivide granitoids into calcic (tholeiitic), calcalkaline, alkaline and peralkaline series (Yang, 2007);* ***b)*** *Shand index plot (fields from Maniar and Piccoli, 1989); ACNK = $Al_2O_3/(CaO+Na_2O+K_2O)$, ANK = $Al_2O_3/(Na_2O+K_2O)$, unit in mole; vertical dashed line indicates ACNK = 1.1, a key parameter discriminating S- and I-type granites (Chappell and White, 1974).*

The SBZ granitoids show varied Na_2O/K_2O ratios ranging from 0.26 to 6.57 (DRI2022012). The samples with low Na_2O/K_2O ratios of <1.0 are likely S-type, whereas those with high Na_2O/K_2O ratios of >1.0 may be I-type (Table 1). These rocks are mostly calcalkaline to high-K calcalkaline series based on the K_2O versus SiO_2 diagram (not shown) of Peccerillo and Taylor (1976), except for the Kiski Lake intrusion sample that is shoshonitic with 6.96 wt. % K_2O and 74.80 wt. % SiO_2. The MOLD granitoids are consistently rich in Na_2O relative to K_2O with Na_2O/K_2O ratios of 1.43 to 1.97. The MLD samples show variable Na_2O/K_2O ratios of 0.50 to 1.13. These granitoids are calcalkaline to high-K calcalkaline series according to Peccerillo and Taylor (1976).

On the SiO_2 versus Fe* and MALI plots (not shown) of Frost et al. (2001), the granitoid samples from the SBZ, MOLD and MLD are mostly magnesian, although few evolved samples are ferroan and attributed to calcic to calcalkalic to alkali-calcic granitoids. Based on the relationship of Zr contents (ppm) versus (10^4Ga/Al) ratios (Whalen et al., 1987), these granitoids plot in the field of I- and S-type granites (not shown). Only one sample from the Nelson River pluton of MLD and two samples from the Jenpeg Dam intrusion in the MOLD plot in the A-type granite field, but these three samples contain low to moderate Zr contents of <200 ppm (DRI2022012), and thus are unlikely A-type granites (e.g., Whalen et al., 1987; Eby, 1990).

In terms of the Shand index (Maniar and Piccoli, 1989), the granitoid samples from the SBZ, MOLD and MD are moderately peraluminous with ACNK values between 1.0 and 1.1, although within the SBZ there are one sample from the Orr Lake intrusion and one from the Setting Lake pluton that are metaluminous, and one sample with an ACNK value of 1.11 from the Kiski Lake intrusion that is strongly peraluminos (Figure 47b).

Figure 48a shows the SBZ, MOLD and MLD granitoid samples portrayed in the CIPW normative albite (Ab)-anorthite (An)-orthoclase (Or) ternary diagram of Barker (1979), indicating bulk compositional variations. The granitoid samples from the SBZ dominantly plot in the field of granite and extend to the fields of granodiorite, tonalite and trondhjemite. The MOLD samples are granodiorite, whereas the MLD samples fall into the fields of granodiorite and granite.

On the Zr/TiO_2 versus Nb/Y classification diagram of Pearce (1996), the SBZ granitoid samples mostly plot in the fields of diorite and granite, and one sample each from the Assean Lake intrusion and Setting Lake pluton, respectively, are located in the monzonite field, and one sample from the Paint Lake pluton falls in the alkali granite field (Figure 48b). The granitoid samples with high Nb/Y ratios (>0.8) and higher Zr contents (>300 ppm) are probably alkaline, but those with lower Nb/Y ratios (<0.8) and lower Zr contents (<250 ppm) are subalkaline (DRI2022012). Therefore, these plotting in the fields of monzonite and alkali granite are probably the product of crustal contamination rather than reflect alkaline affinities (Pearce, 1996), when compared with the TAS diagram (Figure 47a) described above. The MOLD samples fall within the field of monzonite as their Nb/Y ratios are higher than 0.8, whereas the MLD granitoids plot in the fields of granite, alkali granite and syenite. These MLD granites with Nb/Y ratios >0.8 are calcalkaline rocks because of their low Zr contents (up to 165 ppm; see DRI2022012), which are likely caused by contamination of continental crust, in particular for those rocks lacking of sodic-amphibole and/sodic-pyroxene (e.g., Barbarin, 1999; Yang, 2007; Yang et al., 2021).

Trace-element geochemistry

The SBZ granitoid rocks have low Rb, Cs, and moderate to high Sr, Ba contents (DRI2022012) of LILEs. Most of these rocks show very to moderately low Rb/Sr ratios ranging from 0.07 to 0.81, and relatively high K/Rb ratios of 321 to 842, indicating that these rocks are compositionally less fractionated and their source rocks are moderately evolved to unevolved (Blevin, 2004). Exception for two samples from the Paint Lake pluton is evident, however, that display very high Rb/Sr ratios of 4.02 to 19.00 but relatively low K/Rb ratios of 176 to 214 (DRI2022012). The Paint Lake pluton is S-type (Table 2), with relatively high Rb but low Sr contents, suggesting that its source rocks are likely more evolved sedimentary rocks (e.g., Chappell and White, 2001; Blevin, 2004). The MOLD granitoids contain low Rb, Cs and moderate Sr, Ba contents, with low Rb/Sr (0.24 to 0.42) and moderate K/Rb ratios (230 to 292). The MLD granitoids display low Cs (up to 7.3 ppm), moderate and varied Rb, Sr, and Ba contents (DRI2022012), with a large range of Rb/Sr ratios of 0.54 to 23.50 and low to moderate K/Rb ratios of 112 to 266, suggesting a high degree of differentiation of the granitoid magmas that may have been derived from a moderately evolved source region (Blevin, 2004).

Figure 49 shows chondrite-normalized REE patterns in the left panel, and N-MORB–normalized extended trace-element profiles in the right panel, respectively, of the SBZ, MOLD and MLD granitoid rocks. The SBZ granitoid samples display distinct REE patterns, varying from strong to moderate LREE enrichment and HREE depletion without Eu anomalies (e.g., Fox Lake pluton, Assean Lake intrusion, Grass Lake and Setting Lake plutons, Kiski Lake intrusion) or with positive Eu positive anomalies (e.g., Orr Lake and Jock Lake intrusions; Figure 49a, c). Some granitoids (e.g., Ospwagan Lake intrusion, Paint Lake pluton) show moderate to slight enrichment of LREE relative to HREE with pronounced negative Eu or with slightly positive anomalies (Figure 49c). The MOLD granitoid samples (e.g., Jenpeg Dam intrusion) consistently display a strong LREE enrichment relative to HREE without notable Eu anomalies (Figure 49e), typical of TTGs. In contrast, the MLD granitoids exhibit varied REE patterns, from moderately fractionated to flat profiles, without notable to strongly negative Eu anomalies (e.g., Nelson River pluton, Paimusk Creek intrusion; Figure 49e), reflecting that different petrogenetic processes may have been involved in different intrusions. For instance, the Jenpeg Dam intrusion is likely part of TTG displaying geochemical signatures of I-type formed in a magmatic-arc setting, whereas the Paimusk Creek intrusion is an S-type emplaced in a collisional regime.

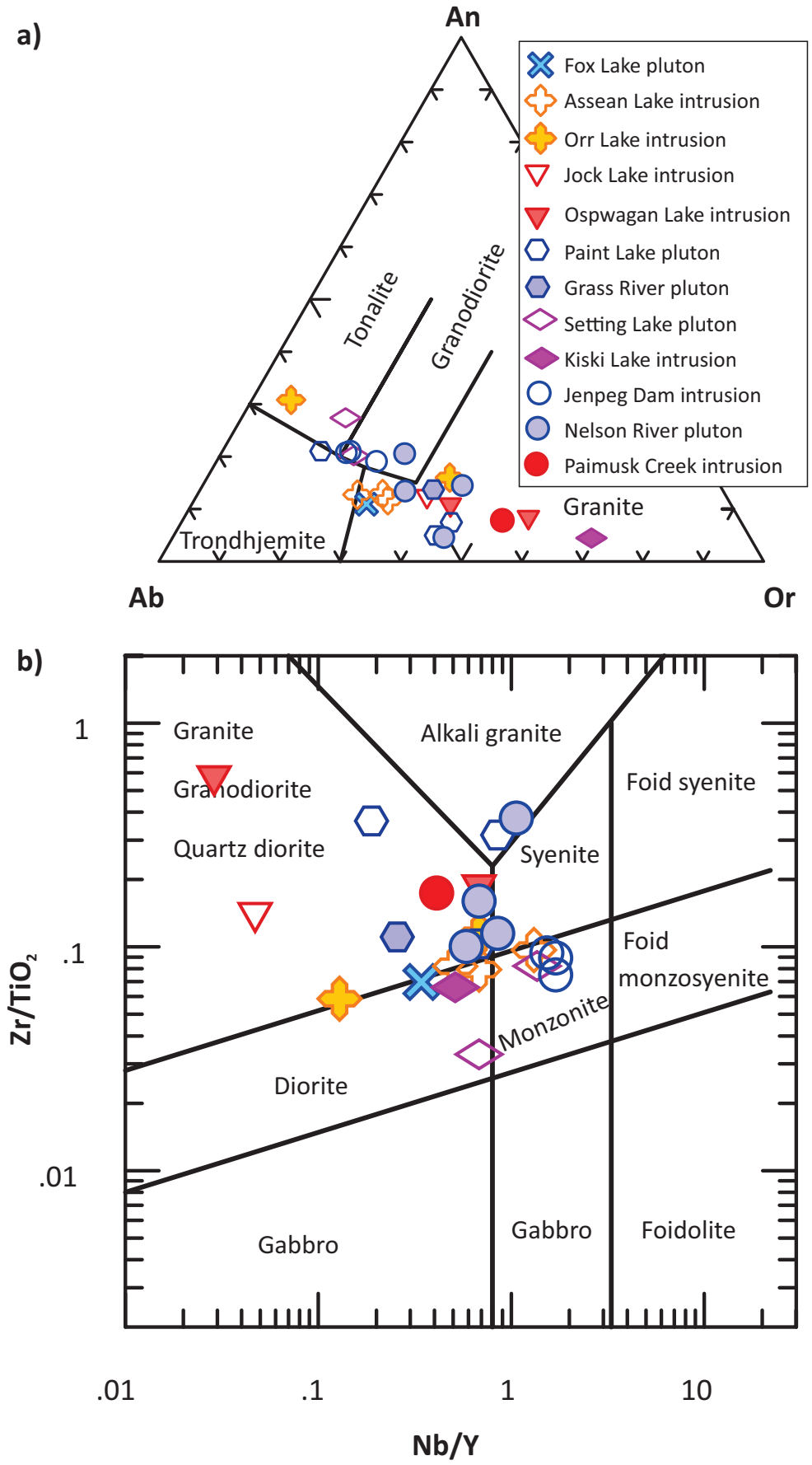

Figure 48: *Chemical classification of granitoids from the Superior boundary zone as well as the Munro Lake and Molson Lake domains in terms of CIPW normative compositions and HFSE:* ***a****) Ab-An-Or ternary diagram (fields from Barker, 1979);* ***b****) plot of* Zr/TiO_2 *versus Nb/Y (after Pearce, 1996). Abbreviations: Ab, albite; An, anorthite; CIPW, Cross, Iddings, Pirsson, Washington; HFSE, high-field-strength element; Or, orthoclase.*

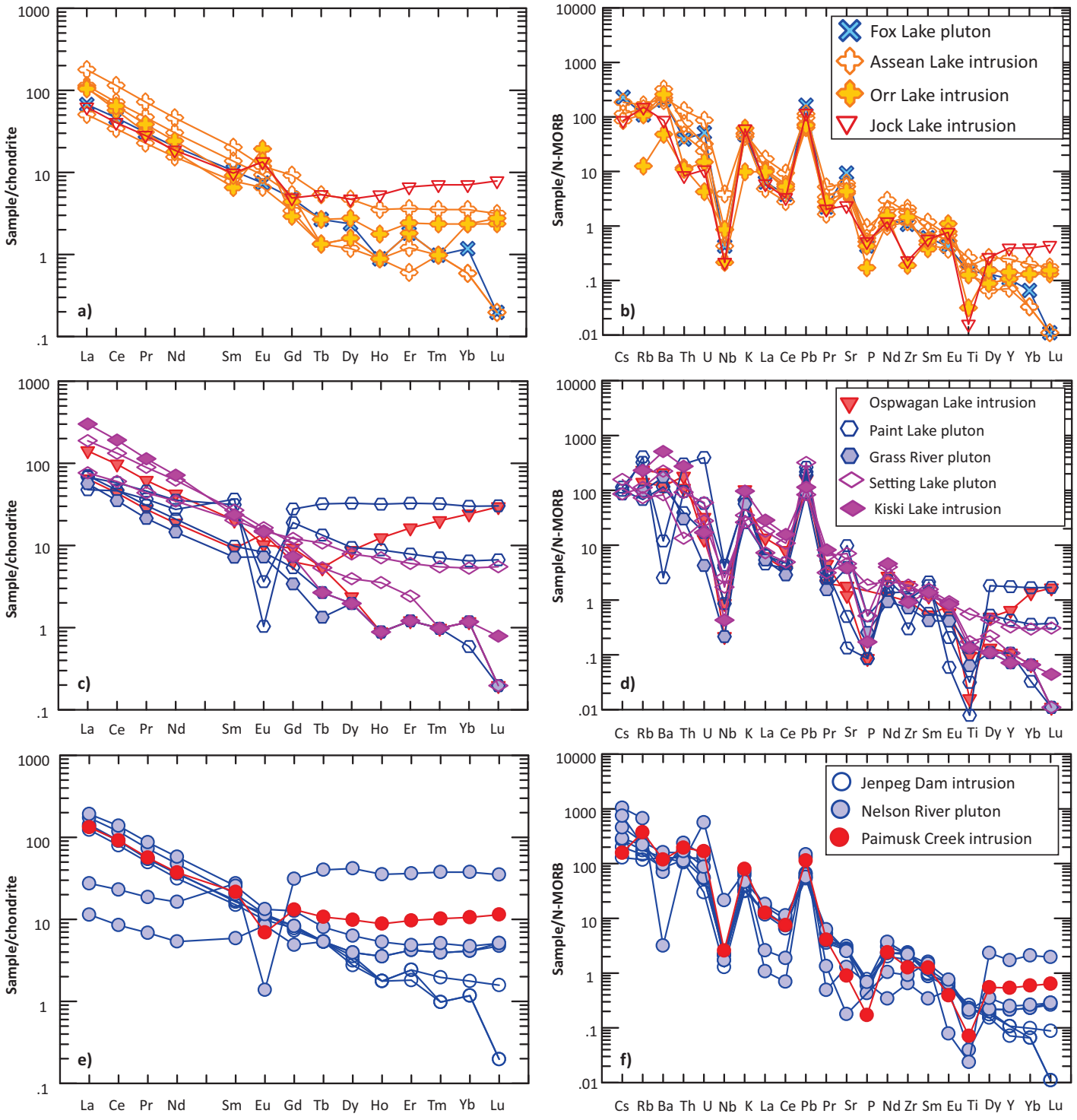

Figure 49: *Trace-element patterns of granitoid rocks from the Superior boundary zone as well as the Munro Lake and Molson Lake domains: left panel* ***a), c), e)*** *chondrite-normalized rare-earth element patterns; right panel* ***b), d), f)*** *N-MORB–normalized extended trace-element profiles. Normalizing values from Sun and McDonough (1989).*

N-MORB–normalized extended trace-element profiles of the SBZ, MOLD and MLD granitoid rocks (Figure 49b, d, and f) show that they are mostly enriched in incompatible elements (e.g., Cs, Rb), display positive Pb, and have pronounced negative Nb, Ti and P anomalies. This is a typical arc signature, suggesting that these granitoids may have formed in a magmatic-arc setting (e.g., Prouteau et al., 1999, 2001; Pearce et al., 2005; Pearce, 2008; Anderson, 2013). However, some of the samples (e.g., Paint Lake pluton in SBZ, and Nelson River pluton in MLD) also display remarkably negatively Ba and/or Sr normalies (Figure 49d, and f), suggesting that feldspar (particularly plagioclase) may have played a major role either in fractionating assemblages or in residues of the source regions (e.g., Rollinson, 1993). This is consistent with their REE patterns of moderately to slightly frac-

tionated LREE relatively to HREE and with pronounced negative Eu anomlies (Figure 49c, e). Although A-type granites commonly exhibit strongly negative Ba and Sr anomlies, they formed in an anorogenic setting (e.g., Whalen et al., 1987; Eby, 1990). However, there is no evidence for such a tectonic setting present in the SBZ at ca. 1850 to 1785 Ma (Machado et al., 2011a, b) and in the MLD during the Neoarchean (Parks et al., 2014).

Figure 50a shows the SZD, MOLD and MLD granitoids portrayed in the Sr/Y and La/Yb discrimination diagram of Moyen and Martin (2012), indicating that most of the samples have ratios of Sr/Y >10 and La/Yb >20. This suggests that these granitoids are likely attributed to low- to high-P TTGs, indicating that garnet in their source region was important during petrogenesis (Zhang et al., 2006; Moyen and Martin, 2012). Few samples (e.g., Ospwagan Lake intrusion, Paint Lake pluton, Paimusk Creek intrusion), however, plot in the field of non-TTG, suggesting absence of garnet in their source rocks. These samples have low Sr/Y ratios (<10) but high Y contents ranging from 48 to 49 ppm (DRI2022012), suggesting that they may have formed in a magmatic-arc setting.

Figure 50b shows distribution of the SBZ, DOLD and DLD granitoid samples on the Rb (ppm) versus Y+Nb (ppm) discrimination diagram of Pearce et al. (1984), indicating that most of the samples are located in the field of volcanic-arc granitoids. Again, exceptions are evident that the Paint Lake pluton sample plots on the boundary of the volcanic-arc and syncollisional granites, and the Kiski Lake intrusion sample falls in the syncollisional granite field; two samples plot in the fields of within-plate granitoids (one from the Paint Lake pluton, and one from the Nelson River pluton). Based on mineral assemblage and MS values (Table 2), the S-type Paint Lake pluton likely formed in a collisional setting, and the sample plotting in the within-plate granite field can be explained by its high Y content of 49 ppm (DRI2022012), indicative of derivation from an arc provenance. The I-type Kiski Lake intrusion must be enriched in culmulative K-feldspar indicated by its high Rb content and positive Ba, Sr and Eu anomalies (Figure 49d). The Nelson River pluton sample falls in the within-plate granite field due to its high Y content of 48 ppm (DRI2022012), which represents I-type (Table 2) formed in a magmatic-arc regime.

On the Nb/Y versus Nb+Y (ppm) and La/Yb versus Nb+Y (ppm) diagrams of Whalen and Hildebrand (2019), the SBZ, MOLD and MLD granitoid samples mostly plot in the field of slab failure magmatism, although few plot in the field of arc and only one in the A-type granite field (Figure 51a, b). Athough A-type granitoids have higher concentration of Nb+Y (>60 ppm) than those emplaced into magmatic arc and/or formed by slab failure magmatism, the high Y contents (>15 ppm) are a diagnostic charcteristics of arc rocks (e.g., Kepezhinskas et al., 2022), and Y behaves similarly to Yb in magmatic system (Rollinson and Pease, 2021). Thus, arc granitoids must have lower Nb/Y and La/Yb ratios than those of slab failure granitoids. Based on these geochemical parameters, the SBZ, MOLD and MLD granitoids are likely to have formed in magmatic arc or by slab failure magmatism, although some (e.g., the Paint Lake pluton) formed in a collisional setting in which their source rocks had inherited geochemical features of magmatic-arc–derived provenance.

In summary, the granitoid rocks from the Superior boundary zone, Munro Lake and Molson domains are mostly attributed to Archean TTG suites with typical features of I-type granites, which formed in magmatic-arc regime and related slab failure magmatism. The Paint Lake pluton, part of the Ospwagan Lake intrusion from the SBZ, and the Paimusk Creek intrusion in the MLD are S-type granites formed at collisional zones between domain boundary.

Geochemistry of granitoid rocks from the Trans-Hudson orogen

Geochemical characteristics of granitoid samples collected from part of the Trans-Hudson orogen are presented in the following sections, starting with the Lynn Lake domain and ending with the Kisseynew domain (Figures 1, 3 and 5).

Lynn Lake domain (LLD)

Geochemical characteristics of 70 granitoid samples from 15 granitoid plutons and/or intrusions (Table 2; DRI2022012) present in the Lynn Lake domain (LLD) are described by using major- and trace-element diagrams and elemental ratios below.

Classification

On the TAS diagram of Middlemost (1994), the LLD granitoid samples spread within a large range of compositions, covering the fields of gabbroic diorite, diorite, monzonite, syenite, granodiorite, and granite (Figure 52a). Both the inter-intrusion and intra-intrusion variation in chemical composition is evident. For instance, the Burge Lake pluton samples have higher contents of (Na_2O+K_2O) and SiO_2 than those from the Cockeram Lake pluton (DRI2022012). The samples from the Cockeram Lake pluton display a positive correlation between (Na_2O+K_2O) and SiO_2 contents. Interestingly, a negative correlation between (Na_2O+K_2O) and SiO_2 contents is evident for the Pool Lake plution, that contrasts with the trend of magmatic fractionation (e.g., Rollinson, 1993). Based on the Rittmann serial index (σ) calculations, the LLD granitoid samples mostly have σ values between 1.2 and 3.5, belonging to the calcalkaline series (Yang, 2007). One sample in the Eden Lake pluton with a σ value of 5.4 is attributed to the alkaline series, which is shoshonitic in magmatic affinity based on its K_2O (5.45 wt. %) and SiO_2 (61.21 wt. %) contents using the discrimination criterion of Peccerillo and Taylor (1976). All eight samples from the Counsell Lake pluton have σ values less than 1.2, indicating that they are calcic (or tholeiitic). Also, one sample each from the Cockeram Lake, Motriuk Lake and Hughs Lake plutons and Late intrusive suite, two from the Farley Lake pluton I, and four from the Pool Lake pluton, respectively, have σ values of less than 1.2, suggesting they are also calcic (or tholeiitic). Obviously, the LLD granitoid samples are dominantly subalkaline in

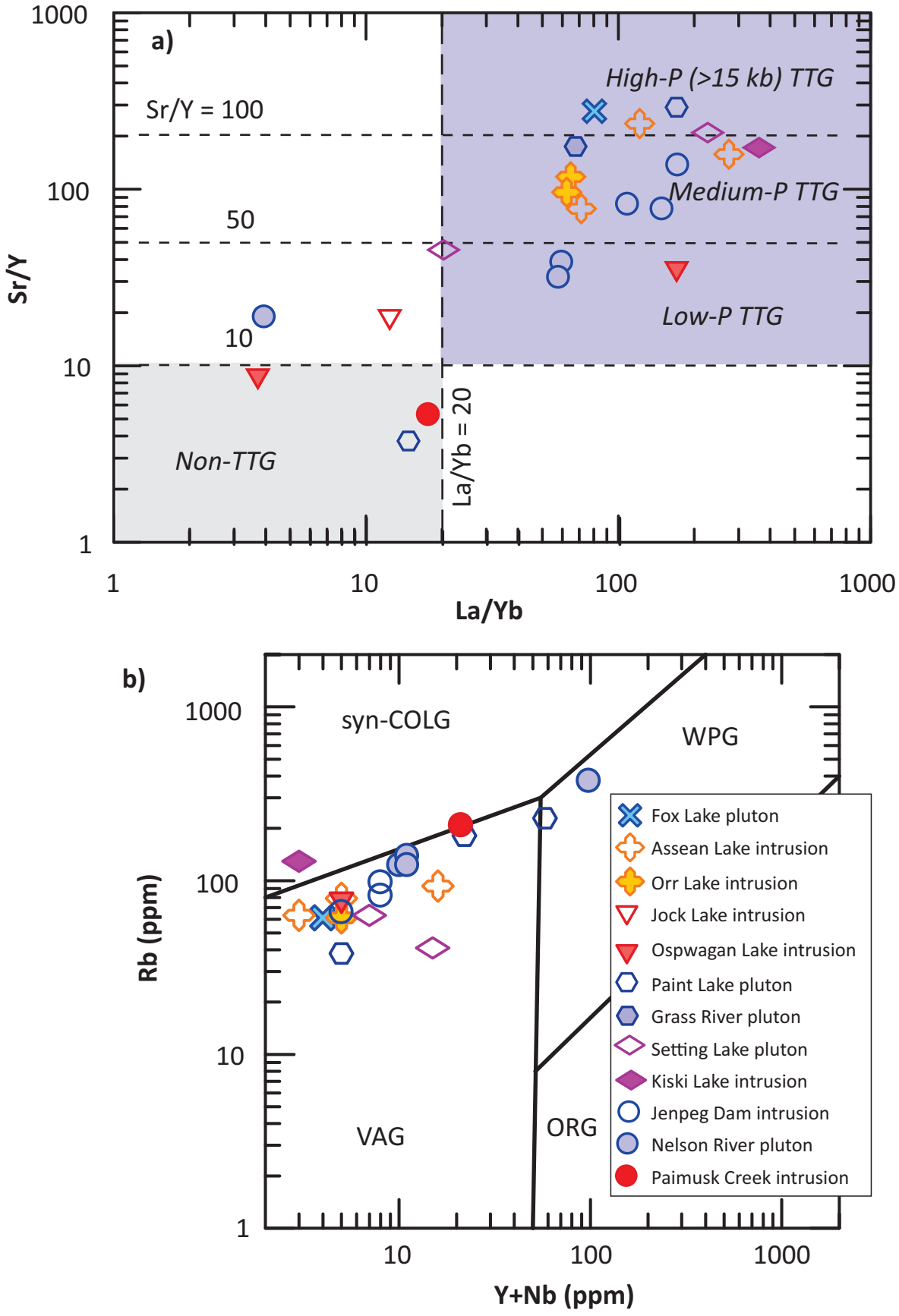

Figure 50: *Discrimination plots for granitoid rocks from the Superior boundary zone as well as the Munro Lake and Molson Lake domains:* ***a)*** *La/Yb versus Sr/Y diagram (the boundaries used to define TTG types from Moyen and Martin, 2012);* ***b)*** *tectonomagmatic discrimination diagram of (Y+Nb) versus Rb contents in ppm (after Pearce et al., 1984). Abbreviations: ORG, ocean-ridge granitoid; syn-COLG, syncollisional granitoid; TTG, tonalite-trondhjemite-granodiorite; VAG, volcanic-arc granitoid; WPG, within-plate granitoid.*

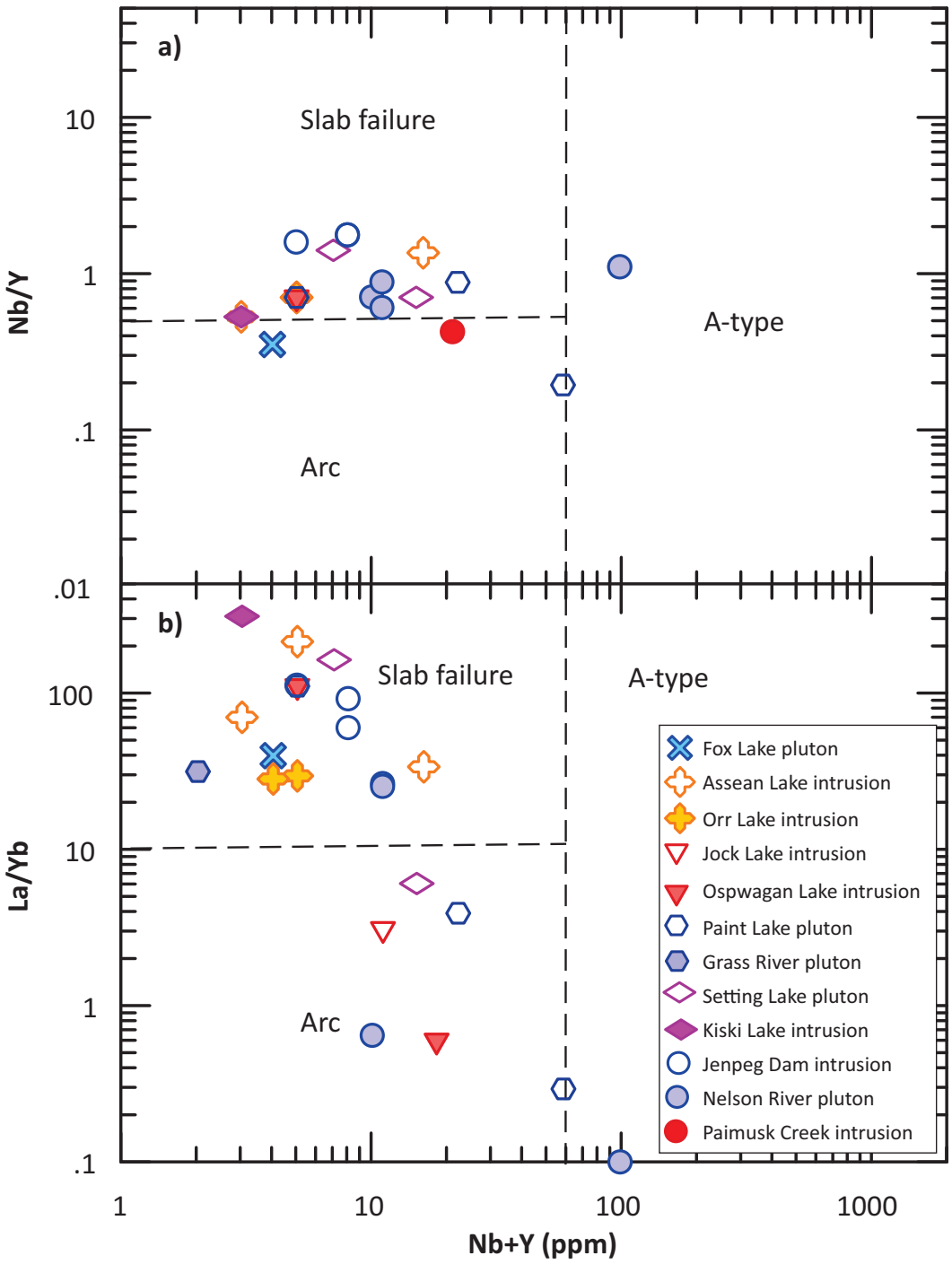

Figure 51: *Discrimination plots of Nb/Y versus Nb+Y (ppm) and La/Yb versus Nb+Y (ppm) for granitoid rocks from the Superior boundary zone as well as the Munro Lake and Molson Lake domains. Boundaries for slab-failure, arc and A-type granitoids from Whalen and Hildebrand (2019).*

terms of the classification scheme based on Irvine and Baragar (1971).

The granitoid samples collected from the LLD are predominantly rich in Na_2O relative to K_2O, mostly with high Na_2O/K_2O ratios of >1.0, although few samples have relatively low Na_2O/K_2O ratios of less than 1.0 (DRI2022012). It is noted that some granite samples from the Late intrusive suite have very high Na_2O/K_2O ratios, up to 61.22. The samples with high Na_2O/K_2O ratios of >1.0 may be I-type, whereas those with low Na_2O/K_2O ratios of <1.0 are likely S-type or evolved I-type (Tables 1 and 2).

Based on the K_2O versus SiO_2 diagram (not shown) of Peccerillo and Taylor (1976), most of the LLD granitoid rocks are calcalkaline, consistent with the discrimination results using the σ values (Figure 52a) mentioned above. Granitoid rocks from the Eden Lake pluton and Farley Lake stock are mostly high-K calcalkaline to calcalkaline series, and granitoids in the Counsell Lake pluton are of the arc tholeiitic series.

On the SiO_2 versus Fe* and MALI plots (not shown) of Frost et al. (2001), the LLD granitoid samples are mostly magnesian although few evolved samples are ferroan, and are attributed to

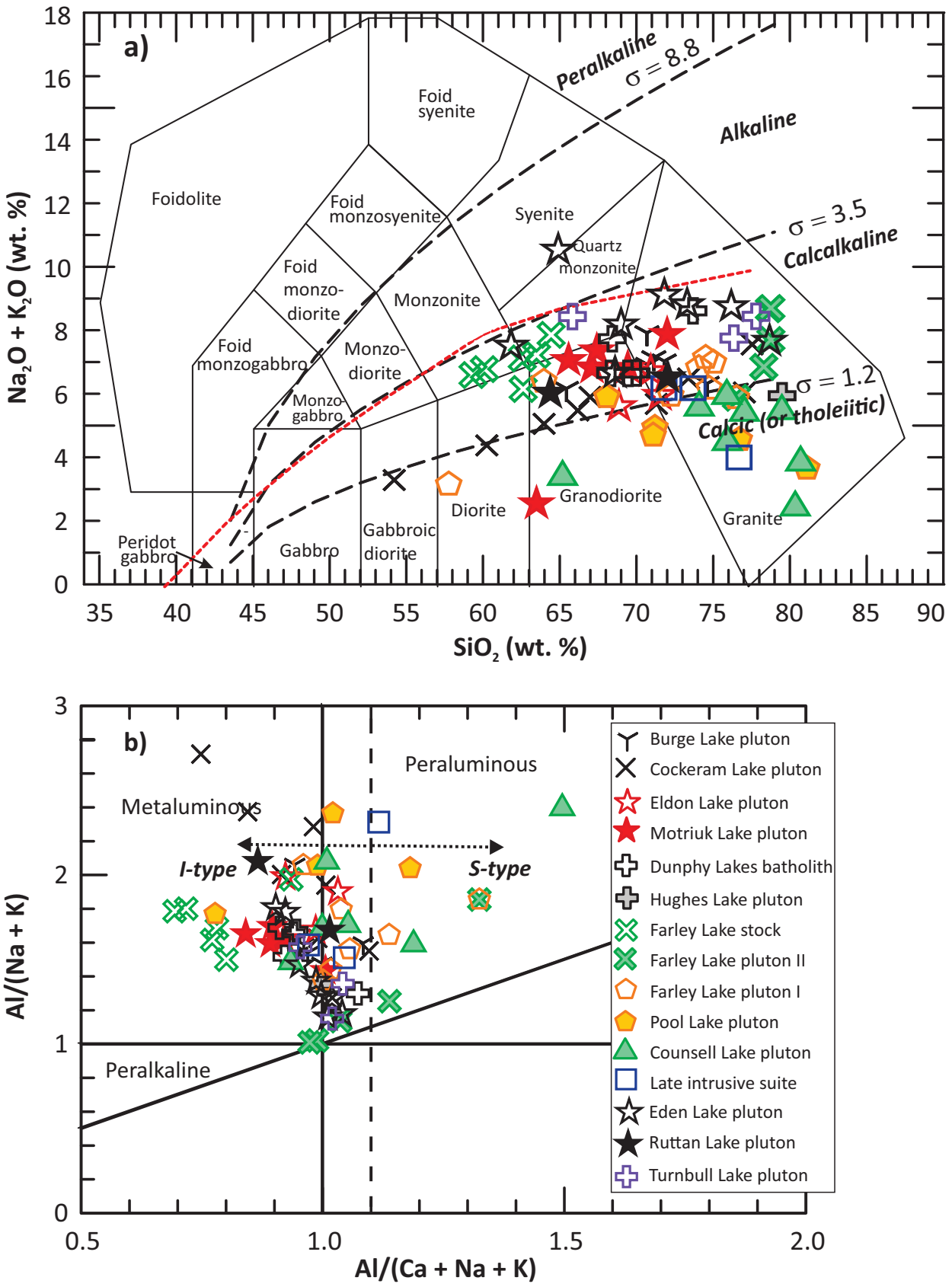

Figure 52: *Chemical classification of granitoids from the Lynn Lake domain based on alkalinity and alumina-saturation index:* ***a)*** *total alkalis (Na_2O+K_2O) versus SiO_2 (TAS; wt. %) diagram (fields from Middlemost, 1994), plotted on the anhydrous basis; boundary (red dashed line) between alkaline and subalkaline series from Irvine and Baragar (1971); Rittmann serial index σ = $(Na_2O+K_2O)^2/(SiO_2–43)$, unit in wt. % (Rittmann, 1973); using σ values to further subdivide granitoids into calcic (tholeiitic), calcalkaline, alkaline and peralkaline series (Yang, 2007);* ***b)*** *Shand index plot (fields from Maniar and Piccoli, 1989); ACNK = $Al_2O_3/(CaO+Na_2O+K_2O)$, ANK = $Al_2O_3/(Na_2O+K_2O)$, unit in mole; vertical dashed line indicates ACNK = 1.1, a key parameter discriminating S- and I-type granites (Chappell and White, 1974).*

calcic to calcalkalic to alkali-calcic. However, granitoids from the Burge Lake pluton, Motriuk Lake pluton, Dunphy Lakes batholith, Farley Lake stock and Pool Lake pluton are exclusively magnesian. Based on the relationship of Zr contents (ppm) versus (10^4Ga/Al) ratios (Whalen et al., 1987), the LLD granitoids plot mostly in the field of I- and S-type granites (not shown). Exceptions are evident, including one sample each from the Burge Lake, Cockeram Lake, Eldon Lake, Farley Lake I, and Turnbull Lake plutons, and two samples each from the Counsell Lake and Eden Lake plutons, which plot in the A-type granite field. These samples have either low Zr contents of <200 ppm, or are low in 10^4Ga/Al ratios of <3 (DRI2022012) and thus are unlikely A-type granites (e.g., Whalen et al., 1987; Eby, 1990). Three samples from the Farley Lake pluton II are truely A-type in terms of both their Zr contents and (10^4Ga/Al) ratios (Yang and Lawley, 2018).

In terms of the Shand index (Maniar and Piccoli, 1989), most of the LLD granitoid samples have metaluminous to moderately peraluminous affinities indicated by ACNK values of less than 1.1, which are ascribed to I-type (Figure 52b). Few samples from the Farley Lake pluton I and II, Pool Lake pluton, Counsell Lake pluton and Late intrusive suite are strongly peraluminous, with ACNK values higher than 1.1. However, these strongly peraluminous granitoids cannot be S-type because of the absence of diagnostic minerals (e.g., garnet, muscovite; Table 2). Three possibilities may account for the formation of the strongly peraluminous granitoids that are not S-type; 1) extreme fractionation of hornblende and/or biotite, 2) removal of Ca, Na and K by suprasolidus aqueous derived fluid from a less peraluminous granite magma, and 3) contamination and/or assimilation of pelitic rocks (Clarke, 1992, 2019; Yang et al., 2008). A fascinating process termed relamination was proposed by Hacker et al. (2011) whereby felsic melts formed from subducted sediments could have emplaced into subarc crust and thus influenced the chemical composition of the continental crust. If correct, such felsic melts (or resultant granites) must have been strongly peraluminous, but may have different implications for geodynamic setting from S-type granites. Furthermore, Figure 52b demonstrates that none of the LLD samples are peralkaline, although three samples from the Farley Lake pluton II plot close to the boundary between metaluminous and peralkaline rocks.

Figure 53a shows the LLD granitoid samples portrayed in the CIPW normative albite (Ab)-anorthite (An)-orthoclase (Or) ternary diagram of Barker (1979), indicating the presence of both inter- and intra-intrusion variation in the contents of normative feldspar components. The Burge Lake pluton samples are dominantly tonalite (only one sample being trondhjemite), whereas the Cockeram Lake pluton samples plot mainly in the fields of tonalite and granodiorite, and two samples as trondhjemite and granite, respectively. The granitoid samples from the Eldon Lake pluton, Motriuk Lake pluton, Dunphy Lakes batholith and Hughes Lake pluton are clustered between the boundaries of tonalite, granodiorite, granite and trondhjemite. Notably, the Farley Lake stock consists exclusively of tonalite; Farley Lake pluton I samples display a wide range covering tonalite, trondhjemite granodiorite and granite; and, the Farley Lake pluton II is composed mainly of granite and An-poor trondhjemite. The Pool Lake pluton comprises dominantly of tonalite although Or-rich granite is also present. The Counsell Lake pluton samples are mainly tonalite and trondhjemite despite the fact that one sample falls in the field of granodiorite. Samples from the Late intrusive suite appears to have low Or components, attributed to trondhjemite and tonalite. The Eden Lake and Turnbull Lake plutons are composed mainly of granite and granodiorite, which appear to be more evolved than the Ruttan Lake pluton that consists of tonalite.

Figure 53b shows the LLD granitoid samples plotted on the Zr/TiO_2 versus Nb/Y classification diagram of Pearce (1996). Most of the samples fall into the fields of diorite and granite. Exceptions are two samples from the Farley Lake stock that plot in the monzonite field and are distributed together with the other samples from this stock on a linear trend with a positive correlation between the Zr/TiO_2 and Nb/Y ratios. One sample from the Farley Lake pluton I is located in the monzonite field with high Nb/Y (1.11), Sr/Y (87) and La/Yb (25.1) ratios (DRI2022012), typical of adakite-like rocks (e.g., Yang and Lawley, 2018). Two samples from the Farley Lake pluton II plot in the field of alkali granite due to high Zr (280 to 302 ppm) and low TiO_2 contents (0.05 to 0.06 wt. %; see DRI2022012). One sample from the Eden Lake pluton has a very high Zr content of 516 ppm and moderate TiO_2 content of 0.63 wt. %, and is located also in the field of alkali granite. This high-Zr sample, however, has a Nb/Y ratio of less than 0.8 and is subalkaline according to Pearce (1996). This sample has a σ value of 5.4, suggesting that it is alkaline (Figure 52a). This contradiction requires further study (see below). The LLD granitoids mostly share common geochemical features, although some intrusions display either high Nb/Y or Zr/TiO_2 ratios. Those samples with high Nb/Y ratios (>0.8) and low Zr contents (<300 ppm) plot in the fields of monzonite and alkali granite probably are the consequence of crustal contamination, whereas the granitoids with low Nb/Y ratios (<0.8) and high Zr contents (>300 ppm) may be alkaline (e.g., Whalen et al., 1987; Eby, 1990; Pearce, 1996).

Trace-element geochemistry

The LLD granitoid rocks show intra- and inter-intrusion variation in contents of LILEs, HFSEs and/or elemental ratios (see DRI2022012), likely reflecting differences in their petrogenesis (e.g., magmatic fractionation degree, source rocks, and geodynamic settings). Granitoid samples from the Burge Lake pluton, Dunphy Lakes batholith, Farley Lake stock, and some of the samples from the Motriuk Lake pluton and Eden Lake pluton have consistently low Rb, Cs, and high Sr, Ba contents of LILEs, with consistently low Rb/Sr ratios ranging from 0.01 to 0.07 and high K/Rb ratios of 461 to 730. This indicates that these granitoid rocks are compositionally less fractionated, and their source rocks are unevolved (Blevin, 2004). The Farley Lake pluton II granite samples display consistently high Rb but low Sr contents, with moderate to very high Rb/Sr ratios of 0.52 to 47.5 and low K/Rb ratios of 214 to 380, suggesting that the rocks are highly fractionated and parental magma may have derived from moderately evolved

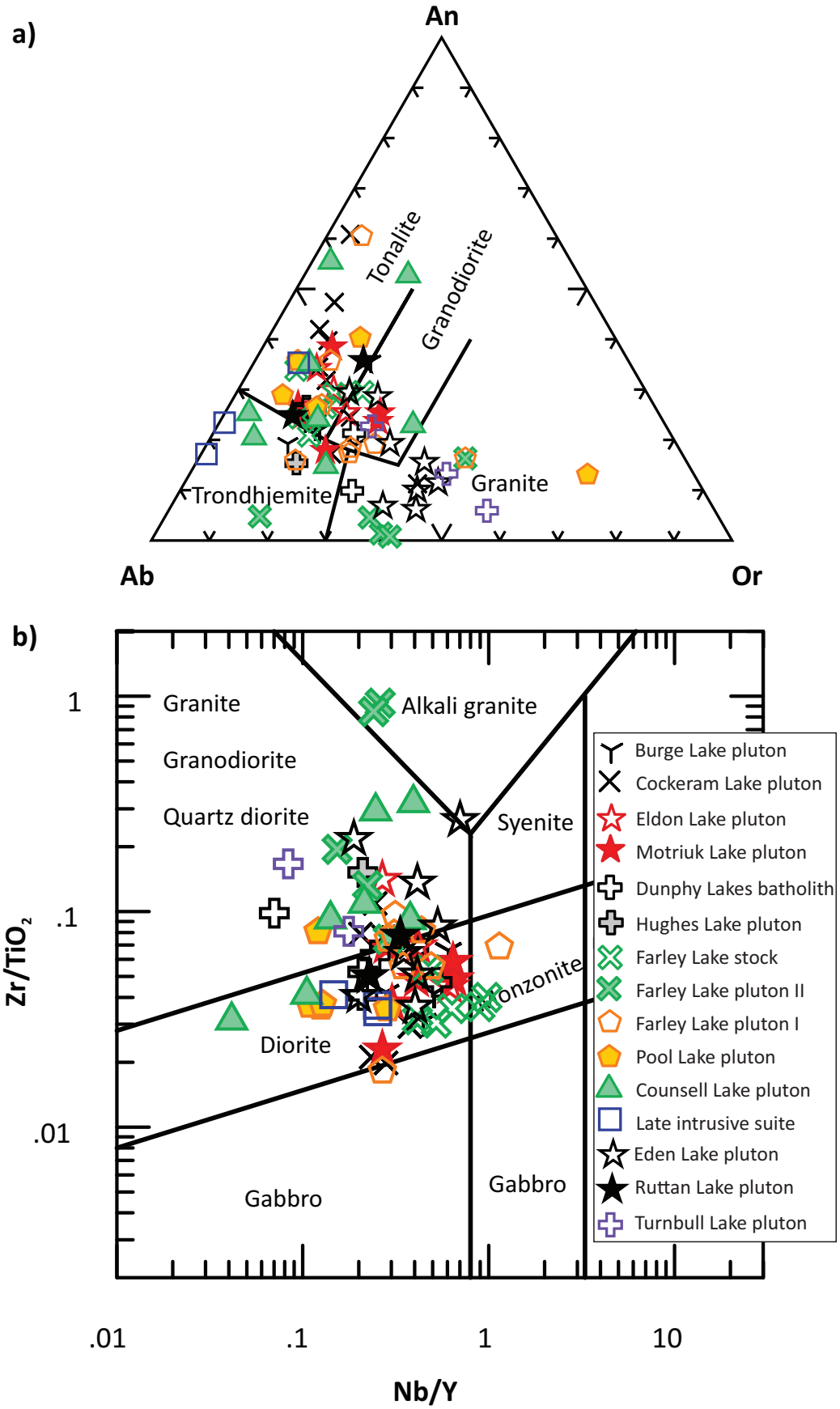

Figure 53: *Chemical classification of granitoids from the Lynn Lake domain in terms of CIPW normative compositions and HFSE:* ***a****) Ab-An-Or ternary diagram (fields from Barker, 1979);* ***b****) plot of* Zr/TiO_2 *versus Nb/Y (after Pearce, 1996). Abbreviations: Ab, albite; An, anorthite; CIPW, Cross, Iddings, Pirsson, Washington; HFSE, high-field-strength element; Or, orthoclase.*

source rock(s). The other intrusions in the LLD share commonalites in LILEs, displaying low to moderate Rb, Cs, and moderate Sr, Ba contents, with a range of moderately low Rb/Sr and moderate to high K/Rb ratios. For example, samples from the Counsell Lake pluton and Ruttan Lake pluton contain Rb contents of 2 to 46 ppm, Sr of 70 to 665 ppm, with Rb/Sr ratios of 0.01 to 0.51 and K/Rb ratios of 360 to 1245 (DRI2022012). A high-Zr syenite sample from the Eden Lake pluton mentioned previously is also enriched in Ba (2456 ppm) and contains SiO_2 of 61.21 wt. %, a low Rb/Sr ratio (0.13) and high K/Rb (497), Sr/Y (39.8) and La/Yb (122.3) ratios. This sample geochemically resembles adakite-like rocks (e.g., Yang and Lawley, 2018). In addition, this syenite sample has a low Mg# of 29.7, but high Nb/Ta (23.3) and high Zr/Hf (51.1) ratios, reflecting the effect of intensive crustal contamination.

In comparison with primitive mantle (Sun and McDonough, 1989) and continental crust (Rudnick and Gao, 2010), most of the LLD granitoid samples have Nb/Ta ratios less than 17.4 and even less than 13.3, suggesting that they may have undergone some degree of magmatic differentiation. These rocks have Zr/Hf ratios mostly higher than 36.2 (DR2022001), consistent with common granitoid rocks elsewhere (e.g., Yang et al., 2008). Those samples (e.g., Burge Lake, Dunphy Lakes batholith, Farley Lake stock) with higher Nb/Ta ratios (>17.4) were likely contaminated by crustal rocks; whereas those with low Zr/Hf ratios (<36.2) are probably related to magmatic fractionation (e.g., Linnen and Keppler, 2002).

Figure 54 shows chondrite-normalized REE patterns in the left panel, and N-MORB–normalized extended trace-element profiles in the right panel, respectively, of various granitoid intrusions in the LLD, demonstrating their commonalities and differences. Granitoid samples from the Burge Lake pluton, Motriuk Lake pluton, Dunphy Lakes batholith, and Farley Lake stocks (Figure 54a, g, i, m) display a strongly (to moderately) fractionated REE pattern, with strong LREE enrichment and HREE depletion without notable Eu anomalies (i.e., Eu/Eu* = 0.90–1.13) except one sample that shows a very positive Eu anomaly (Eu/Eu* = 1.70; DRI2022012). These samples have chondrite-normalized $(La/Yb)_N$ ratios of 15.7 to 57.1, and $(Gd/Yb)_N$ ratios of 2.0 to 4.1, reflecting strongly fractionated LREE relative to HREE. Two samples, however, are less REE fractionated, with $(La/Yb)_N$ ratios of 5.2 to 9.5 and $(Gd/Yb)_N$ ratios of 1.7. N-MORB–normalized extended trace-element profiles of these samples (Figure 54b, h, j, n) exhibit pronounced negative Nb (Ta), Zr, Ti and P anomalies, and strongly positive Ba, Pb and Sr anomalies. These geochemical characteristics are similar to adakite-like (and sanukitoid-like) rocks elsewhere, which are interpreted to have been derived from prior metasomatized lithospheric mantle beneath a magmatic arc and/or direct melting of a subducting slab (e.g., Shirey and Hanson, 1984; Stern et al., 1989; Martin et al., 2005; Lin and Beakhouse, 2013; Yang and Lawley, 2018).

Granitoid samples from the Cockeram Lake pluton, Eldon Lake pluton and Hughes Lake pluton display similar REE patterns in terms of LREE enrichment relative to HREE depletion, and variably negative or pronounced positive Eu anomalies (Figure 54c, e, k). Their moderately fractionated REE patterns are manifested by $(La/Yb)_N$ ratios of 3.6 to 18.8 and $(Gd/Yb)_N$ ratios of 0.9 to 2.0, as well as Eu/Eu* values of 0.67 to 1.39 (DRI2022012). These rocks show in N-MORB–normalized extended trace-element profiles that they are enriched in incompatible elements (e.g., Cs, Rb), display positive Pb, and have pronounced negative Nb, Ti and P anomalies (Figure 54d, f, l).

Granitoid samples collected from the Farley Lake pluton II display flat to slightly enriched REE patterns with pronounced negative Eu anomalies (Figure 54o). These highly evolved granites have $(La/Yb)_N$ ratios of 2.3 to 10.5, $(Gd/Yb)_N$ ratios of 0.9 to 1.3 and Eu/Eu* values of 0.08 to 0.59 (DRI2022012), suggesting that feldspars (e.g., plagioclase) may have been involved, either as an early fractionating phase and/or as a residual phase in their source rocks (e.g., Rollinson, 1993). Interestingly, the REE patterns become flat (i.e., less HREE depletion) and have more pronounced negative Eu anomalies with increasing fractionation. The granites exhibit N-MORB–normalized extended trace-element profiles characterized by Th-, U- and Pb enrichment relative to other HFSEs, and pronounced negative Nb, P, and Ti anomalies (Figure 54p). Two alkali-feldspar granite samples (Figure 53b) are relatively rich in Ta, distinct from continental-arc magmatism, and yielded positive Hf anomalies, typical of an intra-arc extensional environment, and thus are ascribed to A-type granites (Yang and Lawley, 2018).

Granitoid samples from the Farley Lake pluton I exhibit moderately enriched REE patterns (Figure 54q) with $(La/Yb)_N$ ratios of 5.3 to 18.1, $(Gd/Yb)_N$ ratios of 1.0 to 1.7 and varied Eu anomalies (Eu*/Eu values of 0.61 to 2.16), suggesting plagioclase fractionation prior to emplacement and/or the presence of culmulative plagioclase (e.g., Rollinson, 1993). The Counsell Lake pluton granitoids dispay slightly enriched LREE patterns, with $(La/Yb)_N$ ratios of 1.4 to 4.4), $(Gd/Yb)_N$ ratios of 1.0 to 1.2 and negative Eu anomalies (Eu*/Eu values of 0.54 to 0.81; Figure 54u), except for one sample with a positive Eu anomaly (Eu*/Eu value of 1.45; DRI2022012). The granitoid samples from the Farley Lake pluton I and Counsell Lake pluton display similar enriched trace-element patterns with varied REE abundances, negative slopes and pronounced negative Nb, P, and Ti anomalies and positive Pb anomalies (Figure 54r, v), suggesting that they may have been emplaced in a magmatic-arc setting. One quartz diorite sample (111-16-292A01) from the Farley Lake pluton I is characterized by positive Ti, Zr, and Eu anomalies, suggestive of cumulative phases such as Ti-bearing magnetite, zircon and plagioclase.

The Pool Lake pluton and the Late intrusive suite granitoids are characterized by lower REE abundances and slightly enriched REE patterns with slightly negative Eu anomalies (Figure 54s, w). These rocks have $(La/Yb)_N$ ratios of 1.5 to 4.5, $(Gd/Yb)_N$ ratios of 0.9 to 1.3, and Eu*/Eu values of 0.72 to 0.94 (DRI2022012). Notably, the Pool Lake pluton samples have higher incompatible element abundance, and more pronounced negative Nb and Ti anomalies and positive Pb anomalies compared with those

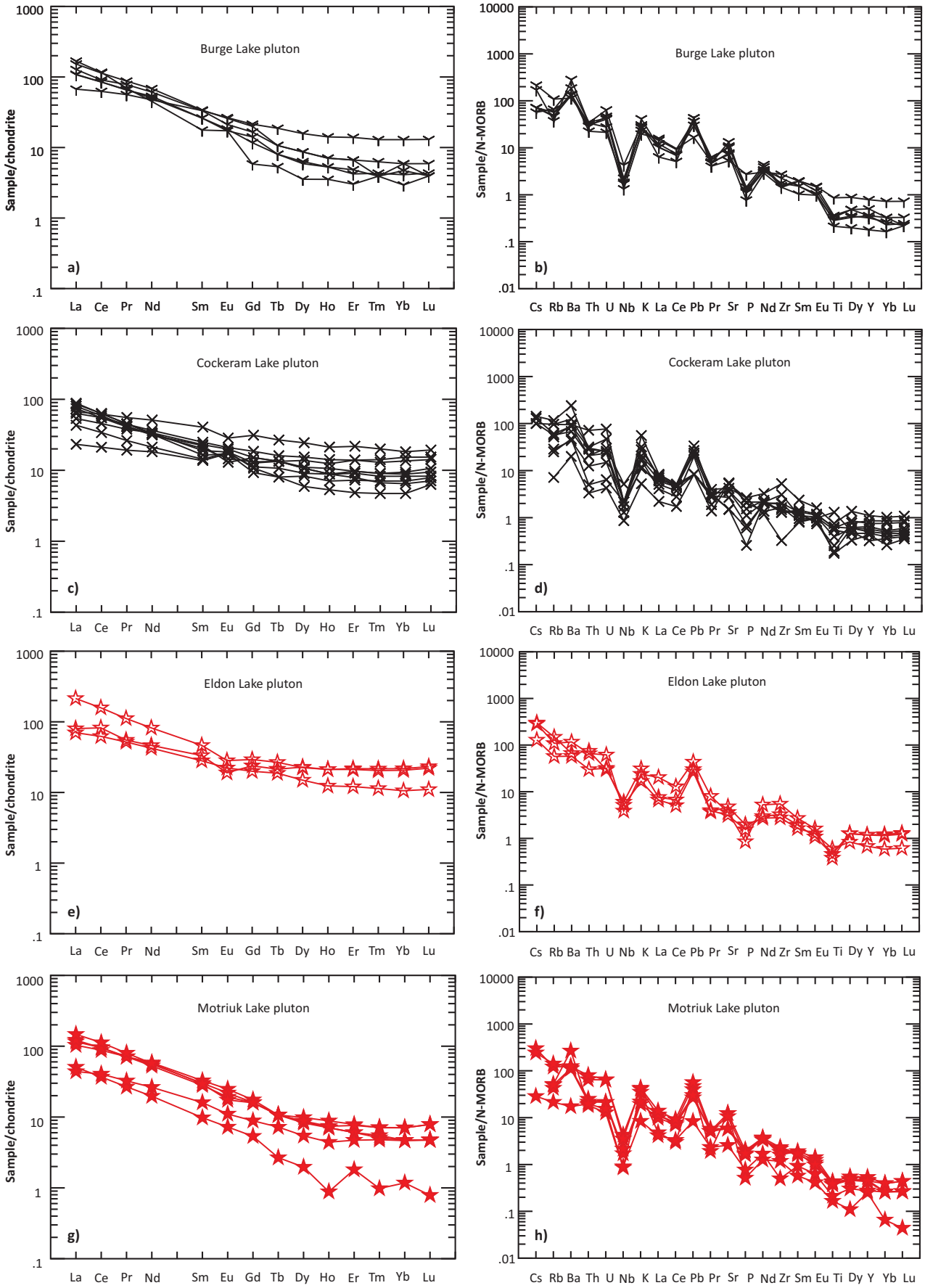

Figure 54: *Trace-element patterns of granitoid rocks from the Lynn Lake domain: left panel showing chondrite-normalized rare-earth element patterns; right panel showing N-MORB–normalized extended trace-element profiles. Normalizing values from Sun and McDonough (1989).*

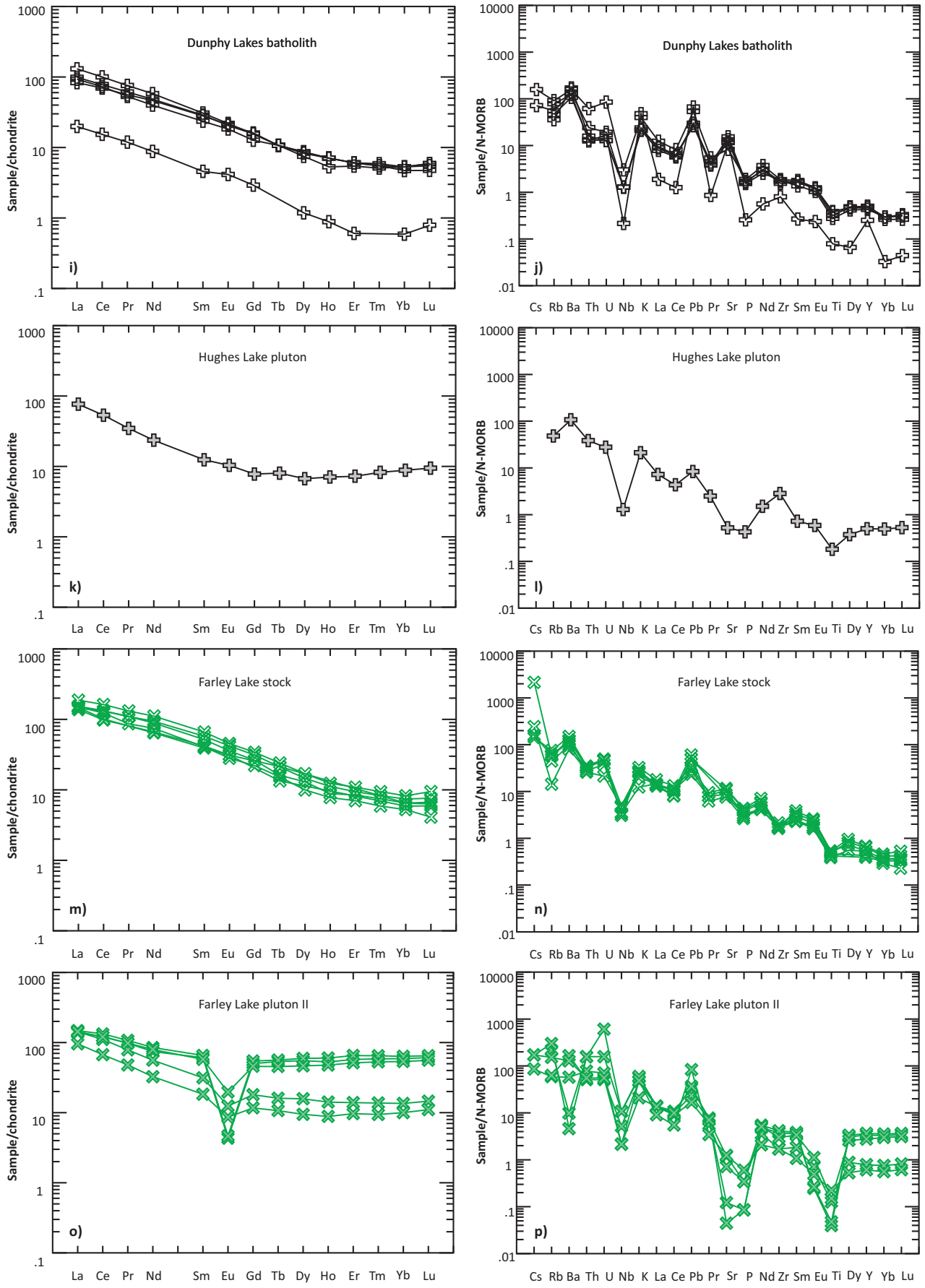

Figure 54 (continued): *Trace-element patterns of granitoid rocks from the Lynn Lake domain: left panel showing chondrite-normalized rare-earth element patterns; right panel showing N-MORB–normalized extended trace-element profiles. Normalizing values from Sun and McDonough (1989).*

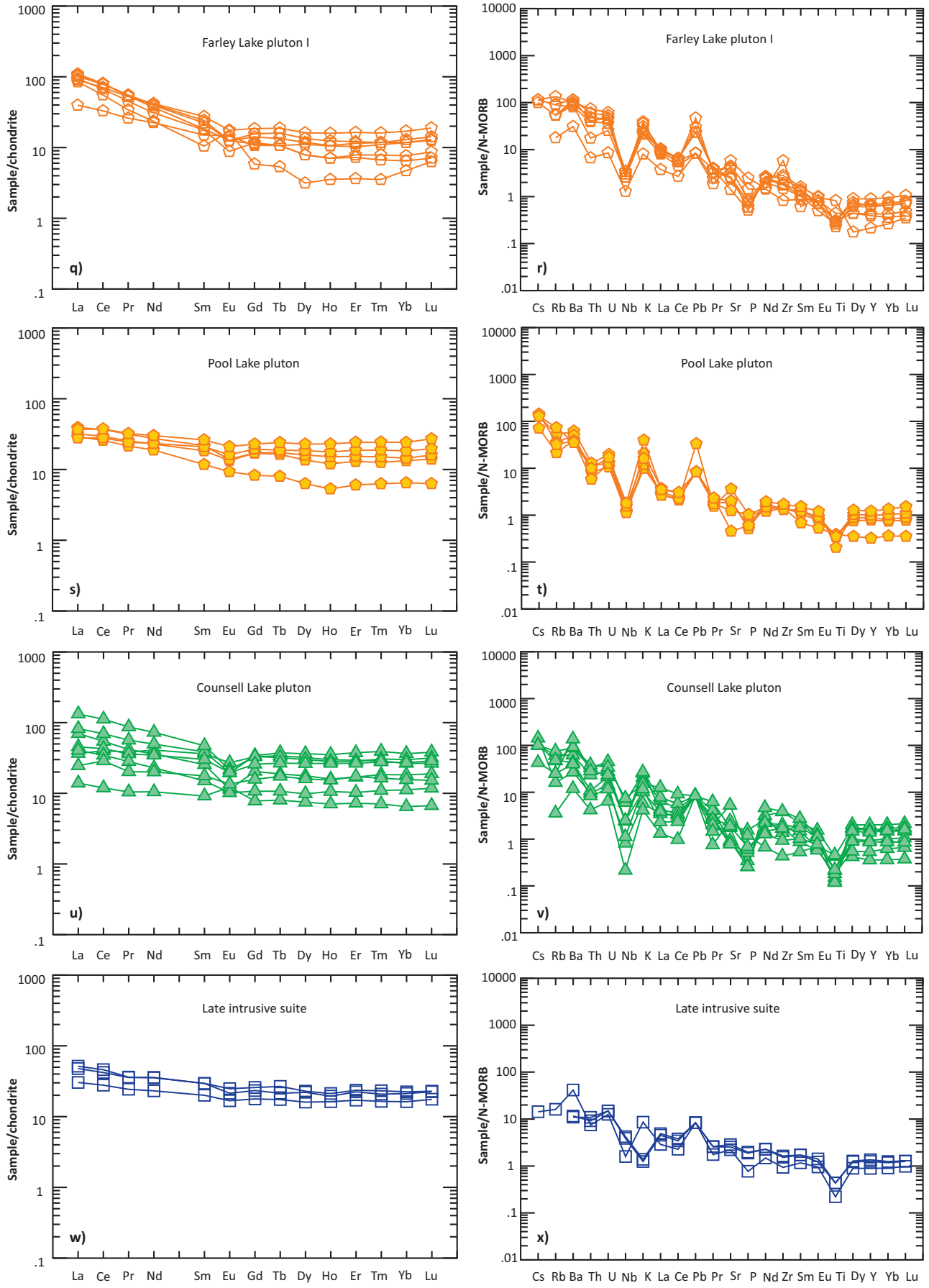

Figure 54 (continued): *Trace-element patterns of granitoid rocks from the Lynn Lake domain: left panel showing chondrite-normalized rare-earth element patterns; right panel showing N-MORB–normalized extended trace-element profiles. Normalizing values from Sun and McDonough (1989).*

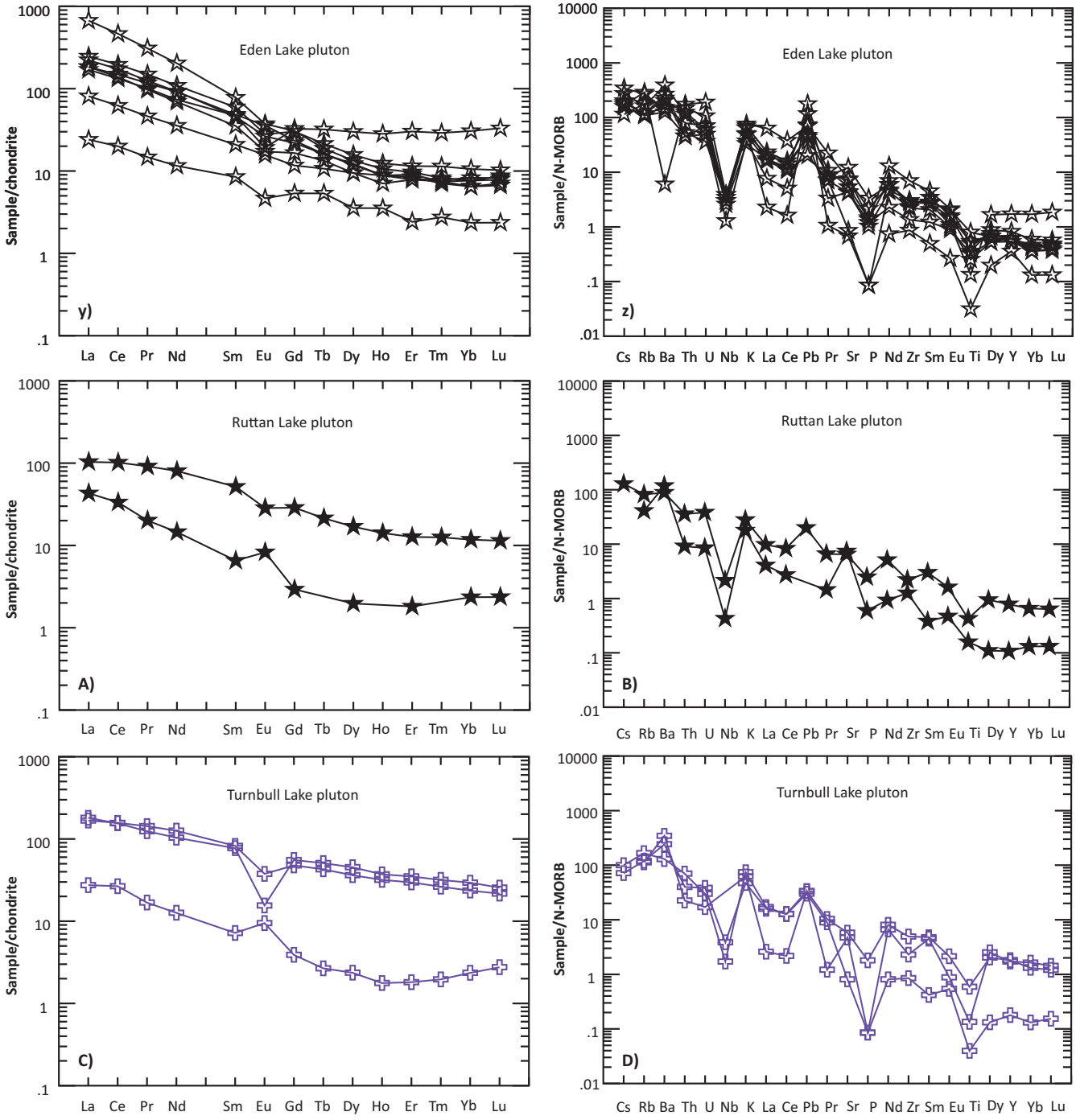

Figure 54 (continued): *Trace-element patterns of granitoid rocks from the Lynn Lake domain: left panel showing chondrite-normalized rare-earth element patterns; right panel showing N-MORB–normalized extended trace-element profiles. Normalizing values from Sun and McDonough (1989).*

from the Late intrusive suite as shown in N-MORB–normalized extended trace-element profiles (Figure 54t, x).

Granitoid samples from the Eden Lake pluton show moderate to strong enrichment of LREE relative to HREE with moderately negative Eu or with slightly positive anomalies indicated by Eu/Eu* values of 0.69 to 1.06 (Figure 54y; DRI2022012). The granitoid rocks can be subdivided into two subgroups; 1) one with high $(La/Yb)_N$ ratios of 22.4 to 88.0 and $(Gd/Yb)_N$ ratios of 2.0 to 4.0, and 2) the other with low $(La/Yb)_N$ ratios of 5.6 to 10.6 and $(Gd/Yb)_N$ ratios of 1.0 to 2.3. Their N-MORB–normalized extended trace-element profiles display enriched LILEs (e.g., Cs, Rb), positive Pb and pronounced negative Nb, P, and Ti anomalies (Figure 54z). One highly evolved granite sample (111-15-169C01) shows much more pronounced negative Ba anomalies.

Granitoid samples from the Ruttan Lake pluton and Turnbull Lake pluton display two comparable enriched REE patterns; one with notable negative Eu anomalies (Eu/Eu* values of 0.24 to 0.74) and relatively low $(La/Yb)_N$ ratios (6.2 to 8.8), and the other with pronounced positive Eu anomalies (Eu/Eu* values of 1.79 to 1.89) and higher $(La/Yb)_N$ ratios (11.7 to 18.3; Figure

54a, c; DRI2022012). The samples with positive Eu anomalies have much lower REE abundances than those with negative Eu anomalies, suggesting that the former contain culmulative feldspars. The samples from these plutons show similar N-MORB–normalized extended trace-element profiles (Figure 54b, d) that show enrichment in incompatible elements (e.g., Cs, Rb), display positive Pb, and have pronounced negative Nb, Ti and P anomalies. This is a typical arc signature, suggesting that these granitoids may have formed in a magmatic-arc setting (e.g., Prouteau et al., 1999, 2001; Pearce et al., 2005; Pearce, 2008; Yang et al., 2008; Anderson, 2013). Positive Ba and Sr anomalies confirm the presence of cumulative feldspars in the samples with positive Eu anomalies mentioned above.

Figure 55a shows the LLD granitoid samples plotted on the Sr/Y and La/Yb discrimination diagram (Moyen and Martin, 2012), indicating that samples from the Burge Lake pluton, Motriuk Lake pluton, Dunphy Lakes batholith, and Farley Lake stock mostly have ratios of Sr/Y >40 and La/Yb >20. This suggests that these granitoids are comparable to medium- to high-P TTGs, indicating the presence of garnet in their source region (Martin et al., 2005, 2010; Zhang et al., 2006; Moyen and Martin, 2012). They are probably adakite-like granitoids (Yang and Lawley, 2018). Samples from the Cockeram Lake pluton, Eldon Lake pluton, Hughes Lake pluton, Farley Lake pluton I, Pool Lake pluton, Counsell Lake pluton, Late intrusive suite, Ruttan Lake pluton and Turnbull Lake pluton display varied to low Sr/Y ratios and low La/Yb ratios (<20), mostly with high Y (>18 ppm) and Yb (>1.9 ppm), typical of magmatic rocks formed in an arc regime. The Farley Lake pluton II samples have low Sr/Y (<10) and La/Yb (<20) ratios, indicative of absence of garnet in its source region. The Eden Lake pluton samples generally exhibit positive correlation between Sr/Y and La/Yb ratios and are likely ascribed to magmatic fractionation, although one sample with high Sr/Y (73.3) and La/Yb (39.4) ratios (see DRI2022012) is akin to adakite-like rocks. The two samples, containing culmulative feldspars, from the Ruttan Lake pluton and Turnbull Lake pluton show very high Sr/Y ratios of 221.7 and 84.8, respectively. These samples have very low Y (3 to 4 mm) and Yb (0.4 ppm) contents (DRI2022012), consistent with very low feldspar-melt partition coefficient (e.g., Rollinson, 1993).

On the Rb (ppm) versus Y+Nb (ppm) tectonomagmatic discrimination diagram of Pearce et al. (1984), most granitoid samples from the LLD are located in the field of volcanic-arc granitoids (Figure 55b). Three granite (*s.s.*) samples from the Farley Lake pluton II together with two from the Counsell Lake pluton plot in the field of within-plate granitoids, and the other samples from these plutons fall also in the field of volcanic-arc granitoids. This indicates that the Farley pluton II is of A-type, suggesting that the tectonic extension may have occurred within an overall magmatic-arc setting during the evolution of the LLD. However, the Counsell Lake pluton is I-type formed in a magmatic-arc setting, and likely experienced differentiation and crustal contamination leading to these two samples plotting in the field of within-plate granitoids. The adakite-like intrusions (i.e., the Burge Lake pluton, Motriuk Lake pluton, Dunphy Lakes batholith, Farley Lake stock) mentioned above exclusively fall into the field of volcanic-arc granitoids, indicating arc signatures.

The LLD granitoid samples mostly plot in the fields of arc and slab failure granitoids and some of the Farley Lake pluton II samples and one from the Counsell Lake pluton fall in the A-type granite field on the Nb/Y versus Nb+Y (ppm) and La/Yb versus Nb+Y (ppm) diagrams (Figure 56a, b) of Whalen and Hildebrand (2019). The Counsell Lake sample is not A-type, because it contains a Y content of 43 ppm (DRI2022012) characterized by magmatic-arc rocks (Kepezhinskas et al., 2022, and references therein). The Burge Lake pluton, Motriuk Lake pluton, Dunphy Lakes batholith, and Farley Lake stock stem from slab failure magmatism, likely emplaced in a post-collisional setting based on their relative high La/Yb (>10) and Nb/Y (>0.4) and relatively low (Nb+Y; <60 ppm) contents (Whalen and Hildebrand, 2019). Basically, the rocks from these intrusions are adakite-like granitoids. The Farley Lake pluton II samples are A-type granitoids that have higher concentrations of Nb+Y than those emplaced into pre-collisional magmatic arc and/or formed by slab failure magmatism. Their high Y (>15 ppm) and Yb (>1.8 ppm) contents are diagnostic characteristics of magmatic-arc rocks (e.g., Kepezhinskas et al., 2022) as Y behaves similarly to Yb in magmatic system (Rollinson and Pease, 2021). Thus, arc granitoids in the LLD must have lower Nb/Y and La/Yb ratios than those generated by slab failure magmatism.

In summary, the granitoid rocks from the Lynn Lake domain (LLD) are mostly attributed to I-type formed by arc magmatism; some (e.g., Farley Lake pluton II) are A-type and formed by tectonic extension within an arc environment, and some are adakite-like granitoids (e.g., Burge Lake pluton, Dunphy Lakes batholith, Motriuk Lake pluton, Farley Lake stock) that formed by partial melting of previously mesomatized mantle induced by upwelling of asthenospheric mantle due to roll-back of slab or by slab failure magmatism. The coexistence of distinct granitoid types in the LLD collectively suggests a geodynamic interplay between sub-arc lithospheric and asthenospheric mantle may have provided the heat and source materials required for their genesis.

Southern Indian domain (SID) and Chipewyan domain (CD)

Classification

Eleven granitoid samples collected from the SID and one from the CD are classified on the basis of their major- and trace-element compositions, using the TAS and Shand index (Figure 57a, b), CIPW normative Ab-An-Or and Zr/TiO_2 versus Nb/Y diagrams (see below). One sample from the Vandekerckhove Lake pluton, one from the Zed Lake pluton and four from the Issett Lake pluton plot the field of granite in the TAS diagram (Figure 57a) of Middlemost (1994). Three samples from the Zed Lake pluton and one from the Issett Lake pluton fall into the granodiorite field. One sample from the South Bay intrusion is located in the field of quartz monzonite, which has a Rittmann serial index (σ) value of

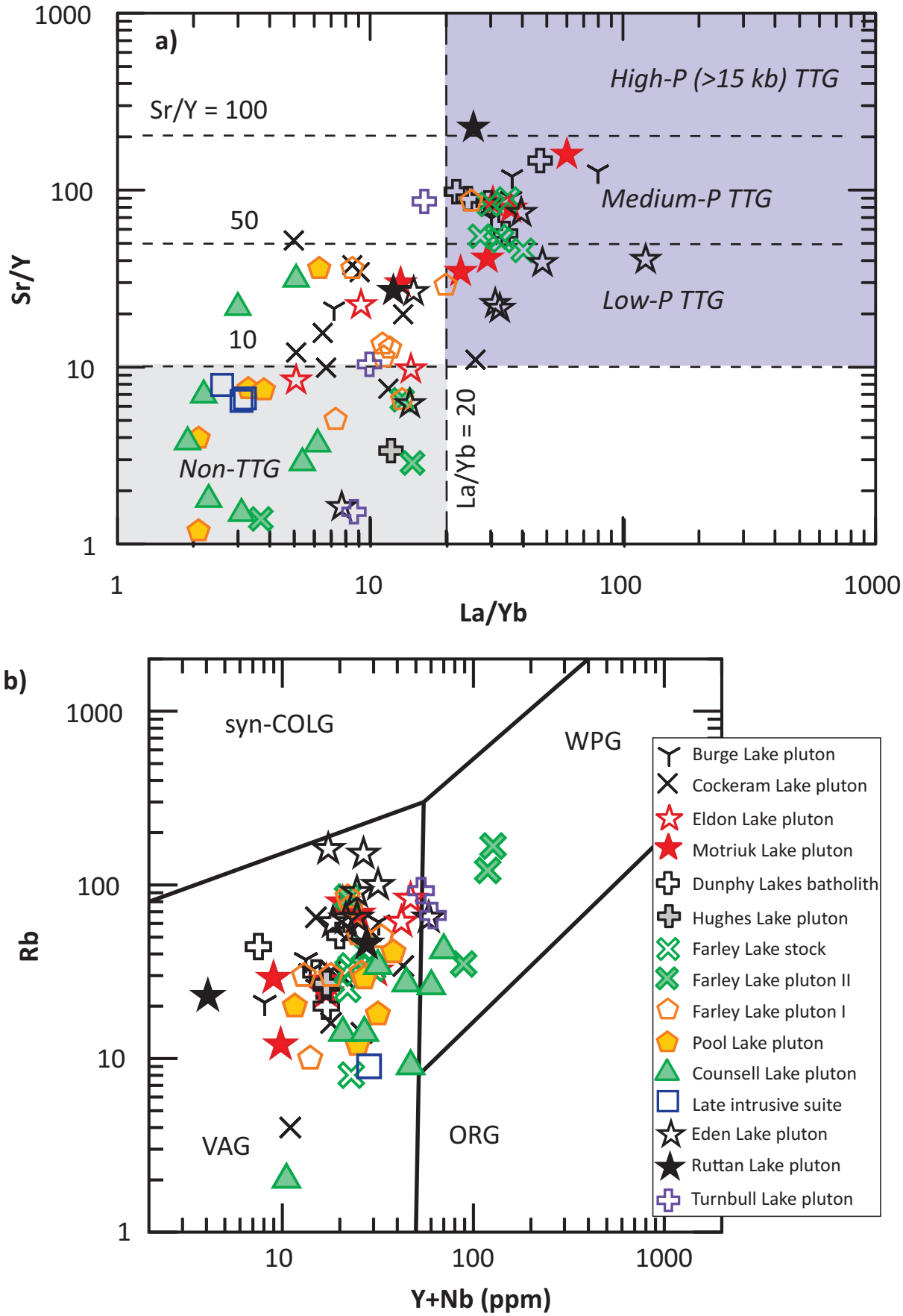

Figure 55: *Discrimination plots for granitoid rocks from the Lynn Lake domain:* ***a)*** *La/Yb versus Sr/Y diagram; boundaries used to define TTG types from Moyen and Martin (2012);* ***b)*** *tectonomagmatic discrimination diagram of (Y+Nb) versus Rb (after Pearce et al., 1984). Abbreviations: ORG, ocean-ridge granitoid; syn-COLG, syncollisional granitoid; TTG, tonalite-trondhjemite-granodiorite; VAG, volcanic-arc granitoid; WPG, within-plate granitoid.*

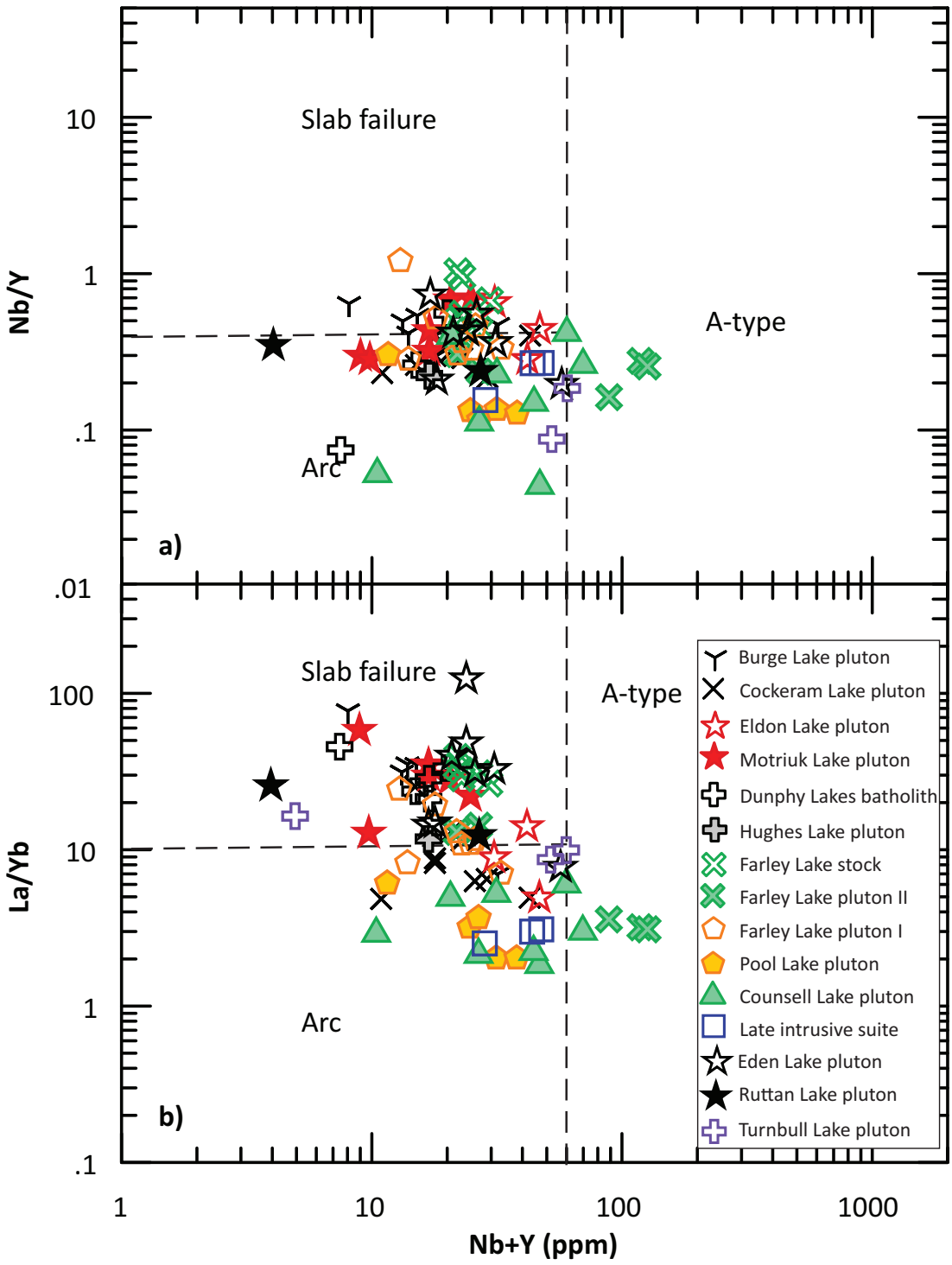

Figure 56: *Discrimination plots of Nb/Y versus Nb+Y (ppm) and La/Yb versus Nb+Y (ppm) for granitoid rocks from the Lynn Lake domain. Boundaries for slab-failure, arc and A-type granitoids from Whalen and Hildebrand (2019).*

3.9, belonging to the alkaline series (Yang, 2007) and comparable to the alkaline series as defined by Irvine and Baragar (1971). In contrast, the other SID samples have σ values between 1.2 and 3.5 indicative of calcalkaline affinity (Yang, 2007), consistent with subalkaline rocks of Irvine and Baragar (1971).

Most of the SID samples have Na_2O/K_2O ratios >1.0 (ranging from 1.23 to 1.78), and few samples from the CD display Na_2O/K_2O ratios <1.0 (0.66 to 0.98). Na_2O/K_2O ratios >1.0 are typical for I-type granites (Table 1), whereas Na_2O/K_2O ratios <1.0 likely indicate high-K granitoids and some S-type granites (Table 2). On the SiO_2 versus Fe* and MALI plots (not shown) of Frost et al. (2001), the SID and CD samples are mostly magnesian and only two samples with higher SiO_2 contents from the Issett Lake pluton are ferroan. Again, the SID granitoids are calcalkalic, except for one sample from the Issett Lake pluton and the South Bay intrusion of the CD are alkali-calcic series, consistent with the result of using the TAS diagram linked with the Rittmann serial index (σ; Figure 57a). Based on the relationship of Zr contents versus (10^4Ga/Al)

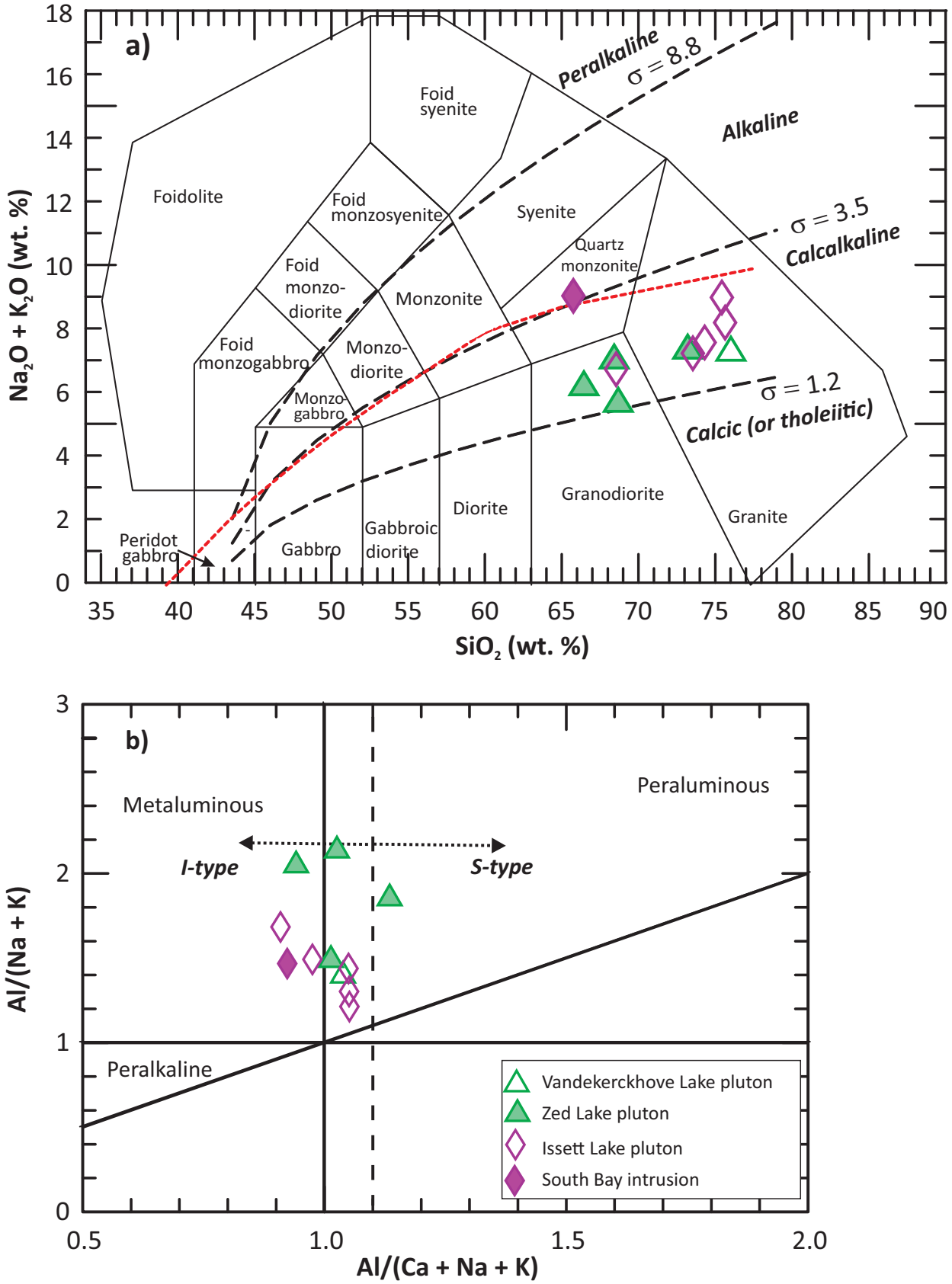

Figure 57: *Chemical classification of granitoids from the Southern Indian and Chipewyan domains in terms of alkalinity and alumina-saturation index:* ***a)*** *total alkalis (Na_2O+K_2O) versus SiO_2 (TAS; wt. %) diagram (fields from Middlemost, 1994); boundary (red dashed line) between alkaline and subalkaline series from Irvine and Baragar (1971); Rittmann serial index σ = $(Na_2O+K_2O)^2/(SiO_2–43)$, unit in wt. % (Rittmann, 1973); using σ values to further subdivide granitoids into calcic (tholeiitic), calcalkaline, alkaline and peralkaline series (Yang, 2007);* ***b)*** *Shand index plot (fields from Maniar and Piccoli, 1989); ACNK = $Al_2O_3/(CaO+Na_2O+K_2O)$, ANK = $Al_2O_3/(Na_2O+K_2O)$, unit in mole; vertical dashed line indicates ACNK = 1.1, a key parameter discriminating S- and I-type granites (Chappell and White, 1974).*

ratios (Whalen et al., 1987), most samples plot in the field of I- and S-type (not shown), although one sample from the Zed Lake and one from the South Bay intrusion fall into the field of A-type as they contain relatively high concentrations of Zr (303 and 316 ppm; DRI2022012).

In terms of the Shand index (Maniar and Piccoli, 1989), the granitoid samples from the SID and CD are mostly metaluminous to moderately peraluminous; only one sample from the Zed Lake pluton is strongly peraluminous (Figure 57b). This suggests that most of the SID and CD granitoid rocks are I-type as indicated by ACNK <1.1, and parts of the Zed Lake pluton and Issett Lake pluton are S-type as evidenced by their ACNK values >1.1 (Chappell and White, 1974, 2001) and/or by their mineral assemblages and MS values (Table 2).

A general positive correlation of Al_2O_3/TiO_2 and a negative correlation of CaO/Na_2O ratios respectively with SiO_2 (wt. %) are evident for granitoid samples from the SID and CD (Figure 58a, b). Such relationships can be explained on the basis of high-T and high-P experimental data on melting of various rocks with Al_2O_3/TiO_2 ratios related to melt temperatures, revealing that higher Al_2O_3/TiO_2 ratios of the melts require lower melt temperatures (Jung and Pfänder, 2007). More recently, Duan et al. (2022) propose a simple equation [T_{SiO2} (°C) = –14.16 × SiO_2 + 1723 (unit of SiO_2 in wt. %)] for calculating temperatures (T_{SiO2}) of granitoid magmas using their SiO_2 contents in terms of statistical analysis in experimental results. Based on SiO_2 contents, the SID and CD granitoid samples can be divided into two groups; one with higher SiO_2 contents (>70.4 wt. %) and Al_2O_3/TiO_2 ratios, and the other having lower SiO_2 contents (<70.4 wt. %) and Al_2O_3/TiO_2 ratios (Figure 58a; DRI2022012). Thus, the latter must have higher T_{SiO2} (796 to 866°C), and the former have relatively low T_{SiO2} (655 to 726°C), that are respectively comparable with high- and low-T granites elsewhere (Chappell et al., 2004).

Furthermore, source rocks of granitoid melts generated by fluid-absent melting can be constrained by CaO/Na_2O ratios (Jung and Pfänder, 2007). Melts sourced from partial melting of pelite have CaO/Na_2O <0.5, melts derived from greywacke or igneous rocks have CaO/Na_2O ratios of 0.3 to 1.5, and melts derived from fluid-absent melting of amphibolite have CaO/Na_2O ratios up to 10 (commonly between 0.1 and 3). This is consistent with the findings of Sylvester (1998) that strongly peraluminous S-type granites display lower CaO/Na_2O if originated from clay-rich source rocks (e.g., pelite) than those souced from plagioclase-rich rocks (e.g., greywacke, mafic rocks). Accordingly, the part with low CaO/Na_2O ratios (<0.5) of the Issett Lake pluton (Figure 58b) could be low-T_{SiO2} S-type granite, likely derived from partial melting of clay-rich sedimentary rocks, consistent with their mineral assemblage and MS values (Table 2).

Use of the CIPW Ab-An-Or ternary diagram of Barker (1979) to portray the SID and CD granitoid rocks (Figure 59a) indicates that they mostly fall into the fields of granodiorite and granite, and two samples (one each from the Zed Lake and Issett Lake plutons, respectively) are located in the tonalite field. Although the sample from the South Bay intrusion of the CD plots in the granite field, it contains a higher An component than two samples of the Issett Lake pluton that also plot in the granite field. On the Zr/TiO_2 versus Nb/Y diagram (Figure 59b), most of the SID and CD granitoid samples are located in the fields of diorite to granite, and two samples from the Zed Lake pluton fall into the field of gabbro. These granitoid rocks display collectively low Nb/Y ratios (<0.8), ascribed to the subalkaline series (Pearce, 1996). This is consistent with the discriminant results in terms of σ values indicated in the TAS diagram (Figure 57a).

Trace elements

Granitoid rocks in the SID and CD mostly have moderate to high Sr (up to 677 ppm), Ba (up to 1707 ppm) and low Rb, Cs contents (DRI2022012). These rocks show relatively low Rb/Sr ratios ranging from 0.07 to 0.79, reflecting low to moderate magmatic fractionation. Also, they have moderate K/Rb ratios ranging from 231 to 408, suggesting that the granitoid magmas may have been derived from a moderately evolved source region (e.g., Blevin, 2004).

Figure 60 shows chondrite-normalized REE patterns (on the right panel; a, c, e, and g) and N-MORB–normalized extended trace-element profiles (on the left panel; b, d, f, and h) for the SID and CD granitoid samples. The SID granitoids collectively display enriched LREE relative to HREE, mostly with moderately to slightly negative Eu anomalies (Eu/Eu* values of 0.51 to 0.87; DRI2022012) except for one sample from the Zed Lake pluton showing slightly positive Eu anomalies (Eu/Eu* value of 1.06). These samples exhibit notable to pronounced negative Nb, Ti and P anomalies, and positive Pb anomaies, typical of arc signatures (e.g., Prouteau et al., 1999, 2001; Pearce et al., 2005; Pearce, 2008; Yang et al., 2008; Anderson, 2013).

Granitoid samples from the SID mostly display low Sr/Y (<40) and La/Yb (<20) ratios, except for two samples from the Issett Lake pluton (Figure 61a). The sample from the South Bay intrusion (CD) has low Sr/Y (20.5) but high La/Yb ratio (30.5), whereas one from the Issett Lake pluton displays low ratios of Sr/Y (22.4) and La/Yb (11.1). Both of them are not attributed to typical TTGs, i.e., sourced from garnet-bearing rocks. Thus, only the two samples from the Issett Lake pluton are ascribed to low- to medium-pressure TTG (Moyen and Martin, 2012), indicative of the presence of garnet in its source rocks.

The SID and CD samples exclusively plot in the field of volcanic-arc granitoids based on their Rb and Y+Nb contents (Pearce et al., 1984; Figure 61b). It is noted that parts of the Issett Lake and Zed Lake plutons are S-type in terms of their mineral assemblages and MS values (Table 2), suggesting that their parental magmas must have contained relatively low Rb concentrations. This is also supported by their moderately evolved source rocks indicated by K/Rb ratios mentioned above.

The SID and CD granitoid rocks display commonality with arc granitoids based on their Nb/Y ratios (<0.5) and (Nb+Y) contents (<60 ppm; Figure 62a). However, most of the granitoid rocks display La/Yb ratios >10 and fall into the field of slab failure

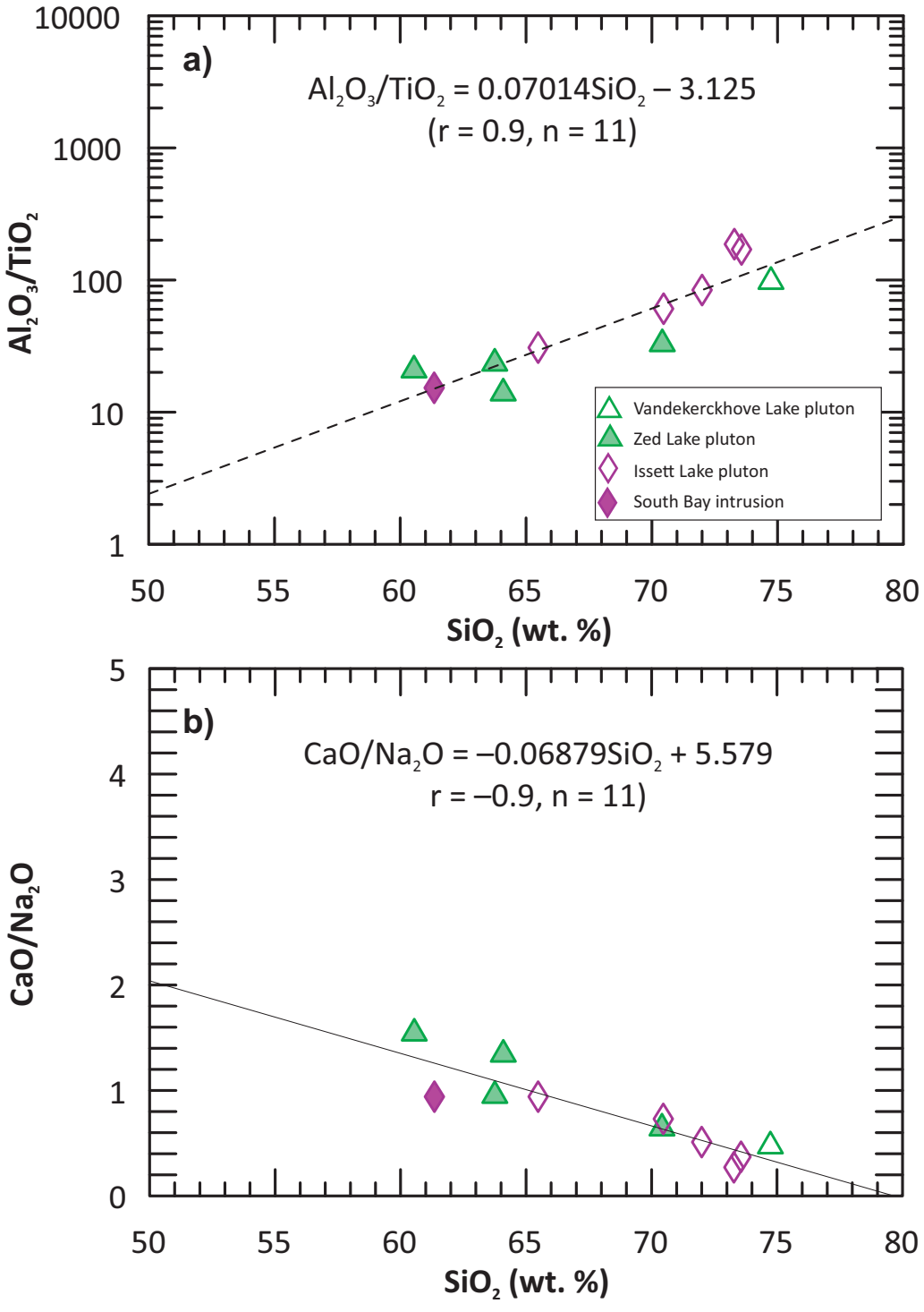

Figure 58: *Diagrams of SiO_2 (wt. %) versus Al_2O_3/TiO_2 (**a**) and CaO/Na_2O (**b**) for granitoid samples from the Southern Indian and Chipewyan domains. Abbreviations: n, number of samples; r, correlation coefficient.*

granitoids (Figure 62b). None of the samples belong to A-type granitoids that should have much higher concentrations of Nb+Y as pointed out by Whalen and Hildebrand (2019).

In summary, the SID and CD granitoid rocks are mostly attributed to typical I-type granites formed in a magmatic-arc setting, although parts of the Zed Lake and Issett Lake plutons belong to the S-type granites formed in a collisional zone. The S-type granites, however, are relatively less evolved and their parental magmas with low Rb contents are likely derived from moderately evolved to unevolved sources. Such S-type granite intrusions may have low potential for generating critical metals (e.g., Li, Cs, Ta) pegmatites. A use fo the Ga-(Nb+Ta)-(Nb/Ta)(Zr/Hf) ternary discrimination diagram (not shown) proposed recently by Mohamadizadeh et al. (2020) reveals that S-type granites from the Zed Lake and Issett Lake plutons emplaced into the southern margin of the Southern Indian domain are barren, suggesting that these plutons may have low potential for producing critical metals (e.g., Li. Cs, Ta) pegmatites.

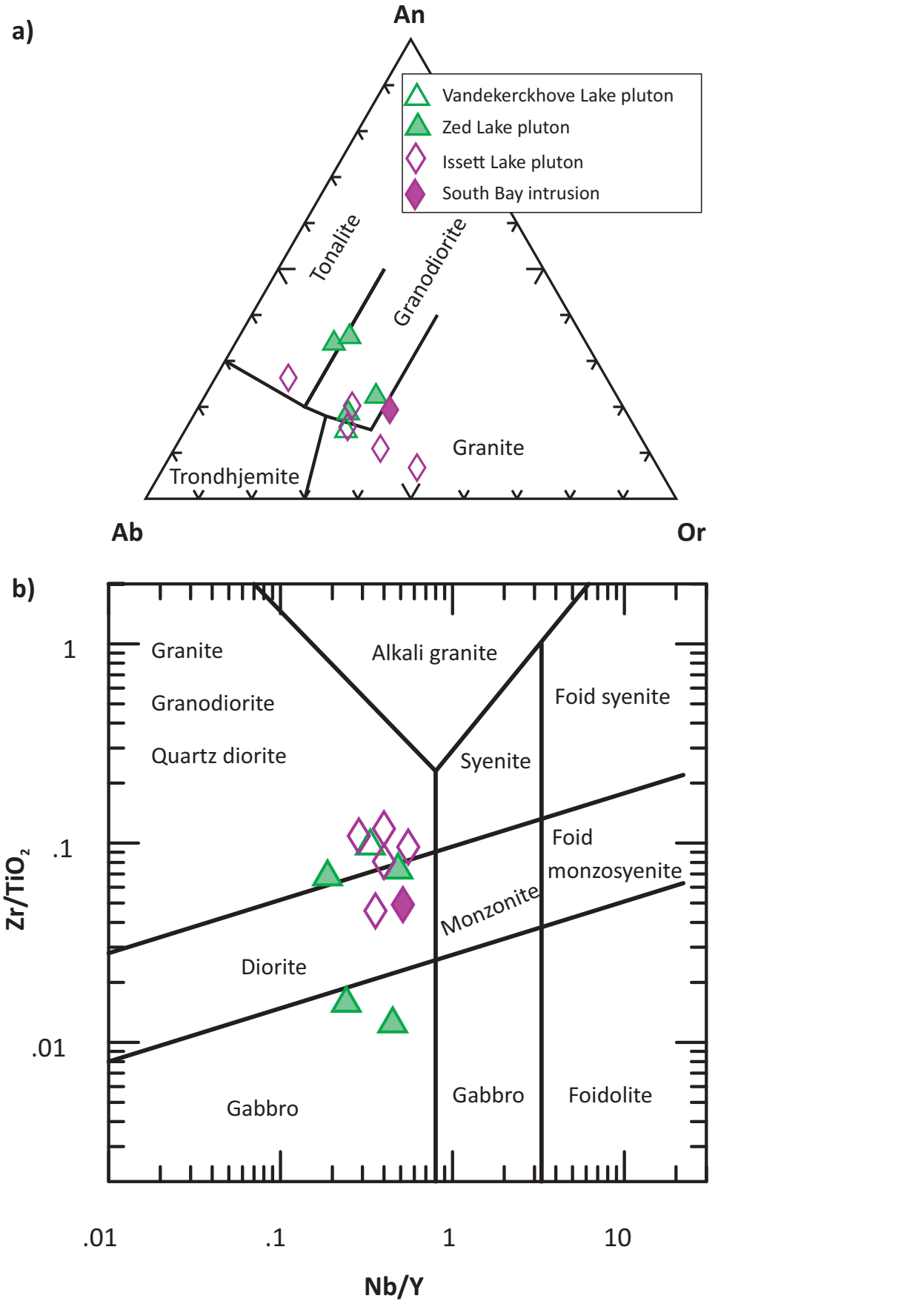

Figure 59: *Chemical classification of granitoids from the Southern Indian and Chipewyan domains in terms of CIPW normative compositions and HFSE:* ***a****) Ab-An-Or ternary diagram (fields from Barker, 1979);* ***b****) plot of Zr/TiO_2 versus Nb/Y (after Pearce, 1996). Abbreviations: Ab, albite; An, anorthite; CIPW, Cross, Iddings, Pirsson, Washington; HFSE, high-field-strength element; Or, orthoclase.*

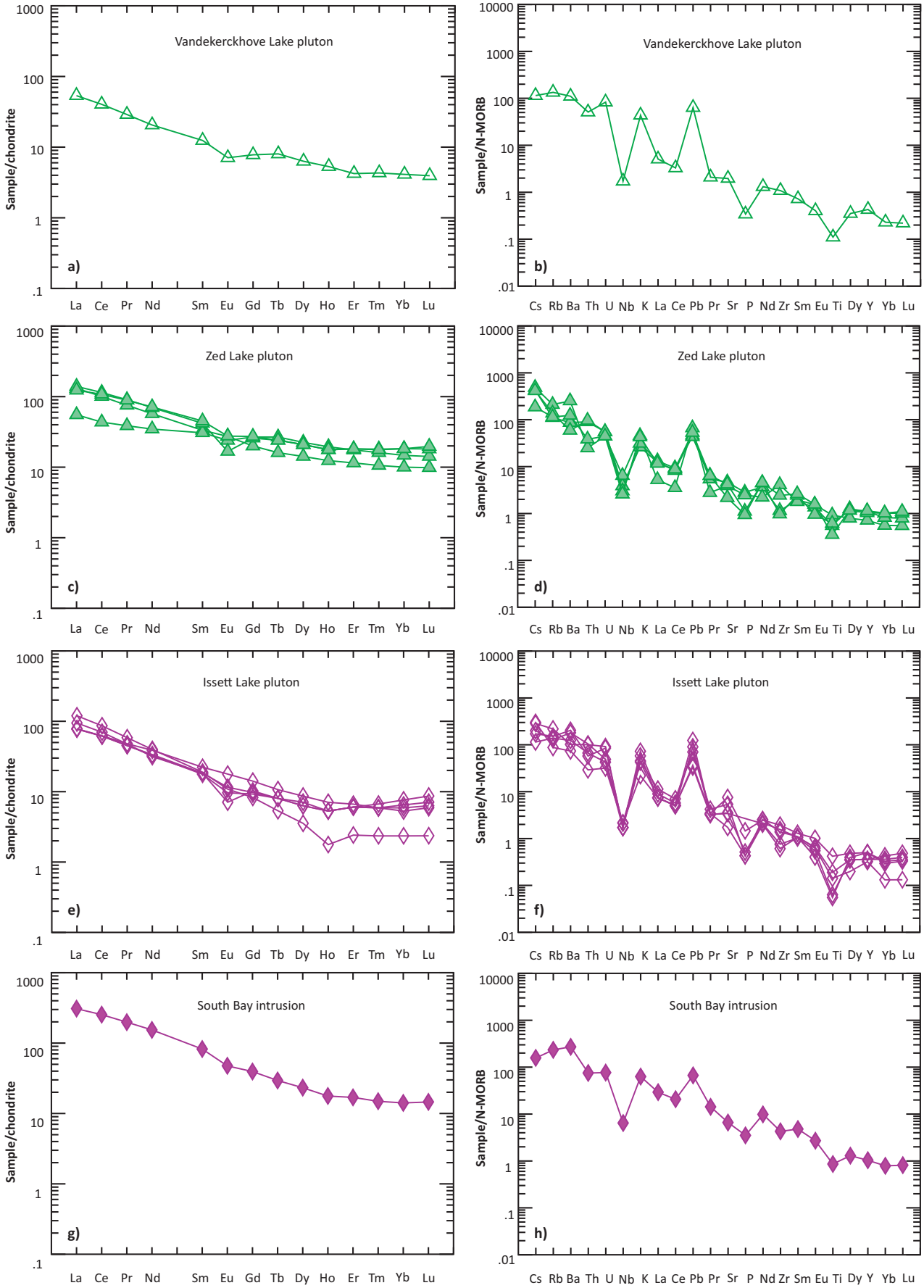

Figure 60: *Chondrite-normalized rare-earth element patterns and N-MORB–normalized extended trace-element profiles of granitoid rocks from the Southern Indian and Chipewyan domains on the left panel and the right panel, respectively:* ***a, b)*** *for the Vandekerckhove Lake pluton;* ***c, d)*** *for the Zed Lake pluton;* ***e, f)*** *for the Issett Lake pluton;* ***g, h)*** *for the South Bay intrusion. Normalizing values from Sun and McDonough (1989).*

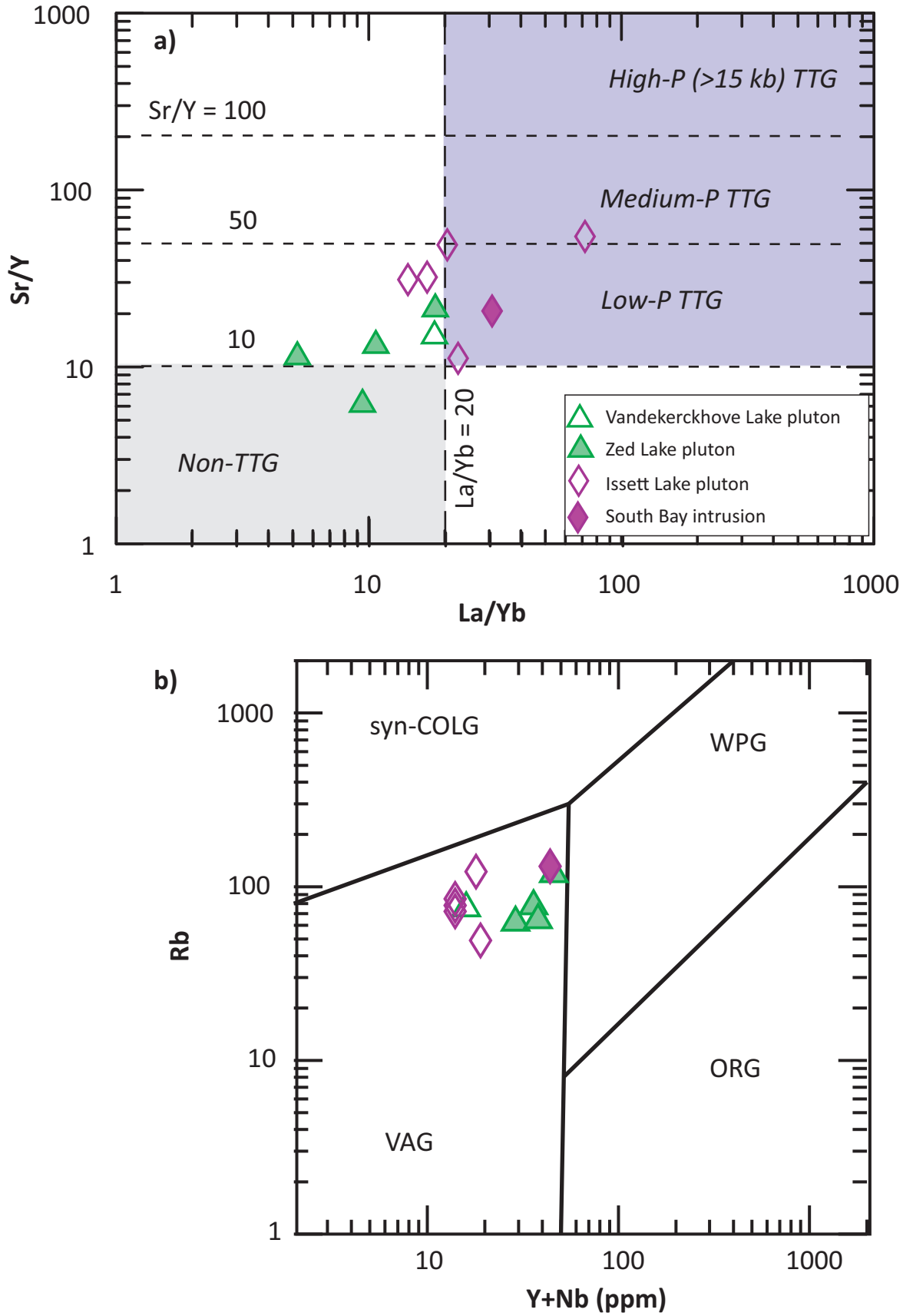

Figure 61: *Discrimination plots for granitoid rocks from the Southern Indian and Chipewyan domains:* ***a)*** *La/Yb versus Sr/Y diagram; boundaries used to define TTG types from Moyen and Martin (2012);* ***b)*** *tectonomagmatic discrimination diagram of (Y+Nb) versus Rb (after Pearce et al., 1984). Abbreviations: ORG, ocean-ridge granitoid; syn-COLG, syncollisional granitoid; TTG, tonalite-trondhjemite-granodiorite; VAG, volcanic-arc granitoid; WPG, within-plate granitoid.*

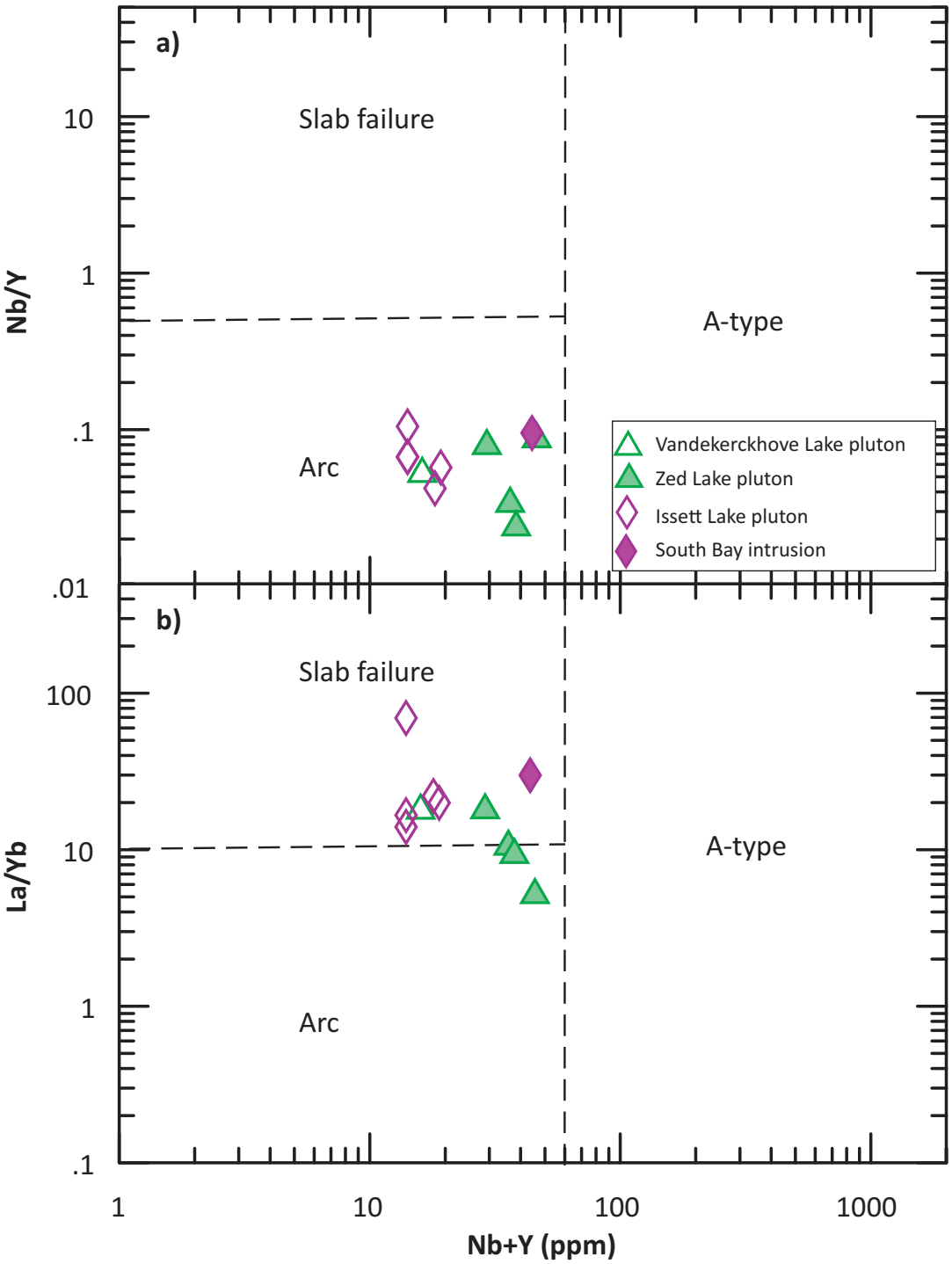

Figure 62: *Discrimination plots of* ***a)*** *Nb/Y versus Nb+Y (ppm) and* ***b)*** *La/Yb versus Nb+Y (ppm) for granitoid rocks from the Southern Indian and Chipewyan domains. Boundaries for slab-failure, arc and A-type granitoids from Whalen and Hildebrand (2019).*

Kisseynew domain (KD)

Classification

Fourteen granitoid samples from three granitoid intrusions in the KD are classified on the basis of their major- and trace-element compositions, using the TAS, Shand index (Figure 63a, b), CIPW normative Ab-An-Or composition, and Zr/TiO_2 versus Nb/Y ratio diagrams (see below). The samples from the Notigi Lake intrusive suite are grouped into two lithological types; most are granite, and two samples are diorite in terms of the TAS diagram (Figure 63a) of Middlemost (1994). Two samples from the Wapisu Lake intrusion together with one from the Costello Lake pluton fall into the field of granite. The other Costello Lake sample is located in the field of granodiorite. All the KD samples display Rittmann serial index (σ) values between 1.2 and 3.5, belonging to calcalkaline series as defined by Yang (2007), which is consistent with the subalkaline series of Irvine and Baragar (1971).

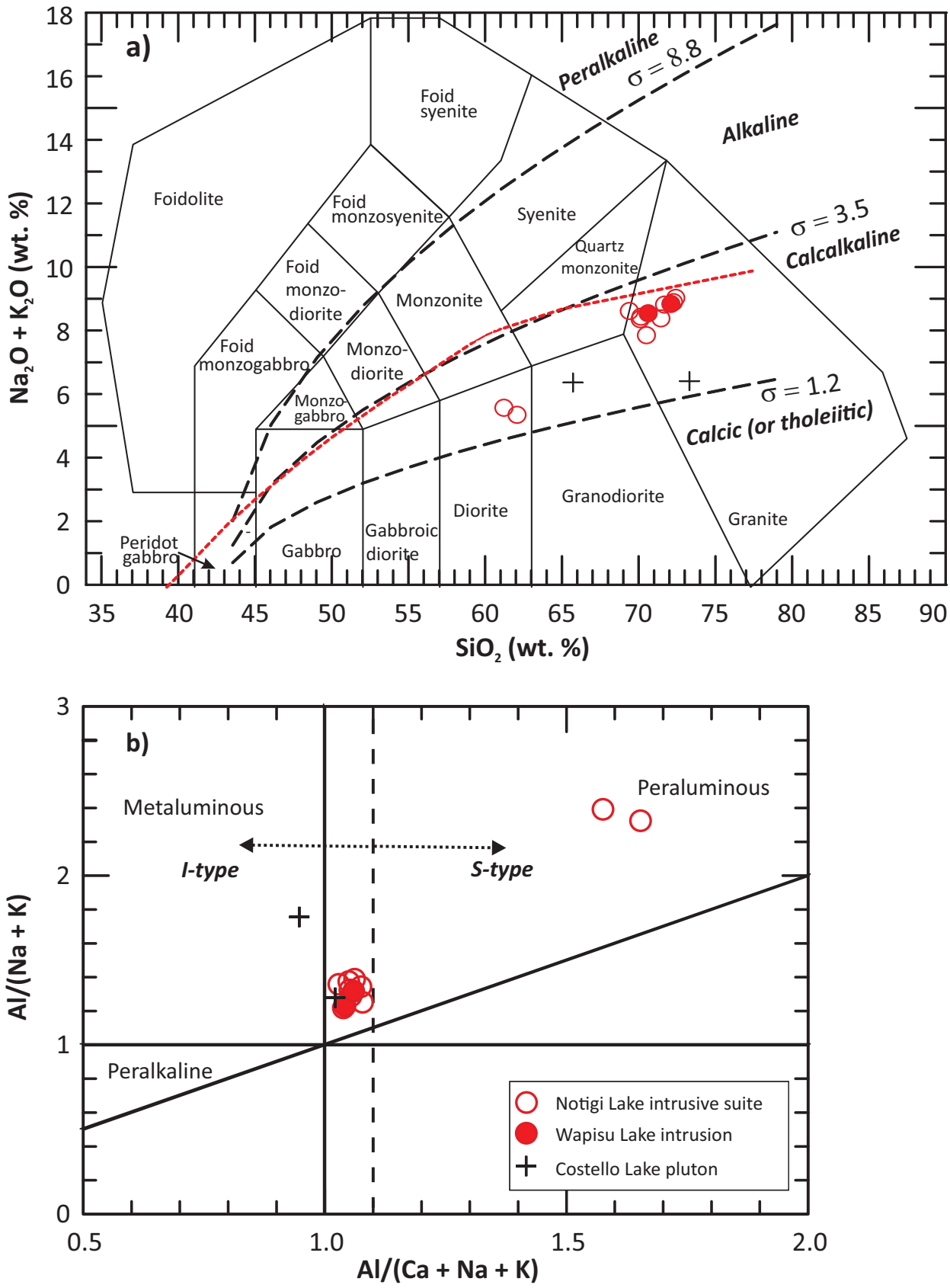

Figure 63: *Chemical classification of granitoids from the Kisseynew domain in terms of alkalinity and alumina-saturation index:* ***a)*** *total alkalis (Na_2O+K_2O) versus SiO_2 (TAS; wt. %) diagram (fields from Middlemost, 1994); boundary (red dashed line) between alkaline and subalkaline series from Irvine and Baragar (1971); Rittmann serial index σ = $(Na_2O+K_2O)^2/(SiO_2–43)$, unit in wt. % (Rittmann, 1973); using σ values to further subdivide granitoid rocks into calcic (tholeiitic), calcalkaline, alkaline and peralkaline series (Yang, 2007);* ***b)*** *Shand index plot (fields from Maniar and Piccoli, 1989); ACNK = $Al_2O_3/(CaO+Na_2O+K_2O)$, ANK = $Al_2O_3/(Na_2O+K_2O)$, unit in mole; vertical dashed line indicates ACNK = 1.1, a key parameter discriminating S- from I-type granites (Chappell and White, 1974).*

Most of the granite samples from the Notigi Lake intrusive suite have Na_2O/K_2O ratios <1.0 (ranging from 0.50 to 0.86), although two samples display Na_2O/K_2O ratios >1.0 (1.08 to 1.63). Granite samples from the Wapisu Lake intrusion and Costello Lake pluton have Na_2O/K_2O ratios exclusively >1.0 (ranging from 1.38 to 2.71; DRI2022012). On the SiO_2 versus Fe* and MALI plots (not shown) of Frost et al. (2001), most of these samples are magnesian and only four samples (i.e., two from the Notigi Lake intrusive suite and two from the Wapisu Lake intrusion) are ferroan. Interestingly, the KD granitoids are mostly alkali-calcic, except for that one sample from the Notigi Lake intrusive suite that is calcalkalic, consistent with the result of using the TAS diagram linked with the Rittmann serial indexndex (Figure 63a). Based on the relationship of Zr contents (ppm) versus (10^4Ga/Al) ratios (Whalen et al., 1987), most samples plot in the field of I- and S-type (not shown), and four samples from the Notigi Lake intrusive suite, one from the Wapisu Lake intrusion and one from the Costello Lake pluton fall into the field of A-type. Only the Costello Lake sample is A-type because it displays both high values of Zr (>300 ppm) and 10^4Ga/Al (>3). However, the other four are unlikely A-type, because two with high Zr (300 and 370 ppm) display 10^4Ga/Al ratios <3 and the other two have low Zr contents (21–106 ppm; DRI2022012).

In terms of the Shand index (Maniar and Piccoli, 1989), most of the KD samples are moderately to strongly peraluminous (Figure 63b). Only one sample from the Costello Lake pluton is metaluminous. Two samples from the Notigi Lake intrusive suite have ACNK values (1.57 to 1.65) >1.1 and are S-type based on Chappell and White (1974, 1992, 2001), and other samples from this suite together with those from the Wapisu Lake intrusion have ACNK values of 1.03 to 1.08 (DRI2022012) and are also attributed to being S-type because of the occurrences of garnet and low MS values (mostly $<0.1 \times 10^{-3}$ SI; see Table 2). One sample from the Costello intrusion displays ACNK value of 0.95, belonging to I-type, although the other sample with high Zr contents (343 ppm) and 10^4Ga/Al ratio (>3) is likely A-type as mentioned above.

Plotting the KD granitoid samples on the CIPW normative Ab-An-Or ternary diagram of Barker (1979; Figure 64a) indicates that they mostly fall into the field of granite, and two samples from the Costello Lake pluton are located in the fields of tonalite and trondhjemite, respectively. The KD samples as a whole have a low An component (mostly <20), although one sample from the Costello Lake pluton has a relatively high An value of 34. Furthermore, the KD granitoids have high normative corundum contents (mostly >1 wt. %) and low An components, consistent with typical S-type granites (Table 1), that distinctively differ from the Costello Lake pluton samples that contain normative corundum contents up to 0.45 wt. %. On the Zr/TiO_2 versus Nb/Y diagram (Figure 64b), most of the KD granitoid samples are located in the fields of diorite to granite, and two samples from the Notigi Lake intrusive suite and one from the Wapisu Lake intrusion fall into the field of monzonite. Interestingly, the granitoid rocks from the Costello Lake pluton display collectively low Nb/Y ratios (<0.8), ascribed to the subalkaline series (Pearce, 1996). This is consistent with the discriminant results in terms of σ values indicated by the TAS diagram (Figure 63a), and the Zr-rich sample can therefore not be attributed to A-type. The three samples with relatively high Nb/Y (>0.8) may be derived of crustal rocks enriched in Nb (e.g., Rudnick and Gao, 2010), which is possibly also indicated by their mineral assemblages (biotite+garnet).

Trace elements

Granitoid rocks from the KD mostly have moderate to high Sr (142 to 1028 ppm) and Ba (538 to 2396 ppm), and low Rb (36 to 120 ppm) and Cs (<0.5 to 2.5 ppm) contents (DRI2022012). They show relatively low Rb/Sr ratios ranging from 0.06 to 0.48, suggesting low to moderate degree of magmatic fractionation. Also, they have moderate to high K/Rb ratios ranging from 225 to 492, suggesting that the granitoid magmas may have been derived from moderately evolved to unevolved source region (e.g., Blevin, 2004). Most of the KD granitoid rocks contain variably low contents of transition metals (e.g., Ni, Co, V, Cr, Cu, Zn), except for two garnet-biotite gneiss samples from the Notigi Lake intrusive suite. These gneiss samples with high $Fe_2O_3^T$ (7.69–8.72 wt. %) and TiO_2 (0.86–0.87 wt. %) contents have moderately high contents of transition metals (50 ppm Ni, 17–22 ppm Co, 154–157 ppm V, 140–150 ppm Cr, 30–50 ppm Cu, and 100–150 ppm Zn; DRI2022012), and likely represent either a cumulative phase or intermediate residual part of source rocks for the Notigi Lake intrusive suite. The first interpretation is preferred because their emplacement depth is about 2.8 to 4.9 km estimated by using the method of Yang (2017) and Yang et al. (2021).

Figure 65 shows chondrite-normalized REE patterns (on the right panel; a, c and e) and N-MORB–normalized extended trace-element profiles (on the left panel; b, d and f) of the KD granitoid rocks. Granitoids rocks of the Notigi Lake intrusive suite display three distinct REE patterns (Figure 65a); 1) strongly fractionated, steep-right-dipping REE pattern characterized by strong enrichment of LREE relative to HREE with high contents of total REE (up to 865.7 ppm in sample 111-16-022A01; DRI2022012) and pronounced negative Eu anomaly (Eu/Eu* value of 0.19); 2) strongly fractionated REE pattern with strong LREE enrichment relative to HREE [$(La/Yb)_N$ ratios of 54.7 to 264.7], low to moderate contents of total REE (32.7 to 271.3 ppm) and slightly to pronounced positive Eu anomalies (Eu/Eu* values of 1.03 to 2.21), and 3) moderately fractionated REE patterns with moderately enriched LREE relative to HREE [$(La/Yb)_N$ ratios of 5.6 to 12.5], low to moderate contents of total REE (54.7 to 264.7 ppm) and moderately to slightly negative or strongly positive Eu anomalies (Eu/Eu* values of 0.56 to 1.47; DRI2022012). Although these samples exhibit notably to pronounced negative Nb, Ti and P anomalies, and positive Pb anomalies (Figure 65b), typical of magmatic-arc signatures (e.g., Prouteau et al., 1999, 2001; Pearce et al., 2005; Anderson, 2013; Rollinson and Pease, 2021), group 1 shows notably higher contents of Th (129 ppm) and U (12.9 ppm) than groups 2 and 3 (DRI2022012). Arc signature of the S-type Notigi Lake intrusive suite, however, reflects that their source region of

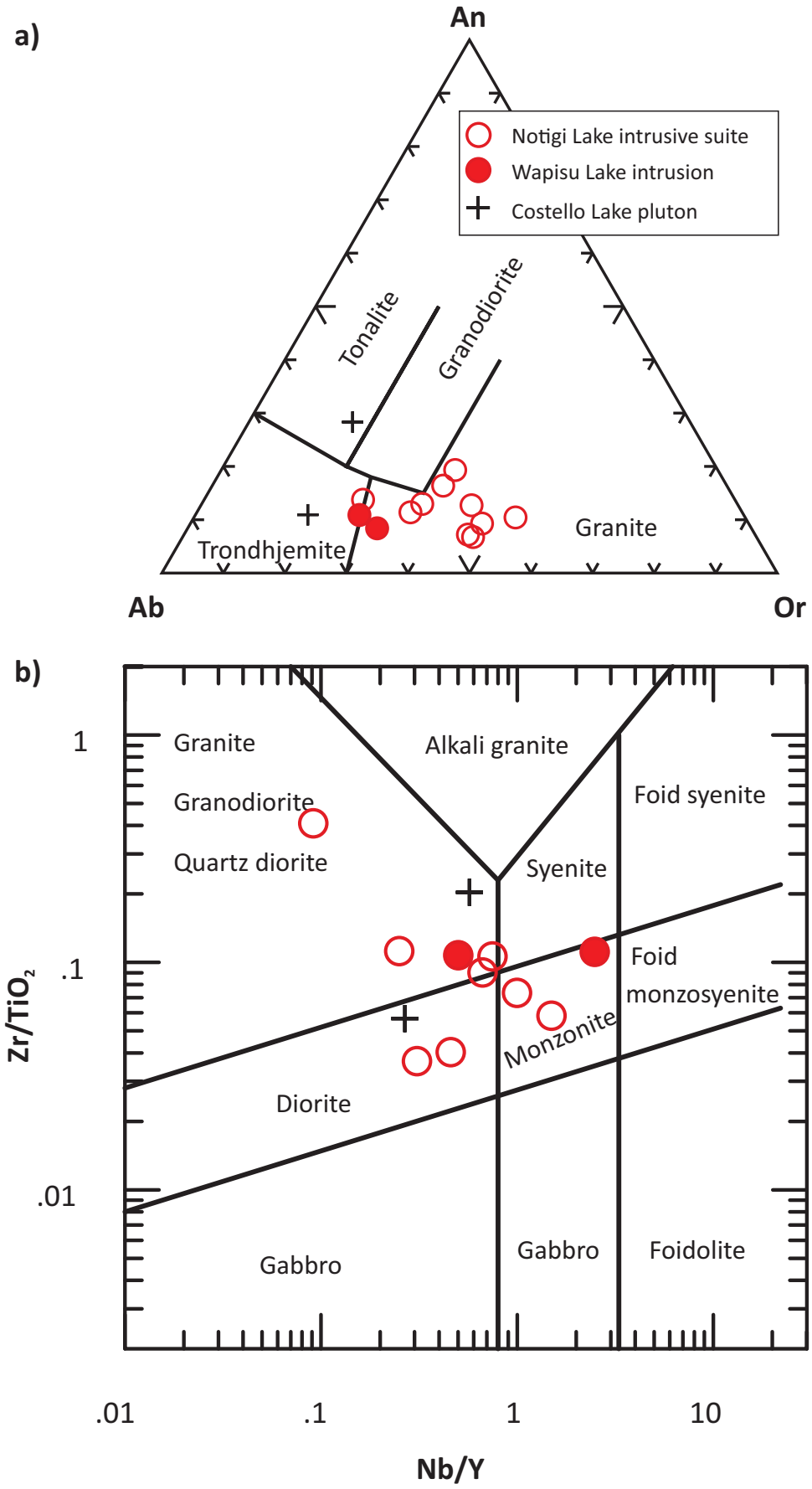

Figure 64: *Chemical classification of granitoids from the Kisseynew domain in terms of CIPW normative compositions and HFSE:* ***a****) Ab-An-Or ternary diagram (fields from Barker, 1979);* ***b****) plot of* Zr/TiO_2 *versus Nb/Y (after Pearce, 1996). Abbreviations: Ab, albite; An, anorthite; CIPW, Cross, Iddings, Pirsson, Washington, HFSE, high-field-strength element; Or, orthoclase.*

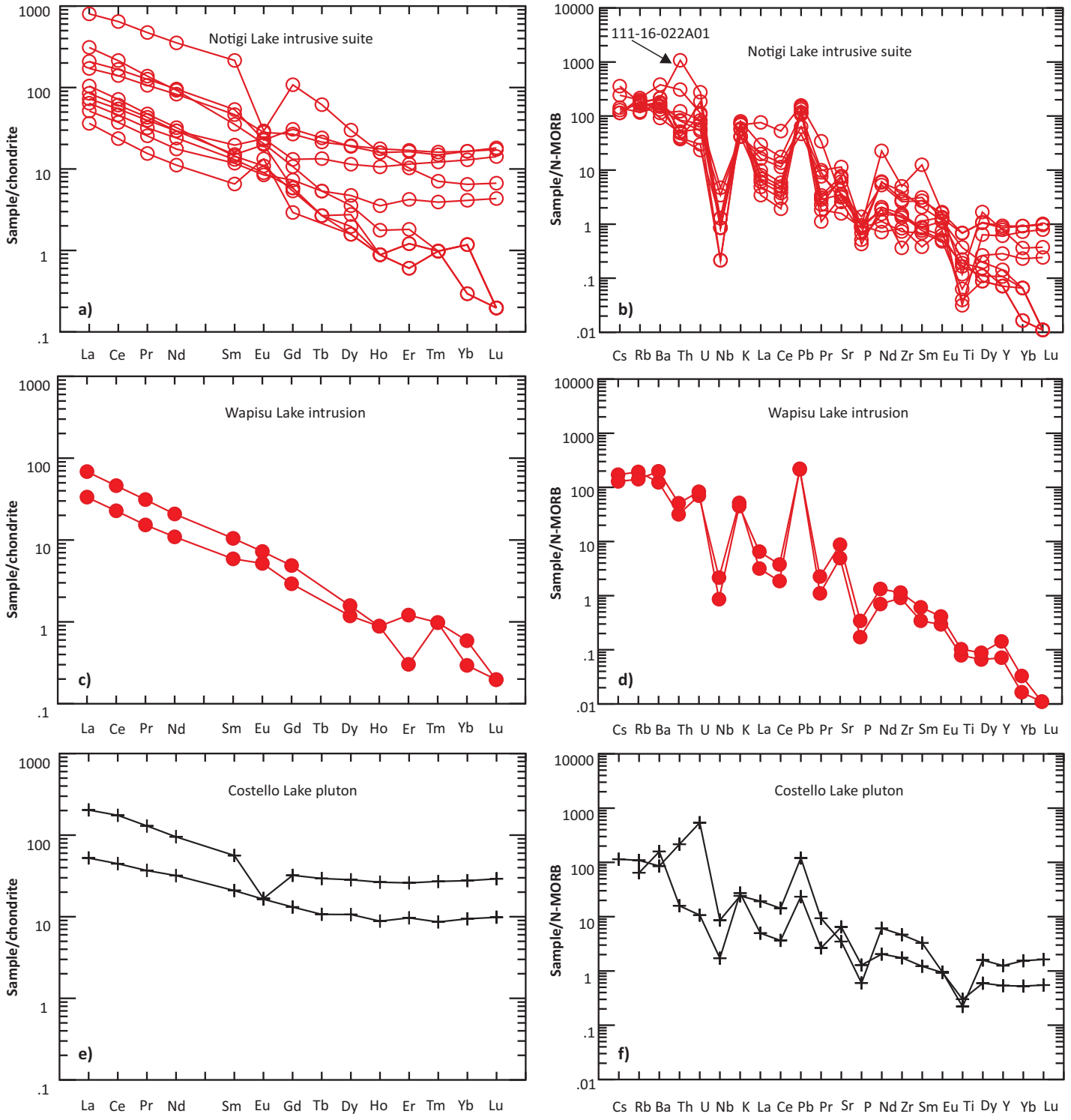

Figure 65: *Chondrite-normalized rare-earth element patterns and N-MORB–normalized extended trace-element profiles of granitoid rocks from the Kisseynew domain on the left panel and the right panel, respectively:* ***a, b)*** *for the Notigi Lake intrusive suite;* ***c, d)*** *for the Wapisu Lake intrusion;* ***e, f)*** *for the Costello Lake pluton. Normalizing values from Sun and McDonough (1989).*

metasedimenry rocks may have been derived from an arc-like provenance.

Granitoid samples from Wapisu Lake intrusion display similar REE patterns (Figure 65c) compared to group 2 of the Notigi Lake intrusive suite as described above, indicated by their $(La/Yb)_N$ ratios of 113.7 to 116.5 (note that sample 111-16-016A01 has Yb content <0.1 ppm, so that a use of 0.05 ppm (i.e., half value of the limit of detection of Yb was used for $(La/Yb)_N$ calculation) and Eu/Eu* values of 1.02 to 1.25 (DRI2022012). Similarly, they exhibit pronounced negative Nb, Ti and P anomalies, and positive Pb anomalies (Figure 65d). Granitoids in the Costello Lake pluton show moderately fractionated REE patterns (Figure 65e) with moderately enriched LREE relative to HREE [$(La/Yb)_N$ ratios of 5.6 to 7.4], low to moderate contents of total REE (72.2 to

248.3 ppm) and moderately negative or no Eu anomalies (Eu/Eu* values of 0.39 to 0.99). These samples exhibit pronounced negative Nb, Ti and P anomalies, and positive Pb anomalies, and sample 111-16-023A01 also shows a positive U anomaly (Figure 65f) due to elevated U (25.3 ppm) and Th (25.9 ppp) abundances (DRI2022012).

Figure 66a shows the KD granite samples plotted on the diagram of Sr/Y versus La/Yb ratios, demonstrating that three samples from the Notigi Lake intrusive suite together with two from the Wapisu Lake intrusion have very high Sr/Y (>100) and La/Yb (>80) ratios, typical of high-pressure TTGs. The other five samples from the Notigi Lake intrusive suite and two from the Costello Lake pluton have low Sr/Y (mostly <20) and La/Yb (<20) ratios, attributed to non-TTGs. One sample from the Notigi Lake intrusive suite shows low Sr/Y (<40) and high La/Yb (>20) ratios, whereas one from the Costello Lake pluton shows high Sr/Y (>40) and low La/Yb (<20) ratios; both belong to atypical TTGs. These features suggest that the S-type Notigi Lake intrusive suite and Wapisu Lake intrusion are interpreted to have derived from heterogeneous, e.g., garnet-present and garnet-absent sources (e.g., Moyen and Martin, 2012). Because the high Sr/Y and La/Yb rocks from the Notigi Lake intrusive suite are rich in silica (>70 wt. %) and poor in MgO and transition elements (DRI2022012), these garnet-bearing (±muscovite) granites are S-type rather than adakite-like granitoids, whose parental magmas must have been derived from partial melting of metasedimentary rocks containing a significant amount of garnet. The I-type Costello Lake pluton may have formed by partial melting of relatively homogeneous igneous rocks lacking of garnet in the source region.

Samples of the KD exclusively plot in the field of volcanic-arc granitoids absed on their Rb and Y+Nb contents (Pearce et al., 1984; Figure 66b), although some of the Notigi Lake intrusive suite samples together with Wapisu Lake intrusion samples with (Y+Nb) contents less than 20 ppm are clustered just below the boundary between the syncollisional and volcanic-arc granitoids. This suggests that the S-type granites in the KD must have contained relatively low Rb concentrations, consistent with their moderately evolved to unevolved source rocks indicated by K/Rb ratios described aboved. The Costello Lake pluton is an I-type granite intrusion formed in a volcanic-arc setting.

Most of the KD granitoid rocks display many similarities to granitoids formed by slab failure magmatism manifested by relatively high Nb/Y (>0.5) and La/Yb ratios (>10) and low (Nb+Y) contents (<60 ppm; Figure 67a, b; Whalen and Hildebrand, 2019), although four samples from the Notigi Lake intrusive suite and one from the Costello Lake pluton display low Nb/Y ratios (<0.5) that are attributed to arc granitoids. Since these granitoid rocks have low (Nb+Y) concentrations, they may have not been affected by contamination of the upper crustal rocks. In addition, it is noted that the KD granites display a large variation in Nb/Y and La/Yb ratios, suggesting that garnet and feldspars played an important role in their source region (Zhang et al., 2006; Moyen and Martin, 2012).

In summary, the KD granitoid rocks are mostly attributed to S-type granites that originated from partial melting of metasedimentary rocks at varied depths from an orogenic basin built upon an arc environment, although some show atypical S-type granites because they have high Sr/Y and La/Yb ratios. In other words, the Notigi Lake intrusive suite is composed likely of granites may have formed as different batches of melts derived from different depths in a thickened crust. Thus, this intrusive suite is a composite pluton, suggesting that the heat required for partial melting could have been provided by upwelling of asthenospheric mantle due to slab failure (Hildebrand et al., 2018; Whalen and Hildebrand, 2019). Also, this suggests that the slab failure granitoids (Whalen and Hildebrand, 2019) are to some extent similar to adakite-like (e.g., Martin et al., 2005, 2010; Yang and Lawley, 2018) granitoids, although their respective geodynamic significance and source rocks are significantly different. Granite samples from the Costello Lake pluton aretypical I-type, which formed in a volcanic-arc setting.

Sm-Nd isotope systematics

To study the nature of their sources and plausible petrogenetic processes (e.g., crustal contamination; see O'Nions et al., 1979; DePaolo, 1981, 1988; Rollinson, 1993; Rollinson and Pease, 2021), thirteen granitoid samples were selected for Sm-Nd isotopic analysis at the University of Alberta. Three samples were re-analyzed for data control. Detailed analytical procedures followed the approach described previously in Böhm et al. (2007) and Anderson (2013), which are also summarized in DRI2022012. The results combined with the data of six samples from the Bird River (Yang and Houlé, 2020) and four from the Lynn Lake (Yang and Lawley, 2018) greenstone belts are presented in Table 3 to address the petrogenetic problems outlined above.

Results

Whole-rock granitoid samples from various domains and/or subprovinces of the western Superior province (southeastern Manitoba) yielded $^{147}Sm/^{144}Nd$ isotope ratios of 0.0542 to 0.1163 and $^{143}Nd/^{144}Nd$ isotope ratios of 0. 0.510048 to 0.511226 (Table 3). The values of 19 samples at the time of crystallization have a large range from –8.0 to +1.9, including two samples from the Uchi domain showing positive values of +1.2 to +1.9, six from the English River basin having positive values of +0.6 to +1.0, six from the Bird River greenstone belt showing values of –0.9 to +1.5, four from the Winnipeg River domain having values of –8.0 to +0.4, and one from the Wabigoon domain having a value of –0.58 (Table 3).

Two depleted-mantle model ages (T_{DM}) for the Uchi domain samples range from 2.96 to 2.89 Ga (Table 3), suggesting that their source rocks (protolith) may have been separated from the mantle source around that time or contain minor amounts of recycled older crust (DePaolo, 1981, 1988; Figure 68). Similarly, six T_{DM} model ages of granitoid samples for the English River

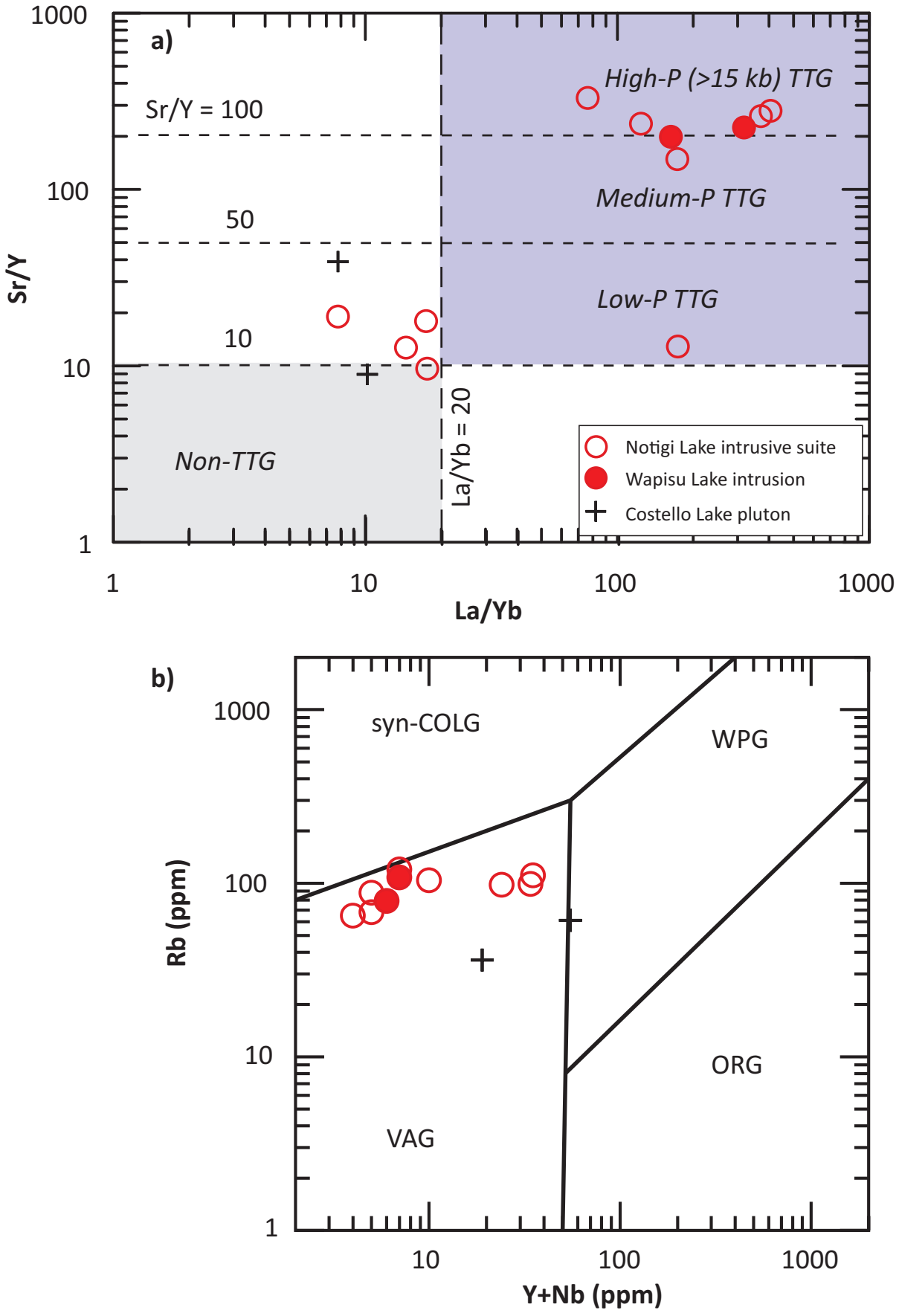

Figure 66: *Discrimination plots for granitoid rocks from the Kisseynew domain:* ***a)*** *La/Yb versus Sr/Y diagram; boundaries used to define TTG types from Moyen and Martin (2012);* ***b)*** *tectonomagmatic discrimination diagram of (Y+Nb) versus Rb (after Pearce et al., 1984). Abbreviations: ORG, ocean-ridge granitoid; syn-COLG, syncollisional granitoid; TTG, tonalite-trondhjemite-granodiorite; VAG, volcanic-arc granitoid; WPG, within-plate granitoid.*

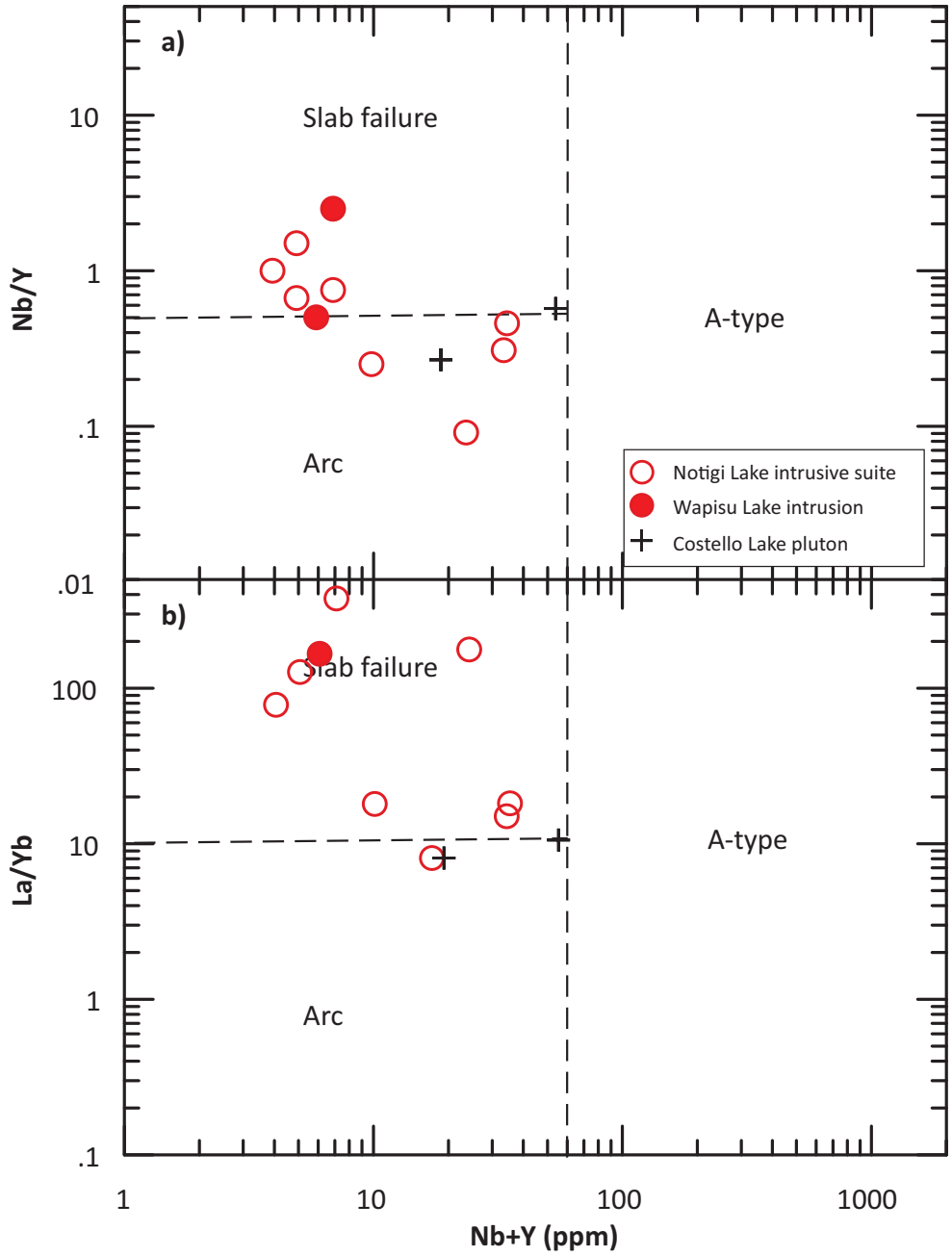

Figure 67: *Discrimination plots of Nb/Y versus Nb+Y (ppm) and La/Yb versus Nb+Y (ppm) for granitoid rocks from the Kisseynew domain. Boundaries for slab-failure, arc and A-type granitoids from Whalen and Hildebrand (2019).*

subprovince are between 3.02 and 2.91 Ga. Granitoids from the Bird River greentone belt have T_{DM} model ages ranging from 3.07 to 2.90 Ga. The Winnipeg River domain granitoids have T_{DM} of 3.56 to 2.95 Ga, significantly older than those from the Wabigoon subprovince sample that has a T_{DM} of 2.89 Ga. Interestingly, the granitoid samples display a range of the fractionation factor $f^{Sm/Nd}$ (Rollinson, 1993), from –0.72 to –0.41, indicating that these samples evolved along different paths with negative values of $\varepsilon_{Nd}^{t=0}$ (–50.5 to –27.5) sourced from varied degrees of compositional differentiation. Such Sm-Nd isotopic systematics require further discussion.

Four granitoid samples collected from the Lynn Lake greenstone belt of the Trans-Hudson orogen display a narrow range of ε_{Nd}^{t} values between +3.3 and +3.6, suggesting that they may have been derived from a similar depleted-mantle source. Three samples yielded depleted-mantle model ages (T_{DM}) of 2.11 to 2.05 Ga (Table 3). Negative fractionation factors $f^{Sm/Nd}$ values of –0.44 to –0.21 indicate that these granitoids evolved along a path to negative $\varepsilon_{Nd}^{t=0}$ values of –17.0 to –6.5, consistent with their LREE-enriched patterns, and similar to the trend of crustal evolution.

Discussion

Plotting the ε_{Nd}^{t} values against crystallization ages of the granitoid samples demonstrates that they may have been derived from distinct sources with different histories of evolution

Table 3: Whole-rock Sm-Nd isotope data of granitoid rocks.

Sample	Easting[1]	Northing[1]	NAD	Zone	Tectonic unit	Pluton	Lithology	Sm (ppm)	Nd (ppm)	$^{147}Sm/^{144}Nd$[2]	$^{143}Nd/^{144}Nd$[3]	Uncert. (2σ)[4]	T_{DM} (Ga)[5]	T (Ma)[6]	εNd_T[7]	$f^{Sm/Nd}$[8]	εNd_0[9]	$T_{2\text{-}DM}$ (Ga)[10]
111-14-230A01	331862	5639923	83	15	Uchi domain	Ross River plutonic suite	Quartz diorite	2.09	12.07	0.1045	0.511079	0.000009	2.89	2724	1.9	-0.47	-30.4	2.75
111-14-265A01	319674	5654294	83	15	Uchi domain	Ross River plutonic suite	Granodiorite	2.85	15.14	0.1137	0.511206	0.000010	2.96	2724	1.2	-0.42	-27.9	2.80
111-14-227A01	332670	5616394	83	15	English River basin	Black River plutonic suite	Granite	2.84	14.85	0.1157	0.511226	0.000010	2.99	2700	0.6	-0.41	-27.5	2.83
111-14-269A01	692867	5640256	83	14	English River basin	Black River plutonic suite	Tonalite	7.00	47.17	0.0898	0.510777	0.000007	2.92	2700	0.9	-0.54	-36.3	2.81
111-14-269A01*	692867	5640256	83	14	English River basin	Black River plutonic suite	Tonalite	7.80	52.84	0.0893	0.510771	0.000008	2.91	2700	0.9	-0.55	-36.4	2.80
111-14-15A01	313105	5613708	83	15	English River basin	Inconnu pluton	Muscovite granite	4.78	24.85	0.1163	0.511222	0.000010	3.02	2670	-0.0	-0.41	-27.6	2.85
111-14-224A01	331803	5606384	83	15	English River basin	Inconnu pluton	Gneissic granite	5.69	32.59	0.1055	0.511049	0.000009	2.96	2700	0.7	-0.46	-31.0	2.82
111-14-223A01	326539	5614495	83	15	English River basin	Inconnu pluton	Granite	3.31	19.41	0.1031	0.511011	0.000011	2.95	2700	0.8	-0.48	-31.7	2.81
111-14-277A01	704262	5613042	83	14	English River basin	Great Falls pluton	Granodiorite	1.21	7.88	0.0929	0.510839	0.000014	2.91	2700	1.0	-0.53	-35.1	2.80
111-13-041A01	323868	5609811	83	15	Bird River greenstone belt	Maskwa Lake batholith II	Tonalite	4.73	29.31	0.0975	0.510806	0.000005	3.07	2725	-0.9	-0.50	-35.7	2.97
111-13-142B01	326107	5609209	83	15	Bird River greenstone belt	Maskwa Lake batholith II	Feldspar porphyry	5.15	29.75	0.1047	0.510985	0.000007	3.02	2725	0.0	-0.47	-32.2	2.89
111-13-167A01	332944	5605444	83	15	Bird River greenstone belt	Maskwa Lake batholith II	Granite	6.44	36.37	0.1071	0.511055	0.000006	3.00	2725	0.5	-0.46	-30.9	2.85
111-13-149A01	327619	5606634	83	15	Bird River greenstone belt	Maskwa Lake batholith I	Granodiorite	2.88	23.68	0.0735	0.510415	0.000007	2.97	2725	-0.2	-0.63	-43.4	2.91
111-13-051A01	323968	5608315	83	15	Bird River greenstone belt	Maskwa Lake batholith I	Granite	5.31	59.31	0.0542	0.510048	0.000008	2.96	2832	1.5	-0.72	-50.5	2.86
111-13-211A01	328790	5606444	83	15	Bird River greenstone belt	Maskwa Lake batholith I	Tonalite	3.67	21.89	0.1013	0.510911	0.000006	3.03	2832	1.1	-0.48	-33.7	2.89
111-14-242A01	301921	5578488	83	15	Winnipeg River domain	Lac du Bonnet batholith	Granite	8.46	60.45	0.0846	0.510674	0.000010	2.92	2660	0.1	-0.57	-38.3	2.84
111-14-242A01*	301921	5578488	83	15	Winnipeg River domain	Lac du Bonnet batholith	Granite	8.77	63.18	0.0839	0.510675	0.000010	2.90	2660	0.3	-0.57	-38.3	2.82
111-14-247A01	294166	5559908	83	15	Winnipeg River domain	Pointe du Bois pluton	Gneissic tonalite	6.87	40.13	0.1035	0.510569	0.000007	3.56	2700	-8.0	-0.47	-40.4	3.49
111-14-247A01*	294166	5559908	83	15	Winnipeg River domain	Pointe du Bois pluton	Gneissic tonalite	6.67	37.60	0.1073	0.510658	0.000008	3.56	2700	-7.6	-0.45	-38.6	3.46
111-14-282A01	327579	5523519	83	15	Winnipeg River domain	Rennie River plutonic suite	Granite	3.58	24.43	0.0887	0.510731	0.000009	2.95	2700	0.4	-0.55	-37.2	2.85
111-14-254A01	320375	5545439	83	15	Winnipeg River domain	Big Whiteshell Lake pluton	Granite	14.75	92.57	0.0963	0.510860	0.000010	2.97	2700	0.2	-0.51	-34.7	2.86
111-14-283A01	337410	5511611	83	15	Wabigoon domain	Falcon Lake igneous complex	Quartz monzonite	5.71	42.12	0.0820	0.510652	0.000008	2.89	2700	1.1	-0.58	-38.7	2.79
111-16-197A01	412573	6307761	83	14	Lynn Lake greenstone belt	Farley Lake stock	Quartz diorite	7.75	42.36	0.11061	0.511769	0.000006	2.05	1854	3.6	-0.44	-17.0	1.95
111-16-199A01	412076	6307467	83	14	Lynn Lake greenstone belt	Farley Lake stock	Diorite	9.62	50.50	0.11515	0.511821	0.000008	2.07	1854	3.5	-0.41	-15.9	1.95
111-15-162A01	411172	6301517	83	14	Lynn Lake greenstone belt	Farley Lake pluton II	Granodiorite	9.58	37.44	0.15481	0.512304	0.000008	N/A	1872	3.6	-0.21	-6.5	1.96
111-16-314A01	411317	6306261	83	14	Lynn Lake greenstone belt	Farley Lake pluton I	Granodiorite	3.50	17.99	0.11763	0.511827	0.000010	2.11	1879	3.3	-0.40	-15.8	1.99

Note: Sample number with * is reanalyzed.
[1] Coordinates in UTM system.
[2] Estimated error is better than 0.5%.
[3] Normalized to $^{146}Nd/^{144}Nd = 0.7219$; external precision based on repeat La Jolla Nd standard runs.
[4] Analytical uncertainty.
[5] Depleted mantle Nd model ages calculated according to the model of DePaolo (1981); T_{DM} not calculated for samples with $^{147}Sm/^{144}Nd > 0.14$.
[6] Known or inferred age.
[7] εNd values at the known or inferred age (T) calculated using present-day chondritic ratios of $^{143}Nd/^{144}Nd = 0.512638$ and $^{147}Sm/^{144}Nd = 0.1967$.
[8] Fractionation factor (see Rollinson, 1993).
[9] εNd values at present calculated using present-day chondritic ratios of $^{143}Nd/^{144}Nd = 0.512638$ and $^{147}Sm/^{144}Nd = 0.1967$.
[10] Two-stage depleted mantle Nd model ages calculated according to the model of Liew and Hofmann (1988).

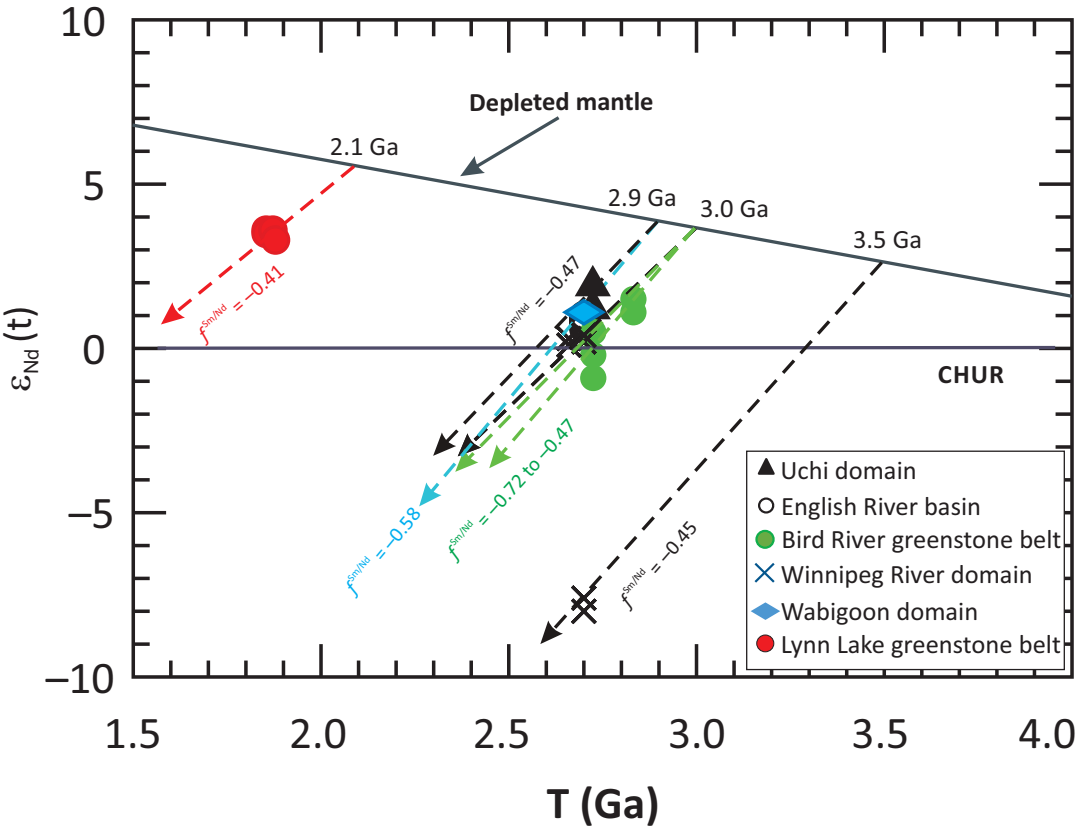

Figure 68: *Time (t) versus ε_{Nd}^{t} evolution diagram for whole-rock samples from the western Superior province and Lynn Lake greenstone belt of the Trans-Hudson orogen. $f^{Sm/Nd}$ denotes fractionation factor (Rollinson, 1993). Depleted-mantle evolution line from Goldstein et al. (1984). Grey box on the y-axis denotes values of $\varepsilon_{Nd}^{t=0}$ at present.*

(Figure 68). Granitoids from the Uchi, English River, Bird River, part of the Winnipeg River and Wabigoon subprovinces are indistinguishable in terms of their protoliths mostly displaying variably depleted mantle signature and separated from the mantle at about 3.0 to 2.9 Ga. However, the Pointe du Bois pluton sample (and its duplicate) from the Winnipeg River domain has an ε_{Nd}^{t} value of –8.0 to –7.6, indicating that it had either a much more evolved crustal precursor that differentiated from the mantle at ca. 3.56 Ga, or partial assimilation of older crust. In the Bird River greenstone belt, three basement granitoid samples from the Maskwa Lake batholith I yielded ε_{Nd}^{t} values of –0.2 to +1.5, indicating that they may have been derived from a protolith akin to a slightly depleted-mantle source (or juvenile crustal material) that was separated from the mantle at ca. 3.03 to 2.96 Ga as indicated by their T_{DM} (Table 3). Three younger TTG samples from the Maskwa Lake batholith II have relatively low ε_{Nd}^{t} values of –0.9 to +0.5, suggesting that they were derived from a fertile juvenile crustal material differeniated from the mantle at ca. 3.07 to 3.00 Ga that was the same as the Maskwa Lake batholith I within uncertainties of model ages.

In addition to the $f^{Sm/Nd}$ values, fractionation degree of LREE relative to HREE in magmatic rocks can also be measured by the Sm/Nd ratios as indicated by their perfectly positive correlation (Table 3). The Sm/Nd ratios for the Uchi domain samples are 0.17 to 0.19 (average 0.18), for the English River basin rocks 0.15 to 0.19 (average 0.17), for the Bird River greenstone TTGs 0.16 to 0.18 (average 0.17) and for the basement granitoids 0.09 to 0.17 (average 0.13), for the Winnipeg River domain granitoids 0.14 to 0.18 (average 0.16), and for the Wabigoon sample is 0.14. These samples have Sm/Nd ratios lower than that of the upper continental crust (0.19; Goldstein et al., 1984) and average continental crust (0.195; Rudnick and Gao, 2010), and much lower than the primitive mantle (0.33) and N-type MORB (0.36; Sun and McDonough, 1989) as well. This suggests that their protoliths must be crustal rocks but had experienced different degrees of evolvement and diffentiation. For example, the basement granitoids in the Bird River greenstone belt appear to have derived to a higher degree from evolved source(s) than TTGs that seem to have similar degree of evolvement as the English River basin granitoids. In contrast, the Lynn Lake greenstone belt granitoid rocks have Sm/Nd ratios of 0.18 to 0.26 (average 0.21), which may have been derived from less evolved source rocks.

The Sm-Nd isotopic data, $f^{Sm/Nd}$ and Sm/Nd ratios (Table 3) reveal that the parental magmas may have been derived mostly from crustal precursors that had differentiated from depleted-mantle at ca. 3.1–3.0 Ga in the western Superior province, although part of the Winnipeg River domain may have an older nuclei of up to ca. 3.6 Ga. In other words, the granitoid rocks were likely sourced from juvenile crust formed via crust-mantle differentiation (Hawkesworth and Kemp, 2006; Frisch et al., 2011; Lee et al., 2011), although it cannot be ruled out that some inputs, in particulary heat, were from the mantle. The TTG and base-

ment granitoids in the Bird River greenstone belt may have been derived from a juvenile crustal source that had also separated from a depleted mantle (e.g., Babuŝka and Plomerová, 2020), at ca. 3.1–3.0 Ga. This is further constrained by the high T-P phase equilibrium relationship suggesting that the granitic melts could not have been in direct chemical equilibrium with the depleted mantle (e.g., Clarke, 1992; Scaillet et al., 2016; Yang, 2017; Clemens, 2018; Hildebrand et al., 2018; Clemens et al., 2020; Yang et al., 2021). Thus, the granitoids with positive values must have been derived from partial melting of juvenile crustal materials, likely of an amphibolite source as constrained by lithogeochemical characteristics described above. However, calculation of single-stage depleted-mantle Nd model ages (Table 3) could not discern the differences in source regions between the granitoid rocks from the granitoid basement and TTG suites.

Therefore, it is necessary to use either a two-stage depleted-mantle Nd model (Liew and Hofmann, 1988; Janoušek, 1999) to constrain the evolution of juvenile crustal source(s) or short-lived crustal material derived from the mantle (Hanson, 1978). The calculations indicate values for the two-stage Nd model ages ($T_{2\text{-}DM}$) of 2.80 to 2.75 Ga for the Uchi domain samples, 2.85 to 2.80 Ga for the English River basin samples, 2.97 to 2.85 Ga for the Bird River greenstone belt TTG rocks and 2.91 to 2.86 Ga for the basement granitoids, 3.49 to 2.84 Ga for the Winnipeg River domain samples, and 2.79 Ga for the Wabigoon domain sample (Table 3). Compared to the depleted mantle Nd model ages (T_{DM}), the duration of juvenile crust for these domains vary for when the granitoid magmas (rocks) were extracted from the crustal source(s). For instance, in the Bird River greenstone belt, the younger TTGs may have been derived from a slightly older, juvenile crustal source than that of the basement granitoids. The source rock(s) of TTGs may have slightly longer duration of cumulative time (~130 m.y.) after differentiating (or separating) from the depleted mantle at ca. 3.1–3.0 Ga, as constrained by the depleted Nd model ages (or single-stage Nd model ages; Table 3; DePaolo, 1981, 1988), than that of the basement granitoids (~100 m.y.). This explanation is also consistent with the requirements of the high P-T experiments mentioned above. However, this study does not rule out the possibility of partial melting of prior metasomatized mantle to produce adakite-like dioritic magmas (e.g., the Farley Lake stock) although it requires fluid-present melting (e.g., Winter, 2014; Rollinson and Pease, 2021).

Granitoid rocks from the Lynn Lake greenstone belt have $T_{2\text{-}DM}$ ages of 1.99 to 1.95 Ga, indicating that their precursors had a duration of time about 110 to 130 m.y. after separation from a depleted mantle at ca. 2.11 to 2.05 Ga. Unfornatunately, there has not been any basement rock(s) identified so far in the belt (e.g., Gilbert et al., 1980; Gilbert, 1993; Beaumont-Smith and Böhm, 2004; Yang and Beaumont-Smith, 2015a, b; Yang, 2021).

Economic considerations

Diverse petrogenetic types of granitoid rocks have been identified to occur in different tectonic units (domains, belts, subprovinces) of the western Superior province and Trans-Hudson orogen within Manitoba. Granitoid rocks, the most abundant exposed Precambrian lithogies, preserve partial primary mineralogy and textures, and bear distinctively different mineral potential. Key petrogenetic information has been acquired in this report in terms of the reconnaissance mapping and sampling conducted in the last eight years since the project was initiated in 2014 by focusing on the field relationships, textures (fabrics), mineral assemblages, MS and presence of mineralization and/or alteration at outcrop scale. In the laboratories, systematic petrography, petrology, geochemical and Nd isotopic studies were carried out to extract detailed geoscientific information on granitoid protoliths, geotectonic settings, magmatic processes, and metallogeny of the granitoid rocks.

A major finding is that muscovite- and/or garnet-bearing granitic rocks (i.e., strongly peraluminous granitoids or S-type) with commonly low MS values ($<0.1 \times 10^{-3}$ SI; Table 2) are mainly intruded into or nearby subprovince boundary zones (or collisional zones) in the western Superior province (Yang, 2014a, b; Yang et al., 2019) and domain boundary zones in the Trans-Hudson orogen (Yang and Beaumont-Smith, 2015a, b; Yang, 2016, 2021), representing a macro-recognizable geological marker to assist in the subdivision of tectonic entities. These peraluminous granitoid rocks likely formed in a thickened crustal setting(s) due to continental collision, are commonly associated with pegmatite intrusions enriched in critical metals (e.g., Li, Cs, Ta, Nb) and may have potential to host Sn-W mineralization. For example, a pegmatitic granite sample 111-13-170D01 from the Inconnu pluton II along the southern margin of the English River basin contains 290 ppm Ta, 195 ppm Be, 95 ppm Nb; this mineralized pegmatitic granite zone extends over 4.3 km along strike (see Yang et al., 2019; Yang and Houlé, 2020). In contrast, granitoid plutons consisting dominantly of tonalite, trondhjemite and granodiorite (i.e., TTG suite) with much higher MS values and mineral assemblages typical of I-type are widely present across the various domains and/or subprovinces in Manitoba's parts of the Canadian shield. These granitoid rocks greatly contributed to continental crustal growth and expansion in the Archean and Paleoproterozoic, and may have been related to plate subduction. Some of the phases in the TTG suites display porphyry Cu-Au and skarn Cu-Au-Ag mineralization, or are overprinted by shear-hosted Au mineralization (Yang and Houlé, 2020).

It is emphasized again that Neoarchean calcalkaline, peraluminous S-type granites are exclusively emplaced along or close to subprovince boundary (or collisional) zones in the western Superior province, southeastern Manitoba (Yang, 2014a; Yang et al., 2019), providing insights into where to explore for critical metals (e.g., Li, Cs, Ta, Nb) hosted in pegmatites genetically associated with S-type granite intrusions.

Furthermore, a new ternary diagram to discriminate fertile from barren rare-metal (Ta) granite-pegmatite systems proposed by Mohamadizadeh et al. (2020) is worthy of testing for its applicability to granite-pegmatites in Manitoba from a critical metals exploration perspective.

In comparison, the Kisseynew domain S-type granite samples with high Sr/Y and La/Yb ratios tend to have low potential for critical rare-metal minerals because they are exclusively attributed to barren granites using the discriminant method of Mohamadizadeh et al. (2020). In contrast, S-type granites from the English River basin are mostly fertile, suggesting that they have high potential for rare metals.

Geochemical and Nd isotope compositions of granitoid rocks from diverse domains and/or subprovinces in Manitoba provide the records of their parental magmas derived from distinct protoliths that had different histories of geological evolution. Detailed bedrock mapping aided by geochemical, U-Pb zircon geochrological and Nd isotope studies provide insight into the tectonic evolution of, for example, the Lynn Lake greenstone belt, that was manifested by arc I-type (i.e., the ca. 1879 Ma Farley Lake pluton 1), intra-arc extension related A-type (the ca. 1972 Ma Farley Lake pluton II), and slab roll-back related adakite-like (the ca. 1854 Ma Farley Lake stock) granitoid rocks that are well exposed in the Farley Lake area (Yang and Beaumont-Smith, 2016; Yang and Lawley, 2018). More importantly, some mineralization may have been generated at specific stages of the tectonic evolution; for instance, gold mineralization at the Gordon (formerly Farley Lake) mine in the Lynn Lake belt is genetically associated with the ca. 1854 Ma Farley Lake stock that shows adakite-like geochemical signatures (Yang and Lawley, 2018).

Abnormally REE enriched granitoids are evident in some of the plutons and/or intrusions from diverse domains in Manitoba. For example, a granite sample (111-16-022A01) collected from the Notigi Lake intrusive suite in the Kisseynew domain contains total ΣREE of 866 ppm (DRI2022012), a sample (111-15-167A01) from the Eden Lake pluton in the Lynn Lake domain has ΣREE of 596 ppm, and a granite sample (111-13-051A01) from the Maskwa Lake batholith I in the Bird River domain contains ΣREE of 506 ppm. Occurrences of local REE concentration in granite plutons therefore justify further evaluation of these critical minerals.

High-K calcalkaline granites from the English River basin and Uchi domain (e.g., Wallace Lake pluton) in the western Superior province require further investigation of their U potential or derivative source of U for mineralization (e.g., Cuney, 2014). For instance, a granite sample (111-14-280A01) from the Black River plutonic suite in the English River basin contains 82 ppm U. Uranium enrichment in Archean and/or Proterozoic basement may have supplied U source for generation of unconformity-related U deposits in sedimentary basins (e.g., Raffensberger and Garven, 1995a, b; Jefferson et al., 2007).

During the course of this project, a numerical method of using CIPW normative composition (i.e., quartz, albite, orthoclase) to estimate crystallization pressure of granite (*s.s.*) intrusions was proposed (i.e., Qtz-geobarometer; see Yang, 2017), which has since widely been applied to various granite plutons elsewhere (Dou et al., 2018; Mulja and Williams-Jones, 2018; Itiga et al., 2019; Yang et al., 2019, 2021; Mohammadi et al., 2020; Devoir et al., 2021; Guo et al., 2022; Secchi et al., 2022). This method is applicable primarily to granites with the contents of total normative quartz, albite, and orthoclase higher than 80 wt. %, which have melt compositions comparable to minima or eutectics of the haplogranite system as defined by Tuttle and Bowen (1958). For less evolved metaluminous to peraluminous granites, their ferric/ferrous oxide ratios dependent upon redox conditions are required to consider to obtain improved pressure estimation and/or emplacement depth of the granite intrusions (Yang et al., 2021). This is important for mineral exploration of ore deposits associated with granite intrusions, indicating their current erosion level and emplacement depth. Furthermore, source of ore-fluids emanating from granitoid intrusions can be tracked in terms of investigation on REE partitioning between fluids and magmas (Yang, 2019b), which provides more clues as to the origin of the fluids.

Going forward, additional work is required to collect and compile granitoid data to cover the entire Precambrian shield in Manitoba. Also, more studies are needed to understand the control of paleo-depth of granite protoliths on metallogeny of mineral deposits associated with the granite intrusions. For example, why do S-type granites with high Sr/Y and La/Yb ratios (suggestive of their derivation from a deep protolith(s) containing significant amount of garnet) from the Kisseynew domain appear to have low potential for critical minerals (e.g., Li, Ta, Cs)? In contrast, why do S-type granites with low Sr/Y and La/Yb ratios from the English River basin and Bird River greenstone belt display high potential for critical minerals?

Acknowledgments

The author thanks L. Lafreniere, S. Kushner, D. Drayson, C. Kovachik, J. Watts, M. Kohli and W. Ezeana from the University of Manitoba and M. Hamilton from Brandon University for assistance in the field. The completion of this report could not have taken place without assistance from the MGS staff present and past (N. Brandson, E. Anderson, C. Epp, P. Belanger, H.P. Gilbert, M.T. Corkery, C.O. Böhm, S.D. Anderson, T. Martins, M.P.B. Nicolas, E.C. Syme, P. Kremer, G. Keller, P. Lenton, L. Chackowsky, H. Adediran, B. Lenton, M. McFarlane, M. Pacey, T. Booth, L. Janower, G. Benger, R. Unruh and V. Varga); A. Polat and P. Sotiriou from the University of Windsor; M.G. Houlé and C.J.M. Lawley from the Geological Survey of Canada. Finally, constructive reviews by C.O. Böhm and G. Keller, and report layout by C. Steffano are gratefully acknowledged.

References

Ames, D.E., Van Breemen, O. and Scoates, J.S. 2002: Evidence for recycled Mesoarchean crust in the Ruttan arc succession, Rusty Lake belt, Trans-Hudson Orogen, Manitoba: U-Pb isotopic data; Radiogenic Age and Isotopic Studies: Report 15, Geological Survey of Canada, Current Research, no. 2002-F2, 7 p., URL <https://doi.org/10.4095/213601>.

Anderson, S.D. 2008: Geology of the Rice Lake area, Rice Lake greenstone belt, southeastern Manitoba (parts of NTS 52L13, 52M4); Manitoba Science, Technology, Energy and Mines, Manitoba Geological Survey, Geoscientific Report GR2008-1, 96 p., URL <https://manitoba.ca/iem/info/libmin/GR2008-1.zip> [December 2022].

Anderson, S.D. 2011: Detailed geological mapping of the Rice Lake mine trend, southeastern Manitoba (part of NTS 52M4): stratigraphic setting of gold mineralization; *in* Report of Activities 2011, Manitoba Innovation, Energy and Mines, Manitoba Geological Survey, p. 94–110, URL <https://manitoba.ca/iem/geo/field/roa11pdfs/GS-10.pdf> [December 2022].

Anderson, S.D. 2013: Geology of the Garner–Gem lakes area, Rice Lake greenstone belt, southeastern Manitoba (parts of NTS 52L11, 14); Manitoba Mineral Resources, Manitoba Geological Survey, Geoscientific Report GR2013-1, 135 p., URL <https://manitoba.ca/iem/info/libmin/GR2013-1.zip> [December 2022].

Anderson, S.D., Beaumont-Smith, C.J. and Böhm, C.O. 2005: Structure and geometry of the Paleoproterozoic Ruttan VMS deposit, southwest Rusty Lake belt (NTS 64B5), Manitoba; Manitoba Industry, Economic Development and Mines, Manitoba Geological Survey, Geoscientific Report GR2005-1, 35 p., URL <https://manitoba.ca/iem/info/libmin/GR2005-1.zip> [December 2022].

Arculus, R.J. 1987: The significance of source versus process in the tectonic controls of magma genesis; Journal of Volcanology and Geothermal Research, v. 32, p. 1–12, URL <https://doi.org/10.1016/0377-0273(87)90033-3>.

Ayer, J.A. and Davis, D.W. 1997: Neoarchean evolution of differing convergent margin assemblages in the Wabigoon Subprovince: geochemical and geochronological evidence from the Lake of the Woods greenstone belt, Superior Province, northwestern Ontario; Precambrian Research, v. 81, p. 155–178, URL <https://doi.org/10.1016/S0301-9268(96)00033-2>.

Ayer, J.A. and Dostal, J. 2000: Nd and Pb isotopes from the Lake of the Woods greenstone belt, northwestern Ontario: implications for mantle evolution and the formation of crust in the southern Superior Province; Canadian Journal of Earth Sciences, v. 37, p. 1677–1689, URL <https://doi.org/10.1139/e00-067>.

Babuška, V. and Plomerová, J. 2020: Growth of primordial continents by cycles of oceanic lithosphere subductions: Evidence from tilted seismic anisotropy supported by geochemical and petrological findings; Solid Earth Sciences, v. 5, p. 50–68, URL <https://doi.org/10.1016/j.sesci.2019.12.003>.

Bailes, A.H. and Syme, E.C. 1989: Geology of the Flin Flon–White Lake area; Manitoba Energy and Mines, Geological Services, Geological Report GR87-1, 313 p., URL <https://manitoba.ca/iem/info/libmin/GR87-1.zip> [December 2022].

Bailes, A.H., Percival, J.A., Corkery, M.T., McNicoll, V.J., Tomlinson, K.Y., Sasseville, C., Rogers, N., Whalen, J.B. and Stone, D. 2003: Geology and tectonostratigraphic assemblages, West Uchi map area, Manitoba / Ontario; Manitoba Industry, Trade and Mines, Open File Report OF2003-1, Geological Survey of Canada, Open File 1522 and Ontario Geological Survey, Preliminary Map P.3461, 1:250 000 scale, URL <https://doi.org/10.4095/213986>.

Baldwin, D.A., Syme, E.C., Zwanzig, H.V., Gordon, T.M., Hunt, P.A. and Stevens, R.D. 1987: U–Pb zircon ages from the Lynn Lake and Rusty Lake metavolcanic belts, Manitoba: two ages of Proterozoic magmatism; Canadian Journal of Earth Sciences, v. 24, p. 1053–1063, URL <https://doi.org/10.1139/e87-101>.

Barbarin, B. 1999: A review of the relationships between granitoid types, their origins and their geodynamic environments; Lithos, v. 46, p. 605–626, URL <https://doi.org/10.1016/S0024-4937(98)00085-1>.

Barker, F. 1979: Trondhjemite: definition, environment and hypotheses of origin; Chapter 1 *in* Trondhjemites, Dacites, and Related Rocks, F. Barker (ed.), Elsevier Scientific Publishing Company, Amsterdam, Netherlands, Developments in Petrology, v. 6, p. 1–12, URL <https://doi.org/10.1016/B978-0-444-41765-7.50006-X>.

Beakhouse, G.P. 1991: Winnipeg River Subprovince; *in* Geology of Ontario, P.C. Thurston, H.R. Williams, R.H. Sutcliffe and G.M. Stott (ed.), Ontario Geological Survey, Special Volume 4, Part 1, p. 279–301.

Beakhouse, G.P. and Davis, D.W. 2005: Evolution and tectonic significance of intermediate to felsic plutonism associated with the Hemlo greenstone belt, Superior Province, Canada; Precambrian Research, v. 137, p. 61–92, URL <https://doi.org/10.1016/j.precamres.2005.01.003>.

Beaumont-Smith, C.J. 2008: Geochemistry data for the Lynn Lake greenstone belt, Manitoba (NTS 64C11–16); Manitoba Science, Technology, Energy and Mines, Manitoba Geological Survey, Open File OF2007-1, 5 p., URL <https://manitoba.ca/iem/info/libmin/OF2007-1.zip> [December 2022].

Beaumont-Smith, C.J. and Böhm, C.O. 2002: Structural analysis and geochronological studies in the Lynn Lake greenstone belt and its gold-bearing shear zones (NTS 64C10, 11, 12, 14, 15 and 16), Manitoba; *in* Report of Activities 2002, Manitoba Industry, Trade and Mines, Manitoba Geological Survey, p. 159–170; URL <https://manitoba.ca/iem/geo/field/roa02pdfs/GS-19.pdf> [December 2022].

Beaumont-Smith, C.J. and Böhm, C.O. 2003: Tectonic evolution and gold metallogeny of the Lynn Lake greenstone belt, Manitoba (NTS 64C10, 11, 12, 14, 15 and 16), Manitoba; *in* Report of Activities 2003, Manitoba Industry, Economic Development and Mines, Manitoba Geological Survey, p. 39–49, URL <https://manitoba.ca/iem/geo/field/roa03pdfs/GS-06.pdf> [December 2022].

Beaumont-Smith, C.J. and Böhm, C.O. 2004: Structural analysis of the Lynn Lake greenstone belt, Manitoba (NTS 64C10, 11, 12, 14, 15 and 16); *in* Report of Activities 2004, Manitoba Industry, Economic Development and Mines, Manitoba Geological Survey, p. 55–68, URL <https://manitoba.ca/iem/geo/field/roa04pdfs/GS-06.pdf> [December 2022].

Beaumont-Smith, C.J., Lentz, D.R. and Tweed, E.A. 2000: Structural analysis and gold metallogeny of the Farley Lake gold deposit, Lynn Lake greenstone belt (NTS 64C/16); *in* Report of Activities 2000, Manitoba Industry, Trade and Mines, Manitoba Geological Survey, p. 73–81, URL <https://manitoba.ca/iem/geo/field/roa00pdfs/00gs-15.pdf> [December 2022].

Beaumont-Smith, C.J., Machado, N. and Peck, D.C. 2006: New uranium-lead geochronology results from the Lynn Lake greenstone belt, Manitoba (NTS 64C11–16); Manitoba Science, Technology, Energy and Mines, Manitoba Geological Survey, Geoscientific Paper GP2006-1, 11 p., URL <https://manitoba.ca/iem/info/libmin/GP2006-1.pdf> [December 2022].

Blackburn, C.E., Johns, G.W., Ayer, J. and Davis, D.W. 1991: Wabigoon Subprovince; in Geology of Ontario, P.C. Thurston, H.R. Williams, R.H. Sutcliffe and G.M. Stott (ed.), Ontario Geological Survey, Special Volume 4, Part 1, p. 303–381.

Bleeker, W. 1990: New structural-metamorphic constraints on early Proterozoic oblique collision along the Thompson nickel belt, Manitoba, Canada; *in* The Early Proterozoic Trans-Hudson Orogen of North America, J.F. Lewry and M.R. Stauffer (ed.), Geological Association of Canada, Special Paper 37, p. 57–73.

Blevin, P.L. 2004: Redox and compositional parameters for interpreting the granitoid metallogeny of eastern Australia: implications for gold-rich ore systems; Resource Geology v. 54, p. 241–252, URL <https://doi.org/10.1111/j.1751-3928.2004.tb00205.x>.

Blevin, P.L. and Chappell, B.W. 1995: Chemistry, origin and evolution of mineralized granitoids in the Lachlan fold belt, Australia: the metallogeny of I- and S-type granites; Economic Geology, v. 90, p. 1604–1619, URL <https://doi.org/10.2113/gsecongeo.90.6.1604>.

Böhm, C.O., Heaman, L.M. and Corkery, M.T. 1999: Archean crustal evolution of the northwestern Superior craton margin: U-Pb zircon results from the Split Lake Block; Canadian Journal of Earth Sciences, v. 36, p. 1973–1987, URL <https://doi.org/10.1139/e99-088>.

Böhm, C.O., Zwanzig, H.V. and Creaser, R.A. 2007: Sm-Nd isotope technique as an exploration tool: delineating the northern extension of the Thompson Nickel Belt, Manitoba, Canada; Economic Geology, v. 102, p. 1217–1231, URL <https://doi.org/10.2113/gsecongeo.102.7.1217>.

Böhm, C.O., Heaman, L.M., Creaser, R.A. and Corkery, M.T. 2000: Discovery of pre-3.5 Ga exotic crust at the northwestern Superior Province margin, Manitoba; Geology, v. 28, p. 75–78, URL <https://doi.org/10.1130/0091-7613(2000)28<75:DOPGEC>2.0.CO;2>.

Böhm, C.O., Heaman, L.M., Stern, R.A, Corkery, M.T. and Creaser, R.A. 2003: Nature of assean lake ancient crust, Manitoba: a combined SHRIMP–ID-TIMS U–Pb geochronology and Sm–Nd isotope study; Precambrian Research, v. 126, p. 55–94, URL <https://doi.org/10.1016/S0301-9268(03)00127-X>.

Böhm, C.O., Hartlaub, R.P., Heaman, L.M., Cates, N., Guitreau, M., Bourdon, B., Roth, A.S.G, Mozsis, S.J. and Blichert-Toft, J. 2018: The Assean Lake complex: ancient crust at the northwestern margin of the Superior craton, Manitoba, Canada; Chapter 28 *in* Earth's Oldest Rocks (2nd edition), M.J. Van Kranendonk, V.C. Bennett and J.E. Hoffmann (ed.), Elsevier, Amsterdam, Netherlands, p. 703–722.

Bonin, B., Janoušek, V. and Moyen, J.-F. 2020: Chemical variation, modal composition and classification of granitoids; *in* Post-Archean Granitic Rocks: Contrasting Petrogenetic Processes and Tectonic Environments, V. Janoušek, B. Bonin, W.J. Collins, F. Farina and P. Bowden (ed.), Geological Society of London, London, United Kingdom, Special Publications, v. 491, p. 9–51, URL <https://doi.org/10.1144/SP491-2019-13>.

Bowen, N.L. 1928: The evolution of the igneous rocks; Princeton University Press, Princeton, New Jersey, 332 p.

Boyle, R.W. 1979: The geochemistry of gold and its deposits (together with a chapter on geochemical prospecting for the element); Geological Survey of Canada, Bulletin 280, 584 p.

Breaks, F.W. 1991: English River Subprovince; in Geology of Ontario, P.C. Thurston, H.R. Williams, R.H. Sutcliffe and G.M. Stott (ed.), Ontario Geological Survey, Special Volume 4, Part 1, p. 239–277.

Breaks, F.W. and Moore, J.M., Jr. 1992: The Ghost Lake batholith, Superior province of northwestern Ontario: a fertile, S-type peraluminous granite – rare element pegmatite system; Canadian Mineralogist, v. 30, p. 835–875.

Brown, M. 2010: Melting of the continental crust during orogenesis: the thermal, rheological, and compositional consequences of melt transport from lower to upper continental crust; Canadian Journal of Earth Sciences, v. 47, p. 655–694, URL <https://doi.org/10.1139/E09-057>.

Bruand, E., Fowler, M., Storey, C., Laurent, O., Antoine, C., Guitreau, M., Heilimo, E. and Nebel, O. 2020: Accessory mineral constraints on crustal evolution: elemental fingerprints for magma discrimination; Geochemical Perspectives Letters, v. 13, p. 7–12, URL <http://doi.org/10.7185/geochemlet.2006>.

Burnham, O.M., Halden, N., Layton-Matthews, D., Lesher, C.M., Liwanag, J., Heaman, L., Hulbert, L., Machado, N., Michalak, D., Pacey, M., Peck, D.C., Potrel, A., Theyer, P., Toope, K. and Zwanzig, H. 2009: CAMIRO project 97E-02, Thompson Nickel Belt: final report, March 2002, revised and updated 2003; Manitoba Science, Technology, Energy and Mines, Manitoba Geological Survey, Open File OF2008-11, 434 p. plus appendices and GIS shape files for use with ArcInfo®, URL <https://manitoba.ca/iem/info/libmin/OF2008-11.zip> [December 2022].

Card, K.D. and Ciesielski, A. 1986: Subdivisions of the Superior province of the Canadian shield; Geoscience Canada, v. 13, p. 5–13.

Černý, P., Trueman, D.L., Ziehlke, D.V., Goad, B.E. and Paul, B.J. 1981: The Cat Lake-Winnipeg River and the Wekusko Lake pegmatite fields, Manitoba; Manitoba Department of Energy and Mines, Mineral Resources Division, Economic Geology Report ER80-1, 216 p., URL <https://manitoba.ca/iem/info/libmin/ER80-1.zip> [December 2022].

Černý, P. and Ercit, T.S. 2005: The classification of granitic pegmatites revisited; The Canadian Mineralogist, v. 43, p. 2005–2026, URL <http://doi.org/10.2113/gscanmin.43.6.2005>.

Chakhmouradian, A.R., Mumin, A.H., Demény, A. and Elliott, B. 2008: Postorogenic carbonatites at Eden Lake, Trans-Hudson orogen (northern Manitoba, Canada): geological setting, mineralogy and geochemistry; Lithos, v. 103, p. 503–526, URL <https://doi.org/10.1016/j.lithos.2007.11.004>.

Chappell, B.W. and White, A.J.R. 1974: Two contrasting granite types; Pacific Geology, v. 8, p. 173–174.

Chappell, B.W. and White, A.J.R. 1992: I- and S-type granites in the Lachlan fold belt; Earth and Environmental Science Transactions of The Royal Society of Edinburgh, v. 83, p. 1–26.

Chappell, B.W. and White, A.J.R. 2001: Two contrasting granite types: 25 years later; Australian Journal of Earth Sciences, v. 48, p. 489–499, URL <https://doi.org/10.1046/j.1440-0952.2001.00882.x>.

Chappell, B.W., White, A.J.R., Williams, I.S. and Wyborn, D. 2004: Low- and high-temperature granites; Earth and Environmental Science Transactions of The Royal Society of Edinburgh, v. 95, p. 125–140, URL <https://doi.org/10.1017/S0263593300000973>.

Clarke, D.B. 1992: Granitoid rocks; Chapman & Hall, London, United Kingdom, 284 p.

Clarke, D.B. 2019: The origins of strongly peraluminous granitoid rocks; The Canadian Mineralogist, v. 57, p. 529–550, URL <https://doi.org/10.3749/canmin.1800075>.

Clemens, J.D. 2018: Granitic magmas with I-type affinities, from mainly metasedimentary sources: the Harcourt batholith of southeastern Australia; Contributions to Mineralogy and Petrology, v. 173, art. 93, URL <https://doi.org/10.1007/s00410-018-1520-z>.

Clemens, J.D. and Stevens, G. 2021: S- to I- to A-type magmatic cycles in granitic terranes are not globally recurring progressions. The cases of the Cape Granite suite of southern Africa and central Victoria in southeastern Australia; South African Journal of Geology, v. 124, p. 565–574, URL <https://doi.org/10.25131/sajg.124.0007>.

Clemens, J.D., Stevens, G. and Bryan, S.E. 2020: Conditions during the formation of granitic magmas by crustal melting – hot or cold; drenched, damp or dry?; Earth-Science Reviews, v. 200, art. 102982, URL <https://doi.org/10.1016/j.earscirev.2019.102982>.

Condie, K.C. 1994: Greenstones through time; Chapter 3 *in* Archean Crustal Evolution, K.C. Condie (ed.), Elsevier Ltd., Amsterdam, Netherlands, Developments in Precambrian Geology, v. 11, p. 85–120, URL <https://doi.org/10.1016/S0166-2635(08)70221-4>.

Corfu, F. 1988: Differential response of U-Pb systems in coexisting accessory minerals, Winnipeg River subprovince, Canadian shield: implications for Archean crustal growth and stabilization; Contributions to Mineralogy and Petrology, v. 98, p. 312–325.

Corfu, F. 1996: Multistage zircon and titanite growth and inheritance in an Archean gneiss complex, Winnipeg River subprovince, Ontario; Earth and Planetary Science Letters, v. 141, p. 175–186, URL <https://doi.org/10.1016/0012-821X(96)00064-7>.

Corfu, F. and Davis, D.W. 1992: A U-Pb geochronological framework for the western Superior province, Ontario; *in* Geology of Ontario, P.C. Thurston, H.R. Williams, R.H. Sutcliffe and G.M. Stott (ed.), Ontario Geological Survey, Special Volume 4, part 2, p. 1335–1346.

Corfu, F., Stott, G.M. and Breaks, F.W. 1995: U-Pb geochronology and evolution of the English River subprovince, an Archean low P-high T metasedimentary belt in the Superior Province; Tectonics, v. 14, p. 1220–1233, URL <https://doi.org/10.1029/95TC01452>.

Corkery, M.T. 1985: Geology of the lower Nelson River project area; Manitoba Energy and Mines, Geological Services, Geological Report GR82-1, 66 p., URL <https://manitoba.ca/iem/info/libmin/GR82-1.zip> [December 2022].

Corkery, M.T., Böhm, C.O. and Heaman, L.M. 2000: Assean Lake ancient crust: an update; *in* Report of Activities 2000, Manitoba Industry, Trade and Mines, Manitoba Geological Survey, p. 155–160, URL <https://manitoba.ca/iem/geo/field/roa00pdfs/00gs-25.pdf> [December 2022].

Corrigan, D. 2012: Paleoproterozoic crustal evolution and tectonic processes: insights from the LITHOPROBE program in the Trans-Hudson orogen, Canada; Chapter 4 *in* Tectonic styles in Canada: the LITHOPROBE perspective, J.A. Percival, F.A. Cook and R.M. Clowes (ed.), Geological Association of Canada, Special Paper 49, p. 237–284.

Corrigan, D., Galley, A.G. and Pehrsson, S. 2007: Tectonic evolution and metallogeny of the southwestern Trans-Hudson orogen; *in* Mineral Deposits of Canada: a synthesis of major deposit-types, district metallogeny, the evolution of geological provinces, and exploration methods, W.D. Goodfellow (ed.), Geological Association of Canada, Mineral Deposits Division, Special Publication 5, p. 881–902.

Corrigan, D., Pehrsson, S., Wodicka, N. and de Kemp, E. 2009: The Palaeoproterozoic Trans-Hudson progen: a prototype of modern accretionary processes; *in* Ancient Orogens and Modern Analogues, J.B. Murphy, J.D. Keppie and A.J. Hynes (ed.), Geological Society of London, London, United Kingdom, Special Publications, v. 327, p. 457–479.

Couëslan, C.G. and Pattison, D.R.M. 2012: Low-pressure regional amphibolite-facies to granulite-facies metamorphism of the Paleoproterozoic Thompson nickel belt, Manitoba; Canadian Journal of Earth Sciences, v. 49, p. 1117–1153, URL <https://doi.org/10.1139/e2012-029>.

Couëslan, C.G, Pattison, D.R.M. and Dufrane, S.A. 2013: Paleoproterozoic metamorphic and deformation history of the Thompson nickel belt, Superior boundary zone, Canada, from in situ U–Pb analysis of monazite; Precambrian Research, v. 237, p. 13–35, URL <http://doi.org/10.1016/j.precamres.2013.06.009>.

Cuney, M. 2014: Felsic magmatism and uranium deposits; Bulletin de la Société Géologique de France, v. 185, p. 75–92, URL <https://doi.org/10.2113/gssgfbull.185.2.75>.

Defant, M.J. and Drummond, M.S. 1990: Derivation of some modern arc magmas by melting of young subducted lithosphere; Nature, v. 347, p. 662–665.

DePaolo, D.J. 1981: Neodymium isotopes in the Colorado front range and crust-mantle evolution in the Proterozoic; Nature, v. 291, p. 193–196.

DePaolo, D.J. 1988: Neodymium isotope geochemistry: an introduction; *S*pringer, Berlin, Germany, 187 p.

Devoir, A., Bloch, E. and Müntener, O. 2021: Residence time of igneous garnet in Si-rich magmatic systems: insights from diffusion modeling of major and trace elements; Earth and Planetary Science Letters, v. 560, art. 116771, URL <https://doi.org/10.1016/j.epsl.2021.116771>.

Dou, J.-Z., Zhang, H.-F., Tong, Y., Wang, F., Chen, F.-K. and Li, S.-R. 2018: Application of geothermo-barometers to Mesozoic granitoids in the Jiaodong Peninsula, eastern China: criteria for selecting methods of pressure estimation and implications for crustal exhumation; Journal of Asian Earth Sciences, v. 160, p. 271–286, URL <https://doi.org/10.1016/j.jseaes.2018.01.019>.

Drayson, D. 2016: Geochemical comparison between the Tin Lake and Osis Lake pegmatitic granites, Bird River greenstone belt, southeastern Manitoba; B.Sc. thesis, University of Manitoba, Winnipeg, Manitoba, 33 p.

Drummond, M.S. and Defant, M.J. 1990: A model for trondhjemite-tonalite-dacite genesis and crustal growth via slab melting: Archaean to modern comparison; Journal of Geophysical Research: Solid Earth, v. 95, p. 21503–21521, URL <https://doi.org/10.1029/JB095iB13p21503>.

Duan, M., Niu, Y., Sun, P., Chen, S., Kong, J., Li, J., Zhang, Y., Hu, Y. and Shao, F. 2022: A simple and robust method for calculating temperatures of granitoid magmas; Mineralogy and Petrology, v. 116, p. 93–103, URL <https://doi.org/10.1007/s00710-021-00769-5>.

Duguet, M., Lin, S., Davis, D.W., Corkery, M.T. and McDonald, J. 2009: Long-lived transpression in the Archean Bird River greenstone belt, western Superior province, southeastern Manitoba; Precambrian Research, v. 174, p. 381–407, URL <https://doi.org/10.1016/j.precamres.2009.09.001>.

Eby, G.N. 1990: The A-type granitoids: a review of their occurrence and chemical characteristics and speculations on their petrogenesis; Lithos, v. 26, p. 115–134, URL <https://doi.org/10.1016/0024-4937(90)90043-Z>.

Foley, S., Tiepolo, M. and Vannucci, R. 2002: Growth of early continental crust controlled by melting of amphibolite in subduction zones; Nature, v. 417, p. 837–840, URL <http://doi.org/10.1038/nature00799>.

Fralick, P., Purdon, R.H. and Davis, D.W. 2006: Neoarchean trans-subprovince sediment transport in southwestern Superior Province: sedimentological, geochemical, and geochronological evidence; Canadian Journal of Earth Sciences, v. 43, p. 1055–1070, URL <https://doi.org/10.1139/e06-059>.

Frisch, W., Meschede, M. and Blakey, R. 2011: Plate tectonics: continental drift and mountain building; Springer, Heidelberg, Germany, 212 p.

Frost, B.R., Barnes, C.G., Collins, W.J., Arculus, R.J., Ellis, D.J. and Frost, C.D. 2001: A geochemical classification for granitic rocks; Journal of Petrology, v. 42, p. 2033–2048, URL <https://doi.org/10.1093/petrology/42.11.2033>.

Frost, C.D. and Da Prat, F.A. 2021: Petrogenetic and tectonic interpretation of strongly peraluminous granitic rocks and their significance in the Archean rock record; American Mineralogist, v. 106, p. 1195–1208, URL <https://doi.org/10.2138/am-2022-8001> [June 2022].

Gilbert, H.P. 1993: Geology of the Barrington Lake-Melvin Lake-Fraser Lake area; Manitoba Energy and Mines, Geological Services, Geological Report GR87-3, 97 p., URL <https://manitoba.ca/iem/info/libmin/GR87-3.zip> [December 2022].

Gilbert, H.P., Syme, E.C. and Zwanzig, H.V. 1980: Geology of the metavolcanic and volcaniclastic metasedimentary rocks in the Lynn Lake area; Manitoba Department of Energy and Mines, Mineral Resources Division, Geological Paper GP80-1, 118 p., URL <https://manitoba.ca/iem/info/libmin/GP80-1.zip> [December 2022].

Gilbert, H.P., Davis, D.W., Duguet, M., Kremer, P.D., Mealin, C.A. and MacDonald, J. 2008: Geology of the Bird River belt, southeastern Manitoba (parts of NTS 52L5, 6); Manitoba Science, Technology, Energy and Mines, Manitoba Geological Survey, Geoscientific Map MAP2008-1, scale 1:50 000, URL <https://manitoba.ca/iem/info/libmin/MAP2008-1.zip> [December 2022].

Gilbert, H.P., Houlé, M.G., Yang, X.M., Scoates, J.S., Scoates, R.F.J., Mealin, C.A., Bécu, V., McNicoll, V.J. and Galeschuk, C.R. 2013: Mafic and ultramafic intrusive rocks and associated Ni-Cu-(PGE) and Cr-(PGE) mineralization in the Bird River greenstone belt, southeast Manitoba; Geological Association of Canada–Mineralogical Association of Canada, Joint Annual Meeting, May 22–24, 2013, Winnipeg, Manitoba, Field Trip Guidebook FT-C2, Manitoba Innovation, Energy and Mines, Manitoba Geological Survey, Open File OF2013-7, 51 p., URL <https://manitoba.ca/iem/info/libmin/gacmac/OF2013-7_FT-C2.pdf> [December 2022].

Goad, B.E. and Černý, P. 1981: Peraluminous pegmatitic granites and their pegmatite aureoles in the Winnipeg River district, southeastern Manitoba; Canadian Mineralogist, v. 19, p. 177–194.

Goldstein, S.L., O'Nions, R.K. and Hamilton, P.J. 1984: A Sm-Nd isotopic study of atmospheric dusts and particulates from major river systems; Earth and Planetary Science Letters, v. 70, no. 2, p. 221–236, URL <https://doi.org/10.1016/0012-821X(84)90007-4>.

Guo, J., Wu, K., Seltmann, R., Zhang, R., Ling, M., Li, C. and Sun, W. 2022: Unraveling the link between mantle upwelling and formation of Sn-bearing granitic rocks in the world-class Dachang tin district, south China; Geological Society of America Bulletin, v. 134, p. 1043–1064, URL <https://doi.org/10.1130/B35492.1>.

Grasso, V.G. 1968: The TiO_2 frequency in volcanic rocks; Geologische Rundschau, v. 57, p. 930–935.

Hacker, B.R., Kelemen, P.B. and Behn, M.D. 2011: Differentiation of the continental crust by relamination; Earth and Planetary Science Letters, v. 307, p. 501–516, URL <https://doi.org/10.1016/j.epsl.2011.05.024>.

Halden, N.M. and Fryer, B.J. 1999: Geochemical characteristics of the Eden Lake Complex: evidence for anorogenic magmatism in the Trans-Hudson Orogen; Canadian Journal of Earth Sciences, v. 36, p. 91–103, URL <https://doi.org/10.1139/e98-08>.

Halden, N.M., Mandziuk, W.S., Young, J., Clark, G.S. and Yang, P. 2007: LAM-ICP-MS zircon dating of the Falcon Lake intrusive complex and Caddy Lake granite, southeastern Manitoba, Canada; Proceedings of the Geologists' Association, v. 118, p. 25–35, URL <https://doi.org/10.1016/S0016-7878(07)80044-7>.

Halla, J. 2018: Highlights on geochemical changes in Archaean granitoids and their implications for early Earth geodynamics; Geosciences, v. 8, art. 353, URL <https://doi.org/10.3390/geosciences8090353>.

Halla, J., Whitehouse, M.J., Ahmad, T. and Bagai, Z. 2017: Archaean granitoids: an overview and significance from a tectonic perspective; *in* Crust–mantle interactions and granitoid diversification: insights from Archaean cratons, J. Halla, M.J. Whitehouse, T. Ahmad and Z. Bagai (ed.), Geological Society of London, London, United Kingdom, Special Publications, v. 449, p. 1–18, URL <https://doi.org/10.1144/SP449.10>.

Hanson, G.N. 1978: The application of trace elements to the petrogenesis of igneous rocks of granitic composition; Earth and Planetary Science Letters, v. 38, p. 26–43, URL <https://doi.org/10.1016/0012-821X(78)90124-3>.

Hawkesworth, C.J. and Kemp, A.I.S. 2006: Evolution of the continental crust; Nature, v. 443, p. 811–817.

Heaman, L.M., Peck, D. and Toope, K. 2009: Timing and geochemistry of 1.88 Ga Molson igneous events, Manitoba: insights into the formation of a craton-scale magmatic and metallogenic province; Precambrian Research, v. 172, p. 143–162, URL <https://doi.org/10.1016/j.precamres.2009.03.015>.

Hildebrand, R.S., Whalen, J.B. and Bowring, S.A. 2018: Resolving the crustal composition paradox by 3.8 billion years of slab failure magmatism and collisional recycling of continental crust; Tectonophysics, v. 734–735, p. 69–88, URL <https://doi.org/10.1016/j.tecto.2018.04.001>.

Hoffman, P.H. 1988: United plates of America, the birth of a craton: early Proterozoic assembly and growth of Laurentia; Annual Review of Earth and Planetary Sciences, v. 16, p. 543–603, URL <https://doi.org/10.1146/annurev.ea.16.050188.002551>.

Holtz, F., Johannes, W., Tamic, N. and Behrens, H. 2001: Maximum and minimum water contents of granitic melts generated in the crust: a reevaluation and implications; Lithos, v. 56, p. 1–14, URL <https://doi.org/10.1016/S0024-4937(00)00056-6>.

Houlé, M.G., McNicoll, V.J., Bécu, V., Yang, X.M. and Gilbert, H.P. 2013: New age for the Mayville intrusion: implication for a large mafic-ultramafic event in the Bird River greenstone belt, southeastern Manitoba (abstract); Geological Association of Canada–Mineralogical Association of Canada, Joint Annual Meeting, Winnipeg, Manitoba, May 22–24, 2013, Program with Abstracts, p. 115.

Hrabi, R.B. and Cruden, A.R. 2006: Structure of the Archean English River subprovince: implications for the tectonic evolution of the western Superior province, Canada; Canadian Journal of Earth Sciences, v. 43, p. 947–966, URL <https://doi.org/10.1139/e06-023>.

Irvine, T.N. and Baragar, W.R.A. 1971: A guide to the chemical classification of the common volcanic rocks; Canadian Journal of Earth Sciences, v. 8, p. 523–548, URL <https://doi.org/10.1139/e71-055>.

Ishihara, S. 1977: The magnetite-series and ilmenite-series granitic rocks; Mining Geology, v. 27, p. 293–305, URL <https://doi.org/10.11456/shigenchishitsu1951.27.293>.

Ishihara, S. 1981: The granitoid series and mineralization; Economic Geology, 75th anniversary volume (1905-1980), p. 458–484.

Ishihara S. 2004: The redox state of granitoids relative to tectonic setting and Earth history: the magnetite-ilmenite series 30 years later; Earth and Environmental Science Transactions of the Royal Society of Edinburgh, v. 95, p. 23–33, URL <https://doi.org/10.1017/S0263593300000894>.

Itiga, Z., Bonin, B., Bardintzeff, J.-M., Wandji, P., Belnoun, R.N.N., Mbassa, B.J., Wotchoko, P., Seuwui, D.T., Nfomou, N. and Bellon, H., 2019: The pan-African post-collision Hosséré Mana plutonic complex and associated Gapi stock (western Cameroon Domain, Cameroon): petrology, mineralogy and geochemistry; Journal of African Earth Sciences, v. 149, p. 398–425, URL <https://doi.org/10.1016/j.jafrearsci.2018.08.019>.

Jacob, J.-B., Moyen, J.-F., Fiannacca, P., Laurent, O., Bachmann, O., Janoušek, V., Farina, F. and Villaros, A. 2021: Crustal melting vs. fractionation of basaltic magmas: part 2, attempting to quantify mantle and crustal contributions in granitoids; Lithos, v. 402–403, art. 106292, URL <https://doi.org/10.1016/j.lithos.2021.106292>.

Janoušek, V. 1999: Interpreting Sr-Nd isotopic data from magmatic and metamorphic rocks: numerical recipes and exercises; Czech Geological Survey, p. 1–15.

Jefferson, C.W., Thomas, D.J., Gandhi, S.S., Ramaekers, P., Delaney, G., Brisbin, D., Cutts, C., Quirt, D., Portella, P. and Olson, R.A. 2007: Unconformity-associated uranium deposits of the Athabasca Basin, Saskatchewan and Alberta; *in* Mineral Deposits of Canada: a synthesis of major deposit-types, district metallogeny, the evolution of geological provinces, and exploration methods, W.D. Goodfellow (ed.), Geological Association of Canada, Mineral Deposits Division, Special Publication 5, p. 273–305.

Jung, S. and Pfänder, J.A. 2007: Source composition and melting temperatures of orogenic granitoids: constraints from CaO/Na_2O, Al_2O_3/TiO_2 and accessory mineral saturation thermometry; European Journal of Mineralogy, v. 19, p. 859–870, URL <https://doi.org/10.1127/0935-1221/2007/0019-1774>.

Kepezhinskas, P., Berdnikov, N., Kepezhinskas, N. and Konovalova, N. 2022: Adakites, high-Nb basalts and copper–gold deposits in magmatic arcs and collisional orogens: an overview; Geosciences, v. 12, art. 29; URL <https://doi.org/10.3390/geosciences12010029>.

Konopásek, J., Janoušek, V., Oyhantçabal, P., Sláma, J. and Ulrich, S. 2018: Did the circum-Rodinia subduction trigger the Neoproterozoic rifting along the Congo–Kalahari craton margin?; International Journal of Earth Sciences, v. 107, p. 1859–1894.

Kremer, P.D. 2008: Geological investigations of the Pukatawakan Bay belt, Southern Indian Lake, Manitoba (part of NTS 64G2); *in* Report of Activities 2008, Manitoba Science, Technology, Energy and Mines, Manitoba Geological Survey, p. 87–98, URL <https://manitoba.ca/iem/geo/field/roa08pdfs/GS-8.pdf> [December 2022].

Kremer, P.D. and Martins, T. 2014: Bedrock geology of the Northern Indian Lake area, Manitoba (parts of NTS 64H3, 5, 6); *in* Report of Activities 2014, Manitoba Mineral Resources, Manitoba Geological Survey, p. 131–139, URL <https://manitoba.ca/iem/geo/field/roa14pdfs/GS-11.pdf> [December 2022].

Kretschmar, U. and McBride, D. 2015: The metallogeny of lode gold deposits: a syngenetic perspective; Elsevier Inc., Amsterdam, Netherlands, 350 p., URL <https://doi.org/10.1016/C2014-0-03103-6>.

Kuiper, Y.D., Lin, S. and Böhm, C.O. 2011: Himalayan-type escape tectonics along the Superior boundary zone in Manitoba, Canada; Precambrian Research, v. 187, p. 248–262, URL <https://doi.org/10.1016/j.precamres.2011.03.009>.

Kushner, D.S. 2016: Petrographic and geochemical analysis of a granitic unit within the Inconnu Batholith, southeastern Manitoba; B.Sc. thesis, University of Manitoba, Winnipeg, Manitoba, 32 p.

Lang, J.R. and Baker, T. 2001: Intrusion-related gold systems: the present level of understanding; Mineralium Deposita, v. 36, p. 477–489, URL <https://doi.org/10.1007/s001260100184>.

Laurent, O., Björnsen, J., Wotzlaw, J.-F., Bretscher, S., Silva, M.P., Moyen, J.-F., Ulmer, P. and Bachmann, O. 2020: Earth's earliest granitoids are crystal-rich magma reservoirs tapped by silicic eruptions; Nature Geoscience, v. 13, p. 163–169.

Lawley, C.J.M., Yang, X.M., Selby, D., Davis, W., Zhang, S., Petts, D.C. and Jackson, S.E. 2020b: Sedimentary basin controls on orogenic gold deposits: new constraints from U-Pb detrital zircon and Re-Os sulphide geochronology, Lynn Lake greenstone belt, Canada; Ore Geology Reviews, v. 126, art. 103790, URL <https://doi.org/10.1016/j.oregeorev.2020.103790>.

Lawley, C.J.M., Selby, D., Davis, W.J., Yang, E., Zhang, S., Jackson, S.E., Petts, D.C., O'Connor, A.R. and Schneider, D.A., 2020a: Paleoproterozoic gold and its tectonic triggers and traps: implications from Re-Os sulphide and U-Pb detrital zircon geochronology, Lynn Lake, Manitoba; *in* Targeted geoscience initiative 5: contributions to the understanding of Canadian gold dystems, P. Mercier-Langevin, C.J.M. Lawley and S. Castonguay (ed.), Geological Survey of Canada, Open File 8712, p. 211–222, URL <https://doi.org/10.4095/326033>.

Le Bas, M.J., Le Maitre, R.W., Streckeisen, A. and Zanettin, B. 1986: A chemical classification of volcanic rocks based on the total alkali silica diagram; Journal of Petrology, v. 27, p. 745–750, URL <https://doi.org/10.1093/petrology/27.3.745>.

Lee, C.-T.A., Luffi, P. and Chin, E.J. 2011: Building and destroying continental mantle; Annual Review of Earth and Planetary Sciences, v. 39, p. 59–90, URL <https://doi.org/10.1146/annurev-earth-040610-133505>.

Le Maitre, R.W., Streckeisen, A., Zanettin, B., Le Bas, M.J., Bonin, B., Bateman, P., Bellieni, G., Dudek, A., Efremova, S., Keller, J., Lameyre, J., Sabine, P.A., Schmid, R., Sorensen, H. and Woolley, A.R. 2002: Igneous rocks: a classification and glossary of terms; Recommendations of the International Union of Geological Sciences Subcommission on the Systematics of Igneous Rocks, Cambridge University Press, Cambridge, United Kingdom, 236 p.

Lemkow, D.R., Sanborn-Barrie, M., Bailes, A.H., Percival, J.A., Rogers, N., Skulski, T., Anderson, S.D., Tomlinson, K.Y., McNicoll, V., Parker, J.R., Whalen, J.B., Hollings, P. and Young, M. 2006: GIS compilation of geology and tectonostratigraphic assemblages, western Uchi Subprovince, western Superior Province, Ontario and Manitoba; Geological Survey of Canada, Open File 5269, Manitoba Science, Technology, Energy and Mines, Manitoba Geological Survey, Open File OF2006-30, Ontario Geological Survey, Miscellaneous Release - Data 203, CD-ROM, URL <https://doi.org/10.4095/222244>.

Lenton, P.G. and Corkery, M.T. 1981: The lower Churchill River project (interim report); Manitoba Department of Energy and Mines, Mineral Resources Division, Open File Report OF81-3, 23 p., URL <https://manitoba.ca/iem/info/libmin/OF81-3.pdf> [December 2022].

Lewry, J.F. and Collerson, K.D. 1990: The Trans-Hudson orogen: extent, subdivisions and problems; *in* The Early Proterozoic Trans-Hudson Orogen of North America, J.F. Lewry and M.R. Stauffer (ed.), Geological Association of Canada, Special Paper 37, p. 1–14.

Liew, T.C. and Hofmann, A.W. 1988: Precambrian crustal components, plutonic associations, plate environment of the Hercynian fold belt of central Europe: indications from a Nd and Sr isotopic study; Contributions to Mineralogy and Petrology, v. 98, p. 129–138.

Lightfoot, P.C., Stewart, R., Gribbin, G. and Mooney, S.J. 2017: Relative contribution of magmatic and post-magmatic processes in the genesis of the Thompson mine Ni-Co sulfide ores, Manitoba, Canada; Ore Geology Reviews, v. 83, p. 258–286, URL <https://doi.org/10.1016/j.oregeorev.2016.12.017>.

Lin, S. and Beakhouse, G.P. 2013: Synchronous vertical and horizontal tectonism at late stages of Archean cratonization and genesis of Hemlo gold deposit, Superior craton, Ontario, Canada; Geology, v. 41, p. 359–362, URL <https://doi.org/10.1130/G33887.1>.

Linnen, R.L. and Keppler, H. 2002: Melt composition control of Zr/Hf fractionation in magmatic processes; Geochimica et Cosmochimica Acta, v. 66, 3293–3301, URL <https://doi.org/10.1016/S0016-7037(02)00924-9>.

Macek, J.J. and Bleeker, W. 1989: Thompson nickel belt project - Pipe Pit mine, Setting and Ospwagan Lakes; *in* Report of Field Activities 1989, Manitoba Energy and Mines, Minerals Division, p. 73–87, URL <https://manitoba.ca/iem/geo/field/rfa89.zip> [December 2022].

Machado, N., Gapais, D., Potrel, A., Gauthier, G. and Hallot, E. 2011a: Chronology of transpression, magmatism, and sedimentation in the Thompson nickel belt (Manitoba, Canada) and timing of Trans-Hudson orogen – Superior province collision; Canadian Journal of Earth Sciences, v. 48, p. 295–324, URL <https://doi.org/10.1139/E10-040>.

Machado, N., Heaman, L.M., Krogh, T.E., Weber, W. and Corkery, M.T. 2011b: Timing of Paleoproterozoic granitoid magmatism along the northwestern Superior province margin: implications for the tectonic evolution of the Thompson nickel belt; Canadian Journal of Earth Sciences, v. 48, p. 325–346, URL <https://doi.org/10.1139/E10-079>.

MacHattie, T.G. 2001: Petrogenesis of the Wathaman batholith and La Ronge domain plutons in the Reindeer Lake area, Trans-Hudson orogen, Saskatchewan; M.Sc. thesis, Memorial University of Newfoundland, St. John's, Newfoundland, 229 p.

Makhluf, A.R., Newton, R.C. and Manning, C.E. 2017: Experimental determination of liquidus H_2O contents of haplogranite at deep-crustal conditions; Contributions to Mineralogy and Petrology, v. 172, art. 77, URL <https://doi.org/10.1007/s00410-017-1392-7>.

Mandziuk, W.S., Brisbin, W.C. and Scoates, R.F.J. 1989: Igneous structure in the Falcon Lake igneous complex, southeastern Manitoba; The Canadian Mineralogist, v. 27, p. 81–92.

Maniar, P.D. and Piccoli, P.M. 1989: Tectonic discrimination of granitoids; Geological Society of America Bulletin, v. 101, p. 635–643, URL <https://doi.org/10.1130/0016-7606(1989)101%3C0635:TDOG%3E2.3.CO;2>.

Manitoba Agriculture and Resource Development 2021: Lynn Lake, Manitoba (NTS 64C14); Manitoba Agriculture and Resource Development, Manitoba Geological Survey, Lynn Lake Bedrock Compilation Map 64C14, scale 1:50 000, URL <https://manitoba.ca/iem/info/libmin/lynn_lake_compilation_2021.zip> [October 2021].

Manitoba Energy and Mines 1986: Granville Lake, NTS 64C; Manitoba Energy and Mines, Geological Services, Bedrock Geology Compilation Map Series, Map 63G, scale 1:250 000, URL <https://manitoba.ca/iem/info/libmin/bgcms/bgcms_granville_lake.pdf> [December 2022].

Manitoba Geological Survey 2006: Manitoba geochronology database; Manitoba Science, Technology, Energy and Mines, Manitoba Geological Survey, Open File OF2006-34, digital web release, v. 1.51, December 2006, URL <http://manitoba.ca/iem/info/libmin/OF2006-34.zip> [October 2014].

Manitoba Geological Survey 2018: Geological map of Manitoba at 1:1 000 000 scale; Manitoba Growth, Enterprise and Trade, Manitoba Geological Survey, URL <https://manitoba.ca/iem/geo/gis/index.html> [January 2022].

Martin, H., Moyen, J.-F. and Rapp, R. 2010: The sanukitoid series: magmatism at the Archaean–Proterozoic transition; Earth and Environmental Science Transactions of The Royal Society of Edinburgh, v. 100, Special Issue 1-2, p. 15–33, URL <https://doi.org/10.1017/S1755691009016120>.

Martin, H., Smithies, R.H., Rapp, R., Moyen, J.-F. and Champion, D. 2005: An overview of adakite, tonalite–trondhjemite–granodiorite (TTG), and sanukitoid: relationships and some implications for crustal evolution; Lithos, v. 79, p. 1–24, URL <https://doi.org/10.1016/j.lithos.2004.04.048>.

Martins, T. 2015: Geological mapping in the northern basin of Southern Indian Lake, north-central Manitoba (parts of NTS 64G7, 8, 9, 10); *in* Report of Activities 2015, Manitoba Mineral Resources, Manitoba Geological Survey, p. 79–88, URL <https://manitoba.ca/iem/geo/field/roa15pdfs/GS-6.pdf> [December 2022].

Martins, T. and Kremer, P.D. 2012: Rare metals in southeastern Manitoba: pegmatites from Bernic Lake and Rush Lake (parts of NTS 52L6); *in* Report of Activities 2012, Manitoba Innovation, Energy and Mines, Manitoba Geological Survey, p. 54–58, URL <https://manitoba.ca/iem/geo/field/roa12pdfs/GS-4.pdf> [December 2022].

Martins, T., Rayner, N., Corrigan, D. and Kremer, P. 2022: Regional geology and tectonic framework of the Southern Indian domain, Trans-Hudson orogen, Manitoba; Canadian Journal of Earth Sciences, v. 59, p. 371–388, URL<https://doi.org/10.1139/cjes-2020-0142>.

Middlemost, E.A.K. 1994: Naming materials in the magma/igneous rock system; Earth-Science Reviews, v. 37, p. 215–224, URL <https://doi.org/10.1016/0012-8252(94)90029-9>.

Milligan, G.C. 1960: Geology of the Lynn Lake district; Manitoba Department of Mines and Natural Resources, Mines Branch, Publication 57-1, 317 p., URL <https://manitoba.ca/iem/info/libmin/PUB57-1.zip> [December 2022].

Miyashiro, A. 1970: Volcanic rock series in island arcs and active continental margins; American Journal of Science, v. 274, p. 321–355, URL <https://doi.org/10.2475/ajs.274.4.321>.

Mohamadizadeh, M., Mojtahedzadeh, S.H. and Ayati, F. 2020: Ga-(Nb+Ta)-(Nb/Ta)(Zr/Hf) ternary diagram: an excellent tool for discriminating barren and Ta-hosting granite-pegmatite systems; Journal of Earth Science, v. 31, p. 551–558, URL <https://doi.org/10.1007/s12583-020-1302-1>.

Mohammadi, N., Lentz, D.R., McFarlane, C.R.M. and Cousens, B. 2020: Geochemistry of the highly evolved Sn-W-Mo-bearing Mount Douglas granite, New Brunswick, Canada: implications for origin and mineralization; Ore Geology Reviews, v. 117, art. 103266, URL <https://doi.org/10.1016/j.oregeorev.2019.103266>.

Moyen, J.-F. 2011: The composite Archaean grey gneisses: petrological significance, and evidence for a non-unique tectonic setting for Archaean crustal growth; Lithos, v. 123, p. 21–36, URL <https://doi.org/10.1016/j.lithos.2010.09.015>.

Moyen, J.-F. and Martin, H. 2012: Forty years of TTG research; Lithos, v. 148, p. 312–336, URL <https://doi.org/10.1016/j.lithos.2012.06.010>.

Moyen, J.-F., Janoušek, V., Laurent, O., Bachmann, O., Jacob, J.-B., Farina, F., Fiannacca, P. and Villaros, A. 2021: Crustal melting vs. fractionation of basaltic magmas: part 1, granites and paradigms; Lithos, v. 402-403, art. 106291, URL <https://doi.org/10.1016/j.lithos.2021.106291>.

Mulja, T. and Williams-Jones, A.E. 2018: The physical and chemical evolution of fluids in rare-element granitic pegmatites associated with the Lacorne pluton, Québec, Canada; Chemical Geology, v. 493, p. 281–297, URL<https://doi.org/10.1016/j.chemgeo.2018.06.004>.

Mumin, A.H. 2002: Discovery of a carbonatite complex at Eden Lake (NTS 64C9), Manitoba; *in* Report of Activities 2002, Manitoba Industry, Trade and Mines, Manitoba Geological Survey, p. 187–197, URL <https://manitoba.ca/iem/geo/field/roa02pdfs/GS-21.pdf> [December 2022].

Murphy, L.A and Zwanzig, H.V. 2007: Preliminary stratigraphy and structure of the Notigi Lake area, Manitoba (parts of NTS 63O14, 64B3); *in* Report of Activities 2007, Manitoba Science, Technology, Energy and Mines, Manitoba Geological Survey, p. 51–62, URL <https://manitoba.ca/iem/geo/field/roa07pdfs/GS-5.pdf> [December 2022].

Musumeci, D., De Benedetti, A.A., Branca, S. and Ingaliso, L. 2022: Rittmann's heritage: a philosophical approach for current research; *in* In the footsteps of Warren B. Hamilton: new ideas in Earth science, G.R. Foulger, L.C. Hamilton, D.M. Jurdy, C.A. Stein, K.A. Howard and S. Stein (ed.), Geological Society of America, Special Paper 553, p. 1–8, URL <https://doi.org/10.1130/2021.2553(03)>.

Nadeau, O., Zelt, C., Leybourne, M.I. and Voinot, A. 2021: Evolution of Archean sanukitoids from the Otto stock by magma mixing and Na–K metasomatism: evidence from petrological observations and lithium isotope geochemistry; Journal of Petrology, v. 62, art. egab047, URL <https://doi.org/10.1093/petrology/egab047>.

Norman, G.W.H. 1933: Granville Lake district, northern Manitoba; Geological Survey of Canada, Summary Report, Part C, p. 23–41, URL <https://doi.org/10.4095/102007>.

O'Nions, R.K., Carter, S.R., Evensen, N.M. and Hamilton, P.J. 1979: Geochemical and cosmochemical applications of Nd isotope analysis; Annual Review of Earth and Planetary Science, v. 7, p. 11–38, URL <https://doi.org/10.1146/annurev.ea.07.050179.000303>.

Parks, J., Lin, S. Davis, D.W., Yang, X.M., Creaser, R.A. and Corkery, M.T. 2014: Meso- and Neoarchean evolution of the Island Lake greenstone belt and the northwestern Superior province: evidence from lithogeochemistry, Nd isotope data, and U–Pb zircon geochronology; Precambrian Research, v. 246, p. 160–179, URL <https://doi.org/10.1016/j.precamres.2014.02.016>.

Pearce, J.A. 1983: Role of the sub-continental lithosphere in magma genesis at active continental margins; *in* Continental Basalts and Mantle Xenoliths, C.J. Hawkesworth and M.J. Norry (ed.), Shiva Publishing Limited, Cheshire, United Kingdom, p. 230–249.

Pearce, J.A. 1996: A user's guide to basalt discrimination diagrams; *in* Trace Element Geochemistry of Volcanic Rocks: Applications for Massive Sulphide Exploration, D.A. Wyman (ed.), Geological Association of Canada, Short Course Notes, v. 12, p. 79–113.

Pearce, J.A. 2008: Geochemical fingerprinting of oceanic basalts with applications to ophiolite classification and the search for Archean oceanic crust; Lithos, v. 100, p. 14–48, URL <https://doi.org/10.1016/j.lithos.2007.06.016>.

Pearce, J.A. and Peate, D.W. 1995: Tectonic implications of the composition of volcanic ARC magmas; Annual Review of Earth and Planetary Sciences, v. 23, p. 251–285, URL <https://doi.org/10.1146/annurev.ea.23.050195.001343>.

Pearce, J.A., Harris, N.B.W. and Tindle, A.G. 1984: Trace element discrimination diagrams for the tectonic interpretation of granitic rocks; Journal of Petrology, v. 25, p. 956–983, URL <https://doi.org/10.1093/petrology/25.4.956>.

Pearce, J.A., Stern, R.J., Bloomer, S.H. and Fryer, P. 2005: Geochemical mapping of the Mariana arc-basin system: implications for the nature and distribution of subduction components; Geochemistry, Geophysics, Geosystems, v. 6, p. 1–27, URL <https://doi.org/10.1029/2004GC000895>.

Pease, V., Percival, J., Smithies, H., Stevens, G. and Van Kranendonk, M. J. 2008: When did plate tectonics begin? Evidence from the orogenic record; *in* When Did Plate Tectonics Begin on Planet Earth?, K.C. Condie and V. Pease (ed.), Special Paper of the Geological Society of America 440, p. 199–228, URL <https://doi.org/10.1130/2008.2440(10)>.

Peccerillo, A. and Taylor, S.R. 1976: Geochemistry of eocene calc-alkaline volcanic rocks from the Kastamonu area, northern Turkey; Contributions to Mineralogy and Petrology, v. 58, p. 63–81.

Peck, D.C., Theyer, P., Hulbert, L.J., Xiong, J., Fedikow, M.A.F. and Cameron, H.D.M. 2000: Preliminary exploration database for platinum-group elements in Manitoba; Manitoba Industry, Trade and Mines, Manitoba Geological Survey, Open File Report OF2000-5, 1 CD-ROM, URL <https://manitoba.ca/iem/info/libmin/OF2000-5.zip> [December 2022].

Percival, J.A. 2007: Geology and metallogeny of the Superior province, Canada; *in* Mineral Deposits of Canada: a synthesis of major deposit-types, district metallogeny, the evolution of geological provinces, and exploration methods, W.D. Goodfellow (ed.), Geological Association of Canada, Mineral Deposits Division, Special Publication 5, p. 903–928.

Percival, J.A., McNicoll, V., Brown, J.L. and Whalen, J.B. 2004: Convergent margin tectonics, central Wabigoon subprovince, Superior Province, Canada; Precambrian Research, v. 132, p. 213–244.

Percival, J.A., McNicoll, V. and Bailes, A.H. 2006a: Strike-slip juxtaposition of ca. 2.72 Ga juvenile arc and >2.98 Ga continent margin sequences and its implications for Archean terrane accretion, western Superior province, Canada; Canadian Journal of Earth Sciences, v. 43, p. 895–927, URL <https://doi.org/10.1139/e06-039>.

Percival, J.A., Sanborn-Barrie, M., Skulski, T., Stott, G.M., Helmstaedt, H. and White, D.J. 2006b: Tectonic evolution of the western Superior province from NATMAP and Lithoprobe studies; Canadian Journal of Earth Sciences, v. 43, p. 1085–1117, URL <https://doi.org/10.1139/e06-062>.

Percival, J.A., Skulski, T., Sanborn-Barrie, M., Stott, G.M., Leclair, A.D., Corkery, M.T. and Boily, M. 2012: Geology and tectonic evolution of the Superior province, Canada; *in* Tectonic Styles in Canada: The Lithoprobe perspective, J.A. Percival, F.A. Cook and R.M. Clowes (ed.), Geological Association of Canada, Special Paper 49, p. 321–378.

Peterson, T.D., Van Breemen, O., Sandeman, H. and Cousens, B. 2002: Proterozoic (1.85–1.75 Ga) igneous suites of the western Churchill province: granitoid and ultrapotassic magmatism in a reworked Archean hinterland; Precambrian Research, v. 119, p. 73–100, URL <https://doi.org/10.1016/S0301-9268(02)00118-3>.

Polat, A. 2012: Growth of Archean continental crust in oceanic island arcs; Geology, v. 40, p. 383–384, URL <https://doi.org/10.1130/focus042012.1>.

Polat, A. and Kerrich, R. 2001: Geodynamic processes, continental growth, and mantle evolution recorded in late Archean greenstone belts of the southern Superior Province, Canada; Precambrian Research, v. 112, p. 5–25, URL <https://doi.org/10.1016/S0301-9268(01)00168-1>.

Polat, A., Frei, R., Deng, H., Yang, X.M. and Sotiriou, P. 2022: Anatomy of a Neoarchean continental arc-backarc system in the Cross Lake-Pipestone Lake region, northwestern Superior Province, Canada; Precambrian Research, v. 370, art. 106556, URL <https://doi.org/10.1016/j.precamres.2021.106556>.

Polat, A., Kokfelt, T., Burke, K.C., Kusky, T.M., Bradley, D.C., Dziggel, A. and Kolb, J. 2016: Lithological, structural, and geochemical characteristics of the Mesoarchean Târtoq greenstone belt, south-west Greenland, and the Chugach-Prince William accretionary complex, southern Alaska: evidence for uniformitarian plate-tectonic processes; Canadian Journal of Earth Sciences, v. 53, p. 1336–1371.

Prouteau, G., Scaillet, B., Pichavant, M. and Maury, R. C. 1999: Fluid-present melting of ocean crust in subduction zones; Geology, v. 27, p. 1111–1114, URL <https://doi.org/10.1130/0091-7613(1999)027%3C1111:FPMOOC%3E2.3.CO;2>.

Prouteau, G., Scaillet, B., Pichavant, M. and Maury, R. 2001: Evidence for mantle metasomatism by hydrous silicic melts derived from subducted oceanic crust; Nature, v. 410, p. 197–200.

Raffensberger, J.P. and Garven, G. 1995a: The formation of unconformity-type uranium ore deposits 1. Coupled groundwater flow and heat transport modeling; American Journal of Science, v. 295, p. 581–636, URL <https://doi.org/10.2475/ajs.295.5.581>.

Raffensberger, J.P. and Garven, G. 1995b: The formation of unconformity-type uranium ore deposits 2. Coupled hydrochemical modeling; American Journal of Science, v. 295, p. 639–696, URL <https://doi.org/10.2475/ajs.295.6.639>.

Rayner, N. and Corrigan, D. 2004: Uranium-lead geochronological results from the Churchill River - Southern Indian Lake transect, northern Manitoba; Geological Survey of Canada, Current Research no. 2004-F1, 1 CD-ROM, URL <https://doi.org/10.4095/214975>.

Rayner, N., Zwanzig, H.V. and Percival, J.A. 2006: Detrital zircon provenance of the Pipe Formation, Ospwagan Group, Thompson Nickel Belt, Manitoba, NTS 63O8; in Report of Activities 2006, Manitoba Science, Technology, Energy and Mines, Manitoba Geological Survey, p. 116–124, URL <https://manitoba.ca/iem/geo/field/roa06pdfs/GS-11.pdf> [December 2022].

Reid, K.D. 2021: Results of bedrock geological mapping in the Stuart Bay–Chickadee Lake area (east of Wekusko Lake), north-central Manitoba (parts of NTS 63J12, 13); *in* Report of Activities 2021, Manitoba Agriculture and Resource Development, Manitoba Geological Survey, p. 29–39, URL <https://manitoba.ca/iem/geo/field/roa21pdfs/GS2021-4.pdf> [December 2022].

René, M. 2020: Geochemistry of granitic rocks of the Moldanubian batholith (central European variscides), Chapter 1 *in* IntechOpen Book Series, URL <https://doi.org/10.5772/intechopen.93189>.

Rinne, M.L. 2017: Preliminary results of bedrock mapping at Bigstone Lake and Knight Lake, northwestern Superior province, Manitoba (parts of NTS 53E11, 12, 13, 14); *in* Report of Activities 2017, Manitoba Growth, Enterprise and Trade, Manitoba Geological Survey, p. 19–29, URL <https://manitoba.ca/iem/geo/field/roa17pdfs/GS2017-3.pdf> [December 2022].

Rittmann, A. 1973: Stable mineral assemblages of igneous rocks; Springer Berlin, Heidelberg, Germany, 262 p., URL <https://doi.org/10.1007/978-3-642-65482-4>.

Rollinson, H.R. 1993: Using geochemical data: evaluation, presentation, interpretation; Routledge, Taylor & Francis Group, London and New York, 352 p.

Rollinson, H. and Pease, V. 2021: Using geochemical data to understand geological processes (2nd edition), Cambridge University Press, Cambridge, United Kingdom, 346 p.

Rudnick, R.L. and Gao, S. 2010: Composition of the continental crust; Chapter 5 *in* Treatise On Geochemistry, H.D. Holland and K.K. Turetian (ed.), Elsevier Ltd., Amsterdam, Netherlands, p. 197–234.

Sanborn-Barrie, M., Skulski, T. and Parker, J. 2001: Three hundred million years of tectonic history recorded by the Red Lake greenstone belt, Ontario; Geological Survey of Canada, Current Research no. 2001-C19, p. 1–14.

Scaillet, B., Holtz, F. and Pichavant, M. 2016: Experimental constraints on the formation of silicic magmas; Elements, v. 12, p. 109–114, URL <https://doi.org/10.2113/gselements.12.2.109>.

Scoates, J.S. and Scoates, R.F.J. 2013: Age of the Bird River sill, southeastern Manitoba, Canada, with implications for the secular variation of layered intrusion-hosted stratiform chromite mineralization; Economic Geology, v. 108, p. 895–907, URL <https://doi.org/10.2113/econgeo.108.4.895>.

Secchi, F., Casini, L., Cifelli, F., Naitza, S., Carta, E. and Oggiano, G. 2022: Syntectonic magmatism and reactivation of collisional structures during late-Variscan shearing (SW Sardinia, Italy); International Journal of Earth Sciences, v. 111, p. 1469–1490, URL<https://doi.org/10.1007/s00531-022-02193-2>.

Shirey, S.B. and Hanson, G.N. 1984: Mantle-derived Archaean monzodiorites and trachyandesites; Nature, v. 310, p. 222–224.

Sotiriou, P., Polat, A., Frei, R., Yang, X.M. and van Vessem, J. 2019: A back-arc origin for the Neoarchaean megacrystic anorthosite-bearing Bird River sill and the associated greenstone belt, Bird River subprovince, western Superior province, Manitoba, Canada; International Journal of Earth Sciences, v. 108, p. 2177–2207.

Sotiriou, P., Polat, A., Frei, R., Yang, X.M. and van Vessem, J. 2020: Evidence for Neoarchean hydrous arc magmatism, the anorthosite-bearing Mayville intrusion, western Superior province, Canada; Lithos, v. 362–363, art. 105482, URL <https://doi.org/10.1016/j.lithos.2020.105482>.

Stauffer, M.R. 1984: Manikewan: an early Proterozoic ocean in central Canada, its igneous history and orogenic closure; Precambrian Research, v. 25, p. 257–281, URL <https://doi.org/10.1016/0301-9268(84)90036-6>.

Stern, R., Hanson, G.N. and Shirey, S.B. 1989: Petrogenesis of mantle-derived, LILE-enriched Archean monzodiorites and trachyandesites (sanukitoids) in southwestern Superior province; Canadian Journal of Earth Sciences, v. 26, p. 1688–1712, URl <https://doi.org/10.1139/e89-145>.

Stott, G.M. and Corfu, F. 1991: Uchi Subprovince; *in* Geology of Ontario, P.C. Thurston, H.R. Williams, R.H. Sutcliffe and G.M. Stott (ed.), Ontario Geological Survey, Special Volume 4, Part 1, p. 145–236.

Stott, G.M., Corkery, M.T., Percival, J.A., Simard, M. and Goutier, J. 2010: Project units 98-006 and 98-007: a revised terrane subdivision of the Superior Province; *in* Summary of Field Work and Other Activities 2010, Ontario Geological Survey, Open File Report 6260, p. 20-1–20-10.

Streckeisen, A.L. and LeMaitre, R.W. 1979: A chemical approximation to the modal QAPF classification of the igneous rocks; Neues Jahrbuch für Mineralogie, v. 136, p. 169–206.

Sun, S.-s. and McDonough, W.F. 1989: Chemical and isotopic systematics of oceanic basalts: implication for mantle composition and processes; Geological Society of London, London, United Kingdom, Special Publications, v. 42, p. 313–345.

Syme, E.C. 1985: Geochemistry of metavolcanic rocks in the Lynn Lake belt; Manitoba Energy and Mines, Geological Services, Geological Report GR84-1, 84 p. plus 1 map at 1:100 000 scale.

Syme, E.C. 1998: Ore-associated and barren rhyolites in the central Flin Flon belt: case study of the Flin Flon mine sequence; Manitoba Energy and Mines, Geological Services, Open File Report OF98-9, 26 p., URL <https://manitoba.ca/iem/info/libmin/OF98-9.pdf> [December 2022].

Sylvester, P.J. 1998: Post-collisional strongly peraluminous granites; Lithos, v. 45, p. 29–44, URL <https://doi.org/10.1016/S0024-4937(98)00024-3>.

Taylor, S.R. and McLennan, S.M. 2009: Planetary crusts: rheir composition, origin and evolution; Cambridge University Press, Cambridge, United Kingdom, 402 p.

Thompson Nickel Belt Geology Working Group 2001: Geology of the Halfway Lake–Pistol Lake area (63O/1 and 63O/2); Manitoba Industry, Trade and Mines, Manitoba Geological Survey, Preliminary Map 2001I-1, scale 1:50 000, URL <https://manitoba.ca/iem/info/libmin/tnb_pdfs/pm_2001i-1.pdf> [December 2022].

Thorne, K.G., Lentz, D.R., Hall, D.C. and Yang, X.M. 2002: Petrology, geochemistry, and geochronology of the granitic pegmatite and aplite dikes associated with the Clarence Stream gold deposit, southwestern New Brunswick; Geological Survey of Canada, Current Research 2002-E12, 13 p.

Tomlinson, K.Y., Stott, G.M., Percival, J.A. and Stone, D. 2004: Basement terrane correlations and crustal recycling in the western Superior province: Nd isotopic character of granitoid and felsic volcanic rocks in the Wabigoon subprovince, N. Ontario, Canada; Precambrian Research, v. 132, p. 245–274, URL <https://doi.org/10.1016/j.precamres.2003.12.017>.

Turek, A., Keller, R., Van Schmus, W.R. and W. Weber 1989: U–Pb zircon ages for the Rice Lake area, southeastern Manitoba; Canadian Journal of Earth Sciences, v. 26, p. 23–30, URL <https://doi.org/10.1139/e89-003>.

Turek, A., Woodhead, J. and Zwanzig H.V. 2000: U-Pb age of the gabbro and other plutons at Lynn Lake (part of NTS 64C); *in* Report of Activities 2000, Manitoba Industry, Trade and Mines, Manitoba Geological Survey, p. 97–104, URL <https://manitoba.ca/iem/geo/field/roa00pdfs/00gs-18.pdf> [January 2023].

Tuttle, O.F. and Bowen, N.L. 1958: Origin of granite in the light of experimental studies in the system $NaAlSi_3O_8$-KAl Si_3O_8-SiO_2-H_2O; Geological Society of America Memoirs, v. 74, 153 p., URL <https://doi.org/10.1130/MEM74>.

Vaughn, E.S. and Ridley, J. R. 2014: Evidence for exsolution of Au-ore fluids from granites crystallized in the mid-crust, Archaean Louis Lake Batholith, Wyoming; in Gold-Transporting Hydrothermal Fluids in the Earth's Crust, P.S. Garofalo and J.R. Ridley (ed.), Geological Society of London, London, United Kingdom, Special Publications, v. 402, URL <http://doi.org/10.1144/SP402.6> [November 2020].

Wang, X. 1993: U-Pb zircon geochronology study of the Bird River greenstone belt, southeastern Manitoba; M.Sc. thesis, University of Windsor, Windsor, Ontario, 96 p.

Wedepohl, K.H. 1995: The composition of the continental crust; Geochimica et Cosmochimica Acta, v. 59, p. 1217–1232., URL <https://doi.org/10.1016/0016-7037(95)00038-2>.

Whalen, J.B. and Chappell, B.W. 1988: Opaque mineralogy and mafic mineral chemistry of I- and S-type granites of the Lachlan fold belt, southeast Australia; American Mineralogist, v. 73, p. 281–296.

Whalen, J.B. and Frost, C.D. 2013: The Q-ANOR diagram: a tool for the petrogenetic and tectonomagmatic characterization of granitic suites (abstract); URL <https://www.researchgate.net/publication/290161821> [December 2022].

Whalen, J.B. and Hildebrand, R.S. 2019: Trace element discrimination of arc, slab failure, and A-type granitic rocks; Lithos, v. 348–349, art. 105179, URL <https://doi.org/10.1016/j.lithos.2019.105179>.

Whalen, J.B., Currie, K.L. and Chappell, B.W. 1987: A-type granites: geochemical characteristics, discrimination and petrogenesis; Contributions to Mineralogy and Petrology, v. 95, p. 407–419.

Whalen, J.B., Percival, J.A., McNicoll, V. and Longstaffe, F.J. 2004: Geochemical and isotopic (Nd-O) evidence bearing on the origin of late- to post-orogenic high-K granitoid rocks in the western Superior province: implications for late Archean tectonomagmatic processes; Precambrian Research, v. 132, p. 303–326, URL <https://doi.org/10.1016/j.precamres.2003.11.007>.

Whalen, J.B., Zwanzig, H.V., Percival, J.A. and Rayner, N. 2008: Geochemistry of an alkaline, ca. 1885 Ma K-feldspar–porphyritic, monzonitic to syenogranitic suite, northeastern Kisseynew Domain, Manitoba (parts of NTS 63O); *in* Report of Activities 2008, Manitoba Science, Technology, Energy and Mines, Manitoba Geological Survey, p. 66–78, URL <https://manitoba.ca/iem/geo/field/roa08pdfs/GS-6.pdf> [December 2022].

White, D.J., Lucas, S.B., Bleeker, W., Hajnal, Z., Lewry, J.F. and Zwanzig, H.V. 2002: Suture-zone geometry along an irregular Paleoproterozoic margin: the Superior boundary zone, Manitoba, Canada; Geology, v. 30, p. 735–738, URL <https://doi.org/10.1130/0091-7613(2002)030%3C0735:SZGAAI%3E2.0.CO;2>.

Windley, B.F. and Garde, A.A. 2009: Arc-generated blocks with crustal sections in the north Atlantic craton of west Greenland: crustal growth in the Archean with modern analogues; Earth-Science Reviews, v. 93, p. 1–30, URL <https://doi.org/10.1016/j.earscirev.2008.12.001>.

Windley, B.F., Kusky, T. and Polat, A. 2021: Onset of plate tectonics by the Eoarchean; Precambrian Research, v. 352, art. 105980, URL <https://doi.org/10.1016/j.precamres.2020.105980>.

Winter, J.D. 2014: Principles of igneous and metamorphic petrology, (2nd edition; Pearson Education Limited, Essex, United Kingdom, 738 p.

Wu, T., Polat, A., Frei, R., Fryer, B.J., Yang, K. and Kusky, T. 2016: Geochemistry, Nd, Pb and Sr isotope systematics, and U–Pb zircon ages of the Neoarchean Bad Vermilion Lake greenstone belt and spatially associated granitic rocks, western Superior province, Canada; Precambrian Research, v. 282, p. 21–51, URL <https://doi.org/10.1016/j.precamres.2016.06.021>.

Wyman, D.A. 2013: A critical assessment of Neoarchean "plume only" geodynamics: evidence from the Superior province; Precambrian Research, v. 229, p. 3–19, URL <https://doi.org/10.1016/j.precamres.2012.01.010>.

Wyman, D., Ayer, J. and Devaney, J. 2000: Niobium-enriched basalts from the Wabigoon subprovince, Canada: evidence for adakitic metasomatism above an Archean subduction zone; Earth and Planetary Science Letters, v. 179, p. 21–30, URL <https://doi.org/10.1016/S0012-821X(00)00106-0>.

Yang, X.M. 2007: Using the Rittmann Serial Index to define the alkalinity of igneous rocks; Neues Jahrbuch für Mineralogie, v. 184, p. 95–103, URL <https://doi.org/10.1127/0077-7757/2007/0082>.

Yang, X.M. 2012: Sulphur solubility in felsic magmas: implications for genesis of intrusion-related gold mineralization; Geoscience Canada, v. 39, p. 17–32.

Yang, X.M. 2014a: Granitoid rocks in southeastern Manitoba: preliminary results of reconnaissance mapping and sampling; *in* Report of Activities 2014, Manitoba Mineral Resources, Manitoba Geological Survey, p. 49–63, URL <https://manitoba.ca/iem/geo/field/roa14pdfs/GS-4.pdf> [December 2022].

Yang, X.M. 2014b: Petrogenetic types, tectonic settings, and mineral potential of granitoids in southeastern Manitoba: evidence from reconnaissance mapping and geological sampling; Geoscientific Presentation PRES2014-T17, Manitoba Mining and Minerals Convention, November 19–21, 2014, Winnipeg, Manitoba.

Yang, X.M. 2016: Granitoid rocks in north-central Manitoba: preliminary results of reconnaissance mapping and sampling; *in* Report of Activities 2016, Manitoba Growth, Enterprise and Trade, Manitoba Geological Survey, p. 115–125, URL <https://manitoba.ca/iem/geo/field/roa16pdfs/GS-10.pdf> [June 2022].

Yang, X.M. 2017: Estimation of crystallization pressure of granite intrusions; Lithos, v. 286–287, p. 324–329, URL <https://doi.org/10.1016/j.lithos.2017.06.018>.

Yang, X.M. 2019a: Preliminary results of bedrock mapping in the Gemmell Lake area, Lynn Lake greenstone belt, northwestern Manitoba (parts of NTS 64C11, 14); *in* Report of Activities 2019, Manitoba Agriculture and Resource Development, Manitoba Geological Survey, p. 10–29, URL <https://www.manitoba.ca/iem/geo/field/roa19pdfs/GS2019-2.pdf> [October 2021].

Yang, X.M. 2019b: Using rare earth elements (REE) to decipher the origin of ore fluids associated with granite intrusions; Minerals, v. 9, p. 426, URL <https://doi.org/10.3390/min9070426> [October 2019].

Yang, X.M. 2021: Bedrock mapping at Ralph Lake, Lynn Lake greenstone belt, northwestern Manitoba (part of NTS 64C14): preliminary results and geological implications; *in* Report of Activities 2021, Manitoba Agriculture and Resource Development, Manitoba Geological Survey, p. 40–58, URL <https://manitoba.ca/iem/geo/field/roa21pdfs/GS2021-5.pdf> [June 2022].

Yang, X.M. and Beaumont-Smith, C.J. 2015a: Geological investigations of the Keewatin River area, Lynn Lake greenstone belt, northwestern Manitoba (parts of NTS 64C14, 15); *in* Report of Activities 2015, Manitoba Mineral Resources, Manitoba Geological Survey, p. 52–67, URL <https://manitoba.ca/iem/geo/field/roa15pdfs/GS-4.pdf> [December 2022].

Yang, X.M. and Beaumont-Smith, C.J. 2015b: Granitoid rocks in the Lynn Lake region, northwestern Manitoba: preliminary results of reconnaissance mapping and sampling; *in* Report of Activities 2015, Manitoba Mineral Resources, Manitoba Geological Survey, p. 68–78, URL <https://www.manitoba.ca/iem/geo/field/roa15pdfs/GS-5.pdf> [October 2021].

Yang, X.M. and Beaumont-Smith, C.J. 2016: Geological investigations in the Farley Lake area, Lynn Lake greenstone belt, northwestern Manitoba (part of NTS 64C16); *in* Report of Activities 2016, Manitoba Growth, Enterprise and Trade, Manitoba Geological Survey, p. 99–114, URL <https://www.manitoba.ca/iem/geo/field/roa16pdfs/GS-9.pdf> [October 2021].

Yang, X.M. and Beaumont-Smith, C.J. 2017: Geological investigations of the Wasekwan Lake area, Lynn Lake greenstone belt, northwestern Manitoba (parts of NTS 64C10, 15); *in* Report of Activities 2017, Manitoba Growth, Enterprise and Trade, Manitoba Geological Survey, p. 117–132, URL <https://www.manitoba.ca/iem/geo/field/roa17pdfs/GS2017-11.pdf> [October 2021].

Yang, X.M. and Gilbert, H.P. 2014: Archean tonalite-trondhjemitegranodiorite (TTG) suite in the Bird River greenstone belt, southeastern Manitoba: lithogeochemical characteristics, geodynamic evolution, and potential for porphyry Cu-(Au) mineralization (abstract); Geological Association of Canada–Mineralogical Association of Canada, Joint Annual Meeting, Fredericton, New Brunswick, May 21–23, 2014, Program with Abstracts, p. 294.

Yang, X.M. and Houlé, M.G. 2020: Geology of the Cat Creek–Euclid Lake area, Bird River greenstone belt, southeastern Manitoba (parts of NTS 52L11, 12); Manitoba Department of Agriculture and Resource Development, Manitoba Geological Survey, Geoscientific Report GR2020-1, 105 p. plus 1 map at 1:20 000 scale, URL <https://manitoba.ca/iem/info/libmin/GR2020-1.zip> [October 2021].

Yang, X.M. and Lawley, C.J.M. 2018: Tectonic setting of the Gordon gold deposit, Lynn Lake greenstone belt, northwestern Manitoba (parts of NTS 64C16): evidence from lithogeochemistry, Nd isotopes, and U-Pb geochronology; *in* Report of Activities 2018, Manitoba Growth, Enterprise and Trade, Manitoba Geological Survey, p. 89–109, URL <https://manitoba.ca/iem/geo/field/roa18pdfs/GS2018-8.pdf> [October 2021].

Yang, X.M. and Lentz, D.R. 2005: Chemical composition of rock-forming minerals in gold-related granitoid intrusions, southwestern New Brunswick, Canada: implications for crystallization conditions, volatile exsolution and fluorine-chlorine activity; Contributions to Mineralogy and Petrology, v. 150, p. 287–305.

Yang, X.M. and Lentz, D.R. 2010: Sulfur isotopic systematics of granitoids, southwestern New Brunswick, Canada: implications for petrogenetic processes, redox conditions and gold mineralization; Mineralium Deposita, v. 45, p. 795–816, URL <https://doi.org/10.1007/s00126-010-0307-6>.

Yang, X.M., Drayson, D. and Polat, A. 2019: S-type granites in the western Superior Province: a marker of Archean collision zones; Canadian Journal of Earth Sciences, v. 56, p. 1409–1436, URL <https://doi.org/10.1139/cjes-2018-0056>.

Yang, X.M., Gilbert, H.P., Corkery, M.T. and Houlé, M.G. 2011: The Mayville mafic–ultramafic intrusion in the Neoarchean Bird River greenstone belt, southeastern Manitoba (part of NTS 52L12): preliminary geochemical investigation and implication for PGE-Ni-Cu-(Cr) mineralization; *in* Report of Activities 2011, Manitoba Innovation, Energy and Mines, Manitoba Geological Survey, p. 127–142, URL <https://manitoba.ca/iem/geo/field/roa11pdfs/GS-12.pdf> [December 2022].

Yang, X.M., Gilbert, H.P. and Houlé, M.G. 2012: Geological investigations of the Cat Creek area in the Neoarchean Bird River greenstone belt, southeastern Manitoba (part of NTS 52L12): new insights into PGE-Ni-Cu-Cr mineralization; *in* Report of Activities 2012, Manitoba Innovation, Energy and Mines, Manitoba Geological Survey, p. 32–53, URL <https://manitoba.ca/iem/geo/field/roa12pdfs/GS-3.pdf> [December 2022].

Yang, X.M., Gilbert, H.P. and Houlé, M.G. 2013: Cat Lake–Euclid Lake area in the Neoarchean Bird River greenstone belt, southeastern Manitoba (parts of NTS 52L11, 12): preliminary results of bedrock geological mapping and their implications for geodynamic evolution and metallogeny; *in* Report of Activities 2013, Manitoba Mineral Resources, Manitoba Geological Survey, p. 70–84, URL <https://manitoba.ca/iem/geo/field/roa13pdfs/GS-6.pdf> [December 2022].

Yang, X.M., Lentz, D.R. and Chi, G. 2021: Ferric-ferrous iron oxide ratios: effect on crystallization pressure of granites estimated by Qtz-geobarometry; Lithos, v. 380-381, art. 105920. URL <https://doi.org/10.1016/j.lithos.2020.105920>.

Yang, X.M., Lentz, D.R., Chi, G. and Thorne, K.G. 2008: Geochemical characteristics of gold-related granitoids in southwestern New Brunswick, Canada; Lithos, v. 104, p. 355–377, URL <https://doi.org/10.1016/j.lithos.2008.01.002>.

Zhang, Q., Wang, Y., Li, C.-D., Jin, W.-J. and Jia, X.-Q. 2006: A granite classification based on pressures; Geological Bulletin of China, v. 25, p. 1274–1278.

Zhou, X., Lin, S. and Anderson, S.D. 2012: Structural study of the Ogama-Rockland gold deposit, southeastern margin of the Ross River pluton, Rice Lake greenstone belt, southeastern Manitoba (NTS 52L14); *in* Report of Activities 2012, Manitoba Innovation, Energy and Mines, Manitoba Geological Survey, p. 59–67, URL <https://manitoba.ca/iem/geo/field/roa12pdfs/GS-5.pdf> [December 2022].

Zhou, X., Lin, S. and Anderson, S.D. 2016: Stratigraphy, structure and lode gold system at the Central Manitoba mine trend, Rice Lake greenstone belt, Archean Superior Province, Manitoba, Canada; Precambrian Research, v. 281, p. 80–100, URL <https://doi.org/10.1016/j.precamres.2016.05.020>.

Zwanzig, H.V. and Bailes, A.H. 2010: Geology and geochemical evolution of the northern Flin Flon and southern Kisseynew domains, Kississing–File lakes area, Manitoba (parts of NTS 63K, N); Manitoba Innovation, Energy and Mines, Manitoba Geological Survey, Geoscientific Report GR2010-1, 135 p., URL <https://manitoba.ca/iem/info/libmin/GR2010-1.zip> [December 2022].

Zwanzig, H.V. and Schledewitz, D.C.P. 1992: Geology of the Kississing-Batty lakes area: interim report; Manitoba Energy and Mines, Geological Services, Open File Report OF92-2, 87 p. plus 1 map at 1:20 000 scale and 2 maps at 1:50 000 scale, URL <https://manitoba.ca/iem/info/libmin/OF92-2.zip> [December 2022].

Zwanzig, H.V., Böhm, C.O. and Etcheverry, J. 2001: Superior Boundary Zone–Reindeer Zone transition in the Pearson Lake–Odei River–Mystery Lake region; *in* Report of Activities 2001, Manitoba Industry, Trade and Mines, Manitoba Geological Survey, p. 51–56, URL <https://manitoba.ca/iem/geo/field/roa01pdfs/01gs-08.pdf> [December 2022].

Zwanzig, H.V., Syme, E.C. and Gilbert, H.P. 1999: Updated trace element geochemistry of the ca. 1.9 Ga metavolcanic rocks in the Paleoproterozoic Lynn Lake belt; Manitoba Industry, Trade and Mines, Geological Services, Open File Report OF99-13, 46 p., URL <https://manitoba.ca/iem/info/libmin/OF99-13.zip> [December 2022].

Zwanzig, H.V., Böhm, C.O., Protrel, A. and Machado, N. 2003: Field relations, U-Pb zircon ages and Nd model ages of granitoid intrusions along the Thompson Nickel Belt–Kisseynew Domain boundary, Setting Lake area, Manitoba (NTS 63J15 and 63O2); *in* Report of Activities 2003, Manitoba Industry, Economic Development and Mines, Manitoba Geological Survey, p. 118–129, URL <https://manitoba.ca/iem/geo/field/roa03pdfs/GS-16.pdf> [December 2022].